UNIVERSITÉ DU LUXEMBOURG

PhD-FHSE-2023-001
The Faculty of Humanities, Education and Social Sciences

DISSERTATION

Defence held on 10/02/2023 in Esch-sur-Alzette

to obtain the degree of

DOCTEUR DE L'UNIVERSITÉ DU LUXEMBOURG

EN GÉOGRAPHIE

by

Yufei WEI
Born on 22 August 1992 in Beijing (China)

ON CENTRALITY AND POPULATION SIZE EFFECTS IN URBAN POLLUTION: A META-ANALYSIS OF NO_2 AND HEAT ISLANDS AND SPATIAL ANALYSIS OF NO_2

Dissertation defence committee

Dr Geoffrey Caruso, dissertation supervisor
Professor, Université du Luxembourg

Dr Rémi Lemoy
Associate Professor, Université de Rouen Normandie

Dr Luisito Bertinelli, Chairman
Associate Professor, Université du Luxembourg

Dr Mirjam Schindler
Lecturer, Victoria University of Wellington

Dr Sophie Legras
Research Scientist, Institut National de la Recherche Agronomique

Abstract

Whether larger cities are greener or not is a controversial topic, and there is a lack of clear understanding about the effect of population size on NO_2 pollution levels and UHI. This is partly because most of the studies quantifying the effects of city size on heat stress and air pollution only concern cities in certain countries, world regions, or a few cities within the top ranks globally. The city center is the most active area for anthropogenic activities, and many single-city studies showed that there is a significant difference in NO_2 levels between the city center and the outskirts of the center. However, we haven't found empirical studies that quantitatively describe how NO_2 levels change with distance to the city center (i.e. centrality) and we are not clear about how population size affects the relationship between NO_2 levels and centrality. We perform a qualitative synthesis and a meta-analysis under the PRISMA guideline to summarize the population effect on NO_2 levels and UHI. We then use annual mean NO_2 surface concentrations and annual mean tropospheric NO_2 columns to test the conclusions of NO_2 derived from the meta-analysis and perform centrality analysis. We use linear regression to investigate the effects of population and centrality on NO_2. We use RMSC and 2-step linear regression to find out how population size affects the relationship between centrality and NO_2 levels. The qualitative synthesis shows remote sensing and monitoring stations are the main ways to measure UHI and NO_2. The meta-analysis shows larger cities always have more heat waves and higher NO_2 levels. Specifically, moving from cities with population from 1 million to 10 million, the max UHI intensity increases by 4 °C and annual mean NO_2 surface concentration increases by 22 $\mu g/m^3$, and moving from cities with population from 100 thousand to 1 million, the max UHI intensity increases by 3 °C and annual mean NO_2 surface concentration increases by 15 $\mu g/m^3$. The coefficients of logarithmic population we derived from empirical studies (i.e. 0.1354 and 0.1911) are very close to the one in meta-analysis (i.e. 0.1587). Logarithmic population is positively correlated with, and logarithmic centrality is negatively correlated with logarithmic NO_2 levels. Population is more important than centrality, and monitoring station background and background NO_2 are more important than population in deciding NO_2 levels. Results of RMSC and 2-step linear regression show that the relationship between NO_2 levels and centrality is affected by population size, and NO_2 levels decrease faster with centrality in large cities.

Acknowledgments

This dissertation would not have been possible without the support of many people. Many thanks to Prof. Dr. Geoffrey Caruso and Prof. Dr. Rémi Lemoy, who gave me this chance, read my writings and offered guidance. I would also like to thank the rest of my thesis committee: Prof. Dr. Luisito Bertinelli, Dr. Mirjam Schindler, and Dr. Sophie Legras for their insightful comments and encouragement, but also for the suggestions which motivated me to broaden my research from new perspectives.

Thanks to the Luxembourg National Research Fund (FNR) CORE program for financing me though the SCALE-IT-UP project. It is a pleasure to complete this thesis and other doctoral courses at the University of Luxembourg.

My work experience at the University of Luxembourg would not have been smooth without the help of my former and current colleagues of DGEO: Dr. Marlène Boura, Dr. Estelle Mennicken, Kerry Schiel, Prof. Dr. Catherine (Kate) Jones, Isabelle Pigeron-Piroth, Nadjia Ekwegbalu, Prof. Dr. Christian Schulz, and Dr. Cyrille Médard de Chardon. I also sincerely thank Régine Poussin and Dr. Elisabeth John, who provided me an opportunity to join their team as an intern.

Heartfelt thanks to the encouragement from Beijing. Sincere thanks to all my friends. Big thanks to Dr. Siwen Guo and Barbara Tijerina Rodriguez who introduced Luxembourgish culture. Special thanks to Dr. Daniela Gierschek and Dr. Elisabeth Wingerter who improved my Luxembourgish and made great conversations.

Table of Contents

List of Tables

List of Figures

Abbreviations and Acronyms

AMF	Air-Mass Factor
ANOVA	ANalysis Of VAriance
API	Air Quality Index
AQ e-Reporting	Air Quality e-Reporting
BP test	Breusch-Pagan test
BRT	Bus Rapid Transit
C	annual mean tropospheric NO_2 vertical columns
C_{min}	minimum annual mean tropospheric NO_2 column per FUA
$\hat{C}$	predicted annual mean tropospheric NO_2 columns
C_f	mean of annual mean NO_2 columns per FUA overlaid with the stations
CFD	Computational Fluid Dynamics
CIs	Confidence Intervals
CO	carbon monoxide
CO_2	carbon dioxide
D	population density
DOAS	Differential Optical Absorption Spectroscopy
EAC4	ECMWF Atmospheric Composition Reanalysis 4
ECMWF	Eruopean Center for Medium-Range Weather Forecasts
EEA	European Environment Agency
EU	European Union
FUAs	Functional Urban Areas
G	annual mean NO_2 surface concentrations
G_f	mean of annual mean NO_2 surface concentrations per FUA overlaid with the columns
$\hat{G}$	predicted annual mean NO_2 surface concentrations
GDP	Gross Domestic Product
HC	hydrocarbons
H_2O	water
H_2O_{liq}	liquid water

H_2O_{vap}	water vapor
IPAT	environmental Impacts, Population, Affluence, Technology
JCR	Journal Citation Reports
LAU	Local Administrative Unit
LUR	Land Use Regression
MODIS	Moderate Resolution Imaging Spectroradiometer
NDVI	Normalized Difference Vegetation Index
NH_3	ammonia
NMC	National Meterological Center
NWP	Numerical Weather Prediction
NO	nitric oxide
NO_x	nitrogen oxides
NO_2	nitrogen dioxide
N_2	nitrogen
N_2O	nitrous oxide
OE	Optimal Estimation
OECD	Organization for Economic Co-operation and Development
OLS	Ordinary Least Squares
OMI	Ozone Monitoring Instrument
O_2	oxygen
O_2-O_2	collisions between two oxygen molecules
O_3	ozone
P	population size
PANs	peroxyacetyl nitrates
PCA	Principal Component Analysis
ppb	parts per billion
PPP GDP	Gross Domestic Product based on Purchasing Power Parity
PRISMA	Preferred Reporting Items for Systematic Reviews and Meta-Analyses
R	the Euclidean distance from each monitoring station to the city center, or the Euclidean distance from the centroid of each pixel of tropospheric NO_2 layer to the city center
RMS	Root Mean Square
RMSC	Root Mean Square Correlation
R^2	coefficient of determination
SCIAMACHY	Scanning Imaging Absorption Spectrometer for atmospheric chartography
SE	Standard Error

SNR	Signal over Noise Ratio
SO_x	sulfur oxides
STIRPAT	STochastic Impacts by Regression on Population, Affluence, and Technology
TROPOMI	TROPOspheric Monitoring Instrument
UHI	Urban Heat Island
VOCs	Volatile Organic Compounds
WHO	World Health Organization
ΔT	UHI intensity

1 Introduction

We are in the process of urbanization that not only harvests huge industrial, technological, and economic achievements, but also reshapes the environment and climate (McPhearson et al. 2021). About 55% of the world's population now lives in urban areas (UN 2013). Meanwhile, urban planners design cities and determine the location of amenities and services such as transportation hubs, hospitals, schools, and other public facilities. Practitioners in the transportation industry work to efficiently connect major residential areas and amenities through highways, mass transit systems, and bike lanes. Socioeconomic researchers investigate how land prices change for housing, factories, and businesses within cities. This can be explained that the population distribution within a city affects the spatial layout of various facilities and infrastructure in the city. The total population of a city affects the urban planning workload, as well as the total capacity of transportation, commercial, and residential facilities. Considering the facts that in most cases cities are considered as "monocentric" models (Alonso 1964) and the characteristics of land use and population density in the city are arranged radially (Lemoy and Caruso 2018), we speculate that the environmental problems caused by impervious surfaces and human activities are also radially distributed within the city. Therefore, this thesis attempts to investigate cities using two key indicators: population size and the Euclidean distance to the city center (i.e. **centrality**).

Some people think that as cities grow in size and population, air quality is increasingly affected. The resulting air pollutants can adversely affect human health, leading to a range of respiratory and cardiovascular diseases. Air pollutants from outdoor and household sources cause 7 million premature deaths each year (WHO 2023). One of the reasons for this worrying phenomenon is the transition from natural soils to impervious surfaces during urban development, which is a prerequisite for building urban infrastructure and amenities. Impervious surfaces cause **Urban Heat Island (UHI)**, which makes cities warmer than countryside and contributes to urban heat waves. Therefore, UHI can be considered as a direct environmental problem caused by built-up areas. As residential areas expand, so does the city's transportation system. Vehicles on highways emit large amounts of harmful gases, including **nitrogen dioxide (NO_2)**. Both UHI and NO_2 adversely affect the health of urban populations (EEA 2016; Robine et al. 2008). Thus,

this thesis chooses UHI and NO_2 as research objects to understand how environmental problems vary with urban population and centrality.

The rest of this introduction is arranged as follows: Section 1.1 introduces UHI and NO_2 briefly and indicates why this thesis focuses on NO_2 when performing empirical analysis. Section 1.2 indicates how to quantify the impact of population size and centrality in urban studies. Section 1.3 illustrates why we need to relate UHI or NO_2 to population size, and why we need to investigate the relationship of NO_2 with centrality. Section 1.4 provides a summary of objectives and outline.

1.1 Introduction to UHI and NO_2

1.1.1 A quick overview of UHI and NO_2

An UHI is defined as an urbanized area that are much warmer than its surrounding rural areas (U.S. EPA 2023). Measuring the temperature difference between urban and rural areas is a way to demonstrate UHI intensity (ΔT) (Howard 1833). In this thesis, we use Δ**T** and **UHI intensity** interchangeably. UHI is caused by a combination of contributors such as urbanization, building density, land use, transportation and climate (Vujovic et al. 2021). For example, large areas of impervious surfaces in cities not only significantly reduce urban biodiversity (Yan et al. 2019), but also are good receivers of solar energy (John et al. 2013; Ndiaye et al. 2018). During the day, impervious surfaces are also far less efficient at evaporating water than grass and soil (Li and Zhang 2021). Building density is also a factor in UHI as poorly designed building density reduces airflow between buildings and makes the building environment hostile to heat dissipation (Tian et al. 2021). Transport also plays a role in the generation of UHI as a chemical reaction of nitrogen (N_2) and oxygen (O_2) in the combustion chamber produces high temperatures (Bose and Maji 2009). UHI is quite noticeable at night and in weak winds (Tan et al. 2010). Studies show that UHI is negatively correlated with humidity, rainfall, and the amount of cloud cover (Brandsma and Wolters 2012; Hu et al. 2019b; Yang et al. 2019).

Every day, millions of cars are driving on the roads, producing N_2, O_2, carbon dioxide (CO_2), water (H_2O), nitrogen oxides (NO_x), sulfur oxides (SO_x), carbon monoxide (CO), hydrocarbons (HC), and dust, etc (Seddiek and Elgohary 2014). Table 1.1 lists the main elements of the exhaust gas and their percentages.

Table 1.1: Typical components and percentages of exhaust gas (Seddiek and Elgohary 2014)

Component	N_2	O_2	CO_2	H_2O	NO_x	SO_x	CO	HC	Dust
%	77.50	13.75	6.25	0.025	0.212	0.17	0.005	0.005	0.0075

We can see from Table 1.1 that not all of these components are toxic: N_2 is non-toxic and inert; O_2 is vital to aerobic organisms, and O_2 toxicity rarely occurs in daily life (Tsan 2006); CO_2 and H_2O are non-toxic; NO_x is a generic expression of two kinds of toxic gas – nitric oxide (NO) and NO_2 (Tschoeke et al. 2010; WHO 1977); SO_x and CO are poisonous; HC is harmful too (Tormoehlen et al. 2014); dust can be irritating and cause health problems (Hilgers and Achenbach 2021).

In this thesis, we choose NO_2 as the only gaseous research object. This is not only because NO_x has the highest percentage compared to other poisonous pollutants in Table 1.1, but also because NO_2 is one of the air pollutants in the European Union (EU) and the World Health Organization (WHO) air quality standards (EU 2008; WHO 2021). In fact, NO_2 is sufficient to replace NO_x for monitoring air quality, since NO_2 is the most common form of NO_x in the atmosphere (U.S. EPA 1999). We therefore consider the quantitative analysis of NO_2 to be an intuitive and fruitful contribution to the sustainable development of cities in Europe and around the world.

1.1.2 Details about UHI

Problems caused by UHI

Although UHI promotes vegetation growth (Kabano et al. 2021), it has a range of negative effects on the environment and humans. First, UHI leads to higher energy and water demands in the cooling process, which increases greenhouse gas emissions and water use (Aboelata and Sodoudi 2020; Guhathakurta and Gober 2010). To make matters worse, UHI interacts with air pollutants. Heated near-surface air and **primary vehicular emissions** (i.e. pollutants emitted directly into the air) create conditions for **secondary air pollutants** (i.e. pollutants obtained from chemical reactions) such as ozone (O_3) (Singh et al. 2020). The turbulence caused by UHI then transports these pollutants further (Sarrat et al. 2006). UHI exacerbates overheating in cities during heat waves (World Bank 2020), and heat waves tend to drag down the cardiovascular system (Havenith 2005). UHI also harms the well-being of urban dwellers by reducing labor productivity and increasing the probability of injury (UNEP 2004). More than 70,000 people died

in Europe during the once-in-500-year (Meteorological Office 2023) summer heat wave of 2003 (Robine et al. 2008).

Ways to mitigate UHI

There are many ways to mitigate the dangerous effects of UHI. One effective way is to increase the area of urban green space and vegetation (Shishegar 2014). Green spaces provide shade and evaporate water, thereby reducing air temperatures. They are also an important tool for fighting climate change and mitigating heat waves (Gilabert et al. 2021; Shazia et al. 2019). Improving roofs and pavements in the built environment can also mitigate UHI. Roofs and pavements made of reflective materials reflect sunlight and reduce heat gain (Cheela et al. 2021; Roman et al. 2016). With the help of **cool roof** (i.e. roofs made of materials that do not heat up easily) and green roof, roof temperatures can be reduced by 25 °C and 20 °C respectively (Costanzo et al. 2016). Policy makers and stakeholders in urban planning can develop policies that favor public transport, cycling, and walking.

Ways to measure UHI

There are many ways to measure UHI such as car traverse, monitoring stations, remote sensing, and climate models. Car traverse is a common method of measuring air temperature by placing the device (Figure 1.1) on top of the car. In car traverse, the thermal probe is wrapped inside a long cylinder made of radiation-proof material to protect it from the sun's rays. Placing this device on the roof of a car is also a good way to avoid engine heat waves (Sahashi 1983). When performing car traverse, the study area should include various land use types such as built-up and rural areas, and the driving route chosen should pass through these different land cover areas in order to measure the air temperature in different environments (Oke 1973; Oke and Maxwell 1975; Sakakibara and Matsui 2005; Torok et al. 2001). The driving speed should be as constant as possible (e.g. 50 km/h), and temperature data is obtained at the distance along the driving route (e.g. every 1.5 km) (Roth and Chow 2012). Although researchers plan driving routes out of research interest and attempt to plan routes covering the pilot area, the data quality is affected by factors such as driving speed and traffic conditions (Clay et al. 2016). Another disadvantage is that a vehicle is required for each car traverse.

Figure 1.1: Device for car traverse (Sakakibara and Matsui 2005)

Monitoring stations measure temperature from a fixed location. Collecting data through the monitoring station is relatively simple and convenient compared to car traverse. However, fixed monitoring stations cannot guarantee coverage of the entire study area (Tian et al. 2021). Remote sensing uses satellites to measure temperatures. Satellites commonly used to measure land surface UHI intensity include Moderate Resolution Imaging Spectroradiometer (MODIS), ASTER, and Landsat (Qiao et al. 2013; Shirani-bidabadi et al. 2019). Satellites routinely measure UHI intensity (Tian et al. 2021) over large geographical areas compared to car traverse and monitoring stations (ibid.), but weather can affect the quality of satellite imagery (Aflaki et al. 2017; Dwivedi and Khire 2018; Wang et al. 2016). Climate model uses existing weather data to predict temperature in urban areas (Chang et al. 2016). Widely used climate models include Numerical Weather Prediction (NWP), ENVI-met, and Computational Fluid Dynamics (CFD) models (Lu et al. 2017; Wong et al. 2010a). One advantage of climate models is that they can reproduce or predict mesoscale and microscale meteorological scenarios using a range of parameters.

Ways to define cities when measuring UHI intensity

For studies using car traverse, visual recognition is the main way to define urban and rural areas (Oke 1973; Oke and Maxwell 1975; Sakakibara and Matsui 2005; Torok et al. 2001). The

measurement of UHI intensity by a monitoring station also mainly relies on visually identifying the background of the station, if there is no official guidance document to clarify the background of the station (Hardin et al. 2018). There are many ways to define cities when measuring UHI intensity by climate models or satellites. For example, Ganeshan et al. (2013) defined that only urban polygons with an impervious surface area greater than 20% can be defined as cities, and rural areas are ring-shaped regions 30 km to 60 km away from cities. Some remote sensing studies such as Zhou et al. (2018) also used the percentage of impervious surface to define cities. Researchers can also distinguish land use types by visual identification (Lee 1993), land cover maps (Du et al. 2016; Zhao et al. 2014), developing city clustering algorithms (Schwarz 2012), or Gaussian surfaces (Tran et al. 2006). We can find that because the visual identification of the city mainly depends on personal judgment, car traverse and monitoring stations lack a clear, quantified definition of city.

1.1.3 Details about NO_2

Multiple sources of NO_2 emissions

Transport is the main source of NO_2 in Europe, and NO_2 concentrations in transport-related places are well above the EU limit (EEA 2016). Diesel vehicles contribute more NO_2 than gasoline cars (Anttila et al. 2011). This is because for gasoline vehicles, only 5% of NO_x is emitted as NO_2, while for diesel vehicles without modern exhaust treatment, 10% to 12% of NO_x is emitted as NO_2 (Grice et al. 2009). NO_2 can be as high as 70% in NO_x emitted by diesel vehicles equipped with oxidation catalysts (ibid.). Other sources and processes that require combustion and heating, such as ships (Vinken et al. 2014), airplanes (Herndon et al. 2004), residential heating (Dedele and Miskinyte 2016), industrial processes (Goldberg et al. 2019) also generate NO_2. Combustion of fossil fuels, including coal, oil and natural gas, is the largest contributor, producing about 46% of NO_x (i.e. 21 teragrams of nitrogen per year / 21 TgN yr^{-1}) (Jacob 1999). Burning biomass for planting and building space emits about 26% of NO_x (i.e. 12 Tg N yr^{-1}) (ibid.). The soil itself emits 13% of NO_x (i.e. 6 Tg N yr^{-1}) (ibid.). The remaining 15% of NO_x in the troposphere comes from sources such as lightning (ibid.) and forest fires (Maurya et al. 2018).

Problems caused by NO_2

NO_2 can cause serious problems for humans and nature. Coughing, wheezing, shortness of breath, and increased susceptibility to respiratory infections are associated with NO_2 (Kelly and Fussell 2011). NO_2 is also linked to lifelong asthma (Gauderman et al. 2005) and other declines in lung function (Schindler et al. 1998), leading to long-term breathlessness and even cancer (Hamra et al. 2015). Exposure to NO_2 also leads to higher rates of cardiovascular disease

such as heart attack (Young and Kindzierski 2019) and stroke (Andersen et al. 2012). This is partly because NO_2 can cause blood clots and damage blood vessels (Reutov et al. 2012). NO_2 may harm pregnant women and premature babies by causing affected placental development (Cahuana-Bartra et al. 2022) and low birth weight (Shmool et al. 2015). NO_2 is one of the main precursors of acid rain (Irwin and Williams 1988), which destroys vegetation, water, and the health of residents and animals. NO_2 also contributes to harmful photochemical smog in cities.

Ways to mitigate NO_2

There are various ways to reduce NO_2 pollution. In fact, some methods for mitigating UHI are also suitable for reducing NO_2. For example, since car emissions are a major source of NO_2, reducing private car use and encouraging public transportation, cycling, and walking can reduce NO_2 levels and improve air quality. For factories and power plants, the use of more efficient technologies and practices, such as energy-efficient light bulbs (Parker and Drake 2018), and more efficient heating and cooling systems can reduce NO_2 emissions (Krieve and Mason 1961). Building large green spaces in cities can reduce NO_2 (Sheridan et al. 2019). Finally, stakeholders can develop far-sighted policies, such as progressively increasing air quality standards and designing walkable neighborhoods.

Ways to obtain NO_2 concentration values

NO_2 concentration values can be obtained from the following sources: emissions inventories, monitoring stations, remote sensing, climate models (i.e. modeled remote sensing data), and samplers. Monitoring stations, remote sensing, and climate models are also applicable when measuring UHI intensity. Satellites used to monitor NO_2 include Ozone Monitoring Instrument (OMI) (NASA 2023a), Scanning Imaging Absorption Spectrometer for atmospheric chartography (SCIAMACHY) (SCIAVALIG 2023) and Sentinel-5P (ESA 2023b). Modeled NO_2 can be retrieved from climate models such as GEOS-Chem (Harvard University 2023) and ECMWF Atmospheric Composition Reanalysis 4 (EAC4) (ECMWF 2023). Samplers detect NO_2 using **solvent extraction** (i.e. to convert NO_2 to nitrate or nitrite ion) (Chaube et al. 1984). Nevertheless, unwanted pyrolysis products during dissolution and some substances that evaporate with the solvent can affect the measurement results when using a sampler (Houck and Siegel 2015). An **emission inventory** is a set of data used to estimate the amount of pollutants emitted into the atmosphere from various sources such as industry, residential, and transportation activities (Li et al. 2017c). The steps of generating an emission inventory are summarized in Figure 1.2.

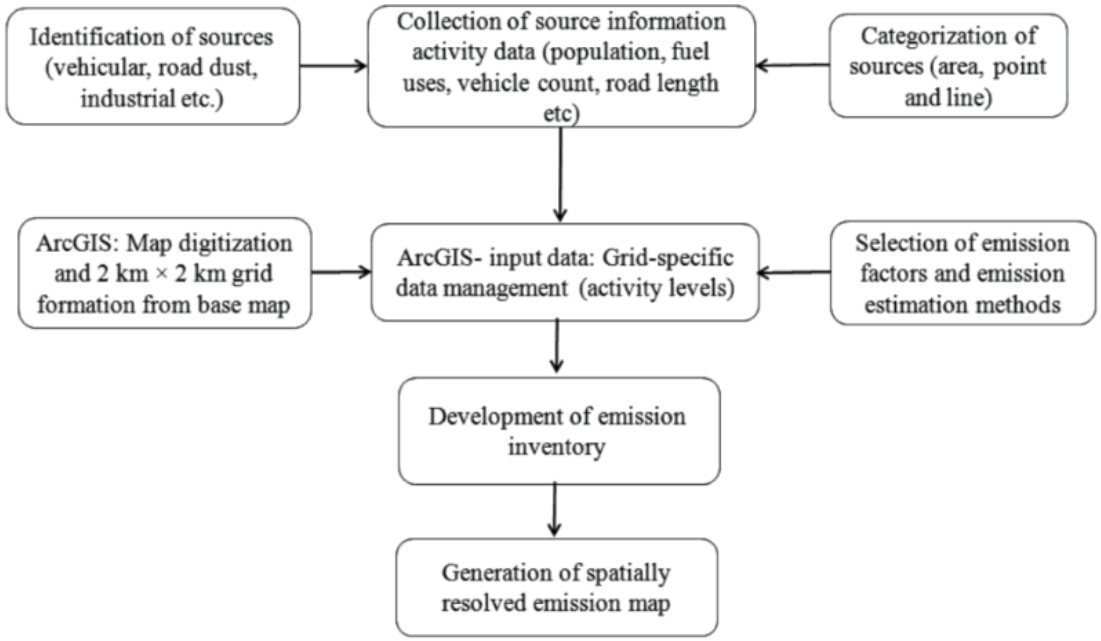

Figure 1.2: Steps of developing an emission inventory (Behera et al. 2011)

First, researchers identify the source of air pollutant and retrieve relevant information about the source, including location, population, and local temperature. Data is digitized in a database. Second, researchers select emission factors and appropriate emission estimation methods. An **emission factor** is a representative value indicating how much emissions a certain amount of fuel will produce (U.S. EPA 2022a). A base map (e.g. with a resolution of 2 km x 2 km) is prepared for further use in this step. The final emission inventory will show the spatial and temporal distribution of air pollutant in the study area, and will also show which emission sources these pollutants are composed of and the percentage of each emission source. Emission inventories allow detection of a wide range of pollutants and continuous monitoring of a single emission source (Zhao et al. 2015). However, emissions inventories may not reflect localized, highly variable pollutant (AQEG 2013).

Chemical reaction of NO_2 in the troposphere

Nearly 95% of NO_x is emitted in the form of NO originally (WHO 2005). The combustion of fossil fuels generates NO through the Zeldovich mechanism (Equations 1.1 to 1.3).

$$N_2 + O \longrightarrow NO + N \tag{1.1}$$

$$N + O_2 \longrightarrow NO + O \tag{1.2}$$

$$N + OH \longrightarrow NO + H \tag{1.3}$$

NO is then released into the troposphere and oxidized to NO_2 (Equations 1.4 and 1.5).

$$2NO + O_2 \longrightarrow 2NO_2 \tag{1.4}$$

$$NO + O_3 \rightleftharpoons NO_2 + O_2 + hv \tag{1.5}$$

Equation 1.5 shows NO reacts with O_3 to release NO_2, O_2 and emit light (i.e. the theory of chemiluminescence, see Appendix E), and under the sunlight, NO_2 and O_2 also generate O_3 and NO. Tropospheric O_3 is equally harmful, although stratospheric O_3, which we cannot breathe, prevents us from being exposed to excessive ultraviolet energy (U.S. EPA 1999). Equation 1.5 is also a part of the chemical reactions of photochemical smog. The remaining chemical reactions of photochemical smog are listed in Equations 1.6 and 1.7,

$$NO_2 + HC \longrightarrow PANs + others \tag{1.6}$$

$$NO + RO_x \longrightarrow NO_2 + others \tag{1.7}$$

where RO_x means oxygenated organic and inorganic compounds.

Volatile Organic Compounds (VOCs) is the main source of HC. Toxic VOCs widely exist in both nature (e.g. forest fires) and anthropogenic activities (e.g. combusting fossil fuels and mining) (Montero-Montoya et al. 2018). The peroxyacetyl nitrates (PANs) in Equation 1.6 belong to secondary air pollutants with a toxicity similar to that of NO_2 (Vyskocil et al. 1998). High concentrations of PANs pose a threat to both humans (Heuss and Glasson 1968) and plants (Taylor 1969; Temple and Taylor 1983). Equations 1.6 and 1.7 show areas with higher concentrations of VOCs also tend to have more tropospheric O_3, this is because VOCs is involved in the reactions with NO and NO_2, resulting in less tropospheric O_3 being consumed in Equation 1.5 (South Australia EPA 2004). The lifetime of NO_x in the lower troposphere is within a day (Geffen et al. 2019). Many studies show that NO_2 remains closely to its source, leading to distinct spatial distribution (Hoek et al. 2008; Liang et al. 1998; Madsen et al. 2011; Marshall et al. 2008; Novotny et al. 2011).

In the lower troposphere, NO_x exists 3.6 h $\pm$ 0.8 h in Switzerland and the Alpine (summer) (Schaub et al. 2007), 4 h in Riyadh (Beirle et al. 2011), 5.9 h in central-eastern China (summer) (Shah et al. 2020), 6 h in Germany (summer) (Beirle et al. 2003), 7.6 h in southeast U.S. (summer) (Lamsal et al. 2010), 8 h in Moscow (Beirle et al. 2011), 13.1 h $\pm$ 3.8 h in Switzerland and the Alpine (winter) (Schaub et al. 2007), 17.8 h in southeast US (winter) (Lamsal et al. 2010), 21 h in

central-eastern China (winter) (Shah et al. 2020), and 18 h to 24 h in Germany (winter) (Beirle et al. 2003).

It is difficult to draw firm conclusions about how long NO_2 stays in the lower troposphere. Factors such as seasons (Bechle et al. 2013), latitude (Beirle et al. 2011), wind speed (Valin et al. 2013), and wind direction (Beirle et al. 2011; U.S. EPA 1999) influence the existence of NO_2. For example, Lamsal et al. (2010) pointed out that the NO_2 detected by the satellite can largely be explained by Air-Mass Factor (AMF). AMF is a measure of the relative length of the average optical path of a photon interacting with a specific absorber in the atmosphere at a specific wavelength with respect to the vertical path (Lorente et al. 2017). One key factor of deciding AMF is zenith angle (i.e. the angle between the sun's rays and the vertical direction). In summer or at low latitudes, the zenith angle is usually small, which means that the path for solar radiation to reach the ground is relatively short. In this case, AMF is smaller and the air pollutant is more easily detected (Honsberg and Bowden 2023). Larger AMF values are induced in winter or at high latitudes. Hong et al. (2017) found that land use type and aerosol are also contributors for AMF. Higher AMF is observed for snowy ground and lower AMF is found for deciduous forest surface (ibid.). In some specific combinations of aerosol parameters, AMF may decrease by up to 240% (ibid.). It has been well known that where the wind speed is low, the NO_2 concentration is high (Donnelly et al. 2011). Grundstrom et al. (2015) found in Gothenburg (Sweden) the concentration of NO_2 decreases with the increase of wind speed, and this relationship can be described by a exponential function. Wind speed and wind direction together can affect NO_2 results (Yu et al. 2004). For example, Carslaw et al. (2006) detected NO_2 from the aircraft at a distance of 2 km from the airport. However, the importance of wind is also affected by other factors (Donnelly et al. 2011). For example, in Glashaboy (Ireland) wind direction has little effect on NO_2, which is due to the fact that there are major traffic roads within less than 1 km of the monitoring point (ibid.). Therefore, the residence time of NO_2 in the troposphere is complicated and affected by many factors. If we want to know the stagnation time of NO_2 in a certain region, we need to consider a series of meteorological factors and emission sources around the region.

1.1.4 Interaction between UHI and NO_2 and a focus on NO_2

The interaction between UHI and NO_2 is complicated, and the interaction can exacerbate the negative effects of these two factors. For example, high temperatures in urban areas produce more NO_2 through a chemical reaction called **thermal decomposition**. Clark (2020) illustrated thermal decomposition of group 2 (i.e. beryllium, magnesium, calcium, strontium and barium) nitrates by giving Equation 1.8,

$$2X(NO_3)_2 \longrightarrow 2XO + 4NO_2 + O_2 \tag{1.8}$$

where X means any of the group 2 nitrates and XO means metal oxide. We can see that at high temperature, group 2 nitrates decompose into meta oxide, and release NO_2. Thus, thermal decomposition leads to an increase in NO_2 under UHI.

The existence of NO_2 also helps to intensify the UHI effect. NO_2 absorbs radiation in visible and ultraviolet bands (Constantin et al. 2015). This radiation-absorbing property of NO_2 is particularly active during thunderstorms (Solomon et al. 1999).

UHI can be regarded as an abnormal temperature phenomenon, while NO_2 is a poisonous gas. At first glance, UHI and NO_2 are different types of environmental problems, but there are many interactions between UHI and NO_2. The existence of UHI exaggerates the pollution of NO_2, and NO_2 is beneficial to the formation of UHI. We also conclude that there are many common factors leading to UHI and NO_2, such as the use of private cars, burning of fossil fuels, heating and cooling, and human activities. We also show that the same approach can be used to reduce UHI and NO_2 such as encouraging public transport, cycling, walking. So we think that if we figure out how urban population and urbanization affect one of these two pollution phenomena, figure out how it is distributed in cities, and improve based on these conclusions, then the other pollution problem will also be alleviated. In addition, focusing on one pollution phenomenon can save investigation time, increase research efficiency, and draw conclusions sooner.

In this thesis we investigate UHI and NO_2 in meta-analysis, but NO_2 is the only environmental problem in the empirical analysis. We focus on NO_2 for a couple of reasons. First, NO_2 is poisonous, and both the EU and WHO have made regulations on the content of NO_2 in the air (EU 2008; WHO 2021). These specific targets can help researchers and stakeholders quantify results and improve air quality over time. Urban residents can also use the quantified NO_2 pollution level as their own reference to improve environmental awareness. Second, NO_2 itself is a local air pollutant (Colvile et al. 2001) as its level varies evidently due to local conditions (Karr et al. 2009; Restrepo 2021). This feature of NO_2 can make it easier for researchers to monitor and improve pollution levels in local areas, effectively improving overall air quality. Finally, due to time constraints, we do not have time to conduct empirical experiments on UHI and NO_2 at the same time, so we choose one of them for in-depth analysis.

1.2 Spatial distribution of population within and across cities

1.2.1 Rank-size rule and the environmental Kuznets curve

A city is defined as a small area with a large number of people, or an urban area having a higher population density than its surrounding areas (O'Sullivan 2012). The development of a city lies in the fact that, there is an efficient transport system linking urban and rural area that enables urban dwellers to provide goods or services in exchange for agricultural products produced by the people outside the city (ibid.). Unlike animal populations that migrate and forage, cities provide human beings with a fixed living place, where urban residents do not need to participate in food production, and residents outside cities provide urban residents with the surplus agricultural products they produce (Bartlett 1998). In other words, cities are the outcome of the evolution of productivity, and only *people* create productivity. Population metrics are therefore more important than others when defining a city. Population metrics are more of perquisites, while other factors are the by-products of productivity to judge how urbanized that area is. If that place is not urbanized enough, then it can't be called a city.

The patterns of the distribution of city sizes around the world can be described by the **rank-size rule**. The rank-size rule says that, *"if the settlements in a country are ranked by population size, the population of a settlement ranked n will be $1/n^{th}$ of the size of the largest settlement (Oxford University Press 2023)"*. If we plot city sizes against ranks then we will get a concave curve; if we plot logarithmic city sizes against logarithmic ranks then we will get a straight line. This straight linear relationship is also known as **Zipf's law** (Gabaix 1999). Rank-size rule and Zipf's law indicate that small cities are more common than large cities. For example, there are only a handful of cities with a population of more than 10 million, but there are thousands of small cities with a population of less than 100 thousand. People may migrate to big cities due to factors such as economic conditions and natural environment (Farhana et al. 2012). However, the relationship between population size and economy is difficult to generalize (Caldwell 1990), as is the relationship between population size and environment (Robinson and Srinivasan 1997). Kelley (1988) summarized the role of population as follows: population has positive and negative impacts on cities, both direct and indirect; the impact of population on the economy will have an impact on the economy no matter whether it is direct or indirect; population can exacerbate problems or cause them to erupt earlier.

Economic factors also affect the relationship between environment and population. As cities develop, the relative cost of production and the exploitation of environmental resources will be beneficial to environmental protection (Robinson and Srinivasan 1997). For example, the **environmental Kuznets curve** (i.e. an inverted U-shaped curve) helps to formulate environmental policy (Yandle et al. 2014) and to predict the optimal size of cities. In the environmental Kuznets

curve, the X-axis can be per capita income and the Y-axis can be environmental degradation. However, Grossman (1993) and Grossman and Krueger (1994) proved that not all environmental problems can be represented by the environmental Kuznets curve and the turning points of the curves are different for different pollutants. Han et al. (2021) pointed out that NO_2 is positively correlated with China's urban economic development, and the turning point of the curve has not yet arrived. But so far we have found no studies on whether European NO_2 emissions fit the environmental Kuznets curve. We also haven't found any studies of the environmental Kuznets curve for the UHI effect.

The relationship between transportation and economy is also very complicated, and there is even interference between different transportation modes. For example, public rapid transit can increase wages and city size, but only in combination with policies that discourage the use of private cars and stimulate the use of public transport (Greenaway-McGrevy and Jones 2022). Examples from the Netherlands (Broersma and Dijk 2007) and the U.S. (Safirova 2002) show that traffic congestion can inhibit economic growth unless teleworking is adopted, a way of generating economic growth without posing a threat to air quality (ibid.). Technological progress and the use of green transportation can indeed improve air quality, although urban expansion will bring air pollution (Lu et al. 2021).

1.2.2 An example of scaling

An integrated urban science is emerging. In this urban science, the growth characteristics of cities can be explained by the allometric theory of biology (Batty 2013; Ramaswami et al. 2018). The relationship between population size and air pollution can be quantified by **scaling, which is a power-law relationship**. Mathematically, it can be expressed by Equation 1.9,

$$Q = \kappa P^{\lambda} \tag{1.9}$$

where Q means air pollution (e.g. CO_2), P means population, and κ and λ are coefficients. If we take the logarithm of both sides of Equation 1.9 we get a straight line (e.g. Figure 1.3).

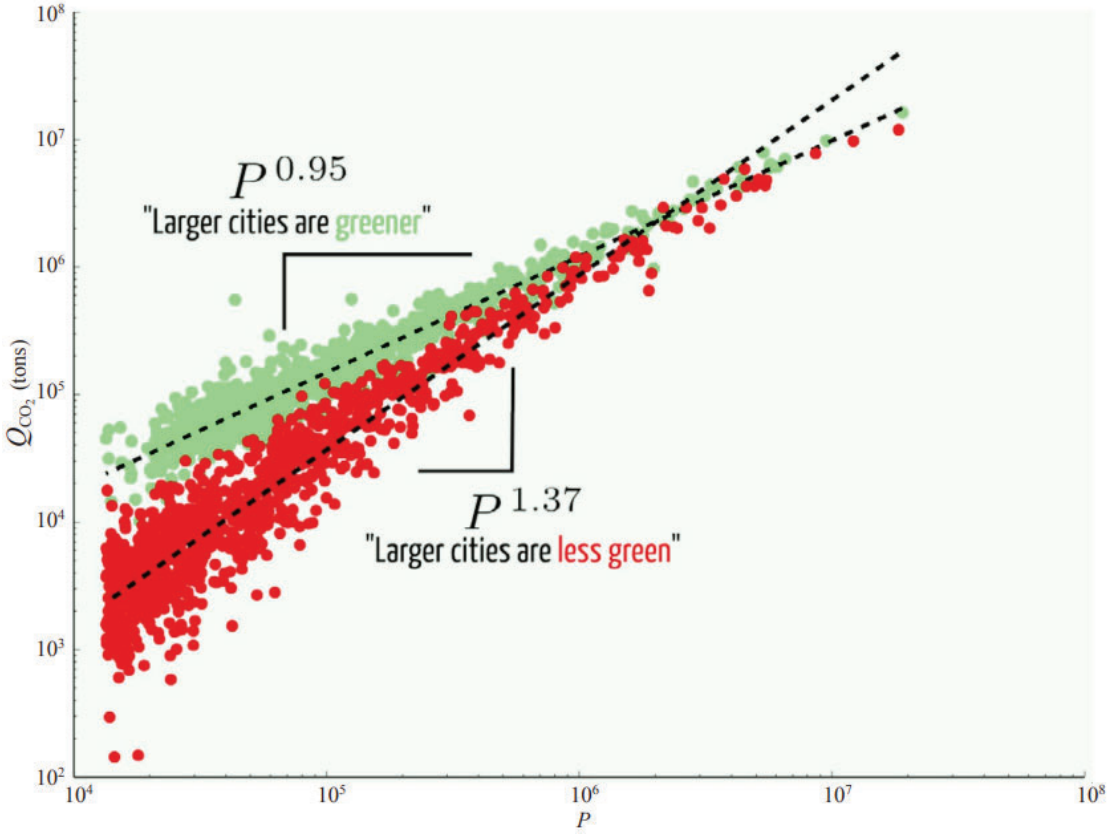

Figure 1.3: Scaling of transport-related CO_2 emissions with the population size of the U.S. cities from the same dataset but at different aggregation levels (Louf and Barthelemy 2014b)

Quantitative changes in environmental and socioeconomic features associated with city size (i.e. in terms of population size) can be also explained by power laws (Bettencourt et al. 2007; Bornstein and Bornstein 1976; Louf and Barthelemy 2014b; Rybski et al. 2017). We present more details of the literature in Section 4.1.2.

1.2.3 Effects of urban residents' choices on air quality

In the classic economic models, Alonso (1964) proposed the **bid-rent curve**, which shows the relationship between land prices and the distance to the city center. Alonso (ibid.) showed retailers and office workers compete for the most profitable or convenient land in the city center, and population density decreases when moving away from the city center. Schindler and Caruso (2014) and Schindler et al. (2017) also used centrality as a variable for the relationship between residents' choice of settlement and air pollution exposure. Schindler et al. (2017) showed that

moving away from the city center can decrease the exposure of traffic-related air pollution, but when households intend to reduce their own exposure, the density profile becomes flatter and total emissions rise.

However, centrality is not the only factor for determining the living places of urban residents. Built-up area is also important. This can be partly explained by the "street canyons" formed by adjacent buildings and tall buildings, causing the **canyon effect**. The canyon effect brings changes in temperature, light, wind direction and air quality caused by tall buildings (Karimimoshaver et al. 2021). The canyon effect increases air temperature, inhibits heat dissipation, causes winds and increases noise levels (Matthews and Kamp 2017). Theoretical models showed that air quality can be significantly improved by changing the urban structure design of the city, such as increasing the green area in the city center (Schindler and Caruso 2014).

1.2.4 An example of homotheticity

The percentage of built-up area of a city is highly positively correlated with the total air pollution level (e.g. $PM_{2.5}$) of that city (Liu et al. 2018b). For the interior of a city, empirical studies showed that the proportion of built-up areas is largely related to their relative distance to the city center, while population size effect is explained by the largest city in the dataset and a scaling exponent, which can be a manifestation of homotheticity (i.e. homothetic scaling) (Lemoy and Caruso 2018).

Homotheticity is a transformation that preserves the shape of an object or system while scaling its size proportionally (Pamfilos 2021). Lemoy and Caruso (2018) expressed homotheticity by Equations 1.10 and 1.11,

$$r' = \frac{r}{(\frac{N}{N_{London}})^{0.5}} \tag{1.10}$$

$$S_N(r') = \frac{S_N(r)}{(\frac{N}{N_{London}})^{0.5}} \tag{1.11}$$

where r is the Euclidean distance from city center, N_{London} is the population of London (i.e. the largest city in the dataset), N is the population size of a city, r' is the rescaled Euclidean distance from city center, $S_N(r)$ is the proportion of build-up area of a city (population size N) at distance r. $S_N(r')$ is the rescaled proportion of build-up area of a city (population size N) at rescaled distance r', $(\frac{N_{London}}{N})^{0.5}$ is the scaling factor as r' = scaling factor * r and $S_N(r')$ = scaling factor * $S_N(r)$. Lemoy and Caruso (ibid.) found a scaling exponent of 0.5 for both land use shares and population size.

Figure 1.4 is a visual expression of how homotheticity works.

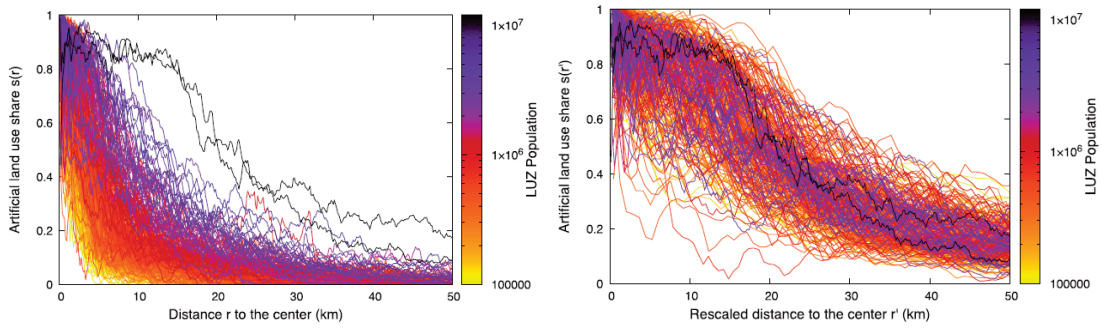

(a) $S_N(r)$ and r (b) $S_N(r')$ and r′

Figure 1.4: Shares of built-up area as functions of the distance to the city center in 300 European cities (Lemoy and Caruso 2018)

We can see stratified lines due to population size in Figure 1.4(a). The lines representing the change of built-up area with distance for large cities tends to be in the upper layer, and the line for the change of built-up area with distance for small cities tends to be in the lower layer. The equations of homothetic scaling (i.e. Equations 1.10 and 1.11) explain the population effect on land use share, so in Figure 1.4(b) the population effect is not evident. The scaling exponent (i.e. 0.5) is tested by two methods: a method called Signal over Noise Ratio (SNR) (Lemoy and Caruso 2018), and a 2-stage linear regression (Lemoy and Caruso 2021). We explain the details in Chapter 5.

Given that facts that the proportion of built-up area and air pollution are highly positively correlated (Liu et al. 2018b), and residents may move out of the city center because of air quality (Schindler et al. 2017), in Chapter 5 we perform a similar analysis on NO_2 levels. We try to find the best exponent(s) to explain the population size effect in the relationship between NO_2 levels and centrality and then test the rationality of our results.

1.2.5 Why need scaling and homotheticity

Both scaling and homotheticity aim to describe urban characteristics with the simplest possible formulas. Scaling uses a power law to express the relationship between urban population and the socioeconomic or environmental characteristics of a city. Homotheticity indicates that a certain feature within a city is largely related to its relative position in the city and population size effect is explained. They all play an important role in urban studies.

Scaling and homotheticity allow cities of different sizes and levels of development to be compared with each other on the same indicators. Their relatively short formulas make analysis easy. Both are also great tools for generalization. Scaling can evaluate the optimal capacity

of urban population (Raan et al. 2016). According to the scaled distance from the city center, homotheticity can find out where the attenuation of a certain phenomenon or indicator is the largest or the smallest (Lemoy and Caruso 2018).

Scaling enables researchers to draw general conclusions about urban processes and phenomena that can be applied to different cities or regions. Using scaling, urban planners can quickly determine the total amount of a certain resource that a city needs (Walker 2011), or how many emissions it will generate (Louf and Barthelemy 2014b). Comparability between cities also helps urban planners draw the best conclusions from different settings.

Homotheticity also allows stakeholders and planners to draw general conclusions applicable to different cities or regions (Kaufmann et al. 2022). Homotheticity focuses on finding the same laws within different cities (Lemoy and Caruso 2018). For example, with the help of homotheticity, urban planners can plan transportation facilities for multiple cities at the same time, and adjust the number of transportation facilities in different regions according to changes in artificial land use, so as to minimize waste of resources. In addition, homotheticity can also be used to obtain the influence of population on a certain phenomenon or indicator. If, after the homothetic scaling, the data representing different cities is still clearly stratified by population size, then stakeholders cannot ignore the impact of population.

1.2.6 Why not study population density and city area

We realize that population density and urban area are also indicators of city size (Gariazzo et al. 2016; Luo et al. 2018). But apart from time constraints, there are other reasons why these two indicators are not studied in this thesis. First, it remains unclear whether there is a significant positive relationship between population density and ΔT. Some studies showed that population density has no significant correlation with ΔT (Debbage and Shepherd 2015; Du et al. 2016; Ward et al. 2016), but there are also many studies showing that population density is significantly positively correlated with ΔT (Elsayed 2012; Steeneveld et al. 2011; Wolters and Brandsma 2012). Interestingly, most of the articles pointing out that there is no significant relationship between population density and ΔT define population density as the total area of the city divided by the total population of the city, while most of the articles pointing out that there is significant positive relationship between population density and ΔT define population density as the area of neighborhood (Steeneveld et al. 2011; Wolters and Brandsma 2012) or city core (Elsayed 2012) divided by the total population of that area. This is because densely populated neighborhoods typically have higher building densities, and dense buildings trap heat (Steeneveld et al. 2011), while the canyon effect becomes less apparent when we define population density as the total city population divided by the total city area. Different definitions of population density also

affect the relationship between NO_2 and population density. When the population density is defined as the total urban population divided by the total urban area, NO_2 has no significant relationship with population density (Bechle et al. 2011; Hosein et al. 1977), and when population density is the population density around monitoring stations, NO_2 is significantly correlated with the population density (Cesaroni et al. 2012; Zhang et al. 2021a). Considering that different definitions of population density are likely to draw opposite conclusions, the empirical analysis of this thesis does not consider population density.

There is usually a positive correlation between the area of a city and its population (Craig and Haskey 1978). However, this relationship is complex and can vary greatly depending on various factors such as natural environment and urban planning. Hong Kong (China) is mountainous and lacks farmland and flat land (Hui 2001). At the end of 1999, Hong Kong had a population of 6,970,000 and an area of only 1,097 km^2 (that is, the population density was 6,360 people/km^2) (ibid.). For comparison, Indianapolis (U.S.), with a similar size (936.5 km^2), had a population of only 887,642 in 2020 (that is, the population density was 948 people/km^2) (US Census Bureau 2020). Because this thesis uses Functional Urban Areas (FUAs) as the definition of cities, and FUAs are defined in terms of employment and economic activity (Section 3.1.1), therefore, the impact of the natural environment on population density is greatly reduced. In fact, after we regress the population size and city area of FUAs, we find that population size and city area are highly positively correlated (Figure 3.2(b)) and the determination of coefficient is 0.73, which means that we are likely to draw similar conclusions if we use city area to replace population size as one of the independent variables. As a result, we don't explore city area in our empirical analysis.

1.3 UHI and NO_2 within and across cities

Though similar positive relations have been found from the majority of current literature which unravels the effects of city size on UHI and NO_2 (Lamsal et al. 2013; Oke 1973), such views need to be consolidated for 3 reasons. First, there are multiple ways of measuring UHI and NO_2. UHI can be expressed either by the land surface ΔT measured by satellites (Lee 1993), or by the near-surface ΔT measured by car traverse (Oke 1973) or monitoring stations (Hardin et al. 2018). Climate models can also model near-surface ΔT difference (Debbage and Shepherd 2015). NO_2 values can be obtained from emission inventories (Sarzynski 2012), monitoring stations (Nguyen and Kim 2006), samplers (Hosein et al. 1977), or satellites (Jiang et al. 2021). Tropospheric NO_2 columns can be modeled to surface NO_2 but the converted values are lower than in-situ surface measurements (Lamsal et al. 2013). Second, we should pay attention to whether the studies use the same metric or specification when comparing. For example, we

have noticed that some population variables are in non-logarithmic form (Tran et al. 2006), some are in natural logarithmic form (Lamsal et al. 2013), and some are in common logarithmic form (Torok et al. 2001). As for the form of specification, we found linear regression (Bechle et al. 2011), Principal Component Analysis (PCA) (Branis and Linhartova 2012), or barely textual description (Nguyen and Kim 2006). Last, most of the studies quantifying the effects of city size on heat stress and air pollution only concern cities in certain countries (Oke 1973), world regions (Lamsal et al. 2013; Oke 1973) or a few cities within the top ranks globally (Bechle et al. 2011). We therefore want to find out whether the relationship between the population size with NO_2 and UHI can be expressed by scaling.

The spatial distribution of NO_2 and UHI within the city is also worthy of study. The city center is the center of commercial activity (Swinney 2011), which provides a large number of jobs and contributes to the national economy (Jeffrey and Enenkel 2020). NO_2 itself is considered as a local air pollutant (Colvile et al. 2001) as its level varies evidently due to local conditions (Karr et al. 2009; Restrepo 2021). The street canyons in the city center of Ljubljana (Slovenia) accumulate low concentrations of NO_2 from low traffic volumes to form a high-polluted area (Vintar Mally and Ogrin 2015). The impact of street geometry in the city center is also observed in Cambridge (UK) where the annual mean NO_2 amounts in the street canyons are higher than the one measured in the radial roads outside the central area (Kirby et al. 1998). The NO_2 gap between the central and suburban roads in Lancaster (UK) is obvious regardless of similar traffic volumes (Nicholas Hewitt 1991). The canyon effect can make the temperature of the city center too high, affecting the health of residents (Matthews and Kamp 2017). Knowing the temperature variation within a city is an effective indicator to monitor the progress of urbanization, as changes in land use types can lead to changes in the spatial temporal distribution of UHI (Li et al. 2012). Residents move away from urban centers because of traffic-related air pollution (Schindler et al. 2017). Due to limited time and other factors (Section 1.1.4), in this thesis we only perform empirical analysis on NO_2. We therefore want to find out how NO_2 changes with the distance to the city center.

In addition, Lemoy and Caruso (2018) used homothetic scaling to show that the proportion of artificial land use area within cities of different sizes changes with distance independently of the urban population and is quite similar. We therefore want to test to what extent the variation of NO_2 with centrality is influenced by the population.

1.4 Objectives

We therefore make hypotheses and propose questions:

1. If the relationship between CO_2 or other socioeconomic indicators and population can be explained by scaling, then the relationship between UHI or NO_2 and population size also follows a power law.
2. If theoretical models suggest that traffic pollution exposure is negatively correlated with centrality, then NO_2 emissions within cities are also negatively correlated with centrality.
3. Whether or not the variation of NO_2 with centrality is influenced by the population.

To prove the hypothesis and answer the questions above, the principle targets of this thesis are

1. summarize published works on revealing the relationship between UHI and city size and quantify the influence of city size on UHI by a meta-analysis,
2. summarize published works on revealing the relationship between NO_2 and city size and quantify the influence of city size on NO_2 levels by a meta-analysis, and test this relationship by measured values from monitoring stations and satellite imagery,
3. quantify the influence of centrality on NO_2 levels by measured values from monitoring stations and satellite imagery, compare the importance of city size and centrality, and propose models showing how surface and tropospheric NO_2 changes according to city size and centrality, and
4. test whether city size differentially affects the relationship between NO_2 and centrality.

These targets are accomplished by 3 chapters.

In Chapter 2, we summarize qualitative and quantitative relations between UHI and NO_2 with city size based on published works. This task is finished by a qualitative synthesis followed by a meta-analysis. The qualitative synthesis utilizes keywords and Boolean operators to select published works from multiple sources. Records from these sources are filtered according to their titles, abstracts, and full-text contents. The filtered records are then subjected to qualitative analysis, i.e. finding their commonalities and differences through textual descriptions only. Quantitative analysis is however indispensable in the subsequent meta-analysis: From the filtered literature, we select quantified environmental and demographic values, group them, and perform ANalysis Of VAriance (ANOVA) on each group. The groups of variables showing statistical significance are fitted by linear regression. Then the linear regression quantifies the effects of population size on UHI and NO_2.

Therefore the objectives of Chapter 2 are

1. perform a qualitative synthesis to collect and filter a corpus of research articles of UHI and NO_2 pollution with population size, and

2. perform a meta-analysis to derive the effects of city size on UHI and NO_2 pollution, based on the results of the qualitative synthesis.

In Chapter 4, we test the effect of population size on NO_2 which is found in Chapter 2. We use 2 kinds of data: NO_2 surface concentrations from air quality monitoring stations and tropospheric NO_2 columns from satellite imagery. The geographical extent and population size of cities in Europe are determined by FUAs. Centrality is defined as the Euclidean distance from a given place to the city center. We further analyze the specifications that showed statistical significance and give the relative importance of city size and centrality.

Therefore the objectives of Chapter 4 are

1. derive the effects of city size on land surface and tropospheric NO_2,
2. quantify the influence of centrality on land surface and tropospheric NO_2, and
3. compare the importance of city size and centrality in determining NO_2.

The data used in Chapter 5 are largely the same as in Chapter 4. We first use a method similar to Lemoy and Caruso (2018) to find out whether the relationship between centrality and NO_2 concentration is independent of population size. Then we use a method similar to Lemoy and Caruso (2021) to test whether our method in the previous step is reliable.

Therefore the objectives of Chapter 5 are

1. find out to what extent city size affects the relationship between NO_2 and centrality.

1.5 Thesis outline

Figure 1.5 lists the layout of this thesis. This thesis is divided into 6 chapters. Chapter 2 is a literature review consisting of qualitative synthesis and meta-analysis. The qualitative synthesis focuses on qualitatively summarizing the effects of city size on UHI and NO_2 in published papers. The meta-analysis then picks out qualified values from the corpus and brings them into regression. In this way the effect of city size is quantified and estimated. Chapter 3 introduces the data and the geoprocessing used in Chapters 4 and 5. Thanks to the wide-spread monitoring stations across European cities and the satellite imagery covering Europe, the effect of city size on NO_2 is verified by measured data in Chapter 4. The centrality effect on NO_2 is also analyzed. Chapter 5 reveals to what extent city size influences the relationship between centrality and NO_2. Finally Chapter 6 provides conclusions.

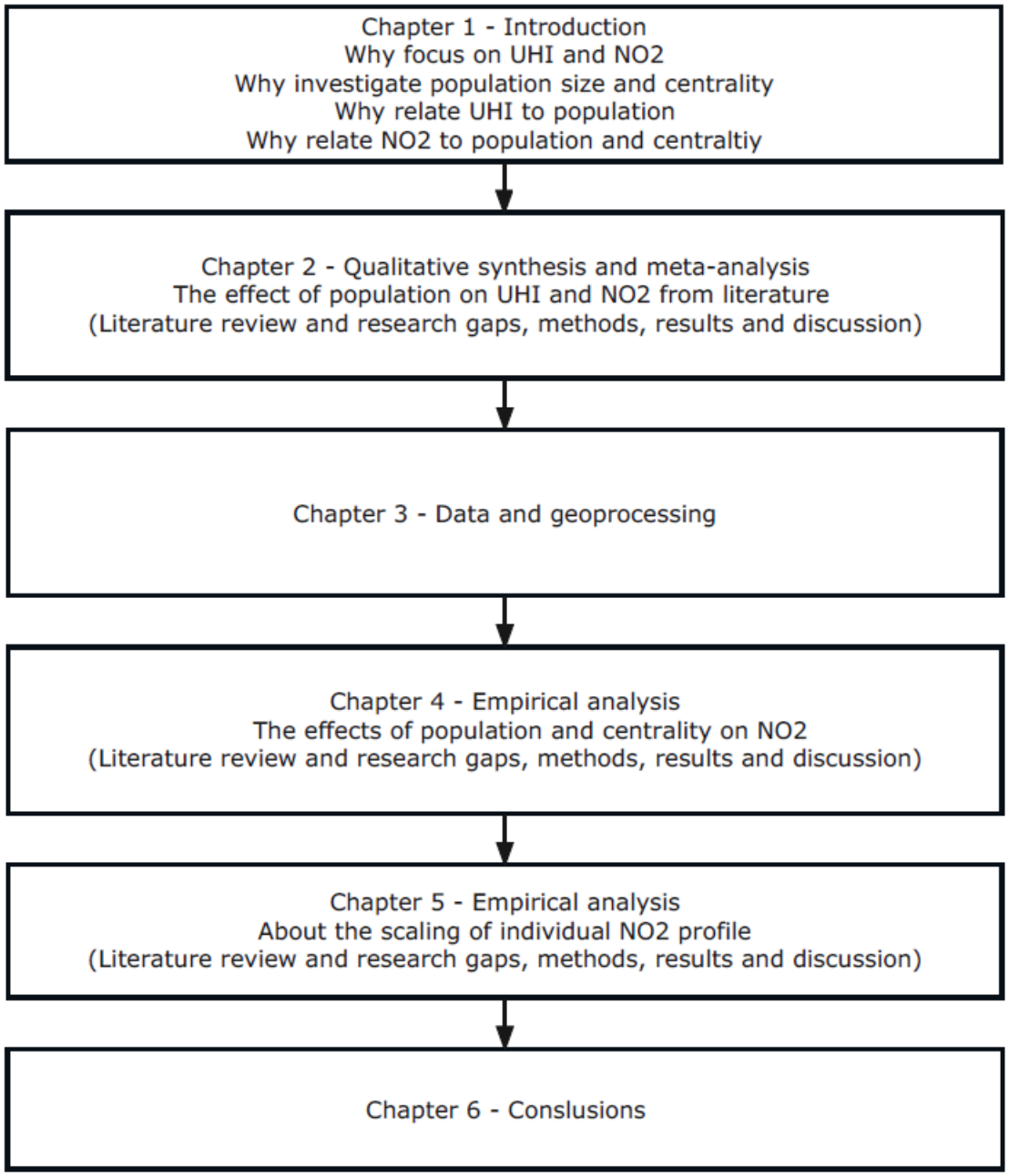

Figure 1.5: Outline of the thesis

2 The effect of city size on UHI and NO_2 in published works

2.1 Literature review and research gaps

Section 1.3 briefly reviews different approaches, metrics, and specifications for quantifying the effect of city size on UHI and NO_2 among research articles. The details of those articles are summarized in this Chapter. Meanwhile, only a few literature reviews have revealed the relationship between UHI and population so far. Common logarithmic population explains 60% of the daily minimum temperature and 38% of the daily maximum temperature of 60 cities in Japan but the coefficients of city sizes are unknown (Fujibe 2011). The annual average maximum temperature and annual maximum temperature of 101 cities in Australia and Asia with a population of more than 300,000 are positively correlated with common logarithmic population, and the coefficient of determination (R^2) varies between 0.55 and 0.65, but the effect of city size is also not given (Santamouris 2015). Tzavali et al. (2015) reviewed UHI around the world but lacked corresponding population data. So far, no literature review has been found to quantify the association between NO_2 and population.

2.2 Methods

First, we assemble the literature on both UHI and NO_2 where a link is drawn, at least qualitatively, with urban population size or density. Second, we review the relationships found in this literature stressing the coefficients or qualitative assessments made in each paper. Since the papers involved in the second step use different measurement methods and metrics, in the third step we collect the values of these papers and use these values to perform regression analysis on UHI and NO_2 with population.

Our literature search and filtering are mainly based on the Preferred Reporting Items for Systematic Reviews and Meta-Analyses (PRISMA) guideline. However, we also conduct a supplementary search, as it appears ex-post that a segment of the literature where environmental effect estimates are made within a broader model, i.e. the environmental Impacts, Population,

Affluence, Technology (IPAT) framework, which could not be retrieved by keywords. Although the IPAT-related literature mainly focuses on carbon emissions, a specific bibliographic search is performed using IPAT and associated models in combination with UHI and NO_2.

Before we present the results, Section 2.2.1 shows our PRISMA filtering and Section 2.2.2 introduces the search under the IPAT framework. Section 2.2.3 then lists the methodological steps used in our quantitative meta-analysis. Figure 2.1 is the workflow of identifying the corpus for this paper.

2.2.1 PRISMA application

The PRISMA guideline first appeared in the field of health care (Moher et al. 2009) and is now also used in urban studies (Cohen 2017; Grekousis 2019). PRISMA is divided into 4 parts: identification, screening, eligibility, and included. *Identification* collects records from different sources. The records are then *screened* to remain non-repeating ones, and are filtered based on titles and abstracts. *Eligibility* judges their full-text contents, and finally *included* carries out qualitative synthesis and meta-analysis. We select UHI and NO_2 papers separately.

Scopus and Google Scholar are the sources for identification. Scopus is the largest multi-disciplinary peer-reviewed abstract and citation database (Elsevier 2019), while Google Scholar covers a wider range of academic citations (Martín-Martín et al. 2018). Keywords such as urban, population, UHI and NO_2 are connected by Boolean operators in Scopus and Google Scholar. The term *city size* is considered as it may refer to population size (Grimm et al. 2008; Tran et al. 2006). The term *urban size* is a synonym of *city size*. The term *population density* is one of the keywords as it has appeared in some UHI and NO_2 papers (Nguyen and Kim 2006; Sakakibara and Matsui 2005). We use the term *NOX* as well because NO_x is a generic term of NO_2. The full search terms are in Appendix A. UHI and NO_2 papers were identified on May 6, 2019 and May 8, 2019 respectively. We did not limit the time of publication, as only 130 UHI and 105 NO_2 records were found in Scopus. We however had found Google Scholar tends to return a large number of research results, so the results in Google Scholar were ordered by relevance, and only the top 200 UHI and top 100 NO_2 items were chosen.

Titles and abstracts of the non-repeating records are screened based on 4 criteria: 1. Peer-reviewed research journal articles written in English. 2. In view of generalizing the relation of UHI and NO_2 with population, papers should aim at deriving the relation of UHI/NO_2 with urban population, or including the measurement of UHI/NO_2 in multiple cities. 3. Of course a simulated environment is very important for prediction, especially when it is needed to assess the health impacts on localized population, but for understanding the effect of city size on built environment at a more aggregated level of cities, circular reasoning should be avoided and only

observed data should be concerned. Thus, papers should use objective, measured data that are generated under non-simulated environment. Papers using subjective UHI/NO_2 values collected from interviews or questionnaires are excluded. 4. To find the agglomerated effect of urban population, papers should consider all the urban population, instead of dividing people into several groups. The excluded UHI and NO_2 records are listed in Appendix B.

Under the PRISMA guideline, we use the following criteria to evaluate full-text contents: 1. As the titles and abstracts of some records do not explicitly indicate whether they fulfill the criteria of title and abstract, the criteria there also apply to their full-text contents. 2. After we reviewed relevant studies, we decide to use UHI intensity and ambient NO_2 concentration (i.e. NO_2 surface concentration) as the metrics of heat stress and NO_2. UHI intensity refers to the temperature difference between a city and its surrounding countryside (Martin-Vide et al. 2015). Ambient NO_2 concentration refers to the measurement of NO_2 contained in an air sample under 25°C and 1 standard atmospheric pressure, and ambient air quality intuitively expresses the hazard of outdoor air pollution to human health (WHO 2022). Papers containing only surface or air temperature but no temperature difference are excluded. Papers containing only bias or difference of NO_2 values are excluded. 3. To avoid circular reasoning, the values of environmental data in the article should not be calculated based on population or transportation, which means values from Land Use Regression (LUR) models and population-weighted UHI/NO_2 data are thus excluded. 4. Correlation/specification/values of population and UHI/NO_2 variables should appear in the full-text. When quantified population and environmental variables appear in the multiple regression model, they should be extractable. 5. Both environmental and population variables should be associated with city boundaries. 6. Correlation/specification/values of population and UHI/NO_2 variables should not duplicate the work of other studies (i.e. data should be newly derived for at least 1 city). The excluded UHI and NO_2 full-text contents are listed in Appendix C.

2.2.2 Search under the IPAT framework

The original IPAT equation (i.e. I = PAT) states that environmental impact (I) is a function of population size (P), affluence (A) and technology (T) (Holdren and Ehrlich 1974), and this equation is extendable by adding additional variables to the right side. Taking the natural logarithmic of the variables on both sides of the IPAT equation will get STochastic Impacts by Regression on Population, Affluence, and Technology (STIRPAT) equation (Dietz and Rosa 1997), a variant of the original IPAT equation under the IPAT framework. The IPAT framework however, focuses primarily on the topic of carbon emissions (Chertow 2000), possibly because carbon footprint is the standard way of judging how the built environment affects the natural

environment (IBM 2021). In the summer of 2022, we searched in Google Scholar using keywords such as "IPAT", "STIRPAT", "NO2", and "UHI" and found 6 articles that include the relationship between NO_2 pollution and population under the IPAT framework. But we haven't found any articles studying UHI and population under the IPAT framework. The results under the IPAT framework obtained are listed in Table 2.2 together with the NO_2 results gained using the PRISMA guideline.

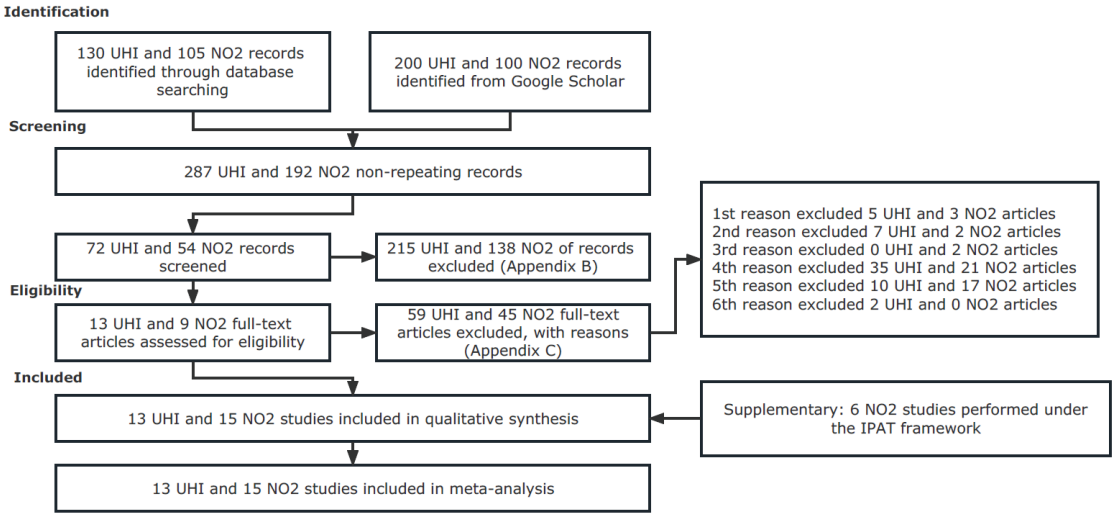

Figure 2.1: Corpus identification

2.2.3 Meta-analysis

13 UHI and 15 NO_2 articles from the qualitative synthesis are included in the meta-analysis of the relationship between UHI and NO_2 with population size. We perform the meta-analysis by:

1. selecting studies having quantified UHI intensity/ambient NO_2 and population size and/or population density. Articles are included if population variables are not specified in the article, but can be calculated from other values described in the article, or can be obtained from sources cited with the article. To obtain as much data as possible, if quantitative data is not clearly stated in the full-text content, we will send queries to the authors for the data,

2. grouping studies having the same combination of environmental and demographic variables,

3. determining the relationship form and unit according to the qualitative synthesis and trial calculation results of the sample data. We decide to derive UHI intensity to the

common logarithmic population variable, the common logarithmic UHI intensity to the common logarithmic population variable, and the common logarithmic ambient NO_2 to the common logarithmic population variable. UHI intensity is in degrees Celsius (°C) and ambient NO_2 is in microgram per cubic meter ($\mu g/m^3$). Ambient NO_2 in parts per billion (ppb) is converted by the equation: 1 ppb = 1.882 $\mu g/m^3$,

4. performing an ANOVA test on each group to assess the extent to which the population variable can explain the variation in UHI/NO_2,

5. for groups showing significant relationships between environmental and demographic factors, their relationships are quantified using linear regression with dummy variables of different papers. That is, when performing each ANOVA test, supposing there are n papers in the group, we create n-1 dummy variables δ_i (i $\in$ [1, n-1]), so the regression becomes

$$Y = \alpha + \sum_{i=1}^{n-1} \lambda_i \delta_i + \beta X + \epsilon, (i \in [1, n-1]) \tag{2.1}$$

where:

Y = UHI intensity (ΔT)/ambient NO_2 (NO2),

α and β = regression coefficients (i.e. intercept and slope),

δ_i = dummy variable associated with the i^{th} paper, δ_i = 1 if ΔT/NO2 belongs to the i^{th} paper, δ_i = 0 otherwise,

λ_i = differential intercept coefficient of δ_i,

X = population size (P)/population density (D),

ϵ = error term, $\epsilon \sim$ N (0, σ^2), and

6. assessing the model.

Differences between ANOVA and linear regression

There are some reasons why we use ANOVA first and then linear regression analysis, although both are used to assess the relationship between dependent and independent variables. First, ANOVA and linear regression have different purposes. ANOVA determines whether there is a significant difference between the means of two or more groups (Kao and Green 2008). Linear regression fits the relationship between a dependent variable and one or more independent variable(s) using a model. Second, ANOVA usually concerns two variables, i.e. one categorical independent variable and one continuous dependent variable (U.S. National University Library 2023), while linear regression concerns one or more independent variable(s) and one continuous

dependent variable. Third, ANOVA uses F-test to test whether there is a significant difference between the means of groups, while linear regression uses coefficients and t-test to describe how the dependent variable changes with the independent variable(s). Last, ANOVA assumes that the variances of the groups are equal (Martin and Games 1977), while linear regression assumes that there is a linear relationship between independent variable(s) and dependent variable. Thus, in this chapter we first use ANOVA to test whether there is a significant difference between population and environmental variables, and then we describe their relationship using linear regression.

2.3 Results and discussion

The studies that pass our criteria and can be understood to relate UHI or NO_2 explicitly to urban population size or density are presented in Tables 2.1 and 2.2. We can already note that the literature is surprisingly thin: 13 papers only relate explicitly UHI to population size, and only 15 papers do so for NO_2. This very low number of studies for such an important global health and environment issue is a first key conclusion and calls for many more cross-section analyses in the field, especially knowing comparability is not necessarily obvious given both UHI and NO_2 are spatio-temporally varying processes and because, as we show below, even within this corpus there is much variety in measurements and methods. Also the IPAT framework does not seem to be used so far for UHI while 6 studies use this more general framework for NO_2. The general conclusion beyond demographics, which includes technology and wealth, is even more rare.

2.3.1 Qualitative synthesis

Tables 2.1 and 2.2 list the qualitative synthesis of UHI and NO_2 studies.

Table 2.1: Qualitative synthesis of UHI studies

Measuring type	Study	Locations and year	ΔT metric	ΔT - population related conclusions
	Oke (1973)	11 cities in Europe, 18 cities in North America *1969-1971* *(car traverse)* *1927-1972* *(literature)*	max/mean aerial ΔT	Canada: mean ΔT = **1.93**$\log_{10}$P - 4.76 R^2 = 0.97 North America: max ΔT = **2.96**$\log_{10}$P - 6.41 R^2 = 0.96 Europe: max ΔT =**2.01**$\log_{10}$P - 4.06 R^2 = 0.74 With the same increment of P, ΔT increases more in a town than in a large city.
	Oke and Maxwell (1975)	1 city in Canada *unspecified*	max aerial ΔT	none
Car traverse	Torok et al. (2001)	7 cities in Australia *1992-1994* *(car traverse)* *1972-1987* *(literature)*	max aerial ΔT	max ΔT = **1.42**$\log_{10}$P - 2.09 R^2 = 0.997 With the same increment P, max ΔT increases less in an Australian town than in a North American/European town. D may decide the association between ΔT and P.
	Sakakibara and Matsui (2005)	16 cities in Japan *2001-2002*	max/mean aerial ΔT	mean ΔT = **1.33**$\log_{10}$P - 3.83 R^2 = 0.96

continued on the next page

continued from the previous page

		(car traverse) *1983-2002* *(literature)*		max ΔT = **2.078**$\log_{10}$P - 4.2176 R^2 = 0.7779 The relationship between P and ΔT is affected by cloud cover and wind speed. The correlation between D and ΔT is not always high comparing with the one between P and ΔT.
Climate models	Ganeshan et al. (2013)	28 cities in U.S. *June, July, August, 2007-2008*	daytime/nighttime mean modeled aerial ΔT	Daytime ΔT in 8 cities is significantly positively correlated with $\log_{10}$P (R^2 = 0.82).
	Debbage and Shepherd (2015)	50 cities in U.S. *2010*	annual mean modeled aerial ΔT	ΔT is insignificant correlated with P (R^2 = 0.27) and D (R^2 = 0.30).
Monitoring stations	Hardin et al. (2018)	4 cities in U.S. May-September *2006-2013*	daily/daytime/ nighttime mean aerial ΔT	P is positively correlated with nighttime mean ΔT.
	Lee (1993)	23 cities in Korea[a] *1986-1989*	max land surface ΔT	max ΔT = **2.38**$\log_{10}$P - 7.75 R^2 = 0.50 P>40000: max ΔT = **3.51**$\log_{10}$P - 14.95 R^2 = 0.50 P<300000: max ΔT = **3.53**$\log_{10}$P - 13.30 R^2 = 0.35

continued on the next page

[a]Cities are counted according to the cities listed in Figure 2 and Table 2 of Lee (1993).

continued from the previous page

	Tran et al. (2006)	8 cities in Asia *2001-2003*	daytime/nighttime/ winter maximum monthly mean land surface ΔT	daytime: $\Delta T = \mathbf{0.4726}(P \div 10^6) + 2.494$ $R^2 = 0.9332$ nighttime: $\Delta T = \mathbf{0.2963}(P \div 10^6) + 0.6586$ $R^2 = 0.7943$
	Zhao et al. (2014)	65 cities in North America *2003-2012*	annual mean daytime/nighttime land surface ΔT	nighttime: $\Delta T = \mathbf{0.64}\log_{10}P - 6.0$ $R^2 = 0.54$
Remote sensing	Du et al. (2016)	101 cities in China *2014*	annual mean daytime/nighttime spring/summer/ autumn/winter mean land surface ΔT	ΔT is insignificantly correlated with D. daytime: spring: $R^2 = 0.057$, summer: $R^2 = 0.387$ autumn: $R^2 = 0.356$, winter: $R^2 = 0.272$ nighttime: spring: $R^2 = 0.258$, summer: $R^2 = 0.261$ autumn: $R^2 = 0.217$, winter: $R^2 = 0.422$
	Ward et al. (2016)	70 cities in Europe *July, 2006*	mean land surface ΔT	ΔT is insignificantly correlated with P and D.
	Zhou et al. (2018)	56 in China *2010-2015*	annual monthly/ summer/winter daytime/nighttime mean land surface ΔT	ΔT is positively correlated with D.

Table 2.1 shows car traverse was a popular way to measure ΔT until the early 21^{st} century. In the 21^{st} century, climate models, monitoring stations and remote sensing are the main ways to gain ΔT, and studies using climate models and remote sensing cover more cities than the one using monitoring stations. Remote sensing measures land surface ΔT while other ways retrieve aerial ΔT, but temperature of the Earth's surface is different from aerial temperature (NASA 2022), and how well they explain each other depends on factors such as terrain and season (Mutiibwa et al. 2015). Perhaps because of the complex measurement procedure, car traverse provides far fewer kinds of ΔT metrics than other ways. As for the related conclusions from the text, 8 papers show ΔT is positively correlated with P, and 6 of which quantify the relation using univariate linear regression. The 2 studies quantifying mean ΔT by car traverse show the coefficients of $\log_{10}$P are 1.93 and 1.33. The studies quantifying max ΔT by car traverse reveal the coefficients of $\log_{10}$P range from 1.42 to 2.96. Climate models and monitoring stations both illustrate the positive relationship between ΔT and P but neither give quantitative equation. The quantitative equations from remote sensing however, could not be compared side by side because of the different ΔT used. The coefficients of $\log_{10}$P in the regression of max land surface ΔT range from 2.38 to 3.53, which are higher than the range of $\log_{10}$P in the regression of max aerial ΔT. Whether ΔT is significantly correlated with D remains inconclusive due to the conflicting conclusions.

Table 2.2: Qualitative synthesis of NO_2 studies

Measuring type	IPAT?	Study	Locations and year	NO_2 metric	Non NO_2/population variables of IPAT	NO_2 - population related conclusions
Emission inventories	Y	Sarzynski (2012)	8032 cities globally	ln(annual emissions) per city	ln(GDP[a] per capita), [ln(GDP per capita)]^2, [ln(GDP per capita)]^3, emission share from energy, emission share from industry, emission share from transport, population growth, rate, annual cooling degree days.	ln(NO_2) = **1.165**lnP - **0.438**lnD + others R^2 = 0.872
	N	Nguyen and Kim (2006)	7 cities in Korea *1998-2003*	annual mean ambient per city		The spatial distribution of NO_2 may associate with D.
	N	Lertxundi-Manterola and Saez (2009)	2 cities in Spain	annual mean/ median/minimum/		none

continued on the next page

[a]Gross Domestic Product (GDP)

continued from the previous page

			1994-2004	maximum ambient per station		
	N	Branis and Linhartova (2012)	39 cities in Czechia *2001*	annual mean ambient per city		Large P is likely to relate with high NO_2. P shows positive significance (**0.886**) in the 2^{nd} factor of PCA
	N	Masiol et al. (2013)	9 cities[a] in Italy *2011*	annual mean ambient per station		none
Monitoring stations	N	Baró et al. (2015)	5 cities in Europe *2011*	annual mean ambient per city		none
	Y	Squalli (2010)	U.S. states *2000*	ln(annual emission) per state	ln(proportion of foreign-born), ln(GDP per capita), $[\ln(\text{GDP per capita})]^2$, ln(electricity output in GDP), ln(manufacturing output in GDP).	$\ln(NO_2)$ = **1.05**lnP + others R^2 = 0.68
	Y	Zhou and Li (2021)	30 provinces	ln(PPP GDP[b]	ln(outward foreign	$\ln(NO_2)$ = **-0.434**lnP + others

continued on the next page

[a]Cities having stations in urban/traffic background are counted. Rural/suburban stations are unselected because of remoteness. The city having stations in industrial background (i.e. Padova) is already counted.

[b]Gross Domestic Product based on Purchasing Power Parity (PPP GDP)

continued from the previous page

		in China *2004-2017*	per terrogram of equivalent industrial emission) per province	direct investment), ln(GDP per capita), ln(GDP per capita^2), ln(proportion of energy consumption in GDP), ln(ratio of pollution discharge costs to GDP), ln(ratio of total imports and exports of goods and services to GDP), ln(oil equivalent. per capita).	R^2 = 0.915
Y	Han et al. (2022)	282 cities in China *2015-2018*	annual mean ambient per city	industrial agglomeration, ln(GDP per capita), ln(energy consumption. per GDP).	NO_2 = **0.161**lnP + others
Y	Cui et al. (2019)	243 cities in China *2005-2012*	ln(annual mean tropospheric column) per city	ln(GDP per capita), ln(the ratio of 2nd industry to 3rd industry), ln(urban road area), ln(total nighttime light value),	ln(NO_2) = **0.7449**lnP + others R^2 = 0.7514

continued on the next page

continued from the previous page

Remote Sensing	Y	Jiang et al. (2021)	65 countries in Africa, Asia, Europe, and Middle East *2005-2018*	ln(annual mean tropospheric column) per country	ln(NDVI[a]), ln(ambient pressure), ln(relative pressure), ln(temperature), ln(wind speed). ln(urbanization level), ln(GDP per capita), ln(GDP per capita^2), ln(access to electricity), ln(foreign direct investment), ln(international trade), ln(industrialization level).	$\ln(NO_2)$ = **0.2441**lnP + others R^2 = 0.649
Remote sensing (modeled)	N	Bechle et al. (2011)	83 cities globally *2005-2007*	$\log_{10}$(modeled annual mean ambient) per city		$\log_{10}NO_2$ is positively correlated with P but is insignificantly related to D. $\log_{10}(NO_2)$ = **0.41**$\log_{10}$P + others
	N	Lamsal et al. (2013)	239 cities in U.S., 757 cities in Europe, 244 cities in China,	ln(modeled annual mean ambient) per city		China: $\ln NO_2$ = **0.66**lnP - 0.38 R^2 = 0.69 Europe: $\ln(NO_2)$ = **0.48**lnP + 0.29, R^2 = 0.67

continued on the next page

[a]Normalized Difference Vegetation Index (NDVI)

continued from the previous page

			265 cities in India *2005*		India: ln(NO_2) = **0.36**lnP - 1.43, R^2 = 0.59 U.S.: ln(NO_2) = **0.42**lnP - 0.02, R^2 = 0.71
Samplers	N	Hosein et al. (1977)	3 cities in U.S. *1972-1974*	annual summer/ winter mean ambient per city	NO_2 is unlikely to relate with D.
	N	Singh and Kulshrestha (2014)	2 cities in India *2012-2013*	annual (summer/ winter/monsoon) mean/median/ minimum/maximum/ 25th/75th percentile ambient per city	none

Table 2.2 shows the only 2 studies using handy samplers measure NO_2 in barely 4 cities. The only study using data from emission inventory however, covers NO_2 pollution across 8,032 cities around the world but ignores cities with less than 50,000 residents. Emission inventory is different from ambient concentration because an emission inventory is made according to indicators including values from emission sources, extrapolated values, and emission factors, and itself needs comprehensive assessment and calculation when updating (U.S. EPA 2022b). Because emission sources have been identified when creating inventories, inventories may fail to reflect localized, highly variable pollutants (AQEG 2013). Compared with NO_2 emission inventories, ambient NO_2 concentration is more suitable to reflect sudden changes in real-world pollutants, especially high vehicular emissions (Fujita et al. 1992). But even ambient NO_2 come in many varieties, including non-logarithmic forms, natural logarithmic forms (*ln()*), and common logarithmic forms ($log_{10}()$). The data of ambient NO_2 itself, can be measured by samplers or monitoring stations, or obtained from the satellite columns through the meteorological model, not to mention that studies aggregate NO_2 at different geographical levels. It is thus difficult to find a consolidated NO_2 metric in evaluating the effect of city size on NO_2 across cities. The only 6 studies under the IPAT framework often contain economic or technological factors along with population variables, but behavior (B), representing environmental impact and residents' choices, is underestimated under the IPAT framework (Schulze 2002). Considering the fact that the use of cars, especially private cars, is largely an individual behavior, the IPAT framework may not be a suitable choice to find the city size effect on ambient NO_2. As for the NO_2-population related conclusions, 4 out of 15 papers do not give corresponding conclusions as they target for other aims. 7 out of 8 articles providing liner regression say non-log/$\log_{10}$/ln NO_2 is positively correlated with $\log_{10}$P/lnP, but they use different metrics or form of relationship. The only paper using PCA gives the conclusion that large cities tend to have high NO_2 pollution. Only 1 article reveals a negative lnP coefficient. Only 3 articles point to a relationship between NO_2 and D, but the conclusions are inconsistent.

2.3.2 Quantitative analysis

6 UHI studies provide quantified environmental and population variables (Hardin et al. 2018; Oke 1973; Oke and Maxwell 1975; Sakakibara and Matsui 2005; Torok et al. 2001; Tran et al. 2006) and we gained data from Zhou et al. (2018). But only 4 papers are enrolled in the meta-analysis (Oke 1973; Oke and Maxwell 1975; Sakakibara and Matsui 2005; Torok et al. 2001). The paper of Hardin et al. (2018) is excluded because it only uses data from May to September. Although Tran et al. (2006) and Zhou et al. (2018) both measure land surface ΔT, these two papers are excluded due to the difference in the definition of ΔT. Tran et al. (2006) approximate ΔT through a fitted

Gaussian surface, while Zhou et al. (2018) define ΔT using absolute difference values between urban and reference pixels. We decide not to include data from climate model into meta-analysis (Debbage and Shepherd 2015; Ganeshan et al. 2013) as a way to avoid circular reasoning. As for the remaining articles in Table 2.1, only Lee (1993) uses max land surface ΔT as an indicator, so its data are not comparable. The time span of Ward et al. (2016) is only 1 month, and thus it is not comparable. We have not got the data of Du et al. (2016), so even with the data from Zhao et al. (2014), no remote sensing studies can be combined to investigate.

5 NO_2 studies provide quantified environmental and population variables (Baró et al. 2015; Hosein et al. 1977; Lertxundi-Manterola and Saez 2009; Nguyen and Kim 2006; Singh and Kulshrestha 2014). Bechle et al. (2011) and Masiol et al. (2013) provided us the data. Data from Jiang et al. (2021), Squalli (2010), and Zhou and Li (2021) are not suitable for our needs as they aggregated the NO_2 data at the level of province/state/country, so even with the data from Cui et al. (2019), no remote sensing studies can be combined to investigate. We did not receive the data from Lamsal et al. (2013), so no modeled ambient NO_2 converted from satellite columns can be studied. We have not received data from Branis and Linhartova (2012) and Sarzynski (2012), and the data source of Han et al. (2022) is not accessible. The paper of Hosein et al. (1977) is excluded due to the abnormal NO_2 comparing with the ones in other studies. Specifically, the summer mean NO2 for Ansonia (U.S.) (108.6 $\mu g/m^3$) with a population of 21,200 (ibid.) is higher than the annual mean NO2 in traffic background of Seoul (South Korea) (102.76 $\mu g/m^3$) (Nguyen and Kim 2006) with a population of 9,895,217 (Turner 2003). Finally, 4 papers are enrolled in the meta-analysis (Baró et al. 2015; Lertxundi-Manterola and Saez 2009; Nguyen and Kim 2006; Singh and Kulshrestha 2014). For the papers of Lertxundi-Manterola and Saez (2009) and Masiol et al. (2013), we average the mean NO_2 values from multiple stations per city as the average of ambient NO_2 per city. For the paper of Lertxundi-Manterola and Saez (2009) we select the maximum value of the maximum ambient NO_2 values gained from stations per city as the maximum ambient NO_2 of that city, and the minimum value of the minimum ambient NO_2 values gained from stations per city as the minimum ambient NO_2 of that city.

ANOVA

An ANOVA test is performed for each combination of environmental and demographic variables. The ANOVA test is performed under the R 3.5.1 environment. Table 2.3 lists the results of the ANOVA test. Appendix D shows the data taken to the ANOVA test.

Table 2.3: Results of ANOVA

Health hazard	Specification/relationship	ρ	Studies
UHI	**max ΔT with $\log_{10}$P**	0.0000	Oke (1973) Oke and Maxwell (1975) Torok et al. (2001) Sakakibara and Matsui (2005)
	$\log_{10}$(max ΔT) with $\log_{10}$P	0.0000	Oke (1973) Oke and Maxwell (1975) Torok et al. (2001) Sakakibara and Matsui (2005)
NO_2	**$\log_{10}$(mean NO2) with $\log_{10}$P**	0.0000	Nguyen and Kim (2006) Lertxundi-Manterola and Saez (2009) Masiol et al. (2013) Singh and Kulshrestha (2014) Baró et al. (2015)
	$\log_{10}$(mean NO2) with $\log_{10}$D	0.0835	Nguyen and Kim (2006) Lertxundi-Manterola and Saez (2009) Singh and Kulshrestha (2014) Baró et al. (2015)
	$\log_{10}$(max NO2) with $\log_{10}$P	0.0746	Lertxundi-Manterola and Saez (2009) Singh and Kulshrestha (2014)
	$\log_{10}$(max NO2) with $\log_{10}$D	0.5192	Lertxundi-Manterola and Saez (2009) Singh and Kulshrestha (2014)

statistical significant relations ($\rho < 0.001$) in bold

Table 2.3 shows max ΔT with $\log_{10}$P, $\log_{10}$(max ΔT) with $\log_{10}$P, and $\log_{10}$(mean NO2) with $\log_{10}$P pass the test of significance at the level of 0.1%. The following analysis is based on these 3 specifications. Although Lertxundi-Manterola and Saez (2009) and Singh and Kulshrestha (2014) provide data to build 2 specifications: min NO2 with $\log_{10}$P, and min NO2 with $\log_{10}$D, but they can not be assessed quantitatively as the minimum annual mean ambient NO_2 of each city in Lertxundi-Manterola and Saez (2009) is 0.

Linear regression

We regress the 3 specifications having statistical significance using Equation 2.1. Tables 2.4, 2.5, and 2.6 show the details of the regression. Appendix D lists the data for the regression. When the dummy variables are absent the regression becomes Ordinary Least Squares (OLS) regression of environmental variables and $\log_{10}$P. For max ΔT, we consider the case where

intercept is 0, as theoretically, cities with no inhabitants should not have UHI. We use R^2 and Breusch-Pagan test (BP test) to assess the regression. F value of the wald test replaces BP test in the OLS regression without intercept (Gibbons 2011).

Table 2.4: Regressions of max ΔT with $\log_{10}$P

	Intercept ≠ 0			Intercept = 0	
	OLS	Dummy variables		OLS	Dummy variables
	(2.1)	(2.2)		(2.3)	(2.4)
Intercept (Oke 1973)	-3.6879***	-2.0007*	Intercept	0	0
	(0.9998)	(0.9522)			
$\log_{10}$P	2.0401***	1.8369***	$\log_{10}$P	1.3006***	1.8369***
	(0.2058)	(0.1847)		(0.0513)	(0.1847)
Oke and Maxwell (1975)		2.5032^{+}	Oke and Maxwell (ibid.)		0.5024
		(1.4685)			(0.9522)
Torok et al. (2001)		-2.1688***	Torok et al. (ibid.)		-4.1695***
		(0.5717)			(1.8140)
Sakakibara and Matsui (2005)		-1.4312**	Sakakibara and Matsui (ibid.)		-3.4319***
		(0.4469)			(1.0241)
			Oke (1973)		-2.0007*
					(0.8587)
R^2	0.6455	0.7581	R^2	0.5562	0.9570
BP test	10.3362**	6.5731	Wald/BP test	642.7377***	6.5731

$^{***}\rho < 0.001$ $^{**}\rho < 0.01$ $^{*}\rho < 0.05$ $^{+}\rho < 0.1$

As we described in Equation 2.1, we use a certain paper as the reference level of the dummy variable. Since we do not have specific coordinates of each study area, we cannot use the climate zone where each study area is located as a dummy variable.

Table 2.4 shows under all circumstances $\log_{10}P$ is positively correlated with max ΔT and passes the test of significance at the level of 0.1%. In the theoretical case (Column 2.3), the slope of $\log_{10}P$ is 1.3006 and $\log_{10}P$ explains more than half of max ΔT. Compared to data in Column 2.1, the dummy variables reduce the slope of $\log_{10}P$ and shows some papers have a significant impact on the regression. In both dummy variables' cases, Torok et al. (2001) passes the test of significance at the level of 0.1% and Oke (1973) passes the test of significance at the level of 5%. The dummy variables also remove the heteroscedasticity in Columns 2.1 and 2.3. In general, $\log_{10}P$ can explain at least 56% or at most 76% of max ΔT (non-theoretical case). The coefficients of $\log_{10}P$ in Columns 2.1 to 2.4 are very close to the ones of Oke (1973), Sakakibara and Matsui (2005), and Torok et al. (2001) in Table 2.1. The R^2 in Column 2.1 (i.e. 0.65) is close to the results Santamouris (2015) (i.e. between 0.55 and 0.65).

Table 2.5: Regressions of $\log_{10}$(max ΔT) with $\log_{10}$P

	Intercept ≠ 0	
	OLS	Dummy variables
	(2.5)	(2.6)
Intercept (Oke 1973)	-0.0442	0.0750
	(0.0770)	(0.0769)
$\log_{10}$P	0.1625***	0.1489***
	(0.0158)	(0.0149)
Oke and Maxwell (1975)		0.0896
		(0.1185)
Torok et al. (2001)		-0.1546**
		(0.0461)
Sakakibara and Matsui (2005)		-0.1082**
		(0.0361)
R^2	0.6607	0.7455
BP test	0.1568	2.4681

***$\rho < 0.001$ ** $\rho < 0.01$ *$\rho < 0.05$ $^{+}\rho < 0.1$

Table 2.5 shows $\log_{10}$P is positively correlated with $\log_{10}$(max ΔT) and passes the test of significance at the level of 0.1%. The dummy variables decrease the coefficient of $\log_{10}$P and describe that Sakakibara and Matsui (2005) and Torok et al. (2001) have influence on deciding the intercept. However, comparing with the significance in Columns 2.2 and 2.4, this time these 2 papers only pass the test of significance at the level of 1%. None of the specifications in Table 2.5 are heteroscedastic. In the $\log_{10}$-$\log_{10}$ specification, the equation of $\log_{10}$P with dummy variables (Column 2.6) is the best to forecast $\log_{10}$(max ΔT). Column 2.6 has a $\log_{10}$P coefficient of 0.1489 and can explain 75% of $\log_{10}$(max ΔT).

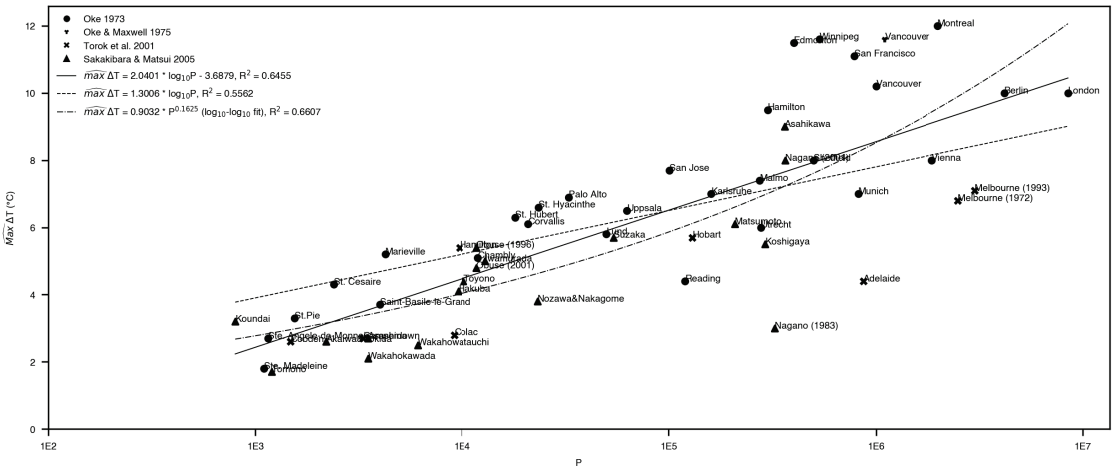

Figure 2.2: Solid line: predicted max UHI intensity ($\widehat{max}$ ΔT) at different P (Column 2.1); short solid line: $\widehat{max}$ ΔT at different P (theoretical case, Column 2.3); solid-dotted line: $\widehat{max}$ ΔT at different P ($\log_{10}$-$\log_{10}$ fit, Column 2.5)

In Figure 2.2, the solid line indicates even small cities of 10,000 inhabitants are likely to have a 4.5°C difference to their surroundings (i.e. 2.0401*$\log_{10}$10000-3.6879=4.4725), and on this basis, when the inhabitants increase by 10 times, the temperature difference increases by an additional 2°C (i.e. 6.5126°C). This coefficient of $\log_{10}$P (i.e. 2.0401) is unsurprisingly close to the coefficients of $\log_{10}$P in the studies of Oke (1973), Sakakibara and Matsui (2005), and Torok et al. (2001) in Table 2.1 as we use their data to produce Figure 2.2. Moreover, this coefficient of $\log_{10}$P is also close to the one using remote sensing (Lee 1993) in Table 2.1. This may indicate land surface ΔT and aerial ΔT are coherent. If we rather consider the $\log_{10}$-$\log_{10}$ fit as the best relationship, we can see that the range is similar for cities with a population of less than 1 million (there is an intersection of the solid and the solid-dotted lines after 1 million) but the heat stress definitely gets worse for mega cities, such as 12°C for a city having 10 million residents.

The specifications highlight the influence from Sakakibara and Matsui (2005) and Torok et al. (2001), but Figure 2.2 shows some significantly low values of max ΔT (e.g. Melbourne in 1972 and 1993, Nagano in 1983) from past literature. It is quite difficult to know the exact reason for these low values as decades have passed, but they can reflect that population is not the only indicator of UHI, perhaps the disproportionate growth of impervious surfaces in cities is one of the reasons (Strohbach et al. 2019).

Table 2.6: Regressions of $\log_{10}$(mean NO2) with $\log_{10}$P

Intercept ≠ 0		
	OLS (2.7)	Dummy variables (2.8)
Intercept (Nguyen and Kim (2006) urban bg.)	0.7045***	0.6547***
	(0.0924)	(0.1528)
$\log_{10}$P	0.1625***	0.1587***
	(0.0164)	(0.0237)
Nguyen and Kim (ibid.) traffic bg.		0.1439***
		(0.0319)
Lertxundi-Manterola and Saez (2009)		-0.0121
		(0.0481)
Masiol et al. (2013) urban bg.		0.0504
		(0.0454)
Masiol et al. (ibid.) traffic bg.		0.1700***
		(0.0447)
Singh and Kulshrestha (2014)		-0.0198
		(0.0672)
Singh and Kulshrestha (ibid.) winter		0.1680*
		(0.0672)
Singh and Kulshrestha (ibid.) summer		-0.0382
		(0.0672)
Baró et al. (2015)		0.0836*
		(0.0366)
R^2	0.7149	0.8982
BP test	0.1169	14.8008^{+}

$^{***}\rho < 0.001$ $^{**}\rho < 0.01$ $^{*}\rho < 0.05$ $^{+}\rho < 0.1$

Table 2.6 shows $\log_{10}$P is positively correlated with $\log_{10}$(mean NO2) and passes the test of significance at the level of 0.1%. The dummy variable reduces the slope of $\log_{10}$P and describes the impacts from the papers of Baró et al. (2015), Masiol et al. (2013), Nguyen and Kim (2006), and Singh and Kulshrestha (2014). NO_2 values measured in traffic background all pass the test of significance at the level of 0.1%. The values taken from urban background in the paper of Nguyen and Kim (2006) also pass the test of significance at the level of 0.1%. None of the specifications in Table 2.6 are severely heteroscedastic. Column 2.8 of $\log_{10}$P with dummy variable is the best one to forecast $\log_{10}$(mean NO2), and its $\log_{10}$P coefficient is 0.1587, which can explain 90% of

$\log_{10}$(mean NO2). The coefficients of $\log_{10}$P in Columns 2.7 and 2.8 are much lower than the ones of Bechle et al. (2011) and Lamsal et al. (2013) in Table 2.2.

The dummy variables on NO_2 studies delineate the obvious impact of measurement background on ambient mean NO2. Values of $\log_{10}$(mean NO2) measured in Italian traffic background pass the test of significance at the level of 0.1% (Masiol et al. 2013). Although the urban background is not a dense area of transportation, but with an average of 10 times the population of Italian cities, $\log_{10}$(mean NO2) values measured in traffic and urban background in South Korea pass the test of significance at the level of 0.1% (Nguyen and Kim 2006), representing the dominant impact from population (Sarzynski 2012). The NO_2 data measured in winter pass the test of significance at the level of 5%, while the data measured in traffic background pass the test of significance at the level of 0.1%. Therefore, traffic background may have a greater impact on NO_2 pollution levels than winter.

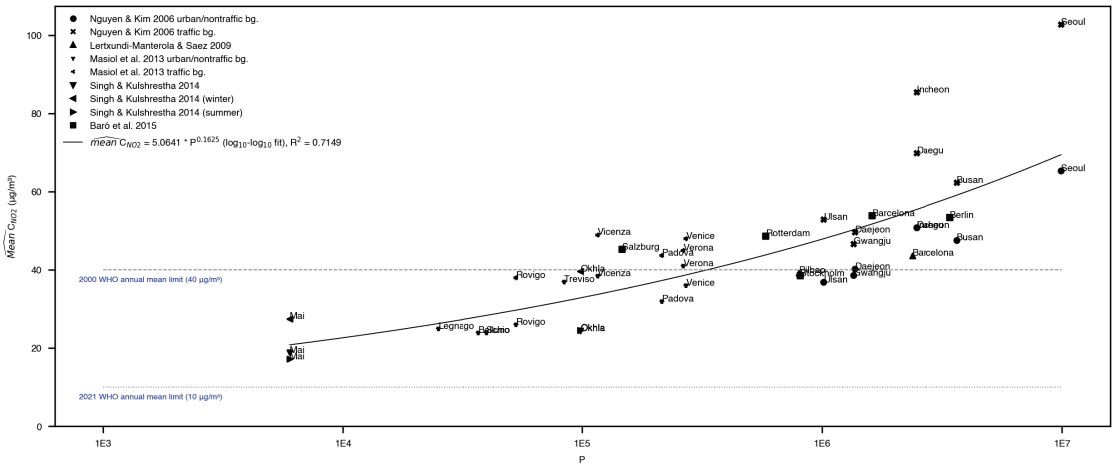

Figure 2.3: Predicted ambient mean NO_2 ($\widehat{mean}$ NO2) at different P (Column 2.7)

Figure 2.3 shows a city of 200,000 inhabitants would then get a 37 $\mu g/m^3$ annual mean intake (i.e. $10^{0.1625*log_{10}200000+0.7045}$=36.8059) while a city of 2 million residents has a 54 $\mu g/m^3$ annual mean intake. The largest cities in the world, i.e. more than 20 million would get a intake of 78 $\mu g/m^3$. We can see however, that some cities can go even largely beyond, such as Seoul on the graph, depending where the ambient NO_2 was measured. We also draw the NO_2 limits suggested by the WHO (WHO 2000, 2021). We can find 53.66% of the data points (i.e. 22/41) are above the WHO annual mean limit in 2000 (i.e. 40 $\mu g/m^3$), and all the points are above the WHO annual mean limit in 2021 (i.e. 10 $\mu g/m^3$). This also means that if the city's mean NO2 meets the WHO annual mean limit in 2000, the population size should be less than 350,000 (i.e. $10^{0.1625*log_{10}350000+0.7045}$=40.3098). The predicted line however is not realistic to

reach the WHO annual mean limit in 2021, as the population size should be less than 100 (i.e. $10^{0.1625*log_{10}100+0.7045}$=10.7029)! So far living in any city is actually detrimental to health.

Our paper is the first to address UHI in cities with inhabitants as small as 800 and ambient NO_2 pollution in cities with inhabitants as small as 6,000, allowing stakeholders of small cities to accurately asses current threats from built environment. Thanks to the inclusion of real small cities, we have a comprehensive view on the contribution of population to the growth rate of max ΔT and mean NO2. Contrary to Sarzynski (2012), who claimed that NO_2 increases faster with population in cities with populations less than 1 million, our $\log_{10}$-$\log_{10}$ specifications of UHI and NO_2 show the growth rates of $\widehat{max}$ ΔT and $\widehat{mean}$ NO2 always increase with population, and the growth rates are not limited by any population threshold. In fact, we couldn't repeat the experiments of Sarzynski (ibid.) as we could not gain the data from her. Sarzynski (ibid.) may make this point because she did not consider cities with inhabitants of less than 50,000. Our findings thus demonstrate that the contribution of population growth to heat stress and NO_2 is unpredictable and inevitable. Based on the results in Figure 2.3, we need to reduce NO_2 emissions if we are to meet the 2021 WHO annual mean limit. Since cars are a major source of NO_2 emissions (EEA 2016), this means we may need to fundamentally change the way we travel or drive.

We suggest that similar meta-analyses can be performed in other databases in the future, such as Web of Science. Second, comparing the cities included in the meta-analysis with inhabitants across continents, heat stress and NO_2 pollution are over-reported in Europe, North America and Oceania, but under-reported in Asia. Apparently African, Latin American, and the Caribbean cities deserve more investigation.

2.4 Code availability

Code links for Table 2.3:

1st ρ **value** - github.com/WeiYufei/PHD_Thesis_University_of_Luxembourg/blob/main/Tab_ANOVA_LOGPOP_MaxUHI.py,

2nd ρ **value** - github.com/WeiYufei/PHD_Thesis_University_of_Luxembourg/blob/main/Tab_ANOVA_LOGPOP_LOGMaxUHI.py,

3rd ρ **value** - github.com/WeiYufei/PHD_Thesis_University_of_Luxembourg/blob/main/Tab_ANOVA_LOGPOP_LOGMeanNO2.py,

4th ρ **value** - github.com/WeiYufei/PHD_Thesis_University_of_Luxembourg/blob/main/Tab_ANOVA_LOGPOPDEN_LOGMeanNO2.py,

5th ρ **value** - github.com/WeiYufei/PHD_Thesis_University_of_Luxembourg/blob/main/Tab_ANOVA_LOGPOP_LOGMaxNO2.py,

6th ρ value - github.com/WeiYufei/PHD_Thesis_University_of_Luxembourg/blob/main/Tab_ANOVA_LOGPOPDEN_LOGMaxNO2.py.

Code links for Table 2.4:
1st column - github.com/WeiYufei/PHD_Thesis_University_of_Luxembourg/blob/main/Tab_MaxUHI_LOGPOP_OLS_withInter.r,
2nd column - github.com/WeiYufei/PHD_Thesis_University_of_Luxembourg/blob/main/Tab_MaxUHI_LOGPOP_FE_withInter.r,
3rd column - github.com/WeiYufei/PHD_Thesis_University_of_Luxembourg/blob/main/Tab_MaxUHI_LOGPOP_OLS_noInter.r,
4th column - github.com/WeiYufei/PHD_Thesis_University_of_Luxembourg/blob/main/Tab_MaxUHI_LOGPOP_FE_noInter.r.

Code links for Table 2.5:
1st column - github.com/WeiYufei/PHD_Thesis_University_of_Luxembourg/blob/main/Tab_LOGMaxUHI_LOGPOP_OLS_withInter.r,
2nd column - github.com/WeiYufei/PHD_Thesis_University_of_Luxembourg/blob/main/Tab_LOGMaxUHI_LOGPOP_FE_withInter.r.

Code links for Table 2.6:
1st column - github.com/WeiYufei/PHD_Thesis_University_of_Luxembourg/blob/main/Tab_LOGMeanNO2_LOGPOP_OLS_withInter.r,
2nd column - github.com/WeiYufei/PHD_Thesis_University_of_Luxembourg/blob/main/Tab_LOGMeanNO2_LOGPOP_FE_withInter.r.

Code link for Figure 2.2:
github.com/WeiYufei/PHD_Thesis_University_of_Luxembourg/blob/main/Fig_UHI_POP_3Lines.py.

Code link for Figure 2.3:
github.com/WeiYufei/PHD_Thesis_University_of_Luxembourg/blob/main/Fig_NO2_POP_1Line.py.

3 Data and geoprocessing

This chapter presents and analyzes the data and geoprocessing methods used in Chapters 4 and 5.

3.1 Data sources and methodology

3.1.1 FUAs

We choose FUAs developed by the Organization for Economic Co-operation and Development (OECD) as the definition of cities (European Comission 2019). FUAs are composed of cities and their surrounding commuting zones. Each city is a Local Administrative Unit (LAU) in which at least half of the residents living in the urban center of the city (Eurostat 2018a). The commuting zone of the city covers the area where the percentage of jobholders hired in the city is at least 15% (Eurostat 2018b). In this way, FUAs define the living areas of commuters in the core city and adjacent metropolitan areas (Simeonova 2019). Thus, FUAs are considered an appropriate geographic domain when formulating transport and planning policies (OECD & European Commission 2020). We download the FUAs dataset from the JRC Big Data Platform (Schiavina et al. 2019). The dataset contains population size and areas of more than 9,000 FUAs globally in 2015. The spatial resolution of the dataset is 1 km x 1 km. Our study area covers 378 FUAs in Europe. We use the population size provided in this dataset as the city size. We use the locations of city halls as the city centers. All city centers are located in FUAs. The coordinates of the city halls are provided by Lemoy, R., Kilgarriff, P. and Mader, M. The city halls were used as the focal points of cities in a study of intra-urban land use profiles (Lemoy and Caruso 2018). We use the locations of city centers to calculate the Euclidean distance from each monitoring station to the city center, or the Euclidean distance from the centroid of each pixel of tropospheric NO_2 layer to the city center (R).

Why choose FUAs

There are several reasons why we choose FUAs as the definition of cities. First, FUAs include not only the core area of the city, but also the surrounding areas delineated according to employment

status. This approach quantifies the socioeconomic activities that take place in and around urban centers. These socioeconomic activities are generated by human activities and also affect the air quality of cities and their surrounding areas. Since the range of human activities are quantified by FUAs, we can assume that UHI effects or NO_2 levels within FUAs are more evident than areas outside FUAs. Second, the boundaries of FUAs do not coincide with the administrative divisions of cities, as the latter rely on the laws and legislation of each country (Dijkstra et al. 2019). FUAs provide a unified city definition, which enables cities to use a unified standard to evaluate economic development and population status, thereby improving the overall economic development level of the region and easing the tension between built and natural environment.

FUAs and urban density

However, due to the definition of FUAs, FUAs may not represent some detailed features of the city's interior, such as urban density, artificial land use, and roads. The definition of FUAs is determined based on the proportion of residents in the city center and the employment status of residents around the city, but this definition does not involve too much the city's infrastructure construction and residents' living conditions (Eurostat 2018a,b). One of the drawbacks of the definition of FUAs is that, FUAs do not reflect how residents commute (e.g. Amsterdam is a city with a well-developed road network but high bicycle usage rate (Ton et al. 2017)) and how much air pollutants are produced on the roads (e.g. the number of people who commute by private car). FUAs also have shortcomings in terms of reflecting urban density. Urban density refers to the number of people or built-up structures per unit of land (Hess 2014), but FUAs ignore urban density because they consider the inhabitants of the entire city as a whole. In addition, FUAs do not show information of housing types, but housing types are related to both energy consumption and pollutant emissions, and housing types also determine the urban density of a certain area (Alrashed and Asif 2014).

FUAs and commuting distance

Since FUAs are defined based on the socioeconomic status of residents, the sizes of FUAs vary from city to city. Therefore, the urban commuting distance of each FUA is different. Among the 378 FUAs, the largest FUA is Paris (France) (19,094 km^2), and the smallest FUA is Andria (Italy) (28 km^2). FUAs of different sizes play a strong supporting role for us to explore the impact of population size on air quality. In Section 3.2 we present the information of FUAs with maps and graphs.

FUAs and suburbanization

Since FUAs take into account both urban core and peri-urban populations, FUAs are inevitably compared with the concept of suburbanization. In fact, FUAs and suburbanization are related but two different concepts. A FUA is a geographical area delineated according to the residence and employment status of residents (Eurostat 2018a,b). Suburbanization is a geographical phenomenon that describes the movement of population from central urban areas to suburban areas, leading to the formation of urban sprawl (Harper 2018; Kok and Kovacs 1999). The size of FUAs is affected to some extent by suburbanization. On the one hand, due to the low land prices in the suburbs and the continuous improvement of the traffic environment, suburbanization is a response to the economic restructuring of the urban core area (Zhou and Ma 2000). On the other hand, suburbanization may negatively affect the city center, leading to the decline of the urban core, thereby concentrating low-income residents in the central area (Gainsborough 2002).

3.1.2 Annual mean NO_2 surface concentrations

We collect annual mean NO_2 surface concentrations (G) in the calendar year 2018 from the Air Quality e-Reporting (AQ e-Reporting) dataset developed by the European Environment Agency (EEA) (EEA 2018b). The annual mean NO_2 surface concentration is in the unit of microgram per cubic meter ($\mu g/m^3$). The AQ e-Reporting dataset contains ground-based air pollutants' records from the monitoring stations of each European Economic Area member country. The AQ e-Reporting dataset we downloaded not only contains the annual mean NO_2 surface concentration recorded by each station, but also includes station coordinates, verification and validity of measured values, time and data coverage of measurement, and monitoring station backgrounds. We choose verified and valid records, then select the ones whose time and data coverage are both greater than 75% (ibid.). Finally, 1,397 monitoring stations are included in our study, of which 674 stations are in mixed background, 566 stations are in traffic background, and 157 stations are in industrial background.

We use dummy variables to show the influence from the backgrounds of different monitoring stations.

3.1.3 Annual mean tropospheric NO_2 vertical columns

The other NO_2 data is annual mean tropospheric NO_2 vertical columns (C), which are calculated from daily tropospheric NO_2 vertical columns. The annual mean tropospheric NO_2 column is in the unit of mole per square meter (mol/m^2). The NO_2 columns are measured by the TROPOspheric Monitoring Instrument (TROPOMI) on the Sentinel-5 Precursor earth observation satellite. We collect daily tropospheric NO_2 vertical columns in the study area from October

25, 2018 to October 24, 2019 from the Sentinel-5P Pre-Operations Data Hub (ESA 2021). We choose this time period is because before October 25, 2018 some data are not available (Eskes and Eichmann 2021). The product has a spatial resolution of 7 km x 3.5 km (Eskes and Eichmann 2021; Eskes et al. 2019).

For further centrality analysis, before obtaining a raster of annual mean tropospheric NO_2 vertical columns, we mosaic the data to gain daily tropospheric NO_2 vertical columns with a spatial resolution of 7 km x 7 km. Because the original data is at the resolution of 7 km x 3.5 km, so generating 3.5 km x 3.5 km pixels without extra algorithms will just bring redundancy (i.e. only the resolution in the X-axis direction increases). The reason why we don't mosaic the data to gain a spatial resolution of 7 km x 3.5 km is because, if we do so, the resulting pixels will be distorted. We found this phenomenon in a trial. In that trial, the length of each pixel in the X-axis direction fluctuated. For example, we found pixels whose X-axis lengths were 8162 m and 7949 m respectively. Since the mosaic is completed by the SNAP software (ESA 2023c), therefore we don't have enough time and authority to understand the algorithm of the software. But to ensure good data quality, only the pixels with *qa_value* higher than 75% are used (Eskes and Eichmann 2021).

3.1.4 Background NO_2 and the impact of agriculture on peri-urban NO_2

For annual mean NO_2 column, we include the minimum annual mean tropospheric NO_2 column of each city as the background NO_2. In this thesis we use **background NO_2** and **minimum annual mean tropospheric NO_2 column per FUA (C_{min})** interchangeably. This is inspired by Nicholas Hewitt (1991) who found the mean *background* ground-level NO_2 pollution in the suburban of Lancaster is around 30 $\mu g/m^3$.

We cannot ignore the fact that agricultural activities also have an impact on NO_2 levels at the urban fringe. Agricultural activities such as using fertilizer, livestock farming and crop burning bring NO_2.

Fertilizers contribute NO_2 mainly through the process of nitrogen deposition (Goulding et al. 1998). The process of nitrogen deposition means reduced N (e.g. ammonia (NH_3)) moves from the atmosphere into the hydrosphere or atmosphere (APIS 2023). Equations 3.1 and 3.2 show a possible way to convert NH_3 to NO_2.

$$NH_3 + O_2 \longrightarrow NO + H_2O \tag{3.1}$$

$$2NO + O_2 \longrightarrow 2NO_2 \tag{3.2}$$

One possible source of NO_2 in livestock farming is manure. Manure produces nitrous oxide (N_2O) (Moeletsi and Tongwane 2015), which can generate NO and H_2O by Equation 3.3. Then NO becomes NO_2 under Equation 3.2.

$$2N_2O + O_2 \longrightarrow 2NO + 2N_2 \tag{3.3}$$

The post-harvest burning of crop residues is another way to generate NO_2. N_2 and O_2 in the air react to produce NO_2 at high temperature.

To mitigate the impact of agriculture on NO_2 levels, one way is to use slow-release fertilizer (Guertal 2009). Slow-release fertilizer releases a small amount of nutrients continuously for a considerable period of time, thereby reducing the release of excess nitrogen (ibid.). NO_2 from manure can be reduced by improving manure management, which includes describing and estimating NH_3 emission in the housing, storage, treatment and spreading of manure (Webb and Misselbrook 2004). Introducing fire-free cultivation is a good way to avoid NO_2 from crop burning (Kato et al. 1999).

3.1.5 Downscaled annual mean tropospheric NO_2 vertical columns

We also downscale NO_2 vertical columns to obtain annual mean tropospheric NO_2 vertical columns with a resolution of 1 km x 1 km. We use the downscaled columns to gain detailed spatial distribution of NO_2 inside cities.

If we don't consider hybrid approaches, there are 4 ways to downscale NO_2 data (Hoek et al. 2008; Jerrett et al. 2005): the proximity method (e.g. Nguyen and Kim 2006), interpolation (e.g. Kumar et al. 2016), LUR model (e.g. Jin et al. 2019), and dispersion model (e.g. Dragomir et al. 2015). The proximity method means that the concentration of a place is expressed by the concentration value near it. Interpolation is the calculation of a value based on known values around it. The LUR model predicts concentration value for a given location based on attributes of the surrounding area, such as traffic, land use, population density, and measured pollution concentrations nearby. The dispersion model is rooted in the Gaussian plume model (Bellander et al. 2001), which estimates air pollution levels from weather, terrain, and emission data (Jerrett et al. 2005). In this thesis however, we do not process data using LUR or dispersion models. It is impractical to use a LUR model with the same predictors for multiple cities (Hoek et al. 2008), and a dispersion model requires quite expensive input (Jerrett et al. 2005). The proximity method simply assigns values without any calculation. As a result, we choose interpolation.

In order to test which method of interpolation is most suitable, we apply spherical, circular, exponential, and Gaussian Kriging on 5 most (Istanbul (Turkey), London (UK), Paris (France), Madrid (Spain), Milan (Italy)) and 2 least (Valjevo (Serbia), Sopron (Hungary)) populous FUAs

and compare the average Standard Error (SE). We find that Gaussian Kriging has the lowest average SE among 6 FUAs. Thus, by using Gaussian Kriging, we gain downscaled annual mean tropospheric NO_2 vertical columns at the resolution of 1 km x 1 km.

3.1.6 Pros and cons to downscale

Downscaling has advantages and disadvantages. One of the benefits is that as the resolution increases, we can obtain a more detailed spatial distribution of NO_2 within the city. The rest of the strength comes from Gaussian Kriging itself. For example, Gaussian Kriging interpolation can accurately represent the interrelationship between independent and dependent variables in a complex space, and because of the use of uncertain parameters, it can explain the spatial relationship at any location in the study area (Kleiber et al. 2012). However, downscaling also brings disadvantages. One of them is the increase in data volume. Increasing spatial resolution can significantly increase data processing time. Second, the improvement in spatial resolution still cannot distinguish the source of NO_2, and NO_2 produced by agriculture still affects the NO_2 levels at the edge of FUAs.

3.1.7 Matching NO_2 with urban boundaries

Although NO_2 and city definitions come from different data sources, there is no boundary mismatch problem in this paper. First, all monitoring stations recording NO_2 surface concentration data are located within city boundaries. Second, for the satellite data, every time we use the city boundary of a FUA to clip the satellite image, we buffer the city edge of the FUA before cropping, and use the FUA with the buffered edge as the reference of cropping, so as to ensure the area of NO_2 column of that FUA is slightly larger than the actual boundary of the FUA.

3.1.8 Year of the data and the effect of choosing a year average

Various factors are considered when we select the year of the data. First, the reason why we choose to study the data on and after October 25, 2018 is that the data on and before October 24, 2018 can no longer be downloaded from the website (Eskes and Eichmann 2021). Second, when selecting the annual average NO_2 surface concentration, it is hoped that the time of the station data is as close as possible to the time of the satellite data, so as to reduce the difference caused by time inconsistency. Our analysis started in November 2019. At that time, there were no annual mean NO_2 surface concentrations in 2019 in the AQ e-Reporting dataset (EEA 2018b), so we can only choose the annual mean NO_2 surface concentrations in 2018.

3.1.9 Pros and cons to choose a year average

There are some advantages of using annual average in measuring NO_2. First, using annual average provides a comprehensive view of the long-term change in NO_2. Thus, the annual mean value is helpful for understanding the overall pollution of NO_2. Second, using the annual average can avoid NO_2 value fluctuations due to short-term disturbances caused by extreme weather (e.g. thunderstorms). Third, the annual average value is a commonly used indicator in weather forecasting (Butryn et al. 2013; Yu et al. 2006). Therefore, the annual averages of different studies can be used for comparison with each other.

However, there are also some disadvantages. First, while the annual mean NO_2 shows a long-term NO_2 trend, using annual averages means that seasonal and diurnal fluctuations in NO_2 may be ignored. For example, urban planners may ignore the high pollution caused by morning peak traffic congestion or heating season. Second, collecting annual averages is expensive and time-consuming. Researchers have to wait a year for satisfactory results. Long-term monitoring can also increase experimental costs.

3.1.10 Data quality

We consider the data quality of the tropospheric NO_2 column from Sentinel-5P to be acceptable for this thesis for several reasons. First of all, in addition to Sentinel-5P, the satellites that measure NO_2 column include OMI and SCIAMACHY. The spatial resolution of OMI is 13 km x 24 km at nadir (Wang et al. 2020a). The spatial resolution of SCIAMACHY is 60 km x 30 km (University of Bremen 2018). The products of Sentinel-5P have a spatial resolution of 7 km x 3.5 km (Eskes and Eichmann 2021; Eskes et al. 2019). Therefore, compared with OMI and SCIAMACHY, the high spatial resolution of Sentinel-5P is more suitable for detecting NO_2 pollution inside cities. Second, TROPOMI has a wide swath width of 2,600 km (NASA 2023b), which enables it to cover large areas at one time. Important spatial variation of NO_2 within a city can thus be captured. Finally, TROPOMI was calibrated before launching (Kleipool et al. 2018) and after collecting NO_2 data (ESA 2023a) to ensure the reliability and validity of the data.

The data quality of NO_2 surface concentrations from the AQ e-Reporting dataset is also acceptable for several reasons. First, the EEA requires all member states to use the same measurement standards (EEA 2023), which helps to ensure data consistency across different European countries. Second, the AQ e-Reporting dataset provides indicators such as time and data coverage, which are convenient for researchers to filter out high-quality data according to experimental needs. Finally, the EEA also annually reviews AQ e-Reporting dataset to ensure that the EU environmental policy is effective (European Court of Auditors 2022).

3.1.11 Influence from wind

Wind can affect NO_2 values by advection and mixing. Advection moves NO_2 horizontally or vertically through the atmosphere, while mixing reduces the NO_2 concentration (Chipperfield et al. 1994; Dieudonne et al. 2013). For example, Ghude et al. (2020) showed that a combination of wind and traffic peaks can make tropospheric NO_2 column concentrations 65% higher measured in the afternoon than in the morning. Ghude et al. (ibid.) pointed out that the temperature inversion formed at night and morning makes a stable air layer above the land surface, which inhibits the advection diffusion of NO_2 in the morning. The NO_2 value measured at noon is not high, because NO_2 is mixed into the photochemical reaction (ibid.). However, from the afternoon to the early evening, a steady low-velocity airflow transfer NO_2 emissions from factories and traffic peaks to surrounding areas, making the measured NO_2 values very high (ibid.). Other factors such as relative humidity (Lee et al. 1992) and sampler types (Masey et al. 2017) can also affect NO_2 measurements. In fact, similar to the situation that NO_2 exists in the troposphere for different lengths of time (Section 1.1.3), the impact of wind on NO_2 is also very complicated, and specific analysis is required for specific regions.

3.2 Maps and graphs

3.2.1 FUAs and city centers

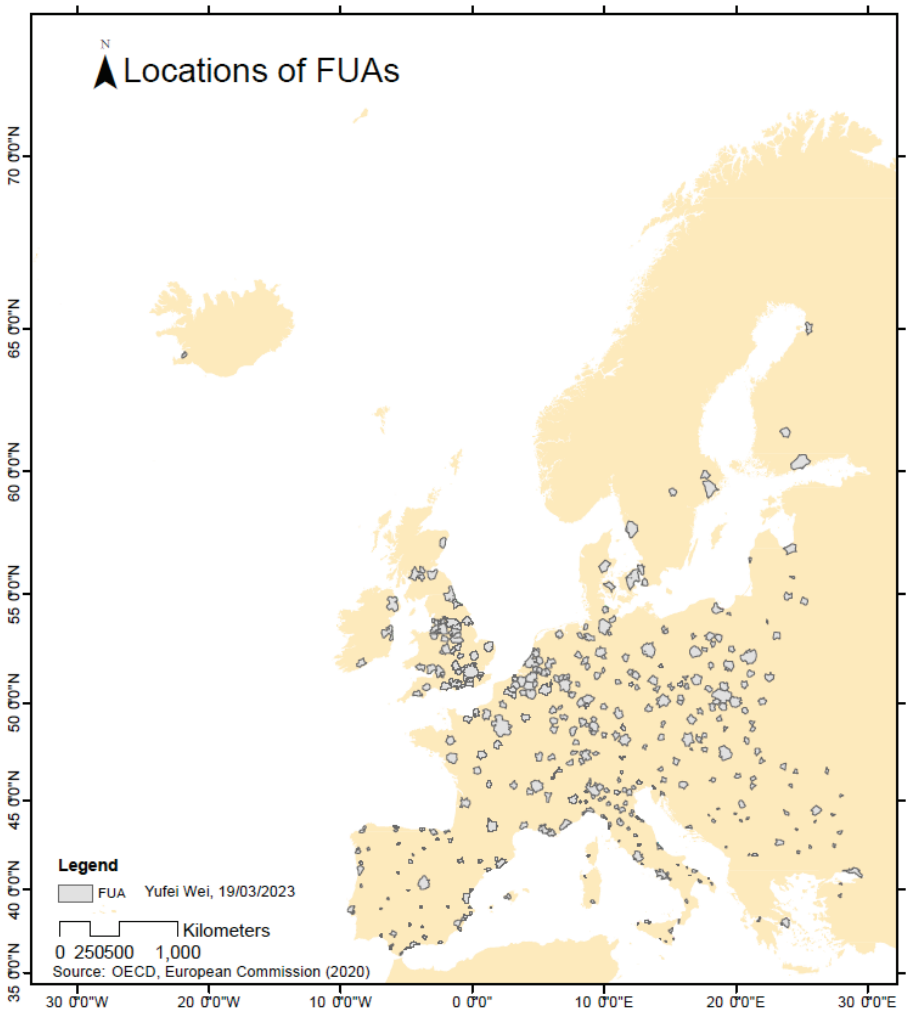

Figure 3.1: Locations of FUAs

Figure 3.1 shows the geographical locations of the 378 FUAs. These 378 FUAs are scattered in Europe. The numbers of FUAs in Northern Europe, Iceland, Southeastern Europe, and Spain are relatively small. FUAs are densely distributed in Central and Eastern Europe and England. The area with the highest density of FUAs is located on both sides of the English Channel, indicating that the region has intensive economic and human activities, and the pollutant content in the air may be relatively high.

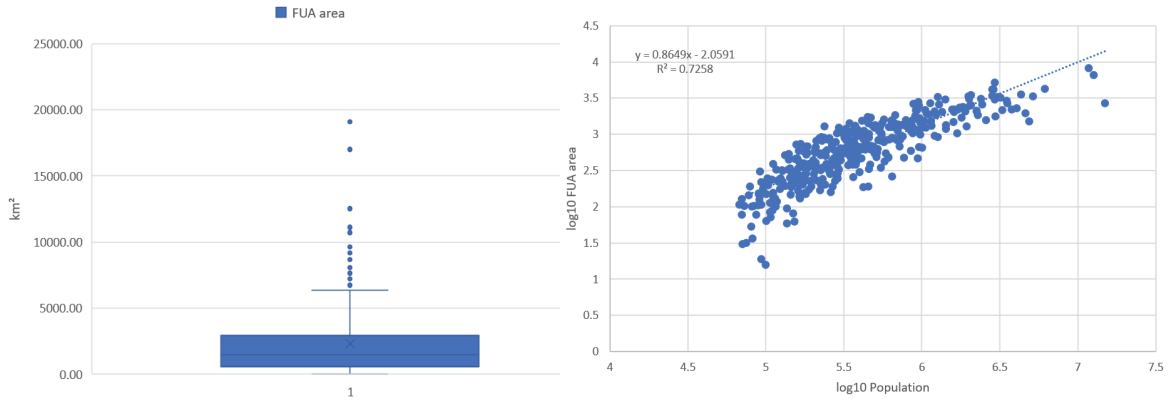

(a) Boxplot of FUA area

(b) $\log_{10}$ FUA area with $\log_{10}$ population

Figure 3.2: Graphs for FUA area

Figure 3.2(a) shows FUAs vary widely in size. The largest FUA covers an area of nearly 20,000 km^2, while the vast majority of FUAs cover an area of around 2,000 km^2. Because in Chapter 2 we have found that the population-environment relationship is suitable to be described by the $\log_{10}$-$\log_{10}$ relationship, so for Figure 3.2(b) and some of the following graphs we also use the $\log_{10}$-$\log_{10}$ relationship. Figure 3.2(b) shows that logarithmic population is positively correlated with logarithmic areas. This results is consistent with the findings from Rozenfeld et al. (2011). Figure 3.2(b) is also one of the evidences that we do not consider the city area in our empirical research (Section 1.2.6).

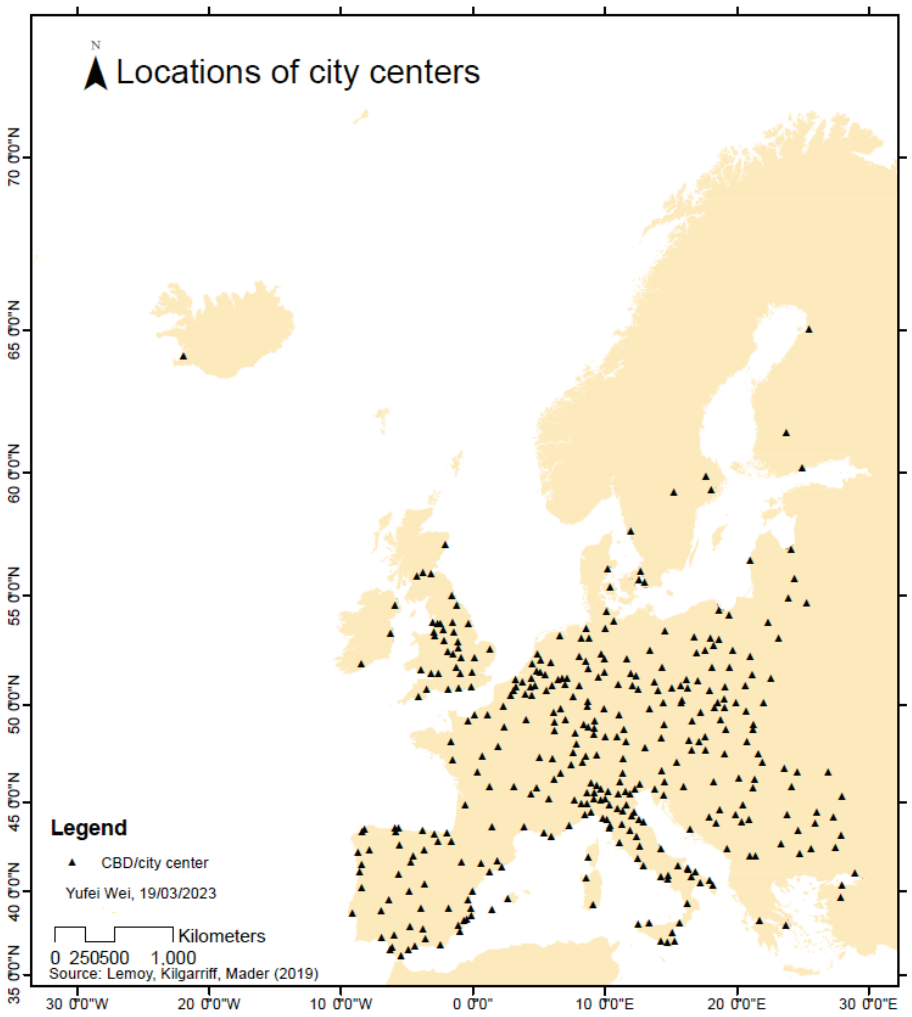

Figure 3.3: Locations of city centers

Figure 3.3 illustrates the locations of city centers in the FUAs. Since each FUA has one and only one city center, the spatial distribution of city centers across Europe is similar to that of FUAs. In this thesis we consider cities are "monocentric" (Alonso 1964).

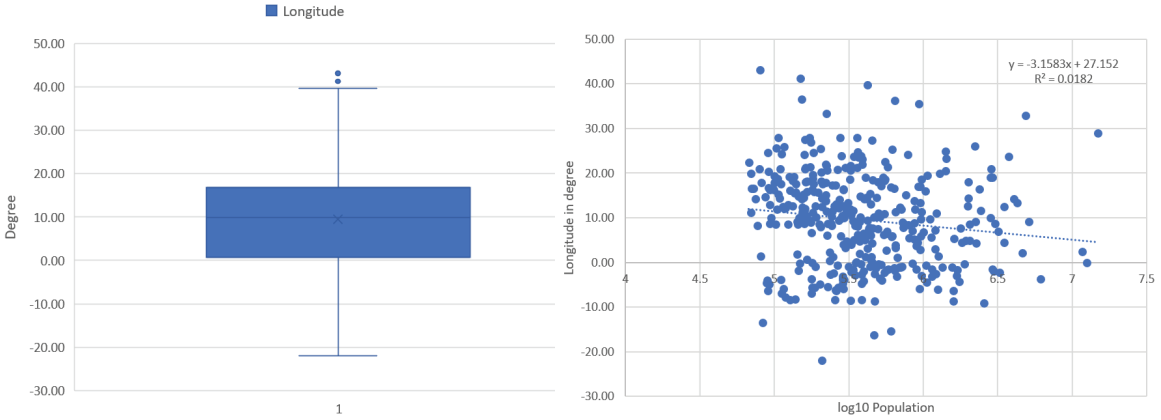

(a) Boxplot of longitude (b) Logitude with $\log_{10}$ population

Figure 3.4: Graphs for longitude

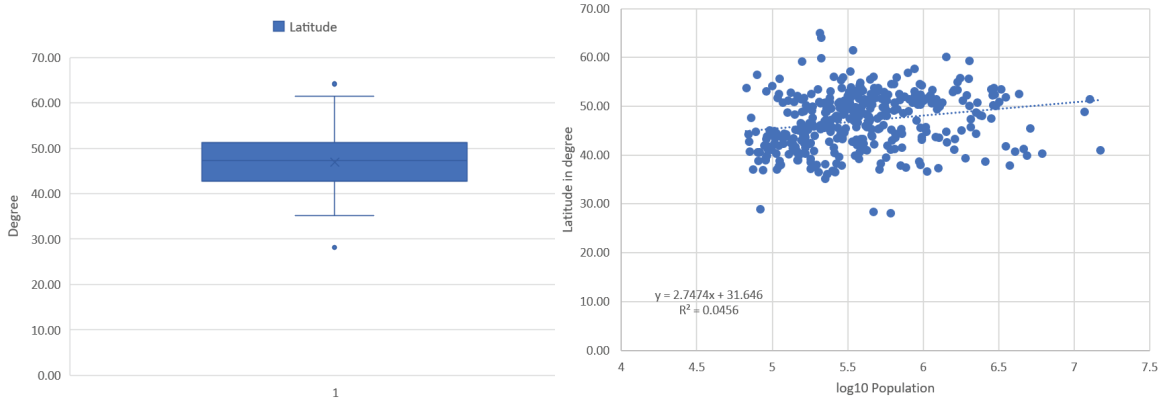

(a) Boxplot of latitude (b) Latitude with $\log_{10}$ population

Figure 3.5: Graphs for latitude

Figures 3.4(a) and 3.5(a) show that the distribution FUAs is mainly concentrated in the area from 0 °E to 20 °E, and 40 °N to 50 °N. The latitudes of FUAs are less discrete than their longitudes. Figure 3.5(b) shows most cities are located south of 50 °N. Kummu and Varis (2011) indicated that important factors such as land surface temperature and rainfall patterns cause approximately half of the world's population to live in regions between 20 °N and 40 °N. Climate classification such as Köppen-Geiger climate classification, also exhibits distinct characteristics according to latitude (Rubel and Kottek 2010).

3.2.2 Köppen-Geiger climate classification

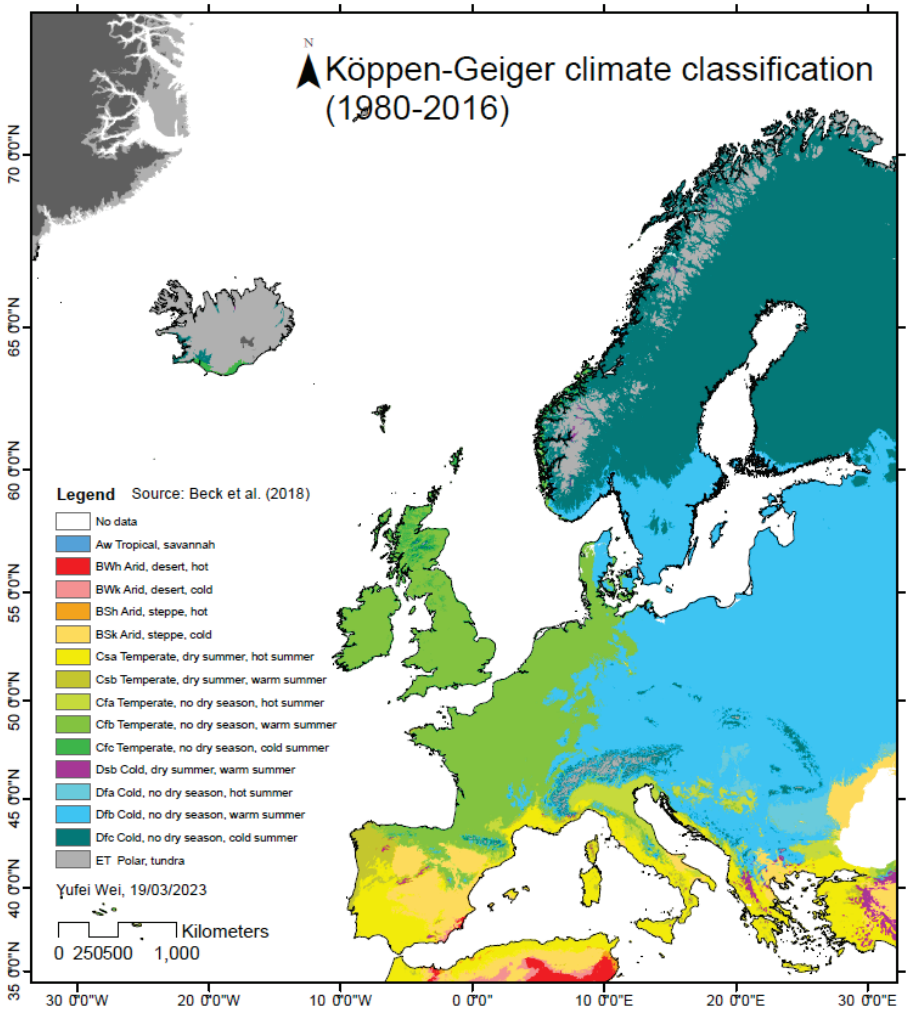

Figure 3.6: Köppen-Geiger climate classification in Europe

Figure 3.6 shows the Köppen-Geiger climate classification in Europe. The data source of the climate classification is Beck et al. (2018). In general, Northern Europe, Iceland, and the Alps have tundra (ET). Denmark, Northern Germany, the Netherlands, Belgium, and Southeastern France form the dividing line between mild (Cfb) and cold (Dfb) year-round. Ireland and most of the UK also fall under the Cfb classification. Dry summer (Csa) appears in Western Spain, Southern France, the Apennines, and the Balkans.

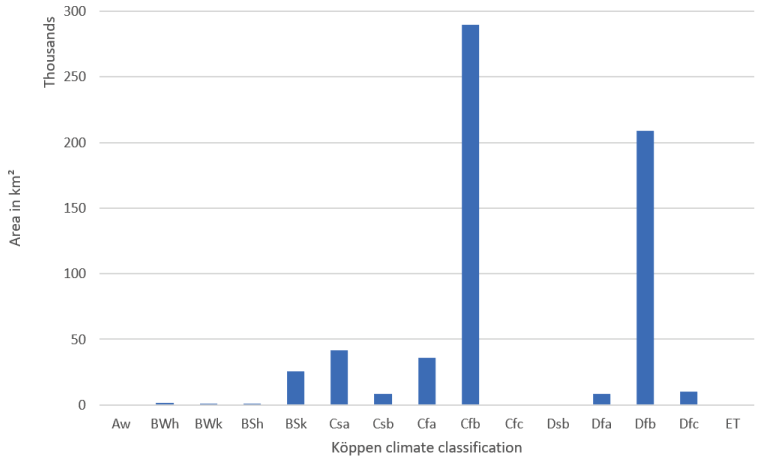

Figure 3.7: Histogram for the Köppen-Geiger climate classification of FUAs

Figure 3.7 shows that the vast majority of FUAs have warm summer and no dry season (Cfb/Dfb). Areas of FUAs with dry or hot summers (Csa/Csb/Cfa) are small. No FUAs in the tundra (ET). Although no dry season and cold summers (Dfc) predominate in Scandinavia, only a few FUAs belong to Dfc.

3.2.3 Wind speed

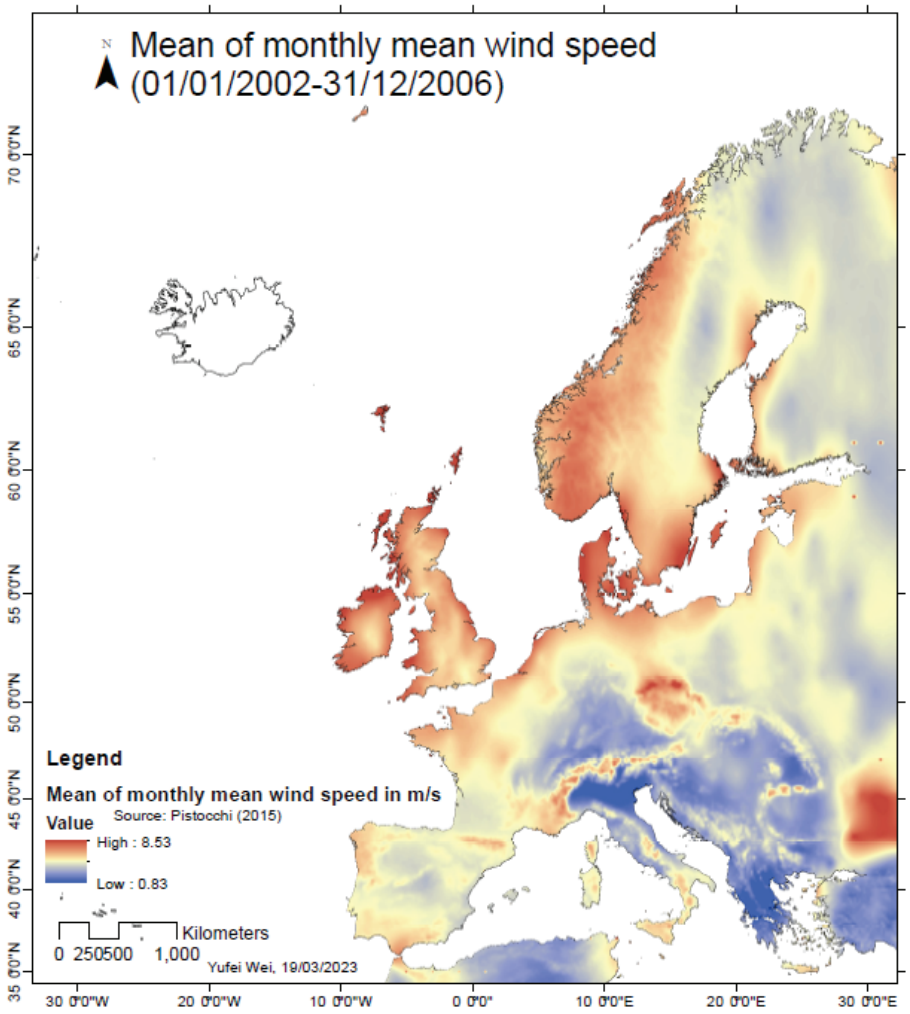

Figure 3.8: Mean of monthly mean wind speed in Europe

Figure 3.8 shows the mean of monthly mean wind speed in Europe from 2002 to 2006. The data source is Pistocchi (2015). We can see high wind speeds, for example, in Ireland, Denmark, Norway and Southeastern Sweden. The wind speed is low in Eastern France, Southwestern Germany, Northern Italy and the Balkans.

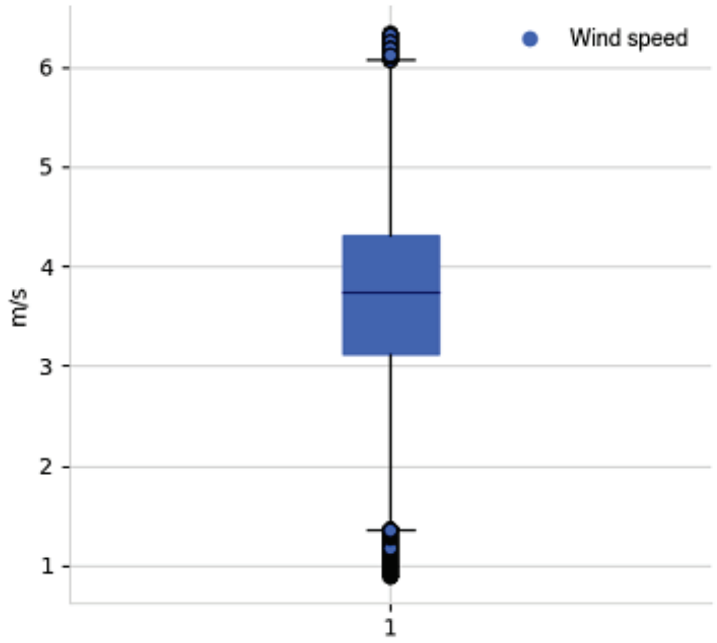

Figure 3.9: Boxplot for mean of monthly mean wind speed of FUAs

Figure 3.9 shows the median of mean of monthly mean wind speed over the FUAs is about 3.7 m/s. Most FUAs have wind speeds between 3 m/s and 4.3 m/s. The maximum wind speed of FUAs (about 6.3 m/s) is smaller than the maximum wind speed (8.53 m/s) in Europe, and the minimum wind speed of FUAs (about 0.9 m/s) is quite close to the minimum wind speed (0.83 m/s) in Europe.

3.2.4 Annual mean NO_2 tropospheric columns

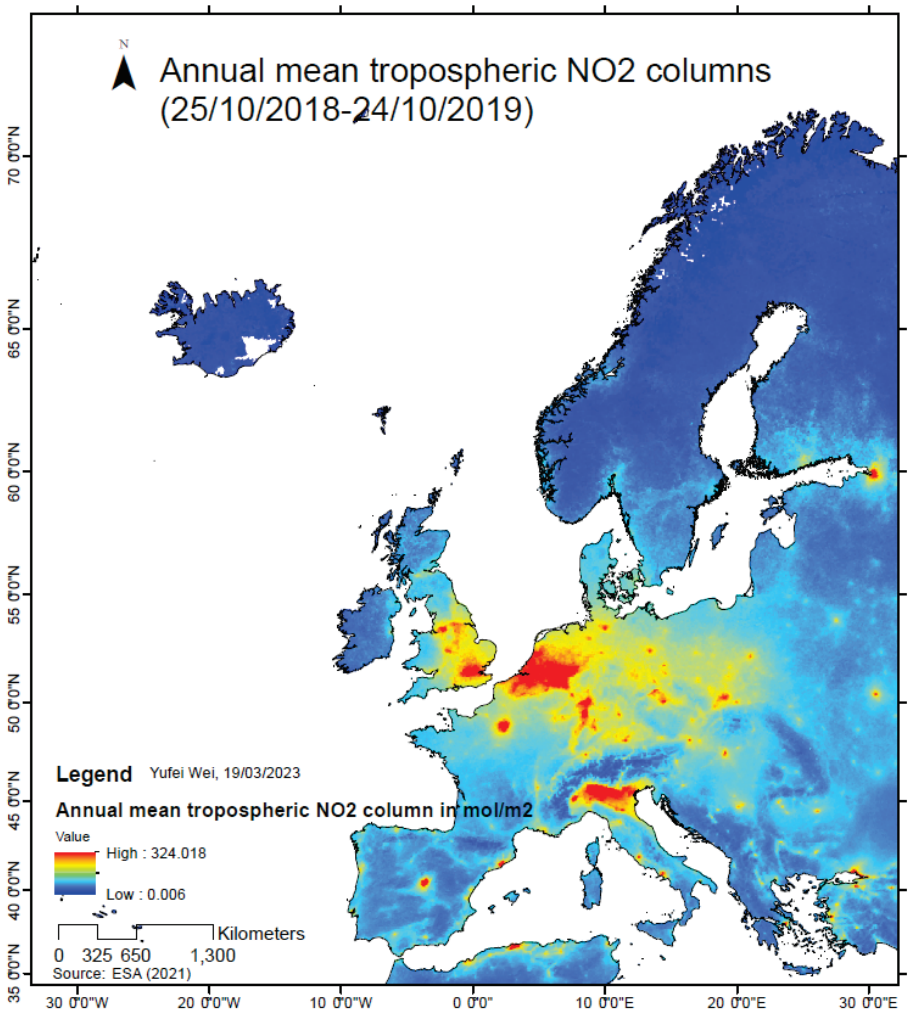

Figure 3.10: Annual mean tropospheric NO_2 columns in Europe

Donnelly et al. (2011) pointed out that NO_2 concentration is negatively correlated with wind speed, and their conclusions can be partly explained from Figure 3.10. We can see that in general, Ireland and Norway with high wind speeds have low NO_2 concentrations, while Eastern France and Southwestern Germany with low wind speeds have high NO_2 concentrations. Figure 3.10 shows that the most polluted areas are in London, the Netherlands, Belgium, Paris and Northern Italy, and the wind speed in these areas is around 4 m/s to 6 m/s (Figure 3.8). However, as we introduced in Section 1.1.3, NO_2 concentrations are affected by many factors, so Figure 3.10 also

shows that regions with low wind speeds, such as Spain (except Madrid) and the Balkans, also have low NO_2 levels.

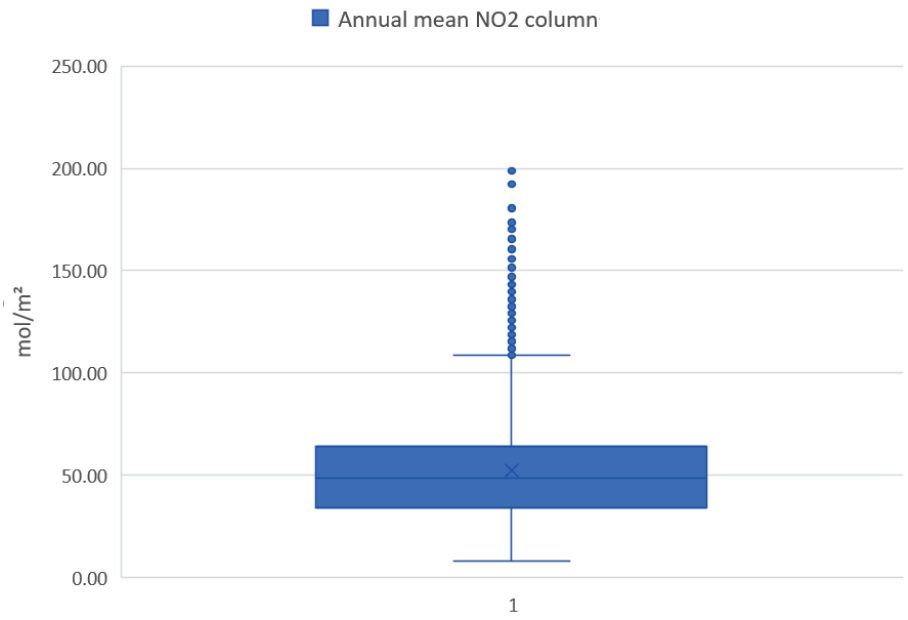

Figure 3.11: Boxplot for annual mean tropospheric NO_2 column of FUAs

Figure 3.11 shows that most of the NO_2 column concentration values are between 40 mol/m^2 and 60 mol/m^2, but the highest NO_2 column concentration can reach about 200 mol/m^2, which is 4 times the median.

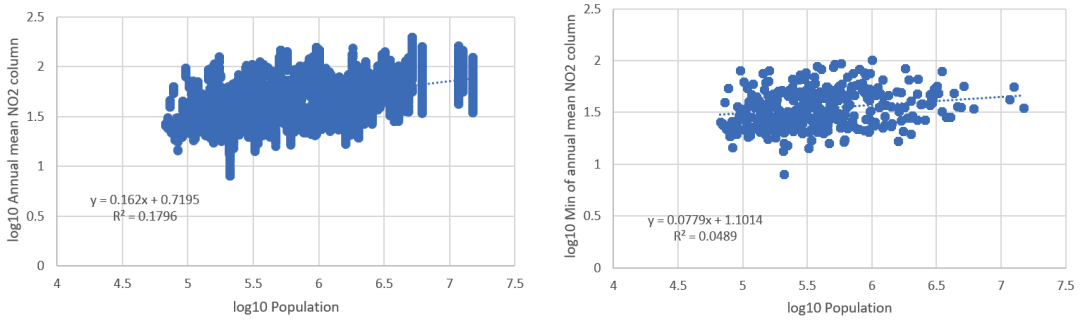

(a) $\log_{10}$ annual mean tropospheric NO_2 column with $\log_{10}$ population

(b) $\log_{10}$ minimum of annual mean tropospheric NO_2 column per FUA with $\log_{10}$ population

Figure 3.12: Graphs for NO_2 column

Figures 3.12(a) and 3.12(b) show logarithmic population is positively correlated with logarithmic annual mean NO_2 columns or logarithmic background NO_2 per FUA. The coefficient in Figure 3.12(a) is higher than the one in Figure 3.12(b). This may be because background NO_2 is affected by more factors than annual average NO_2. We have shown in Section 3.1.4 the impact of agriculture on NO_2 at the urban fringe. We also find that neighboring cities also have an impact on the distribution of NO_2 within the city, which makes the distribution of NO_2 in the city deviate from the theoretical model proposed by Schindler et al. (2017). In Sections 3.2.7 and 3.2.8, we use some FUAs as examples to illustrate this phenomenon.

3.2.5 Annual mean NO_2 surface concentrations

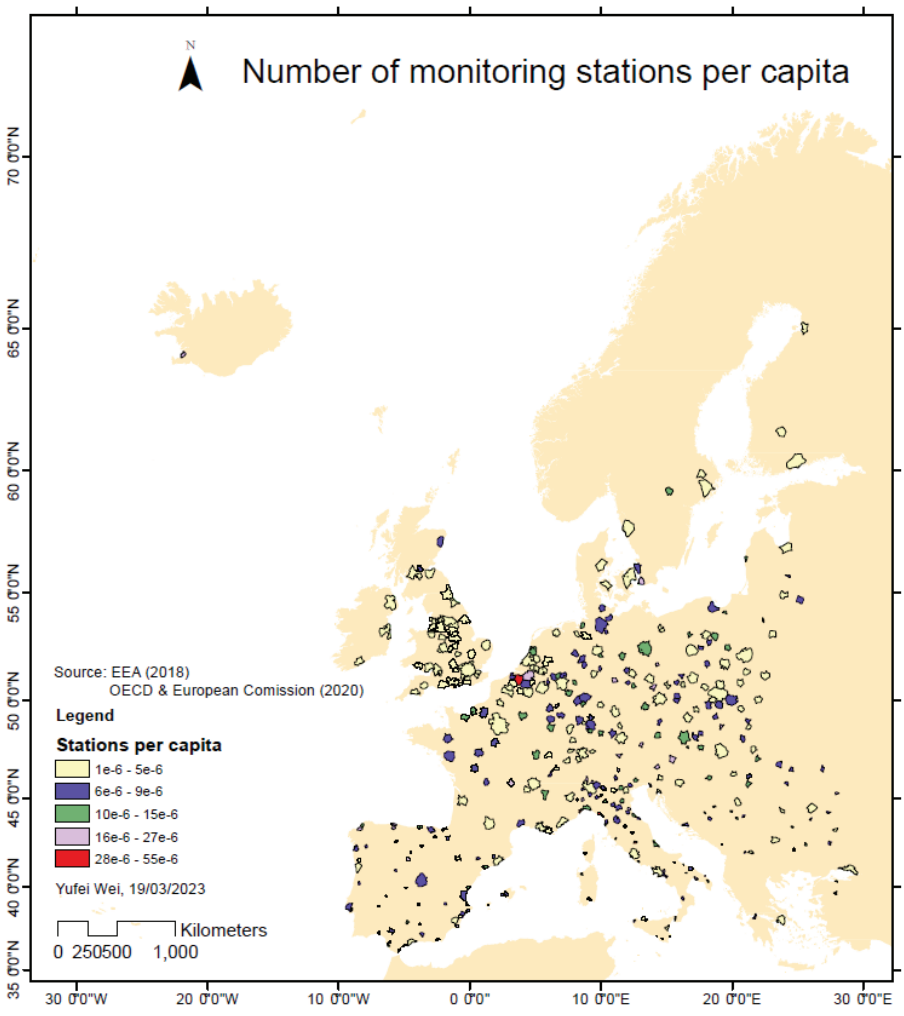

Figure 3.13: Number of monitoring stations per capita in Europe

Figure 3.13 shows that generally speaking, areas with high NO_2 levels in Figure 3.10 (e.g. the Netherlands, Belgium, Western Germany, Eastern France, and Northern Italy) also have higher numbers of stations per capita. Surprisingly, in large cities like London and Paris, the number of measuring stations for NO_2 per capita is very low, which may indicate that the problem of NO_2 pollution in large cities has not received enough attention. Capital cities such as Copenhagen and Rome also have too few stations per capita.

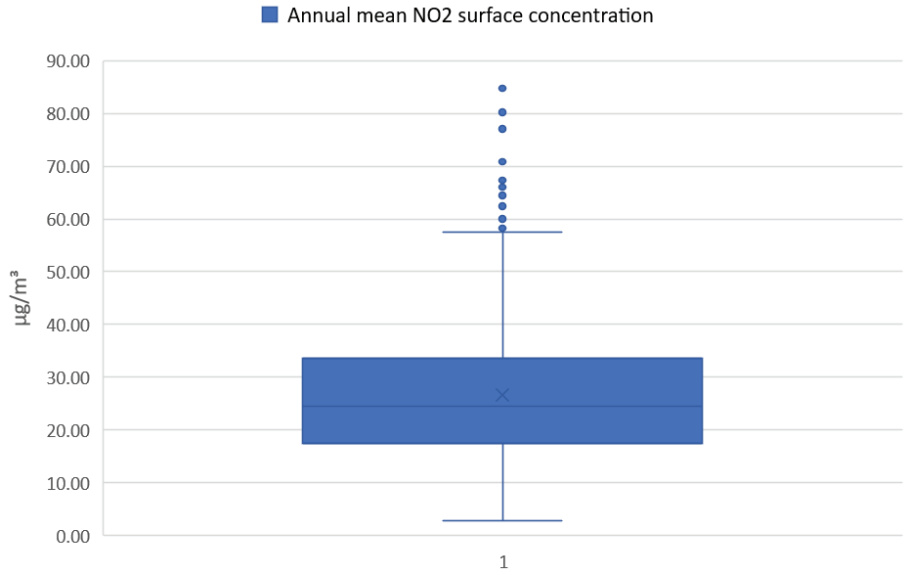

Figure 3.14: Boxplot for annual mean NO_2 surface concentration

Figure 3.14 shows that most of the NO_2 surface concentrations are between 18 $\mu g/m^3$ and 33 $\mu g/m^3$, but the highest NO_2 column concentration can reach more than 80 mol/m^2, which is nearly 4 times the median. Interestingly, the highest value of the NO_2 columns is also about 4 times the median (Figure 3.11). This shows the consistency between NO_2 columns and NO_2 surface concentrations.

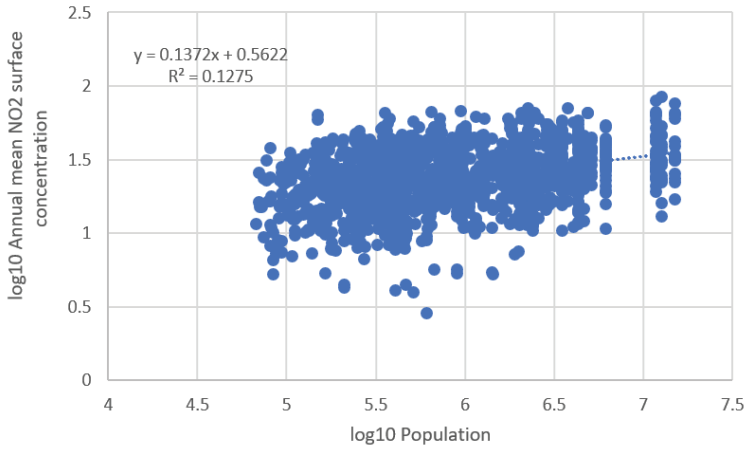

Figure 3.15: $\log_{10}$ annual mean NO_2 surface concentration with $\log_{10}$ population

Same as the positive effect of the population on the NO_2 column in Figure 3.12(a), Figure 3.15 shows logarithmic population is positively correlated with logarithmic annual mean NO_2 surface concentration.

3.2.6 Neighborhood analysis

To find out the effect of proximity to neighboring cities, we conduct a neighborhood analysis. We create a buffer zone with a radius of 50 km from the boundary of each FUA and find out how many neighboring city centers are within the buffer zone.

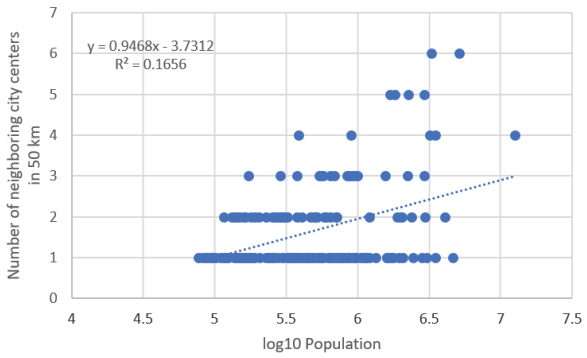

Figure 3.16: Number of neighboring city centers in 50 km with $\log_{10}$ population

Figure 3.16 shows logarithmic population is positively correlated with the number of neighboring city centers in 50 km. This means that, overall, the larger the city, the more neighboring

cities it has. This may also suggest that the larger the city, the more its pollution may potentially affect its surrounding cities.

3.2.7 Sample FUAs

We select 8 FUAs as sample cities to find their detailed characteristics of geography, climate and NO_2. We choose Paris (France) as a representative city with a population greater than 10 million. We choose Madrid (Spain) and Milan (Italy) as representative cities with a population of 5 million, of which Madrid is far from its surrounding FUAs, and Milan is close to its surrounding FUAs. We choose Nuremberg (Germany) and Dublin (Ireland) as representative cities with a population of around 1 million, where Nuremberg is far from the coast and Dublin is close to the coast. We choose Blackpool (UK), Kiel (Germany) and Ghent (Belgium) as representative cities with a population of less than 1 million, where Blackpool is close to other cities, Kiel is a coastal city but has no other cities nearby, and Blackpool is a coastal city but is adjacent to other cities.

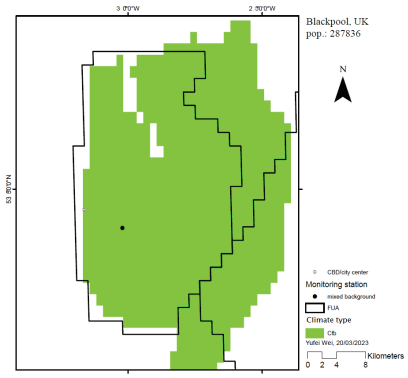

(a) Blackpool, UK

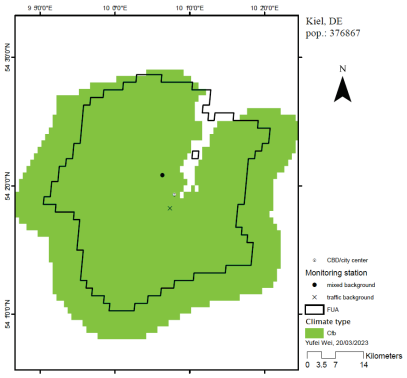

(b) Kiel, Germany

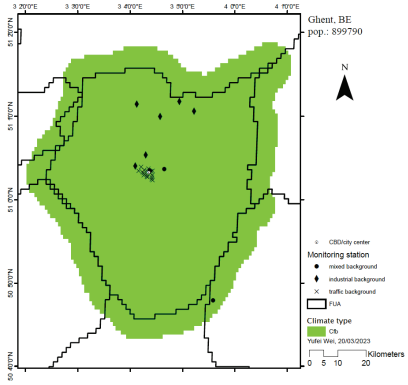

(c) Ghent, Belgium

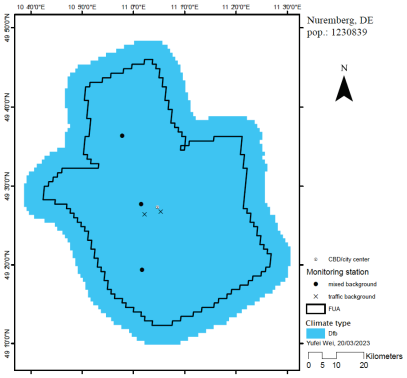

(d) Nuremberg, Germany

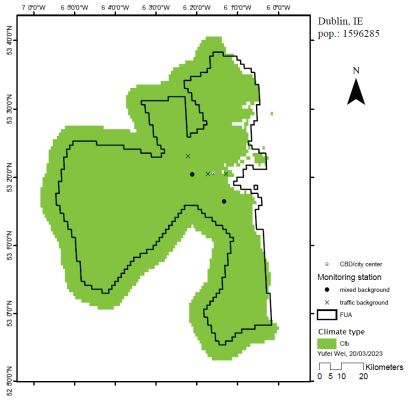

(e) Dublin, Ireland

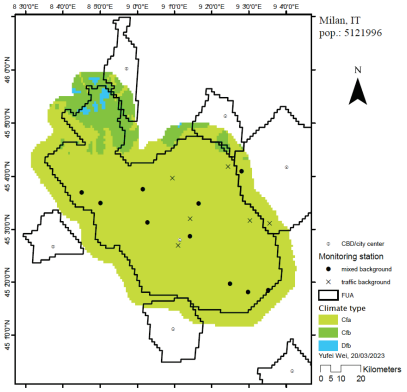

(f) Milan, Italy

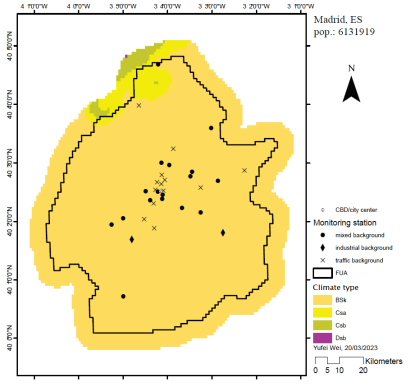

(g) Madrid, Spain

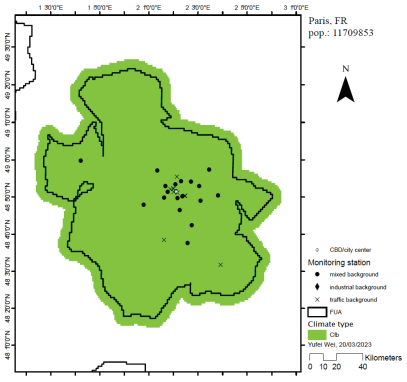

(h) Paris, France

Figure 3.17: Köppen-Geiger climate classification of sample cities

Figure 3.17 shows that the climate type of 5 of the 8 cities is Cfb, and the dominant climate types of the remaining 3 cities are Dfb, Cfa and Bsk respectively. Both Cfa and Cfb belong to the temperate climate type and have no dry season. The difference is that Cfa has hot summer and Cfb has warm summer. Summers in Dfb are warm but cold year-round. Bsk is dry steppe but not hot. Generally speaking, the climate types within the sample FUAs have little or no spatial variation.

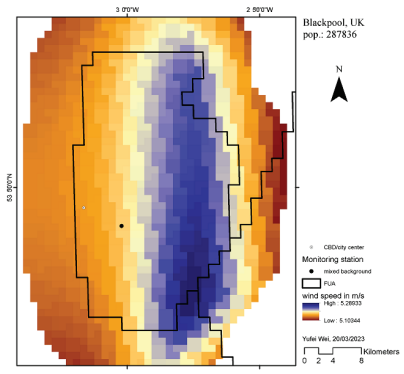

(a) Blackpool, UK

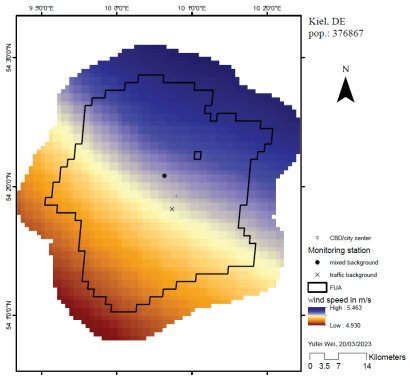

(b) Kiel, Germany

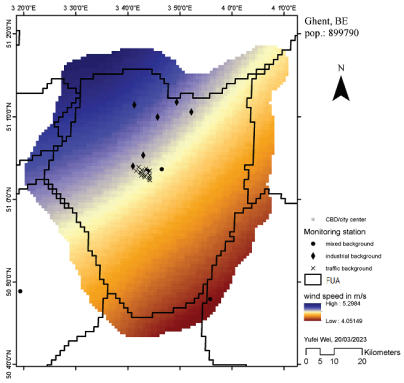

(c) Ghent, Belgium

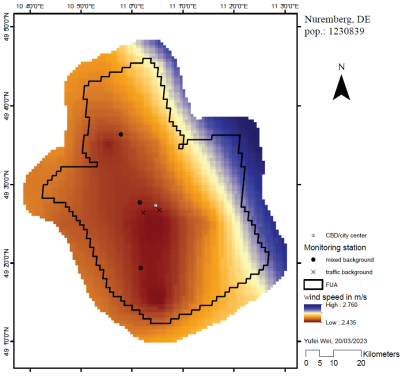

(d) Nuremberg, Germany

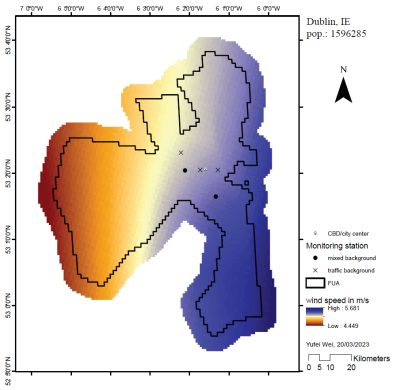

(e) Dublin, Ireland

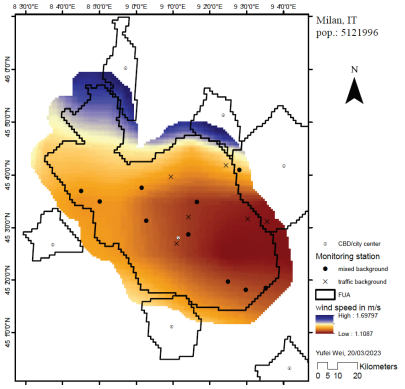

(f) Milan, Italy

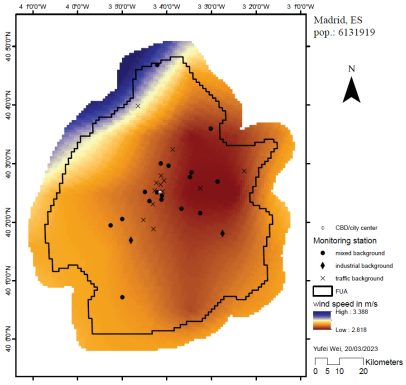

(g) Madrid, Spain

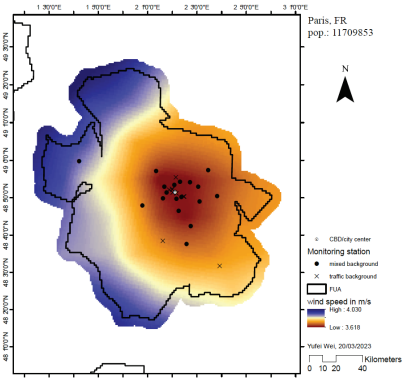

(h) Paris, France

Figure 3.18: Wind speed of sample cities

Figure 3.18 shows that with the exception of Kiel, Ghent and Dublin, wind speeds are lower in the city centers. It is worth noting that Kiel, Ghent and Dublin are coastal cities, and their average wind speed is generally higher than that of inland cities (Nuremberg, Milan, Madrid, Paris). Stations with traffic background in inland cities are located in areas with low wind speed.

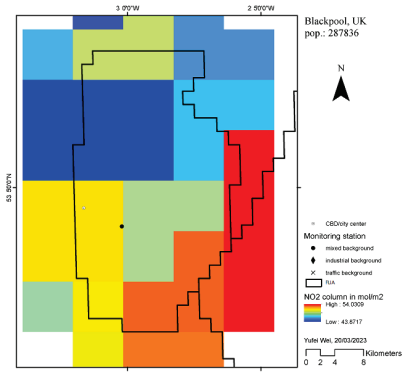

(a) Blackpool, UK

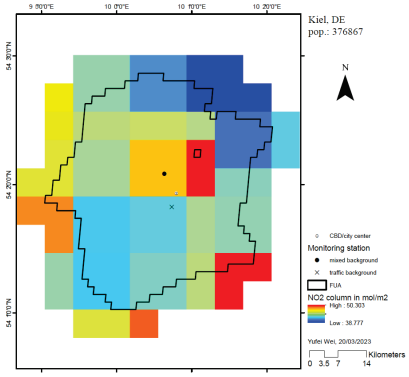

(b) Kiel, Germany

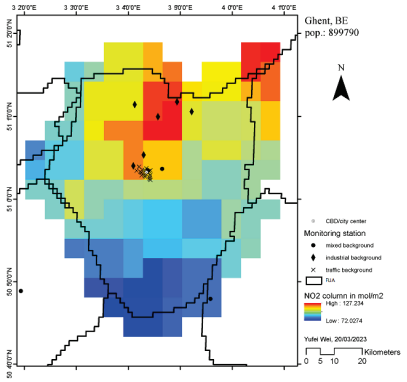

(c) Ghent, Belgium

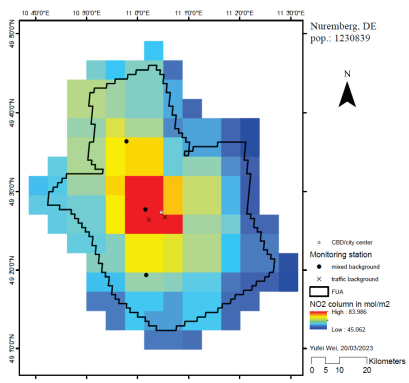

(d) Nuremberg, Germany

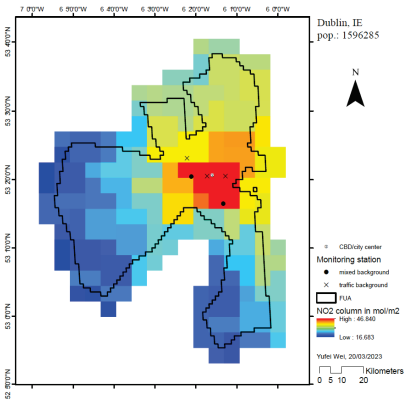

(e) Dublin, Ireland

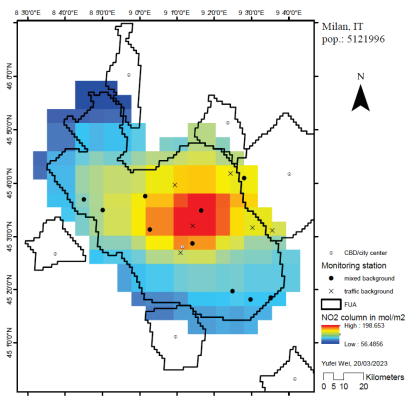

(f) Milan, Italy

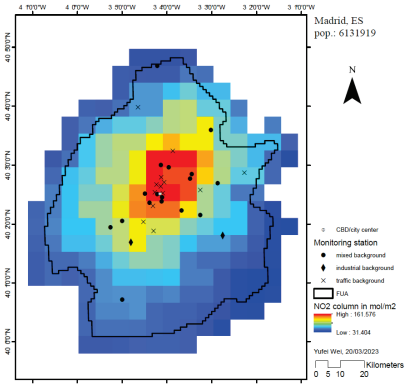

(g) Madrid, Spain

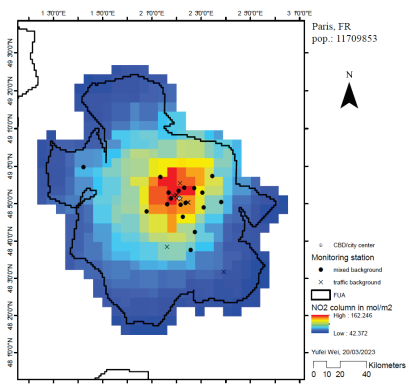

(h) Paris, France

Figure 3.19: Annual mean tropospheric NO_2 columns (resolution: 7 km x 7 km) of sample cities

Figures 3.19 shows that satellite imagery with a resolution of 7 km x 7 km fails to show the spatial distribution of NO_2 in cities with populations less than 1 million, especially for Blackpool. It seems that there are sources of NO_2 pollution at the fringes of Blackpool, Ghent and Milan.

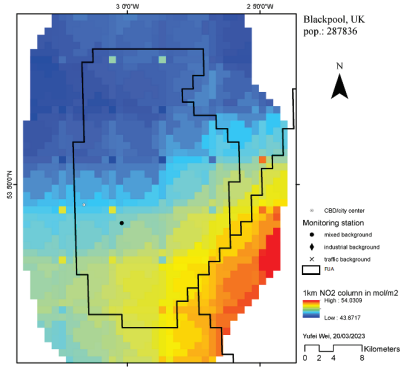

(a) Blackpool, UK

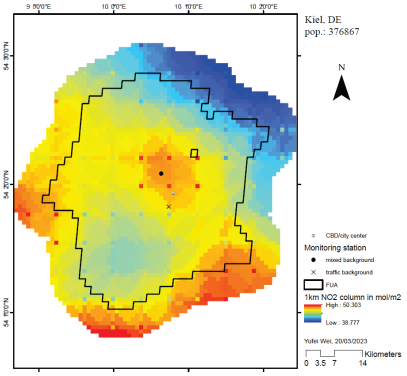

(b) Kiel, Germany

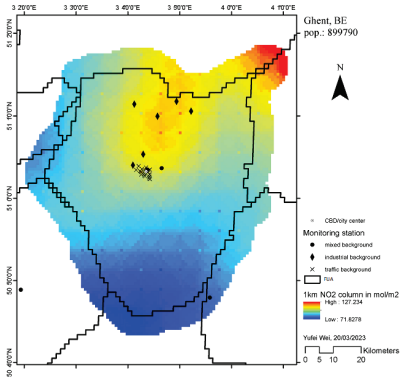

(c) Ghent, Belgium

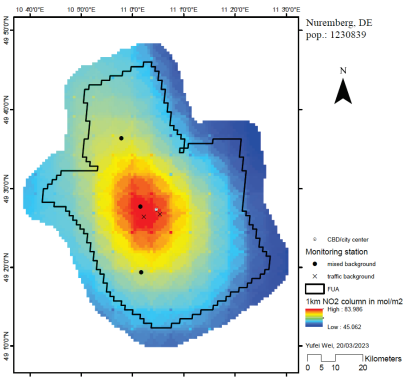

(d) Nuremberg, Germany

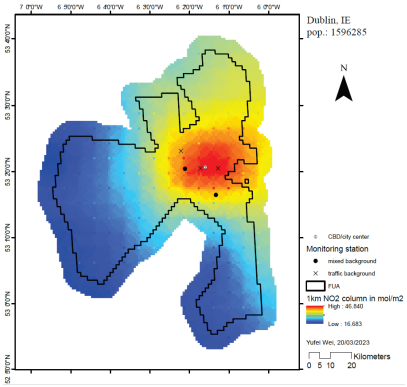

(e) Dublin, Ireland

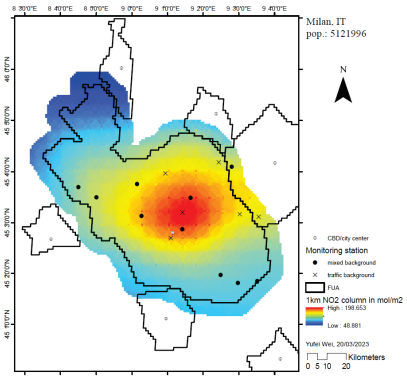

(f) Milan, Italy

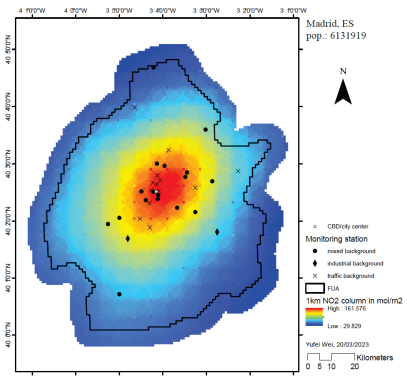

(g) Madrid, Spain

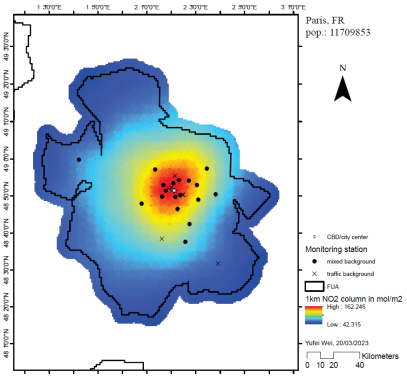

(h) Paris, France

Figure 3.20: Downscaled annual mean tropospheric NO_2 columns (resolution: 1 km x 1 km) of sample cities

Figure 3.20 shows that downscaled NO_2 columns are capable of showing the NO_2 distribution of small cities. For example, we can observe the obvious influence from the neighboring city of Blackpool. The NO_2 levels in the north of Ghent and in the center of Ghent are lower than those in the northeast corner of Ghent, possibly because of lower wind speeds in the northeast corner than in the north, and also possibly because Ghent's northeast borders another city, Antwerp (Belgium). However, wind speed appears to have little effect on the NO_2 levels in Dublin. The east of Dublin has high wind speed (Figure 3.18(e)), but the NO_2 levels are high there as well.

3.2.8 Regular and irregular intra-urban NO_2 distribution

To quantify the NO_2 levels inside cities, we decide to use a scatter plot to show how NO_2 changes with centrality. Figure 3.21 shows how NO_2 is distributed inside sample cities.

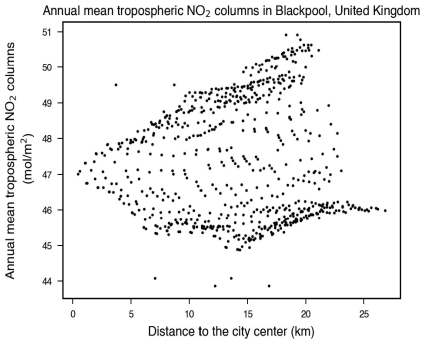

(a) Blackpool, UK

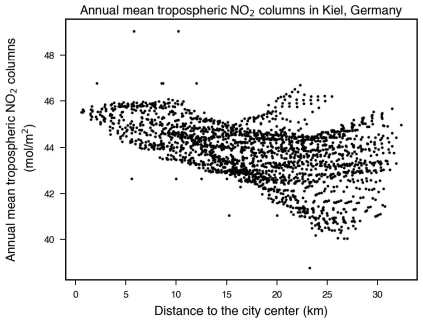

(b) Kiel, Germany

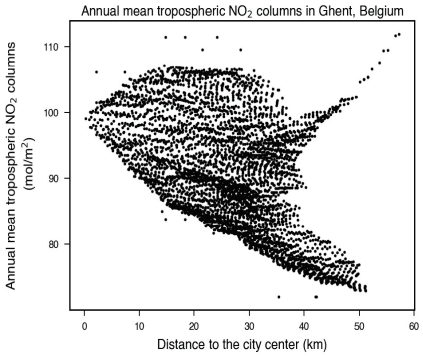

(c) Ghent, Belgium

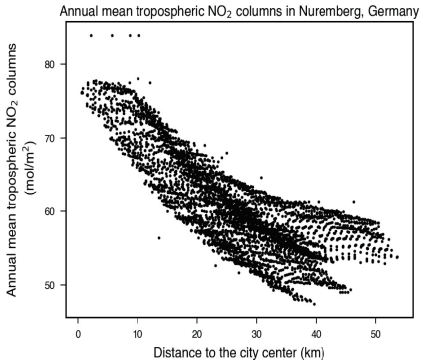

(d) Nuremberg, Germany

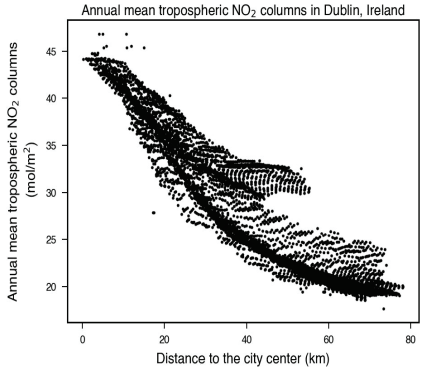

(e) Dublin, Ireland

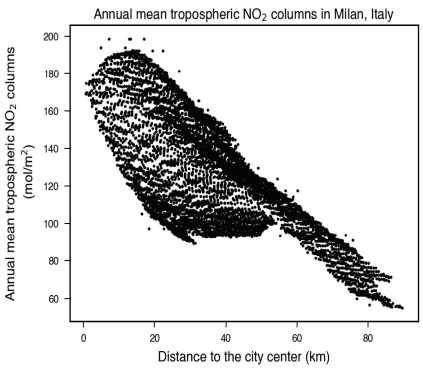

(f) Milan, Italy

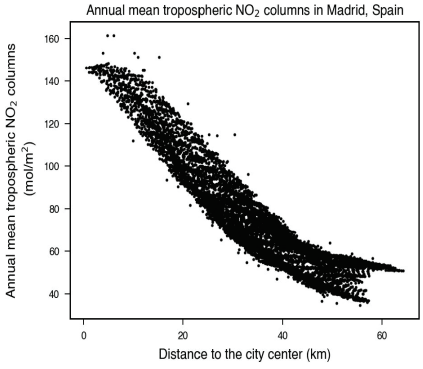

(g) Madrid, Spain

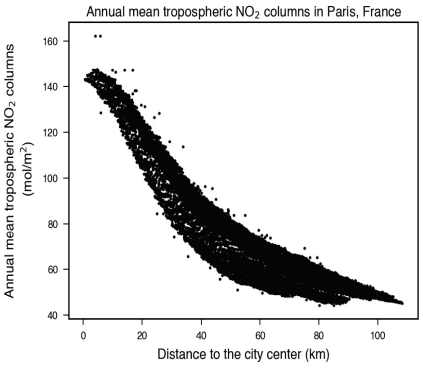

(h) Paris, France

Figure 3.21: Scatter plots of downscaled annual mean tropospheric NO_2 columns of sample cities

Due to the patterns of the points in Figure 3.21 we classify FUAs into 2 types: **regular** and **irregular**. We use this classification in Chapter 5. We define that if the NO_2 distribution inside a city can be described by the following standards, then this city is a regular city.

1. The NO_2 levels near the city center do not change a lot, or can increase a bit around the city center, and then the NO_2 levels should decrease evidently along the distance to the city center.
2. The NO_2 levels at the city fringe cannot be higher than those near the city center.
3. The distribution of point sets should be striped, not suddenly thick or thin.

Taking Figure 3.21 as an example, Nuremberg, Dublin, Madrid, and Paris are regular cities. Blackpool, Kiel, Ghent, and Milan are irregular cities. According to our judgment, among the 378 FUAs, 139 FUAs are regular cities, 239 are irregular cities.

The spatial distribution of NO_2 in regular cities is very similar to the spatial distribution of land use in cities (Lemoy and Caruso 2018). The fluctuation of NO_2 around the city center may be related to the complex built environment of the city center. For example, a town hall might appear next to a square or park (e.g. Hôtel De Ville, Esch-sur-Alzette (Luxembourg)), and the place where the traffic jam usually occurs is far from the city center (e.g. Rue de l'Arbed, Esch-sur-Alzette). The maximum traffic volume is also determined by factors such as road curvature and friction (Zhu and Zhang 2012). The reason for the weakening decline at the urban fringe may be that people prefer to live in the suburbs due to low housing prices, and the population activities in the suburbs generate NO_2.

Irregular cities are formed for many reasons, and they can be analyzed in conjunction with Figure 3.20 and population data from European Comission (2019). Taking Blackpool as an example, it is a seaside city and the city center is about 1 km away from the sea, which leads to the low NO_2 level in the city center. The high NO_2 in the southeast of the city is mainly caused by Preston (UK) in the southeast. Preston has a population of 385,143 and Blackpool has a population of 287,836, which may imply that larger cities produce more NO_2. The distribution of NO_2 in Ghent may also be explained by the influence of neighboring cities. Northeast of Ghent is heavily polluted, while Antwerp lies northeast of Ghent. Ghent has a population of 899,790 and Antwerp has a population of 1,817,176. Although Milan (5,121,996 residents) is surrounded by 5 cities, it seems that only its neighboring city to the east, Bergamo (Italy), has an impact on the distribution of NO_2 within Milan. This may also be because Bergamo is the largest of these neighbors (958,533 residents). The remaining four cities are Lecco (Italy) (172,672 residents), Lugano (Italy) (176,322 residents), Novara (Italy) (159,270 residents), and Pavia (Italy) (142,506 residents). However, FUAs may be flawed in how to define cities, for example when we need to

explain the distribution of NO_2 in Kiel. Kiel (376,867 residents) does not have any neighboring cities. The nearest city is Lübeck (Germany) (329,527 residents), which is about 10 km away in the southeast. However, Figures 3.20(b) and 3.21(b) shows that Kiel may be affected by three nearby NO_2 emission sources. We speculate that those emission sources may be factories. This may be because FUAs are defined by employment in and around the city center (European Comission 2019), while factories are less likely to be located in the city.

4 How city size and centrality affect land surface and tropospheric NO_2

In this chapter, we want to test the conclusions about NO_2 drawn in Chapter 2 using empirical data. We also explore how NO_2 changes with centrality.

4.1 Literature review and research gaps

4.1.1 Links between land surface and tropospheric NO_2

Both tropospheric NO_2 columns and NO_2 surface concentrations are the indicators of NO_2 levels, but they are measured in different ways.

Chemiluminescence is the reference method used by the monitoring stations in European Economic Area member countries to measure NO_2 surface concentrations (EU 2008). The details of chemiluminescence are in Appendix E. Simply speaking, chemiluminescence relies on two principles: NO reacts with O_3 to emit light; NO_2 can be converted into NO. So the first step is to react the sampled air with O_3, and calculate the NO concentration in the sampled air by calculating the intensity of emitted light. In the second step, all the NO_2 in the sampled air is converted into NO and react with O_3, and the light intensity is calculated again to obtain the NO concentration. The subtraction of these two NO concentrations can determine how much NO was converted from NO_2 in the second step, and thus we can get the NO_2 concentration in the sampled air.

The details for measuring tropospheric NO_2 vertical columns are in Appendix F. Simply speaking, there are 3 steps to measure tropospheric NO_2 vertical columns. First, total NO_2 slant columns are measured by a step called Differential Optical Absorption Spectroscopy (DOAS), which is a step to compare modeled and measured reflectance spectra. Second, a data assimilation system separates total NO_2 slant columns into tropospheric NO_2 slant columns and stratospheric NO_2 slant columns. Last, the satellite uses AMF tables to convert tropospheric NO_2 slant columns to tropospheric NO_2 vertical columns.

NO_2 columns are ideal to describe background NO_2 concentrations, but are not suitable to illustrate NO_2 near the land surface (Lövblad et al. 1997). Due to the way how NO_2 vertical

columns are obtained, NO_2 columns therefore, don't indicate the amount of NO_2 people breathe in (NASA 2020). They are actually the average of NO_2 concentrations over the optical path from land surface to the satellite's sensor (Lövblad et al. 1997). This means that even if the NO_2 surface concentration is 0 somewhere, the tropospheric NO_2 column cannot be 0 there, because NO_2 also exists in the troposphere. We can also see from Figure 3.10 that the minimum annual mean NO_2 column is 0.006 mol/m^2. *Therefore, this thesis does not contain any specification with an intercept of 0 when the NO_2 column is used as the dependent variable.*

In fact, to the best of our knowledge, we are probably one of the few articles comparing land surface and column concentrations of NO_2 in Europe. Only few studies compared NO_2 surface concentrations to tropospheric NO_2 columns (Blond et al. 2007; Paraschiv et al. 2017; Wallace and Kanaroglou 2009). Blond et al. (2007) compared annual mean NO_2 surface concentration measured by 439 monitoring stations in the UK, France, and the Netherlands with annual mean tropospheric NO_2 columns measured by the satellite SCIAMACHY, and found that the column is positively correlated with the surface concentration (coefficient: 0.33, R^2: 0.45), and if only the stations in rural background are considered, then the coefficient rises to 1.04 and R^2 increases to 0.90. Wallace and Kanaroglou (2009) also found positive relationship between these 2 NO_2 sources in Hamilton (Canada), and found that R^2 fluctuates between 0.20 and 0.35. The annual mean NO_2 surface concentration measured at the stations in traffic background is positively correlated to the annual mean NO_2 column, and R^2 is between 0.51 and 0.86 (i.e. 0.51 in Bucharest (Romania), 0.53 in Athens (Greece), 0.53 in Rotterdam (the Netherlands), 0.58 in Lisbon (Portugal), 0.65 in Rome (Italy), 0.69 in Paris (France), 0.81 in Madrid (Spain), 0.86 in Berlin (Germany)) (Paraschiv et al. 2017).

Many factors influence the relationship between land surface and tropospheric NO_2. Zhao et al. (2020) found that adding wind speed and direction to the image of tropospheric NO_2 columns significantly increases the fitness of these 2 kinds of NO_2 data. Zhao et al. (ibid.) rotated the satellite pixels around the monitoring station according to the wind direction and speed data collected from the meteorological model. Rainfall washes away land surface NO_2, causing a negative relationship between precipitation and NO_2 (Song et al. 2011; Wei et al. 2011). Rainfall also raises relative humidity, and relative humidity changes air temperature (Harkey et al. 2015). Temperature also has an impact on NO_2, and the impact is inseparable from diurnal circulation (Delaney and Dowding 1998), season (Ahmad and Aziz 2013), and sunshine (Harkey et al. 2015). In addition, the cloud cover presented during rainfall influences the fitness of tropospheric NO_2 columns and NO_2 surface concentrations (Markovic et al. 2008). Nevertheless, in this paper we use observed annual mean NO_2 surface concentrations and annual mean NO_2 columns (including atmospheric, climate and seasonal effects) as the data sources. This is because we

hope that our assessment of NO_2 is objective and realistic, and can serve as an intuitive reference that can be used by urban planners and policy makers.

4.1.2 Population effects on socioeconomics and environment

We show in Section 1.2.2 that there is a positive correlation between urban population size and CO_2 emissions. As early as 1976, Bornstein and Bornstein (1976) found a positive correlation between population size and pedestrian walking speed. Bettencourt et al. (2007) used Equation 1.9 and data from China, Germany, and the U.S. to link population size with 23 factors related to economy (e.g. wages, employment rates), health (e.g. the number of AIDS cases), scientific research (e.g. the number of patents, research funding), and energy (e.g. household water and electricity consumption).

$$Q = \kappa P^{\lambda} \tag{1.9}$$

Bornstein and Bornstein (1976) found that the when the indicator is related to wealth and innovation, the value of λ in Equation 1.9 is greater than 1, and when the indicator is related to infrastructure, the value of λ is less than 1. Equation 1.9 can also explore the relationship between city size and environment. Louf and Barthelemy (2014b) summarized the published literature on whether large cities emit less CO_2 per capita or smaller cities emit less CO_2 per capita, and pointed out that air pollution emissions may be underestimated when traffic congestion is ignored. Louf and Barthelemy (ibid.) also explained through Equation 1.9 that different definitions of cities will lead to diametrically opposite conclusions on the question of whether big cities are greener or not. Rybski et al. (2017) classified urban population according to the level of economic development and pointed out that the relationship between CO_2 and the level of urban development conforms to the environmental Kuznets curve (i.e. the per capita CO_2 emissions in developed countries is negatively correlated with population size, while the per capita CO_2 emissions in developing countries is positively correlated with population size).

However, as can be seen from the few relevant studies in Table 2.2, the impact of urban population on NO_2 levels seems to have received insufficient attention. Only Lamsal et al. (2013) explored NO_2 using the Equation 1.9, and pointed out that NO_2 is positively correlated with population size. But Lamsal et al. (ibid.) did not use the NO_2 surface concentration measured by the station, and because of the early publication time, the data from the Sentinel-5P satellite with higher spatial resolution was not used. Therefore, in this chapter, we use data from monitoring stations and Sentinel-5P to study the relationship between population and NO_2 levels.

4.1.3 Centrality effect on NO_2

Apart from a theoretical model (Schindler and Caruso 2014), so far we have found only 2 studies introducing the relationship between centrality and NO_2. 1 empirical study focuses on 6 U.S. cities (Wang et al. 2020c) and the other one considers Germany (Borck and Schrauth 2021). For each U.S. city, Wang et al. (2020c) drew straight lines from the city center to the urban fringe, and calculated the NO_2 surface concentration on these lines. (ibid.) found that annual average NO_2 levels are highest in urban centers and decrease along centrality. However, (ibid.) did not use equations or specifications to quantify the impact of centrality, so applying this method to other cities or the 378 cities in this thesis is quite inefficient. Plus, Wang et al. (ibid.) didn't consider population size. Although Borck and Schrauth (2021) pointed out that the centrality and hourly average NO_2 surface concentration can be expressed by ln-ln relationship and the coefficient is -0.00321, Borck and Schrauth (ibid.) did not consider population size as well.

Hien et al. (2020) used a LUR model to show that the distribution of annual mean NO_2 surface concentration within Hanoi (Vietnam) decreases with centrality, and the NO_2 at the urban fringe is about 50% to 60% of that in the city center. However, so far we have not found any research on the relationship between NO_2 at the urban fringe and centrality of European cities. Therefore, in this chapter, we also use data from monitoring stations and Sentinel-5P to study the relationship between centrality and NO_2 levels.

4.2 Methods

4.2.1 Data

In this chapter we use annual mean NO_2 surface concentrations (G) and annual mean tropospheric NO_2 columns (at the resolution of 7 km x 7 km) (C) as the data sources of NO_2. Centrality is denoted as R. Population size is noted as P. Background NO_2 is denoted as C_{min}. We include dummy variables as the backgrounds of NO_2 monitoring stations. For details of the data, see Chapter 3.

4.2.2 NO_2 per FUA comparison

To find out to what extent annual mean NO_2 surface concentration and annual mean tropospheric NO_2 column of each city are correlated, we overlay the NO_2 column layer on top of the land surface NO_2 layer. We then select the monitoring stations overlapping with the column layer, and the column pixels overlapping with the land surface layer, and calculate the mean of the overlapping stations per city and the mean of the overlapping pixels per city. We then regress the 378 mean values of overlapping pixels on the 378 mean values of overlapping stations. We

also add population size as another independent variable to see how population affects the regression.

We use the R package *sandwich* (Zeileis et al. 2021) when regressing. This package provides information about heteroscedasticity (Mohr 2018).

We then perform the regressions of mean of annual mean NO_2 columns per FUA overlaid with the stations (C_f), mean of annual mean NO_2 surface concentrations per FUA overlaid with the columns (G_f), and P using Equations 4.1 to 4.4,

$$C_f = \kappa_0 \, G_f + \epsilon \tag{4.1}$$

$$C_f = \kappa_0 \, G_f + \kappa_1 \, P + \epsilon \tag{4.2}$$

$$log_{10}C_f = \kappa_0 \, log_{10}G_f + \epsilon \tag{4.3}$$

$$log_{10}C_f = \kappa_0 \, log_{10}G_f + \kappa_1 \, log_{10}P + \epsilon \tag{4.4}$$

where κ_0 and κ_1 are coefficients, ϵ is error term.

4.2.3 Regressing NO_2 on city size and centrality

We then focus on the whole study area. Due to the results of Chapter 2, we regress common logarithmic G ($\log_{10}$G) and common logarithmic C ($\log_{10}$C) against the common logarithmic R ($\log_{10}$R) and common logarithmic P ($\log_{10}$P) respectively and together.

For the regressions of $\log_{10}$G, We use dummy variables to show different backgrounds of monitoring stations. Stations in mixed background are the reference of the dummy variables.

For the regressions of $\log_{10}$C, we include the common logarithmic C_{min} ($\log_{10}C_{min}$) as the background factor. Equations 4.5 to 4.14 are the specifications to regress $\log_{10}$G and $\log_{10}$C. We exclude the cells having the values of C_{min} when performing Equation 4.14,

$$log_{10}G = \kappa_0 \, log_{10}R + \epsilon \tag{4.5}$$

$$log_{10}G = \kappa_0 \, log_{10}R + \sum_{j=1}^{2} \lambda_j \delta_j + \epsilon, (j \in [1,2]) \tag{4.6}$$

$$log_{10}G = \kappa_0 \, log_{10}P + \epsilon \tag{4.7}$$

$$log_{10}G = \kappa_0 \, log_{10}P + \sum_{j=1}^{2} \lambda_j \delta_j + \epsilon, (j \in [1,2]) \tag{4.8}$$

$$log_{10}G = \kappa_0 \, log_{10}R + \kappa_1 \, log_{10}P + \epsilon \tag{4.9}$$

$$log_{10}G = \kappa_0\, log_{10}R + \kappa_1\, log_{10}P + \sum_{j=1}^{2} \lambda_j \delta_j + \epsilon, (j \in [1,2]) \tag{4.10}$$

$$log_{10}C = \kappa_0\, log_{10}R + \epsilon \tag{4.11}$$

$$log_{10}C = \kappa_0\, log_{10}P + \epsilon \tag{4.12}$$

$$log_{10}C = \kappa_0\, log_{10}R + \kappa_1\, log_{10}P + \epsilon \tag{4.13}$$

$$log_{10}C = \kappa_0\, log_{10}R + \kappa_1\, log_{10}P + \kappa_2\, log_{10}C_{min} + \epsilon \tag{4.14}$$

where κ_0 to κ_2 are coefficients, ϵ means error term, δ_j means dummy variable associated with the j^{th} kind of station background, λ_j means differential intercept coefficient of δ_j, and there are 2 dummy variables in total[1].

4.2.4 Predicted and measured tropospheric NO_2 comparison

After we get the regression results, we calculate predicted annual mean tropospheric NO_2 columns ($\hat{C}$) through Equation 4.13 and compare them with the measured C. Unlike stations that cannot cover the entire spatial extent of a city, the pixels of satellite imagery can cover the entire area of a city with constant spatial resolution, so they are very suitable to evaluate the regression. *In fact, in a trial, we also tried to calculate predicted annual mean NO_2 surface concentrations ($\hat{G}$) through Equation 4.9, and compare them with the measured G. However, due to the uneven distribution of stations within the city, the deviation between $\hat{G}$ and G was too large. This is because the location of monitoring stations have to fit some EU criteria. European Commission (2010) defines that the NO_2 concentrations measured by the monitoring stations represent the NO_2 exposure of general population, the NO_2 quality near a road of at least 100 meters in traffic background, and the NO_2 concentrations at an industrial site with an area of at least 250 m x 250 m.*

We then rank cities in ascending order of population size and choose the first, the middle, and the last 10^{th} percentiles of the cities, and calculate the average values of each group as the representatives of small (group S), medium (group M), and large (group L) cities. The average values of population for groups S, M, and L are 93,744.5, 341,002.5, and 4,312,730.1 respectively. The details of the 3 groups are listed in Table 4.1.

We then bring the average values of groups S, M, and L and their R values to Equation 4.13 to get $\hat{C}$. Then, for each group, we plot the average and SD (i.e. error bar) of C every 5 km.

[1]Because we have 3 kinds of monitoring station backgrounds, so we set 2 dummy variables to avoid multicollinearity.

Table 4.1: Group S, M, and L

Group	Range of percentile	No. of FUAs	Min P	Max P	Ave P	Min R (m)	Max R (m)
S	min to 10^{th}	38	67160.9	111179.4	93744.5	636.3	35036.3
M	45^{th} to 55^{th}	38	300393.4	380293.0	341002.5	179.2	56429.2
L	90^{th} to max	38	1687394.8	14921595	4312730.1	495.8	121995.8

4.3 Results and discussion

4.3.1 NO_2 per FUA comparison

Table 4.2 shows the results of Equations 4.1 and 4.2. Table 4.3 shows the results of Equations 4.3 and 4.4.

Table 4.2: Regressions of C_f with G_f and P

		C_f	
		(4.1)	(4.2)
coefficients			
	intercept	24.5667***	27.0337***
		(3.1726)	(2.9456)
	G_f	1.1739***	0.8795***
		(0.1242)	(0.1203)
	P	n/a	6.1807e-06***
		n/a	(7.6155e-07)
relative importance			
	G_f	n/a	0.4635
	P	n/a	0.5365
R^2		0.1919	0.3126
		378 FUAs, 33 countries, 1085 cells	
		***$\rho < 0.001$ **$\rho < 0.01$ *$\rho < 0.05$ $^{+}\rho < 0.1$	

Table 4.2 shows that C_f is positively correlated with G_f and P. G_f and P pass the test of significance at the level of 0.1%. G_f can explain around 20% of C_f by itself. The result of Column

4.2 shows after adding P, G_f and P together can explain more than 30% of C_f, and the slope of G_f drops slightly from 1.17 to 0.88.

The results of relative importance show that, comparing with G_f, P has more explanatory ability in influencing C_f, but the difference of the relative importance between P and G_f is less than 10%.

The coefficient of G_f in Column 4.2 is similar to the value (i.e. 1.04) of Blond et al. (2007), and R^2 in Column 4.2 is similar to the one of the results (i.e. 0.35) of Wallace and Kanaroglou (2009).

Table 4.3: Regressions of $\log_{10}C_f$ with $\log_{10}G_f$ and $\log_{10}P$

	$\log_{10}C_f$	
	(4.3)	(4.4)
coefficients		
intercept	0.9627***	0.1717^{+}
	(0.0678)	(0.0979)
$\log_{10}G_f$	0.5320***	0.3449***
	(0.0499)	(0.0478)
$\log_{10}P$	n/a	0.1868***
	n/a	(0.0183)
relative importance		
$\log_{10}G_f$	n/a	0.3946
$\log_{10}P$	n/a	0.6054
R^2	0.2320	0.3995
	378 FUAs, 33 countries, 1085 cells	

$^{***}\rho < 0.001$ $^{**}\rho < 0.01$ $^{*}\rho < 0.05$ $^{+}\rho < 0.1$

Table 4.3 shows that $\log_{10}C_f$ is positively correlated with $\log_{10}G_f$ and $\log_{10}P$. $\log_{10}G_f$ and $\log_{10}P$ pass the test of significance at the level of 0.1%. $\log_{10}G_f$ can explain around 23% of $\log_{10}C_f$ by itself. The result of Column 4.4 shows after adding $\log_{10}P$, $\log_{10}G_f$ and $\log_{10}P$ together can explain nearly 40% of $\log_{10}C_f$, and the slope of $\log_{10}G_f$ drops from 0.53 to 0.34.

The results of relative importance show that, the influence of population becomes more evident in Column 4.4 than in Column 4.2. The difference of the relative importance between $\log_{10}P$ and $\log_{10}G_f$ is around 20%.

So far we haven't found any article comparing G and C using the $\log_{10}-\log_{10}$ relationship, we think the $\log_{10}-\log_{10}$ relationship is better for comparing G and C than the non-logarithmic relationship as it stresses the relative importance of P.

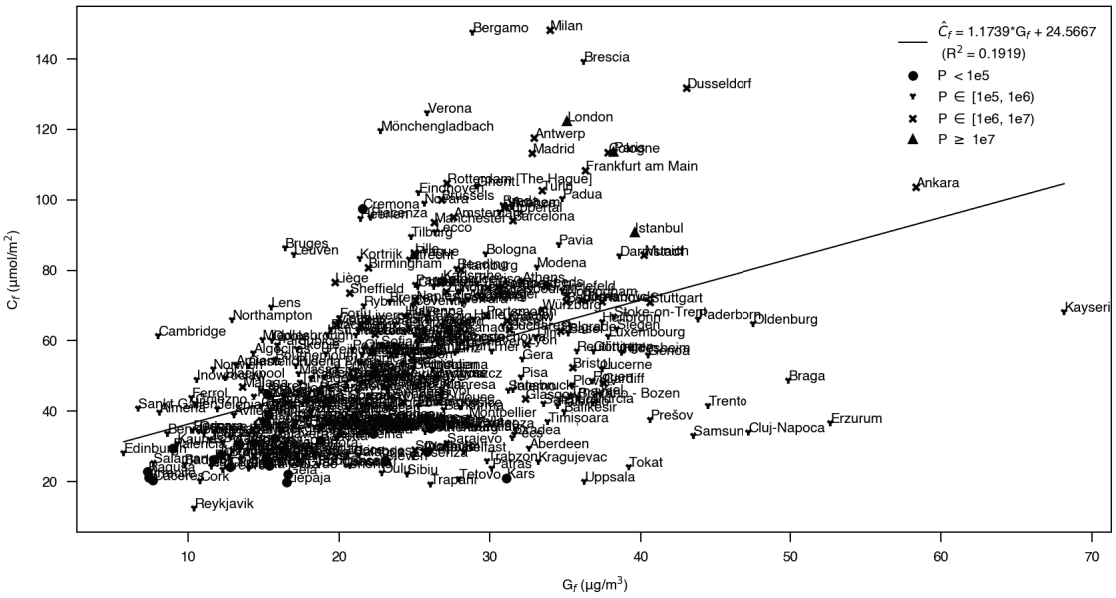

Figure 4.1: Plot of the regression of C_f with G_f

We plot the regression result of Column 4.1 in Figure 4.1. Figure 4.1 shows that in most cases G_f is less than 40 μg/m^3 and C_f is less than 75 μmol/m^2. When P is small, the points tend to stay close with the line, and when P increases, the points spread. This figure shows that P is an important factor in deciding C_f and G_f.

When examining Figure 4.1, we can find the top 3 FUAs with the highest values of C_f (Bergamo, Milan, and Brescia (Italy)) and the top 2 FUAs with the highest values of G_f (Ankara and Kayseri (Türkiye)) are all located in the Southern Europe. Cyrys et al. (2012) also indicated high NO_2 concentrations in Southern Europe and Mediterranean cities, and attributed these phenomena to transportation, climate conditions, compact built-up environment, and diesel cars. Diesel cars emit more NO_2 than gasoline cars (Bares et al. 2018), and today's diesel cars have a higher NO_2/NO_x emission ratio than the past ones (Degraeuwe et al. 2016).

The coefficient of G_f in Figure 4.1 is similar to the value (i.e. 1.04) of Blond et al. (2007), and R^2 in Figure 4.1 is similar to one of the results (i.e. 0.19) of Wallace and Kanaroglou (2009).

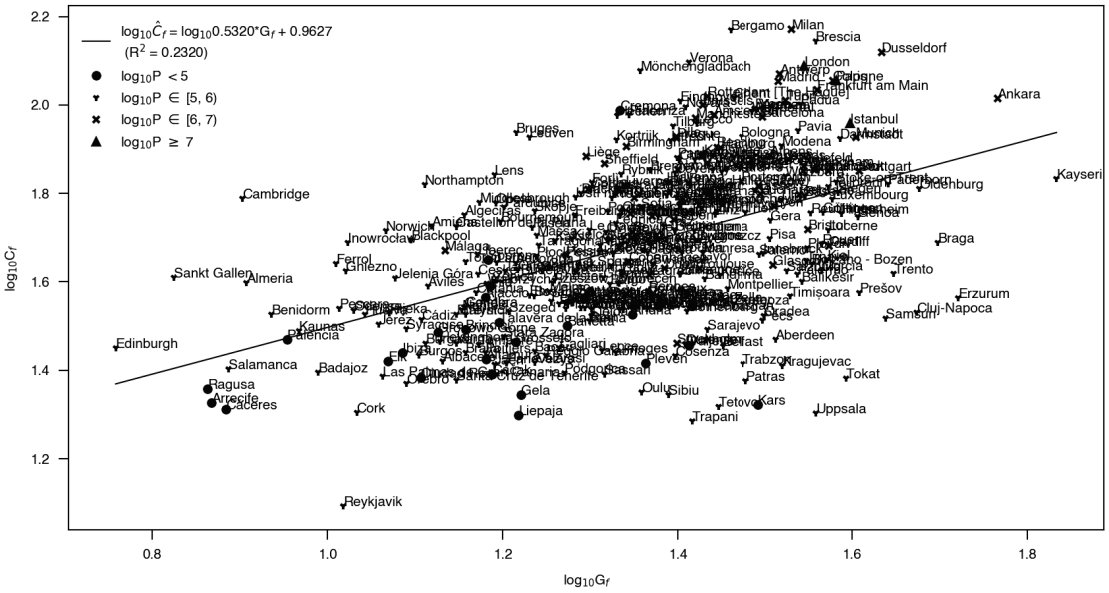

Figure 4.2: Plot of the regression of $\log_{10}C_f$ with $\log_{10}G_f$

We plot the regression result of Column 4.3 in Figure 4.2. Compared with Figure 4.1, we can find that the points are more evenly distributed, and the NO_2 levels of small and medium-sized cities can be clearly distinguished in Figure 4.2.

Given the small number of countries covered by current articles comparing G and C (e.g. 3 countries in Blond et al. (2007), 1 country in Wallace and Kanaroglou (2009), and 8 countries in Paraschiv et al. (2017)), we believe that the $\log_{10}$-$\log_{10}$ relationship is more suitable to compare G and C in regional studies.

4.3.2 Regressing NO_2 on city size and centrality

Tables 4.4 and 4.5 are the regressions results of Equations 4.5 to 4.14.

Table 4.4: Regressions of $\log_{10}$G with $\log_{10}$R, $\log_{10}$P

	$\log_{10}$G					
	(4.5)	(4.6)	(4.7)	(4.8)	(4.9)	(4.10)
coefficients						
intercept (dummy variable-mixed bg.)	1.6537***	1.3581***	0.5622***	0.4831***	0.7278***	0.5890***
	(0.0380)	(0.0331)	(0.0574)	(0.0452)	(0.0524)	(0.0430)
$\log_{10}$R	-0.0734***	-0.0189*	n/a	n/a	-0.1763***	-0.1162***
	(0.0100)	(0.0085)	n/a	n/a	(0.0097)	(0.0083)
$\log_{10}$P	n/a	n/a	0.1372***	0.1343***	0.2208***	0.1911***
	n/a	n/a	(0.0096)	(0.0075)	(0.0098)	(0.0081)
dummy variable-traffic bg.	n/a	0.2379***	n/a	0.2458***	n/a	0.2201***
	n/a	(0.0098)	n/a	(0.0087)	n/a	(0.0083)
dummy variable-industrial bg.	n/a	-0.0475**	n/a	-0.0269*	n/a	0.0021
	n/a	(0.0150)	n/a	(0.0136)	n/a	(0.0129)
relative importance						
$\log_{10}$R	n/a	0.0554	n/a	n/a	0.3463	0.1155
$\log_{10}$P	n/a	n/a	n/a	0.2620	0.6537	0.3093
dummy variables	n/a	0.9446	n/a	0.7380	n/a	0.5752
R^2	0.0371	0.3555	0.1275	0.4742	0.2943	0.5395

378 FUAs, 33 countries, 1397 stations in total, 674 stations in mixed background, 566 stations in traffic background, 157 stations in industrial background

$^{***}\rho < 0.001$ $^{**}\rho < 0.01$ $^{*}\rho < 0.05$ $^{+}\rho < 0.1$

In Table 4.4, all 4 specifications having $\log_{10}$R show $\log_{10}$R is negatively correlated with $\log_{10}$G. The coefficients of $\log_{10}$R range from -0.1763 to -0.0189. 3 of 4 $\log_{10}$R coefficients pass the test of significance at the level of 0.1%. All 4 specifications considering $\log_{10}$P show larger cities have higher levels of $\log_{10}$G. The coefficients of $\log_{10}$P range from 0.1343 to 0.2208. All the coefficients of $\log_{10}$P pass the test of significance at the level of 0.1%. Comparing with Column 4.9, the introduction of dummy variables dampens both the negative profile of $\log_{10}$R and the positive profile of $\log_{10}$P. All the coefficients of dummy variables of traffic background fluctuate between 0.22 and 0.25, and are statistically significant at the level of 0.1%.

Among the 6 specifications, the one of $\log_{10}$R, $\log_{10}$P, and dummy variable has the strongest ability of estimating $\log_{10}$G. This specification has a $\log_{10}$R coefficient of -0.1162 and a $\log_{10}$P coefficient of 0.1911. It also indicates concentrations measured at the traffic background station are 22% higher than the $\log_{10}$G measured at the mixed background station.

The coefficient of $\log_{10}$P in Column 4.10 is close to the one we derived (i.e. 0.1587 in Column 2.8) from the meta-analysis. The difference between these two coefficient values may be partly due to the different ways of counting P (Louf and Barthelemy 2014b). Other possible reasons are the differences in wind speed (Figure 3.8) and climate types (Figure 3.6), etc.

If we express the coefficient of $\log_{10}$P in Column 4.10 according to Equation 1.9 we get a value of 1.5527 for λ. According to the points of Bornstein and Bornstein (1976), we infer that this indicates land surface NO_2 levels are related to the way of creating wealth or other socioeconomic factors.

Table 4.5: Regressions of $\log_{10}C$ with $\log_{10}R$, $\log_{10}P$, and $\log_{10}C_{min}$

	$\log_{10}C$			
	(4.11)	(4.12)	(4.13)	(4.14)
coefficients				
intercept	1.7142***	0.7195***	1.2004***	0.1585***
	(0.0176)	(0.0131)	(0.0164)	(0.0080)
$\log_{10}R$	-0.0082*	n/a	-0.1823***	-0.1453***
	(0.0040)	n/a	(0.0040)	(0.0018)
$\log_{10}P$	n/a	0.1620***	0.2161***	0.1354***
	n/a	(0.0022)	(0.0024)	(0.0011)
$\log_{10}C_{min}$	n/a	n/a	n/a	0.8692***
	n/a	n/a	n/a	(0.0027)
relative importance				
$\log_{10}R$	n/a	n/a	0.1314	0.0295
$\log_{10}P$	n/a	n/a	0.8686	0.1623
$\log_{10}C_{min}$	n/a	n/a	n/a	0.8082
R^2	0.0002	0.1796	0.2434	0.8531

378 FUAs, 33 countries, 24816 cells for (9)-(11), 24238 cells for (12)
$^{***}\rho < 0.001$ $^{**}\rho < 0.01$ $^{*}\rho < 0.05$ $^{+}\rho < 0.1$

In Table 4.5, all the specifications considering $\log_{10}R$ indicate $\log_{10}R$ is negatively correlated with $\log_{10}C$. The coefficients of $\log_{10}R$ range from -0.1823 to -0.0082. 2 of 3 $\log_{10}R$ coefficients pass the test of significance at the level of 0.1%. All the specifications considering $\log_{10}P$ show larger cities have higher levels of $\log_{10}C$. The coefficients of $\log_{10}P$ range from 0.1354 to 0.2161. All the $\log_{10}P$ coefficients pass the test of significance at the level of 0.1%. Comparing with Column 4.13, $\log_{10}C_{min}$ restrains the profile of both the $\log_{10}R$ and $\log_{10}P$. Its coefficient is 0.8692 and it passes the test of significance at the level of 0.1%.

R^2 values show when specifications contain only 1 independent variable, $\log_{10}R$ is much less capable of explaining $\log_{10}C$ than $\log_{10}P$. $\log_{10}R$ and $\log_{10}P$ together can explain nearly 30% of $\log_{10}C$. Adding $\log_{10}C_{min}$ improves explanatory ability evidently. The specification of $\log_{10}R$, $\log_{10}P$, and $\log_{10}C_{min}$ is the best to forecast $\log_{10}C$. This specification has a $\log_{10}R$ coefficient of -0.1453 and a $\log_{10}P$ coefficient of 0.1354. The relatively high R^2 in Column 4.14 may indicate the importance of background NO_2. Also, after we consider background NO_2, the effect of $\log_{10}P$ becomes less strong.

The patterns of relative importance in Tables 4.4 and 4.5 are quite similar. $\log_{10}P$ is always more important than $\log_{10}R$ regardless of the NO_2 sources. The explanatory ability of dummy variables and $\log_{10}C_{min}$ are higher than $\log_{10}P$, if any of them appears in the specifications. This means the ground NO_2 levels are mainly determined by the background of the monitoring

station while the tropospheric NO_2 levels depend heavily on background NO_2. R is not an influential factor in affecting the NO_2 levels. The relative importance of $\log_{10}$P in Column 4.14 is lower than the one in Column 4.10.

The coefficient of $\log_{10}$P is still close to the one we derived from the meta-analysis (i.e. 0.1587 in Column 2.8). Compared with Table 4.4, 1 new factor causing the difference between the two coefficients is the troposphere. This is due to the fact that Table 4.5 uses tropospheric NO_2 columns, while the values used in the meta-analysis are NO_2 surface concentrations. These 2 kinds of data are collected in different ways (Section 4.1.1).

If we express the coefficient of $\log_{10}$P in Column 4.14 according to Equation 1.9, we get a value of 1.3658 for λ. According to the points of Bornstein and Bornstein (1976), we infer that this may indicate tropospheric NO_2 levels are also related to the way of creating wealth or other socioeconomic factors. The 2 similar λ values (i.e. 1.5527 and 1.3658) also show the coherence of G and C.

4.3.3 Regression summary

The coefficients of $\log_{10}$R in Tables 4.4 and 4.5 are always negative. This results confirms the theory proposed by Schindler et al. (2017) and the results of Borck and Schrauth (2021) and Wang et al. (2020c). We have only found 1 paper so far stating that centrality and hourly average NO_2 surface concentration can be expressed by the ln-ln relationship with a coefficient of -0.00321 (Borck and Schrauth 2021), and our coefficients of $\log_{10}$R are lower than theirs (-0.1162 in Column 4.10 and -0.1453 in Column 4.14). One of the reasons is that our specifications are different. Borck and Schrauth (ibid.) used independent variables including population density, distance to the city center and distance to street but did not consider population size.

$\log_{10}$R is always the least important factor when other variables are in the specifications. The R^2 value reveals that $\log_{10}$R can only explain 4% $\log_{10}$G and 0.02% $\log_{10}$C if it is the only variable in the specification. This may be due to the fact that the NO_2 concentration may drop rapidly within 200 m from the main road (Bermejo-Orduna et al. 2014; Gilbert et al. 2003; Laffray et al. 2010). The ability of satellite data to explain centrality is weaker than that of stations data is partly due to differences in the way satellites and stations collect NO_2 data (Section 4.1.1). NO_2 columns don't indicate the amount of NO_2 people breathe in (NASA 2020). They are actually the average of NO_2 concentrations over the optical path from land surface to the satellite's sensor (Lövblad et al. 1997). Another possible explanation is that satellites are subject to more atmospheric factors when collecting NO_2 data, and the same climate conditions may have different influences on stations and satellites. For example, we have explained the impact

of rainfall on NO_2 data in Section 4.1.1, but for satellites, the cloud over the land surface during rainfall is also one of the influencing factors (Markovic et al. 2008).

$\log_{10}P$ is always more important in deciding the NO_2 levels when $\log_{10}P$ and $\log_{10}R$ appear simultaneously. Among all of our specifications, $\log_{10}P$ always passes the test of significance at the level of 0.1% and its coefficient is constantly positive. The positive effect of city size on NO_2 ground and tropospheric concentrations have been reported in Cyrys et al. (2012) and Lamsal et al. (2013). There are many reasons that make city size more important than centrality. These factors include but are not limited to: First, huge volumes of anthropogenic activities brought by large population size increase NO_2 emissions. Second, NO_2 emissions from those anthropogenic activities could be exacerbated by urban canyons (Vintar Mally and Ogrin 2015) and large cities tend to have more urban canyons as a way of utilizing land intensively. Third, adsorbed and re-radiated solar energy from urban land use and anthropogenic heat are the main causes of UHI in cities (Rizwan et al. 2008). UHI can change thermal structure of cities and dispersion patterns of air pollutants (Ngarambe et al. 2021).

Dummy variables and $\log_{10}C_{min}$ are always the most important factor in affecting NO_2 concentrations if any of them appears in the specification. Monitoring stations at traffic background record higher NO_2 surface concentrations than other types of stations as NO_2 levels are mainly contributed by transportation in Europe (EEA 2016). Our results are similar to those of Cyrys et al. (2012), who showed that the NO_2 surface concentration depends largely on the background of the measuring site. However, for the coefficient of the dummy variable of the industrial monitoring station, we find its value can be positive or negative, and it doesn't pass the test of significance at the level of 0.1%. This is probably because the industrial areas are too far to affect the NO_2 in urban areas (Coppalle et al. 2001). Furthermore, only 157 of the 1,397 stations are located in industrial areas, and not all FUAs have stations in industrial areas (e.g. Paris, Figure 3.19(h)).

4.3.4 Regression-based prediction for NO_2

To visualize the effects of centrality and city size, we plot $\hat{G}$ according to Column 4.9 in Figure 4.3 and $\hat{C}$ according to Column 4.13 in Figure 4.4.

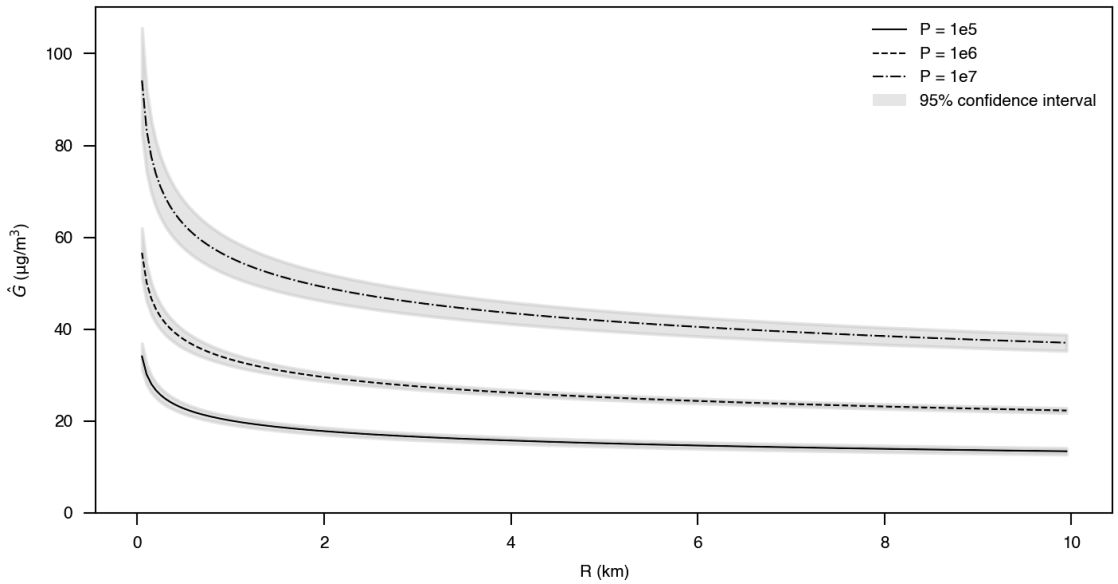

Figure 4.3: $\hat{G}$ at different R by Column 4.9

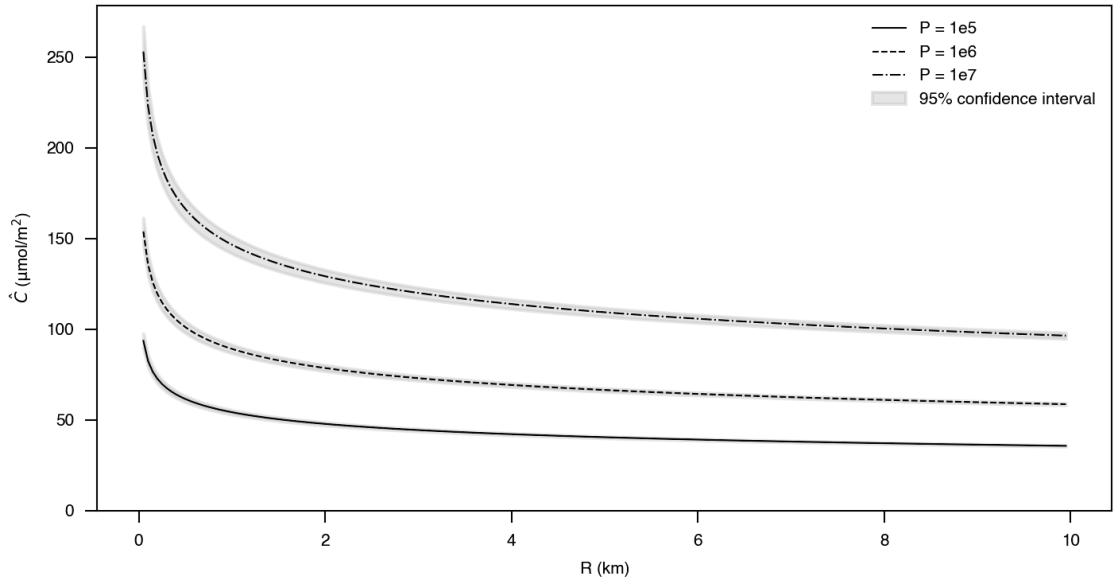

Figure 4.4: $\hat{C}$ at different R by Column 4.13

Figures 4.3 and 4.4 show how $\hat{G}$ and $\hat{C}$ vary for cities with populations of 100 thousand, 1 million and 10 million inhabitants residents. The variation of $\hat{G}$ and $\hat{C}$ with R is similar in both figures. The difference in NO_2 caused by population size is higher near the city center than in places far away. When R is the same, the $\hat{G}$ and $\hat{C}$ levels of big cities are always higher than those

of small cities. For each city, $\hat{G}$ and $\hat{C}$ decrease sharply near the city center and then the rate of decline of $\hat{G}$ and $\hat{C}$ decreases sharply. The attenuation of NO_2 levels off when R is larger than 4 km. As can be expected, the 3 curves of each figure are also highly unlikely to intersect at the far end.

However, Figures 4.3 and 4.4 are predicted values, but the reality is more complicated. For example, we can see from Figure 3.21 that the C_{min} value and the maximum value of C in Milan are higher than those in Paris. This is partly because the high mountains around Milan trap air pollutants, causing high NO_2 levels in the city center (Park et al. 2021). Area of FUAs also affects background NO_2. We can see that the area of Milan is smaller than the area of Paris (Figure 3.20). This shows that residents at the fringe of Paris tend to work in the center of Paris, but may live in suburban because of the low housing prices. Milan does not provide as many employment opportunities as Paris, so residents not far from the center of Milan may consider finding employment in neighboring cities. As a result, Milan's background is higher than that of Paris (Figure 3.21).

Figures 4.3 and 4.4 also show that the suburban of a large city may have the same level of NO_2 as the center of a small city. For example, the values of $\hat{C}$ at 500 meters from the center of a city with a population of 1 million are similar to the values of $\hat{C}$ at about 8 km from the center of a city with a population of 10 million. In fact, the reality is more complicated. For example, we know that the population of Paris is about 10 times that of Nuremberg (Figure 3.20). Figure 3.21 shows that C is still around 140 mol/m^2 at a distance of 8 km from the center of Paris, while the maximum C in Nuremberg is only 84 mol/m^2. We speculate that this may be partly due to the tall buildings in the center of Paris exacerbates NO_2 pollution levels, which may make commuting more expensive for residents living in large cities than predicted in Figure 4.4, if they want to reduce their NO_2 exposure.

When examining the patterns of the 95% Confidence Intervals (CIs), we find that first, in general, the width of CIs in Figure 4.3 is wider than the ones of Figure 4.4. This means the number of monitoring stations are much less than the quantity of satellite columns. Second, for each figure, the width of CIs of the larger cities is wider than the ones of the smaller cities. This indicates our data set includes more smaller cities than larger cities. Third, for Figure 4.3, the width of CIs is not consistent when moving from the city center to the places far away. This shows the spatial heterogeneity of the distribution of monitoring stations. All of these findings can be verified by observing the maps in Section 3.2.

To quantify and generalize the effects of centrality and city size on G and C, we calculate $\hat{G}$ and $\hat{C}$ for cities with a population of 100 thousand, 1 million and 10 million inhabitants at different R. The results of $\hat{G}$ and $\hat{C}$ are listed in Tables 4.6 and 4.7.

Table 4.6: $\hat{G}$ by Column 4.9 and relative changes at different R

	$\hat{G}$ ($\mu g/m^3$) and its relative change comparing to the left column				
R (km)	0.1	0.5	1	5	10
P = 1e5	30.1439	22.6972	20.0863	15.1242	13.3844
(% decrease)	(n/a)	(24.70%)	(11.50%)	(24.70%)	(11.50%)
P = 1e6	50.1187	37.7374	33.3964	25.1462	22.2536
(% decrease)	(n/a)	(24.70%)	(11.50%)	(24.70%)	(11.50%)
P = 1e7	83.3297	62.7439	55.5265	41.8092	36.9999
(% decrease)	(n/a)	(24.70%)	(11.50%)	(24.70%)	(11.50%)

Table 4.7: $\hat{C}$ by Column 4.13 and relative changes at different R

	$\hat{C}$ ($\mu mol/m^2$) and its relative change comparing to the left column				
R (km)	0.1	0.5	1	5	10
P = 1e5	82.4708	61.5004	54.2001	40.4183	35.6205
(% decrease)	(n/a)	(25.43%)	(11.87%)	(25.43%)	(11.87%)
P = 1e6	135.6438	101.1528	89.1456	66.4780	58.5868
(% decrease)	(n/a)	(25.43%)	(11.87%)	(25.43%)	(11.87%)
P = 1e7	223.1002	166.3711	146.6223	109.3397	96.3607
(% decrease)	(n/a)	(25.43%)	(11.87%)	(25.43%)	(11.87%)

Although $\hat{G}$ and $\hat{C}$ are derived from different NO_2 data sources, however, it is interesting to find some similarities from the relative changes in Tables 4.6 and 4.7. The relative changes of $\hat{G}$ when R increases from 100 m to 500 m are as same as the ones when R increases from 1 km to 5 km. The relative changes of $\hat{G}$ when R increases from 500 m to 1 km are equal to the ones when R increases from 5 km to 10 km. These 2 characteristics can also be found in the relative change of $\hat{C}$. Moreover, when R increases from 100 m to 500 m and from 1 km to 5 km, the relative changes of $\hat{G}$ and $\hat{C}$ are very close (i.e. 24.70% vs. 25.43%). We can also find the same patterns on the relative changes of $\hat{G}$ and $\hat{C}$ when R increases from 500 m to 1 km and from 5 km to 10 km (11.50% vs. 11.87%). The similarity of the relative changes of $\hat{G}$ and $\hat{C}$ are due to the similar coefficients of $\log_{10}$R and $\log_{10}$P in Equations 4.9 and 4.13. These are good results showing the coherence between land surface and tropospheric NO_2.

Given the above results, we think urban planners can rely on both to evaluate NO_2 levels. Monitoring stations are close to the emission sources and they may neglect the accumulated NO_2

up into the street canyon and other built environment (e.g. street geometry, proportion of diesel cars) and climate (e.g. topography, winds). That is a probable reason why the R^2 of Equation 4.10 is only 54%, comparing with the one of Equation 4.14 (85%) by Sentinel-5P. Sentinel-5P not only captures the effects of population size and centrality, but also includes the impacts from other sources such as climate. In other words, $\hat{G}$ guides people to choose a place considering surrounding environment while $\hat{C}$ is good at telling background NO_2 in a holistic view. Urban planners and policy makers can rely on NO_2 surface concentrations to evaluate the inhaled NO_2 of a specific location in a city, and count on NO_2 tropospheric columns to assess the level of sustainability and development of the city. And both kinds of NO_2 concentrations have similar abilities when required to show the effects of city size and centrality on NO_2.

4.3.5 Predicted and measured tropospheric NO_2 comparison

Figure 4.5 shows the comparison results of $\hat{C}$ and C every 5 km for the population group S, M, and L.

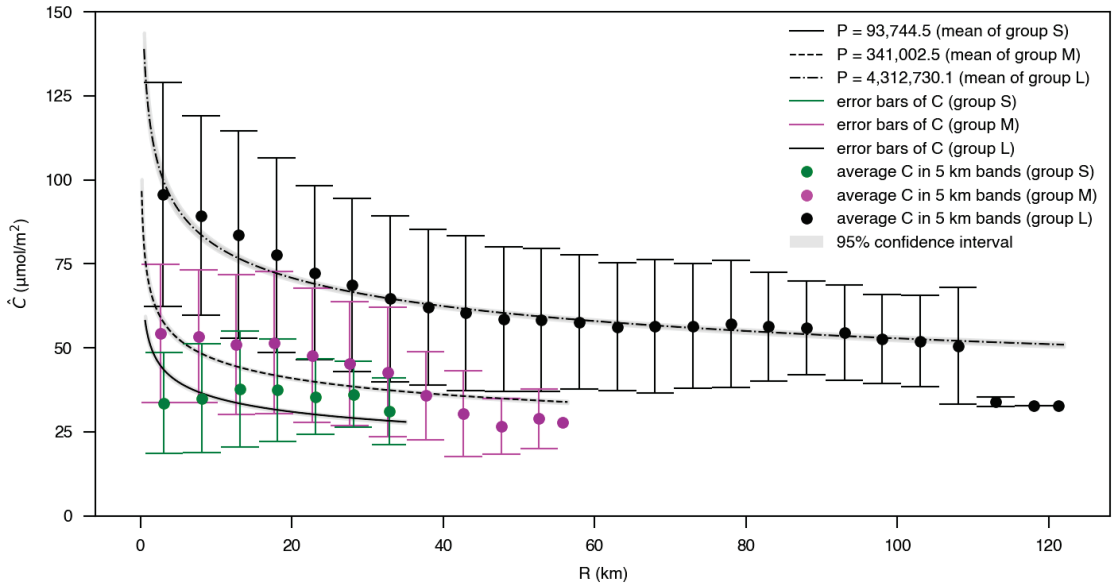

Figure 4.5: $\hat{C}$ by Column 4.13 and C

The values of R in Figure 4.5 are completely determined by the data, and we do not specify a maximum value for R as we do in Figures 4.3 and 4.4. Therefore we can find that cities with larger population expand further. The regression results of Equation 4.13 are credible as the mean values of C are situated closely with the predicted $\hat{C}$. The huge deviation of the last 3 points around the curve of group L are acceptable, because in this group only 10 tropospheric

columns have R values greater than 110 km. SE decreases with R. This is because more imagery cells appear as R increases.

The data points in Figure 4.5 show that the NO_2 levels at the urban fringes of Groups L and M are roughly 50% to 60% of those in the city center, which is the same as the results obtained in Hien et al. (2020), and we find that the variation of NO_2 with centrality in Group S is not obvious. This may be because the spatial resolution of the satellite imagery we use is 7 km x 7 km, and the R value of the S group is about 40 km. We also show in Figure 3.19 that 7 km x 7 km satellite resolution fails to reveal the detail of NO_2 variation with centrality in small cities.

4.4 Limitations

To our knowledge, this is the first paper exploring the effects of city size and the Euclidean distance to the city center on NO_2 data gained by monitoring stations and the satellite across European cities. However, our studies have some limitations. First, in this study we use FUAs as the definition of cities. Therefore, results may vary when defining cities in other ways (e.g. municipal boundaries (Branis and Linhartova 2012), population density (Lamsal et al. 2013) or satellite imagery (Bechle et al. 2011)). Second, we use logarithmic variables in the specifications. But because of the undefined *log(0)*, so the monitoring stations situated close to the city center and the NO_2 columns overlapped with the city center should be examined separately to find out the NO_2 concentration at the exact point of the city center, which shows that there are some difficulties in using power laws to predict real-world air pollution. Third, although Figures 3.18 and 3.20 show a certain correlation between wind speed and NO_2 levels, our specifications do not add wind correction. Our specifications also do not include the relationship between climate classification (e.g. Figure 3.17) and NO_2, although climate classification is related to the land surface feature, and the land surface feature affects the NO_2 column (Hong et al. 2017). Last, we believe that the intra-urban profiles of land surface NO_2 concentrations could be better described if more monitoring stations were built. Cyrys et al. (2012) made a similar point.

4.5 Suggestions for urban planners

We show that both land surface NO_2 and NO_2 columns are reliable and useful tools for exploring urban NO_2 levels. Monitoring stations are close to the emission sources, therefore they are suitable for describing changes in NO_2 concentration over short distances, while NO_2 columns are suitable for describing the extent of NO_2 in the whole city.

We also find out that our regression-based prediction underestimates the pollution levels in the central areas of large cities, thus residents living in large cities need to move farther than

predicted to obtain lower NO_2 exposure. We therefore suggest that urban planners should decrease NO_2 levels in the urban core (e.g. building green spaces (Sheridan et al. 2019), introduce congestion charges (Tonne et al. 2008)) and optimize the transportation network connecting the urban core and suburbs (e.g. subways). Finally, urban planners cannot only count on economic or population growth to gain reduced NO_2 levels, as so far we've found that relationship between NO_2 and city size does not conform to the environmental Kuznets curve.

4.6 Code availability

Code link for Table 4.1:
github.com/WeiYufei/PHD_Thesis_University_of_Luxembourg/blob/main/GroupSML_and_Boxplot.py.

Code links for Table 4.2:
1st column - github.com/WeiYufei/PHD_Thesis_University_of_Luxembourg/blob/main/Tab_Satellite_Station_C1.r,
2nd column - github.com/WeiYufei/PHD_Thesis_University_of_Luxembourg/blob/main/Tab_Satellite_Station_Pop_C2.r.

Code links for Table 4.3:
1st column - github.com/WeiYufei/PHD_Thesis_University_of_Luxembourg/blob/main/Tab_Satellite_Station_C1a.r,
2nd column - github.com/WeiYufei/PHD_Thesis_University_of_Luxembourg/blob/main/Tab_Satellite_Station_Pop_C2a.r.

Code links for Table 4.4:
1st column - github.com/WeiYufei/PHD_Thesis_University_of_Luxembourg/blob/main/Tab_Station_LOGNO2_LOGDIS_C3.r,
2nd column - github.com/WeiYufei/PHD_Thesis_University_of_Luxembourg/blob/main/Tab_Station_LOGNO2_LOGDIS_FIX_C4.r,
3rd column - github.com/WeiYufei/PHD_Thesis_University_of_Luxembourg/blob/main/Tab_Station_LOGNO2_LOGPOP_C5.r,
4th column - github.com/WeiYufei/PHD_Thesis_University_of_Luxembourg/blob/main/Tab_Station_LOGNO2_LOGPOP_FIX_C6.r,
5th column - github.com/WeiYufei/PHD_Thesis_University_of_Luxembourg/blob/main/Tab_Station_LOGNO2_LOGDIS_LOGPOP_C7.r,
6th column - github.com/WeiYufei/PHD_Thesis_University_of_Luxembourg/blob/main/

Tab_Station_LOGNO2_LOGDIS_LOGPOP_FIX_C8.r.

Code links for Table 4.5:
1st column - github.com/WeiYufei/PHD_Thesis_University_of_Luxembourg/blob/main/Tab_Satellite_LOGNO2_LOGDIS_C9.r,
2nd column - github.com/WeiYufei/PHD_Thesis_University_of_Luxembourg/blob/main/Tab_Satellite_LOGNO2_LOGPOP_C10.r,
3rd column - github.com/WeiYufei/PHD_Thesis_University_of_Luxembourg/blob/main/Tab_Satellite_LOGNO2_LOGDIS_LOGPOP_C11.r,
4th column - github.com/WeiYufei/PHD_Thesis_University_of_Luxembourg/blob/main/Tab_Satellite_LOGNO2_LOGDIS_LOGPOP_minFUA_C12.r.

Code link for Table 4.6:
github.com/WeiYufei/PHD_Thesis_University_of_Luxembourg/blob/main/Tab_calculatePredictedStation.r.

Code link for Table 4.7:
github.com/WeiYufei/PHD_Thesis_University_of_Luxembourg/blob/main/Tab_calculatePredictedRS.r.

Code link for Figure 4.1:
github.com/WeiYufei/PHD_Thesis_University_of_Luxembourg/blob/main/Fig_Satellite_Station_Pop_B_and_W.py.

Code link for Figure 4.2:
github.com/WeiYufei/PHD_Thesis_University_of_Luxembourg/blob/main/Fig_Satellite_Station_Pop_B_and_W1.py.

Code link for Figure 4.3:
github.com/WeiYufei/PHD_Thesis_University_of_Luxembourg/blob/main/Fig_EffectPlot_Model7_B_and_W.py.

Code link for Figure 4.4:
github.com/WeiYufei/PHD_Thesis_University_of_Luxembourg/blob/main/Fig_EffectPlot_Model11_B_and_W.py.

Code link for Figure 4.5:
github.com/WeiYufei/PHD_Thesis_University_of_Luxembourg/blob/main/GroupSML_and_Boxplot.py.

5 About the scaling of individual NO_2 profile

5.1 Literature review and research gaps

5.1.1 Motivation

In Chapter 4, we have found that larger cities have higher NO_2 levels, and NO_2 concentrations inside the city decrease with centrality, and we have tested how well the measured annual mean NO_2 columns match the predicted values using three sets of FUA population data. However, since we do not control population effect in Chapter 4, we cannot explore further the details of urban centrality and intra-urban NO_2 levels. In other words, if we follow Figure 4.4 to plot the NO_2 levels of cities of different sizes, the curves will not overlap, which make them difficult for us to compare side by side. After studying the relationship between air pollution indicators (i.e. $PM_{2.5}$, Air Quality Index (API)) and urban form attributes of 83 Chinese cities, Liu et al. (2018b) found that the relationship between air pollution indicators and urban form attributes showed consistency only when cities with similar populations were grouped together for analysis. Liu et al. (ibid.) also suggested that the impact of urban population size should be explained for a clear relationship between urban air pollution and urban form.

In fact, we can also see the direct or indirect impact of population on NO_2 levels by combining the data in Chapter 3 and the specifications in Chapter 4. For example, for Paris, whose population is about 10 times that of Nuremberg, the measured annual mean NO_2 column at a distance of 8 km from the city center is about 140 mol/m^2 (Figure 3.21(h)), which is higher than the concentration predicted by Column 4.13 (i.e. 103.84 mol/m^2). The highest annual average column concentration near the center of Nuremberg is 84 mol/m^2 (Figure 3.21(d)), but this value is lower than the predicted value by Column 4.13 (i.e. 105.80 mol/m^2 when R equals 500 m).

We have pointed out in previous chapters that human activities including car emissions, industrial processes (Section 1.1.3) and agricultural activities at the urban fringe (Section 3.1.4) are important contributors to NO_2 emissions. Another possible reason for high NO_2 levels in large cities is that cities with large populations have large built-up areas (Wania et al. 2014).

Large areas of impervious surfaces not only provide conditions for human activities that emit air pollution, but also create canyon effects (Karimimoshaver et al. 2021) and UHI (Clark 2020), which exacerbate NO_2 pollution levels. So in this chapter we explore the impact of population size on centrality.

Meanwhile, in Chapter 4, we have found that no matter we use NO_2 columns or NO_2 surface concentrations as the data source, the logarithm of centrality is always negatively correlated with the logarithm of NO_2 level. This offers us the possibility to describe the effect of centrality on NO_2 using simple models such as radial analysis. Although radial analysis may ignore NO_2 fluctuations far away from the city center (e.g. industrial emission sources), it can reflect the contribution of the city center to the overall pollution level of the city, thus providing the possibility of comparing cities side by side.

So far we have found some experiments using radial analysis to investigate UHI and land use inside the cities. The annual mean UHI intensity of Chinese cities decays exponentially from the built-up area to the area of 6 times the built-up area (Zhou et al. 2015). But Zhou et al. (ibid.) used the entire built-up area instead of a single point in the city center as the starting area for the radial analysis, which made the method unsuitable for the NO_2 analysis inside the city as the NO_2 changes obviously around the emission source (Colvile et al. 2001). Irwin and Bockstael (2007) and Schneider and Woodcock (2008) also used the urban core area rather than a point as the starting area for the radial analysis. Although Seto and Fragkias (2005) used the city center as the starting point for the radial analysis of the urban landscape, Seto and Fragkias (ibid.) built 3 buffer zones (i.e. 0 km to 3km, 3 km to 10 km, 10 km to 20 km) from the city center and summarized the landscape within these 3 buffer zones, this method thus could not continuously observe the changes of geographical phenomena with centrality. Although Jiao (2015) used a radial analysis starting from the city center to describe how urban land use density changes continuously with centrality, the function he used was too complicated. We hope to use a model as simple as possible to describe how population affects the relationship between centrality and NO_2 levels, so as to provide an intuitive and clear reference for citizens and urban planners.

5.1.2 Radial analysis and homothetic scaling of land use

Lemoy and Caruso (2018) proposed an innovative approach to study the relationship between artificial land use share and centrality. This method not only includes a radial analysis with the city center as the starting point, but also systematically describes the impact of population size on the relationship between centrality and artificial land use share.

In order to conduct profile analysis, Lemoy and Caruso (ibid.) made concentric rings with the city center as the start point, and the width of each ring was about 141 m. Lemoy and Caruso

(ibid.) then calculated the Euclidean distance from each ring to the city center and the artificial land use share within the ring. To find out population effects on artificial land use share and centrality, Lemoy and Caruso (2018) then performed homothetic scaling on artificial land use share of each ring and the Euclidean distance from the ring to the city center.

We have introduced the definition of homothetic scaling (i.e. homotheticity) in Section 1.2.4. In short, homothetic scaling makes the relationship between centrality and artificial land use share largely explained by the city's population, the largest city's population, and a scaling exponent, making the intra-urban land use distribution across cities presents similar characteristics (i.e. homotheticity) (Equations 1.10 and 1.11).

$$r' = \frac{r}{(\frac{N}{N_{London}})^{0.5}} \tag{1.10}$$

$$S_N(r') = \frac{S_N(r)}{(\frac{N}{N_{London}})^{0.5}} \tag{1.11}$$

The reason why Lemoy and Caruso (ibid.) chose 0.5 (i.e. the reciprocal of 2) as the scaling exponent is that the artificial land use share is a geographical phenomenon that occurs in 2-dimensional space and thus conforms to the **square-cube law**[1]. Lemoy and Caruso (ibid.) then performed homothetic scaling in both X and Y directions. The scaled centrality and artificial land use share are shown in Figure 1.4(b).

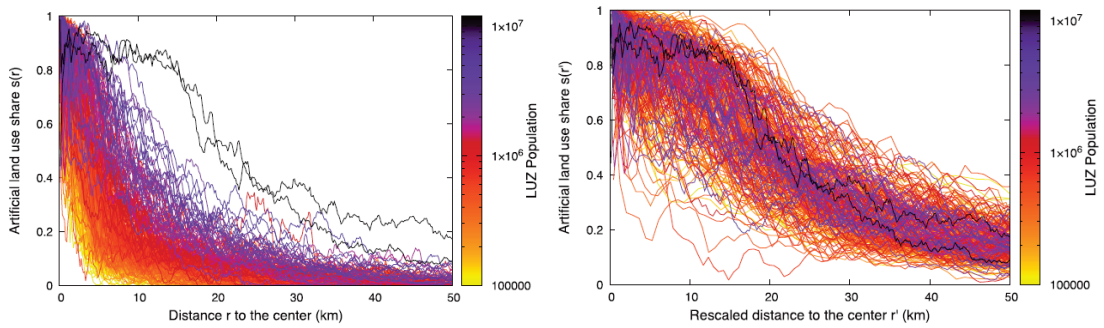

(a) S_N(r) and r (b) S_N(r′) and r′

Figure 1.4: Shares of built-up area as functions of the distance to the city center in 300 European cities (Lemoy and Caruso 2018)

[1] Area scales with the square of length while volume scales with the cube of length. (Hey 2023)

5.1.3 Ways to find/test a scaling exponent

SNR

Lemoy and Caruso (2018) tested the rationality of using 0.5 as the scaling exponent in Equations 1.10 and 1.11 using a method called SNR. Assuming α is the scaling exponent, Lemoy and Caruso (ibid.) stated that for a given rescaled Euclidean distance from the city center r', the rescaled proportion of build-up area of a city (population size N) at this rescaled distance $S_N(r')$ is the signal, and in this situation, the standard deviation $\sigma(S_\alpha(r))$ is the noise. The SNR is defined as the average value of signal over ratio between r' = 0 and r', such that the value of $S_\alpha(r)$ is a threshold value t. Lemoy and Caruso (ibid.) tried different combinations of α and t to get a variety of SNR values (Figure 5.1).

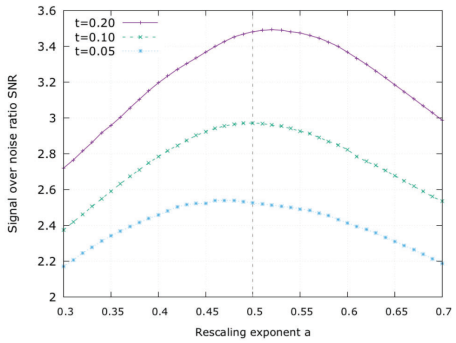

Figure 5.1: SNR for the artificial land use share (Lemoy and Caruso 2018)

Figure 5.1 shows the highest value of SNR appears when α is close to 0.5. Therefore 0.5 is a suitable scaling exponent in expressing the relationship between centrality and artificial land use share.

2-step linear regression (Lemoy and Caruso 2021)

Lemoy and Caruso (2021) proposed another way to find the scaling exponent by performing a 2-step linear regression. This 2-step linear regression can be carried out in 2 ways: either by linear fits or by nonlinear fit. The details of the 2-step linear regression are:

1. for each city Lemoy and Caruso (ibid.) regress artificial land use share $S_N(r)$ on centrality r as a way to predict artificial land use share in the city center a_N and characteristic distance l_N. This step can be finished by a linear fit (Equation 5.1) or a nonlinear fit (Equation 5.2),

$$log_{10}(S_N(r)) = log_{10}(a_N) - \frac{r}{l_N} + \epsilon \tag{5.1}$$

$$S_N(r) = a_N \, e^{\frac{-r}{l_N}} + \epsilon \tag{5.2}$$

where S_N(r) is the proportion of build-up area of a city (population size N) at distance r, a_N is the proportion of build-up area in the city center, r is the Euclidean distance from city center, l_N is the predicted characteristics distance, ϵ is error term.

2. regress l_N on population size N. This step can also be finished by a linear fit (Equation 5.3) or a nonlinear fir (Equation 5.4),

$$log_{10}(l_N) = log_{10}(l_1) + \alpha \, log_{10}N + \epsilon \tag{5.3}$$

$$l_N = l_1 \, N^{\alpha} + \epsilon \tag{5.4}$$

where l_1 is a constant, N is population size, α **is the scaling exponent**, ϵ is error term.

Lemoy and Caruso (2021) summarized the results of the 2-step linear regression in Table 5.1. Simple nonlinear regression (SNL) is a theoretical scenario where the proportion of built-up area in city center is 100% (i.e. $S_N(0) = 1$). SNL20 and NL20 only consider continental cities.

Table 5.1: Regression of l_N with N (Lemoy and Caruso 2021)

Model	L	NL	SNL	NL20	SNL20
Scaling exponent α	0.317	0.499	0.496	0.500	0.494
	(0.024)	(0.013)	(0.013)	(0.012)	(0.011)
l_1 (m)	114.4	7.43	7.04	7.38	7.69
	(42.3)	(1.32)	(1.34)	(1.28)	(1.19)
Observations	293	293	293	237	237
R^2	0.372	0.845	0.826	0.877	0.895

L=linear, NL=nonlinear, SNL=simple nonlinear,
NL20=continental cities only, nonlinear,
SNL20=continental cities only, simple nonlinear

Table 5.1 shows that the NL model is the optimal choice when all cities are considered, because it has the highest R^2 (i.e. 0.845) and the lowest SEs (i.e. 0.013 and 1.32). If only continental cities are considered, then the SNL20 model is the optimal choice, because it has the highest R^2 (i.e. 0.895) and the lowest SEs (i.e. 0.011 and 1.19). But no matter whether we choose the NL or

the NL20 model, the scaling exponent is very close to 0.5. Therefore, Lemoy and Caruso (2021) showed that the homothetic scaling expressing the impact of population on the relationship between land use share and centrality is appropriate to use a scaling exponent of 0.5.

5.1.4 Comparison and expectations

SNR and 2-step linear regression give very close exponents when deriving the relationship between centrality and land use share under cities of different sizes. The difference is that SNR calculates and compares all possible SNR values by trying to build all possible combinations of exponent and land use share threshold, so as to test the rationality of 0.5 as the exponent proposed by Lemoy and Caruso (2018). In the 2-step linear regression, instead of specifying an exponent value, Lemoy and Caruso (2021) put raw data into linear or nonlinear regression, and then the exponent appears as part of the regression results.

We are not sure what exponent we would get if we applied something like SNR or 2-step linear regression to find the relationship between centrality and NO_2 levels, since land use is a 2-dimensional geographic phenomenon and NO_2 is distributed in 3-dimensional space. The NO_2 concentration fluctuates with factors such as meteorological conditions (e.g. Section 3.1.11) and built environment (e.g. canyon effect). Thus, in this case, the obtained exponent may not be 0.5. However, we hope to explain the influence of population size on the relationship between centrality and NO_2.

5.1.5 Importance and significance

The model proposed by Lemoy and Caruso (2018) shows that the relationship between built-up share and centrality can be described by homotheticity, and this relationship can be explained by population size. This simple model facilitates regional geographic research from many perspectives. On one thing, it involves few parameters, so it is simple and easy to understand for both the public and researchers. For another thing, by using this model, urban planners can compare cities of different sizes and cultural backgrounds side by side, and can predict the land use challenges that will arise in a city as urbanization accelerates. Urban planners can also formulate plans based on the homotheticity of artificial land use, such as estimating the amount of built-up land resources required for a certain place and the location and quantity of infrastructure based on centrality, thereby allocating resources efficiently. The homotheticity of artificial land use share also inspires us to further explore urban forms, for example, whether or not the air pollution that occurs on artificial land is also homothetic. Answering this question helps us build sustainable cities and resilient urban environment.

5.2 Methods

5.2.1 Data

In this chapter we use annual mean tropospheric NO_2 columns (at the resolution of 1 km x 1 km) (C) as the data source of NO_2. Centrality is denoted as R. Population size is noted as P. Background NO_2 is denoted as C_{min}. The reason why we don't include NO_2 surface concentrations this time is because stations cannot cover the entire spatial extent of a city, therefore we cannot gain land surface NO_2 data covering the entire area of a city with constant spatial resolution. Because we want to gain details about how NO_2 levels decrease along centrality so we interpolate satellite data and use annual mean tropospheric NO_2 columns at the resolution of 1 km x 1 km this time. For details of the data, see Chapter 3.

We use 2 ways to find how city size affects centrality: RMSC and 2-step linear regression.

5.2.2 RMSC

Inspired by Lemoy and Caruso (2018), the method of RMSC is very similar to the one of SNR. We need to find the minimum value of RMSC and the corresponding scaling exponents of centrality and NO_2 levels. We assume the scaling exponents of centrality and NO_2 levels may not be the same.

We select 30 *regular FUAs* to calculate the scaling factors. The definition of *regular FUAs* is in Section 3.2.8. Table 5.2 lists the 30 FUAs.

Table 5.2: Selected FUAs for RMSC

FUA	Country	FUA population
1. Altamura	Italy	70389.22
2. Caceres	Spain	89925.35
3. Ravenna	Italy	119043.26
4. Ceske Budejovice	Czech Republic	156917.20
5. Erfurt	Germany	239680.63
6. Oldenburg	Germany	241914.29
7. Salzburg	Austria	261062.85
8. Split	Croatia	289206.83
9. Pilsen	Czech Republic	311181.29
10. Aberdeen	United Kingdom	327687.31
11. Timisoara	Romania	358871.40
12. Salerno	Italy	379125.53
13. Plymouth	United Kingdom	397096.87
14. Bratislava	Slovakia	523360.46
15. Augsburg	Germany	547174.87
16. Ostrava	Czech Republic	550274.95
17. Rennes	France	569011.48
18. Skopje	Macedonia	576711.20
19. Leicester	United Kingdom	691528.57
20. Riga	Latvia	788480.59
21. Bremen	Germany	868843.17
22. Nantes	France	895937.40
23. Wroclaw	Poland	926637.90
24. Kayseri	Turkey	936403.55
25. Bordeaux	France	1045640.53
26. Budapest	Hungary	2822154.57
27. Athens	Greece	3747423.88
28. Berlin	Germany	4290482.74
29. Madrid	Spain	6131919.00
30. Paris	France	11709852.56

We define that α is the scaling exponent of centrality R and β is the scaling factor of NO_2 levels C. We use a similar expression to Equations 1.10 and 1.11 to express how we find scaling exponents using Equations 5.5 and 5.6,

$$R' = \frac{R}{(\frac{P}{P_{Paris}})^{\alpha}} \tag{5.5}$$

$$C_P(R') = \frac{C_P(R)}{(\frac{P}{P_{Paris}})^{\beta}} \tag{5.6}$$

where R is the Euclidean distance from the centroid of the pixel of satellite imagery to the city center, P_{Paris} is the population of the largest city in the dataset (i.e. Pairs), P is the population size of a city, R' is the rescaled Euclidean distance from the centroid of the pixel of satellite imagery to the city center, C_P(R) is the annual mean tropospheric NO_2 column of a city (population size P) at distance R. C_P(R') is the rescaled annual mean tropospheric NO_2 column of a city (population size P) at rescaled distance R'.

For each city of the dataset, we calculate the square of Pearson correlation coefficient between C_P(R') and $\log_{10}$ P. We repeat calculating Pearson correlation coefficient between R = 0 and R = T, such that T is the maximum centrality of each city. We use a set of values of α and β to calculate RMSC each time. $\alpha \in$ [0,1]. $\beta \in$ [0,1]. We then compare all the RMSC values, and the α and β values corresponding to the lowest RMSC value are the desired scaling factors. We use Equation 5.7 to find the lowest value of RMSC,

$$RMSC = \sqrt{\frac{\sum_{i=1}^{30} \rho^2(C_P(R'),\, log_{10}P)}{30}} \tag{5.7}$$

where ρ^2 means the square of Pearson correlation coefficient.

5.2.3 2-step linear regression

Inspired by Lemoy and Caruso (2021), we use 2-step linear regression as the second method to find the population effect on the relationship between centrality and NO_2 levels. In the first step, we perform linear regression on each city, and in the second step, we regress all the cities together.

The details of the 2-step linear regression are:

1. for each city we regress $\log_{10}$C on $\log_{10}$R, so we perform 378 linear regression (Equation 5.8) and we can derive 1 **intercept (A)** value, 1 **slope (B)** value, and 1 $\log_{10}$P value from each fitted line,

$$\forall_i,\ i \in [1{,}378] : log_{10}C = A_i + B_i\ log_{10}R + \epsilon \tag{5.8}$$

where ϵ is error term.

2. we regress all intercepts (A) on $\log_{10}$P (Equation 5.9), and regress all slopes (B) on $\log_{10}$P (Equation 5.10),

$$A = \alpha_0 + \alpha_1\ log_{10}P + \epsilon \tag{5.9}$$

$$B = \beta_0 + \beta_1\ log_{10}P + \epsilon \tag{5.10}$$

where α_0, α_1, β_0, and β_1 are coefficients.

We create 3 variations based on Equations 5.8 to 5.10.

1. We replace $\log_{10}$C with logarithmic annual mean tropospheric NO_2 columns without background effects ($\log_{10}$(C-C_{min})) to find out the effect of background NO_2.
2. We calculate R from the centroid of the pixel with the highest annual mean NO_2 column as the starting point (if a city has multiple pixels with the same highest NO_2 value, the position of the highest value is the average value of the coordinates of these pixels) to find out the effect of the location of the city center.
3. We replace $\log_{10}$R with R to find out the effect of logarithm.

To sum up, we perform 2-time linear regression by using Equations 5.11 to 5.18.

$\log_{10}$R calculated from the highest NO_2 pixel:

$$log_{10}C = \alpha_0 + \alpha_1\ log_{10}P + (\beta_0 + \beta_1\ log_{10}P)\ log_{10}R + \epsilon \tag{5.11}$$

$$log_{10}(C - C_{min}) = \alpha_0 + \alpha_1\ log_{10}P + (\beta_0 + \beta_1\ log_{10}P)\ log_{10}R + \epsilon \tag{5.12}$$

$\log_{10}$R calculated from the city center:

$$log_{10}C = \alpha_0 + \alpha_1\ log_{10}P + (\beta_0 + \beta_1\ log_{10}P)\ log_{10}R + \epsilon \tag{5.13}$$

$$log_{10}(C - C_{min}) = \alpha_0 + \alpha_1\ log_{10}P + (\beta_0 + \beta_1\ log_{10}P)\ log_{10}R + \epsilon \tag{5.14}$$

R calculated from the highest NO_2 pixel:

$$log_{10}C = \alpha_0 + \alpha_1\, log_{10}P + (\beta_0 + \beta_1\, log_{10}P)\, R + \epsilon \tag{5.15}$$

$$log_{10}(C - C_{min}) = \alpha_0 + \alpha_1\, log_{10}P + (\beta_0 + \beta_1\, log_{10}P)\, R + \epsilon \tag{5.16}$$

R calculated from the city center:

$$log_{10}C = \alpha_0 + \alpha_1\, log_{10}P + (\beta_0 + \beta_1\, log_{10}P)\, R + \epsilon \tag{5.17}$$

$$log_{10}(C - C_{min}) = \alpha_0 + \alpha_1\, log_{10}P + (\beta_0 + \beta_1\, log_{10}P)\, R + \epsilon \tag{5.18}$$

5.3 Results and discussion

5.3.1 RMSC

By using Equation 5.7, we get the lowest RMSC value (i.e. 5.1106e-15) when α = 0.45 and β = 0.95. We then apply these values of α and β on Equations 5.5 and 5.6 for 30 *regular* FUAs (Figure 5.2(a)) and all the cities (Figure 5.2(c)). The rescaled results are Figures 5.2(b) and 5.2(d).

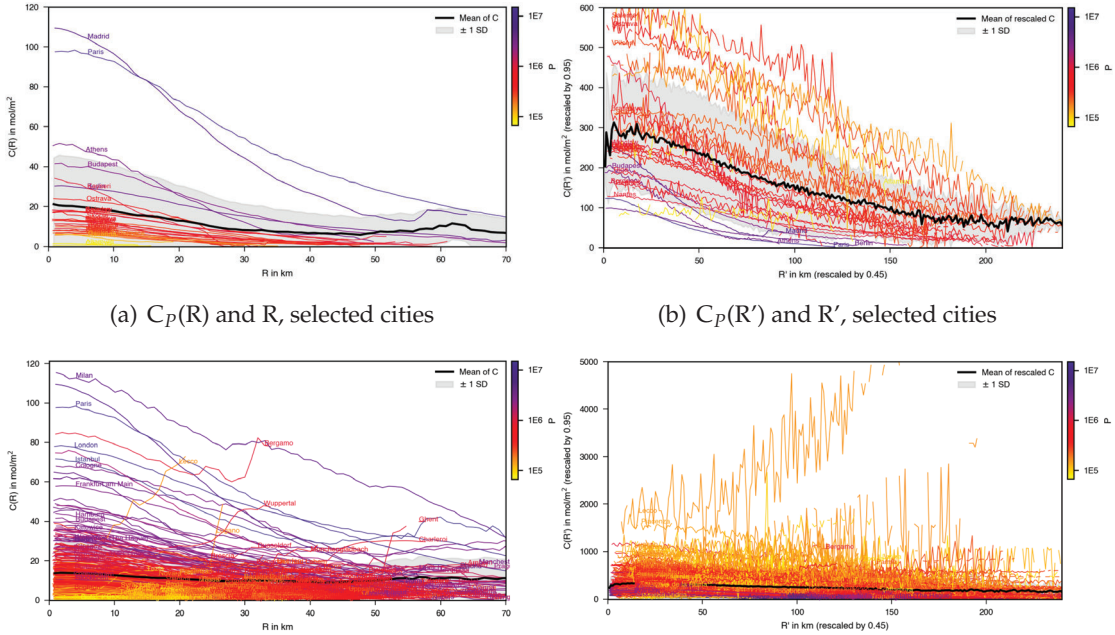

(a) $C_P(R)$ and R, selected cities

(b) $C_P(R')$ and R', selected cities

(c) $C_P(R)$ and R, all cities

(d) $C_P(R')$ and R', all cities

Figure 5.2: Applying RMSC on selected or all cities, before (a, c) and after (b, d)

Figure 5.2(b) shows that RMSC is not suitable to find out the effect of population size on the relationship between centrality and NO_2 levels. This is because, although the relative position of the lines in Figure 5.2(b) changes compared to Figure 5.2(a), if we compare Figure 5.2(b) with the results of rescaled centrality and artificial land use share in Figure 1.4(b), we find that the relative position of the lines in Figure 5.2(b) is still mainly determined by population size.

When we apply RMSC on all the cities, the results again show that RMSC is not a suitable tool. First, the RMSC does not largely attenuate, or explain, the effect of population size. For example, the purple lines representing large cities at the top of Figure 5.2(c) move to the bottom in Figure 5.2(d), and the bright yellow lines representing small cities at the bottom in Figure 5.2(c) just move to the upper layer of the line group in Figure 5.2(d). Second, RMSC cannot eliminate or weaken the influence of surrounding cities. For example, the rescaled NO_2 levels in Lecco increase evidently with rescaled centrality in Figure 5.2(d). Because Lecco is one of the neighboring cities of Milan, so we use Figure 5.3 as an example to illustrate why the NO_2 levels of Lecco show an upward trend in Figure 5.2(d).

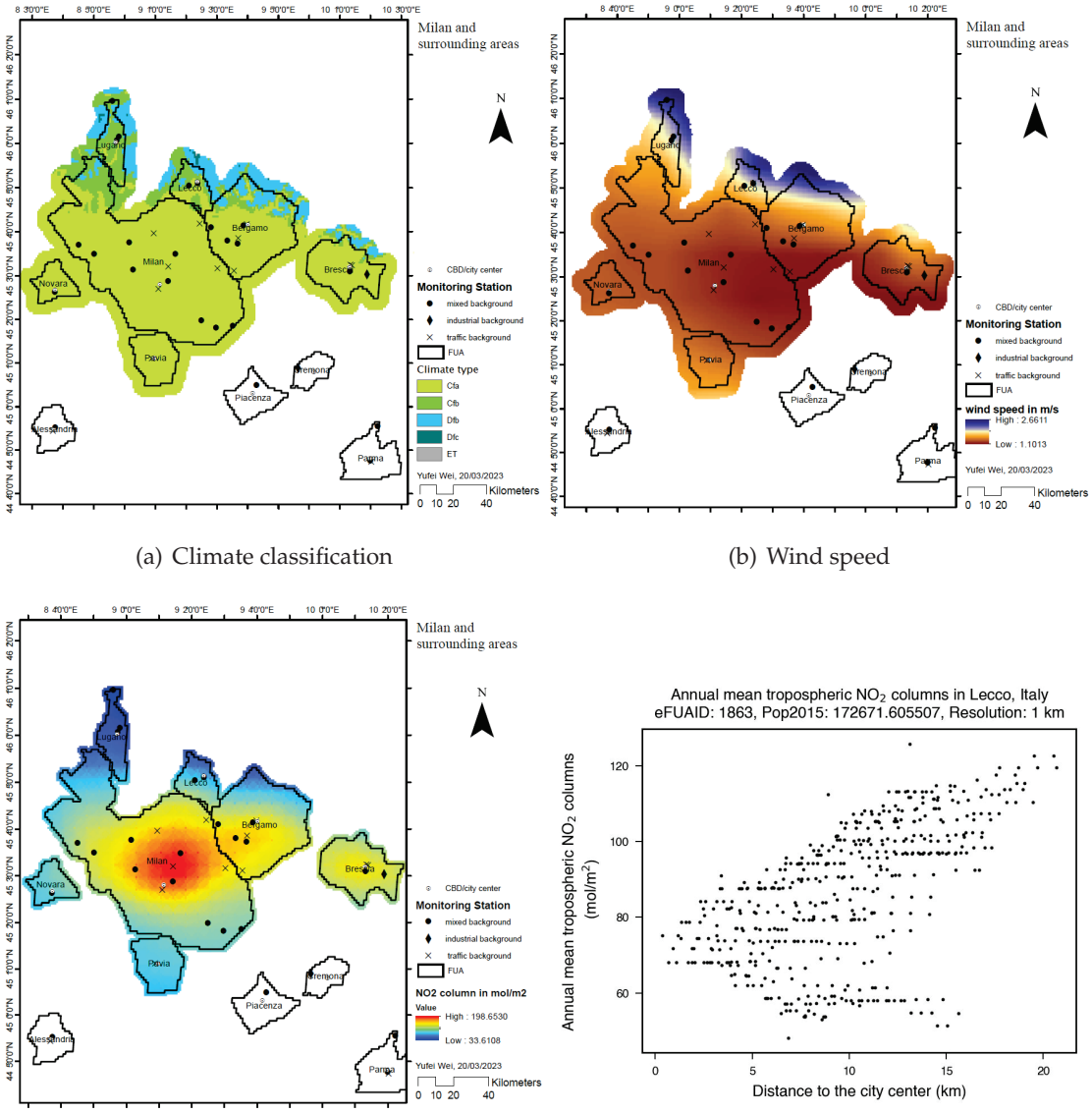

(a) Climate classification

(b) Wind speed

(c) Annual mean NO_2 columns

(d) Scatter plot of annual mean NO_2 columns

Figure 5.3: Milan and surrounding FUAs (i.e. Bergamo, Brescia, Lecco, Lugano, Novara, Pavia)

We use Milan and its surrounding FUAs (Figure 5.3) to illustrate why the use of RMSC is not suitable to find the scaling exponents of centrality and NO_2 columns. Lecco is a small city located in the northeast of Milan (Figure 5.3(a)). Influenced by the Alps, the climate type in the north of Lecco is different from that in the south (Figure 5.3(a)), and the wind speed is high in the north of Lecco and low in the south (Figure 5.3(b)). The city center of Lecco is located in a place with low

wind speed, but it is affected by the neighboring large city Milan, thus the NO_2 concentration on the south side of Lecco city is higher than that of the city center. From Figure 5.3(c) we can see that the NO_2 pollution levels of Milan have a great impact on the surrounding cities, so that the city of Brescia, which is a little far from Milan, does not show that the concentration of NO_2 decreases with centrality. That is why we see the NO_2 levels increase with centrality in Lecco in Figure 5.3(d).

Thus, we think RMSC is not suitable to find the effect of population size on centrality. Different from artificial land use share used in SNR (Lemoy and Caruso 2018), the NO_2 concentration is affected by many factors such as climate type, wind speed, and influence from surrounding cities. Although similar to Lemoy and Caruso (ibid.), the relative position of the lines representing cities of different sizes changes after using RMSC, suggesting that population affects the relationship between centrality and NO_2 to some extent, but we think in the future, scaling factors considering climate type, terrain, and proximity should be added to improve the performance of RMSC.

5.3.2 2-step linear regression

Tables 5.3 and 5.4 are the regression results of the 2-step linear regression.

Table 5.3: Regressions of A and B with $\log_{10}$P (log_{10}R is used in the regression)

R calculated from the highest NO_2 pixel			R calculated from the city center		
	$\log_{10}$C (5.11)	$\log_{10}$(C-C_{min}) (5.12)		$\log_{10}$C (5.13)	$\log_{10}$(C-C_{min}) (5.14)
α_0	-2.6456***	-8.6668***	α_0	-2.7186***	-11.4110***
	(0.1821)	(0.6980)		(0.1662)	(0.6973)
α_1	0.8343***	2.0820***	α_1	0.8330***	2.4862***
	(0.0325)	(0.1246)		(0.0297)	(0.1244)
β_0	0.7069***	1.1166***	β_0	0.7350***	1.8556***
	(0.0367)	(0.1640)		(0.0370)	(0.1676)
β_1	-0.1425***	-0.2936***	β_1	-0.1442***	-0.4052***
	(0.0065)	(0.0293)		(0.0066)	(0.0299)
R^2 (Equation 5.9)	0.6368	0.4263	R^2 (Equation 5.9)	0.6772	0.5150

continued on the next page

continued from the previous page

R^2 (Equation 5.10)	0.5574	0.2113	R^2 (Equation 5.10)	0.5589	0.3280

$^{***}\rho < 0.001$ $^{**}\rho < 0.01$ $^{*}\rho < 0.05$ $^{+}\rho < 0.1$

Table 5.3 shows that the signs of the coefficients of α_0, α_1, β_0, and β_1 do not change from Columns 5.11 to 5.14, and the coefficients all pass the test of significance at the level of 0.1%. α_1 indicates the positive effect of $\log_{10}$P on $\log_{10}$C or $\log_{10}$(C-C_{min}). Columns 5.11 and 5.13 show a 1% increase in $\log_{10}$P leads to 0.83% increase in $\log_{10}$C, and Columns 5.12 and 5.14 show a 1% increase in $\log_{10}$P leads to around 2% increase in $\log_{10}$(C-C_{min}).

β_1 shows how $\log_{10}$P changes with slope (B) (Equation 5.10) and the values of β_1 are negative in Table 5.3. This means the value of B of a big city is low, and the value of B of a small city is high. B shows how $\log_{10}$C or $\log_{10}$C-C_{min} changes with $\log_{10}$R (Equation 5.8), and in most cases B is negative (i.e. NO_2 levels decrease with centrality). This means for example, if the value of B of a big city is -2, then the value of B of a small city can be -1, which means that the NO_2 levels decrease faster with centrality in large cities. This can be explained by the siphon effect of large cities. The centripetal road networks agglomerate commercial activities, bring resources and population far away to the city center of big cities (Wang et al. 2018), generate high NO_2 emission at the city center, and result in a greater decline in NO_2 levels within the city.

We also compare the data in Column 5.13 with the data in Column 4.13 of Chapter 4. The coefficient of $\log_{10}$P in Column 5.13 is 0.8330, while the coefficient of $\log_{10}$P in Column 4.13 is 0.2161. We also collect all the values of B when calculating Column 5.13, and we find the mean of all the values of B is -0.0707. As a comparison, the coefficient of $\log_{10}$R in Column 4.13 is -0.1823. This means Columns 5.13 and 4.13 derive similar scaling exponents of P and R.

Table 5.4: Regressions of A and B with $\log_{10}$P (R is used in the regression)

R calculated from the highest NO_2 pixel			R calculated from the city center		
	$\log_{10}$C (5.15)	$\log_{10}$(C-C_{min}) (5.16)		$\log_{10}$C (5.17)	$\log_{10}$(C-C_{min}) (5.18)
α_0	0.1682	-3.3670***	α_0	0.1490	-3.8588
	(0.1062)	(0.2126)		(0.1015)	(0.2010)
α_1	0.2714***	0.7968***	α_1	0.2728***	0.8710***
	(0.0190)	(0.0379)		(0.0181)	(0.0359)

continued on the next page

continued from the previous page

β_0	7.4235e-6***	-7.1207e-5***	β_0	1.2152e-5***	3.1579e-6
	(1.3085e-6)	(1.2794e-5)		(1.4093e-6)	(1.1461e-5)
β_1	-1.7972e-6***	9.1697e-6***	β_1	-2.5368e-6***	-3.1508e-6
	(2.3349e-7)	2.2830e-6)		(2.5148e-7)	(2.0451e-6)
R^2 (Equation 5.9)	0.3530	0.5398	R^2 (Equation 5.9)	0.3763	0.6106
R^2 (Equation 5.10)	0.1361	0.0411	R^2 (Equation 5.10)	0.2130	0.006

$^{***}\rho < 0.001$ ** $\rho < 0.01$ * $\rho < 0.05$ $^{+}\rho < 0.1$

Table 5.4 shows compared with $\log_{10}$R, R is not a suitable independent variable in finding how city size affects centrality. In Table 5.4, the signs of the coefficients of α_0, α_1, β_0, and β_1 are not consistent from Columns 5.15 to 5.18, and only part of the coefficients pass the test of significance at the level of 0.1%. In each column, the coefficient of α_1 is lower than the coefficient of α_1 in Table 5.3, and the coefficient of β_1 is much lower than the coefficient of β_1 in Table 5.3, which means that using R as an independent variable does not reflect the effects of $\log_{10}$P and $\log_{10}$R on $\log_{10}$C or $\log_{10}$(C-C_{min}) well.

We also compare the data in Column 5.17 with the data in Column 4.13 of Chapter 4. The coefficient of $\log_{10}$P in Column 5.17 is 0.2728, while the coefficient of $\log_{10}$P in Column 4.13 is 0.2161. We also collect all the values of B when calculating Column 5.17, and we find the mean of all the values of B is -2.0196e-06. As a comparison, the coefficient of $\log_{10}$R in Column 4.13 is -0.1823. This means Columns 5.13 and 4.13 only derive similar scaling exponent of P.

We then calculate predicted C ($\hat{C}$) by Columns 5.13 and 5.17 and compare those values with the values of $\hat{C}$ in Table 4.7 of Chapter 4. We list the results in Tables 5.5 and 5.6.

Table 5.5: $\hat{C}$ by Column 5.13 and relative changes at different R

$\hat{C}$ (μmol/m^2) and its relative change comparing to the left column and over-(+)/under-(-)estimated volume of $\hat{C}$ compared to $\hat{C}$ in Table 4.7					
R (km)	0.1	0.5	1	5	10
P = 1e5	29.8126	32.6493	30.7893	31.4909	31.7980
(% decrease)	(n/a)	(-9.5152%)	(5.6969%)	(-2.2788%)	(-0.9751%)
(+/-)	-52.6582	-28.8511	-23.4108	-8.9274	-3.8225
P = 1e6	104.4720	84.7216	77.4105	62.7761	57.3588
(% decrease)	(n/a)	(66.2486%)	(22.3927%)	(47.5310%)	(17.2026%)
(+/-)	-31.1718	-16.4312	-11.7351	-3.7019	-1.2280
P = 1e7	366.1002	235.3979	194.6256	125.1419	103.4666
(% decrease)	(n/a)	(76.8584%)	(67.115%)	(67.7452%)	(54.1650%)
(+/-)	+143.0000	+69.0268	+48.0033	+15.8022	+7.1059

Table 5.5 shows $\hat{C}$ declines faster in large cities than in small ones. Different from the data in Table 4.7, the values of "% decrease" in Table 5.5 are all different. Compared with Table 4.7, Table 5.5 tends to underestimate the NO_2 pollution levels of small cities and overestimate the NO_2 levels of large cities, and the overestimation or underestimation is very obvious within 1 km from the city center. When the centrality is 10 km, the difference between the estimates of Tables 4.7 and 5.5 is within 10 mol/m^2.

Table 5.6: $\hat{C}$ by Column 5.17 and relative changes at different R

$\hat{C}$ (μmol/m^2) and its relative change comparing to the left column and over-(+)/under-(-)estimated volume of $\hat{C}$ compared to $\hat{C}$ in Table 4.7					
R (km)	0.1	0.5	1	5	10
P = 1e5	32.5797	32.5637	32.5438	32.3847	32.1870
(% decrease)	(n/a)	(0.0490%)	(0.0612%)	(0.4888%)	(0.6106%)
(+/-)	-49.8911	-28.9367	-21.6563	-8.0336	-3.4335
P = 1e6	61.0229	60.8507	60.6361	58.9462	56.9000
(% decrease)	(n/a)	(0.5287%)	(0.6591%)	(5.1926%)	(6.3186%)
(+/-)	-74.6209	-40.3021	-28.5095	-7.5318	-1.6868
P = 1e7	114.2982	113.7096	112.9781	107.2932	100.5875
(% decrease)	(n/a)	(46.7615%)	(46.6746%)	(47.8251%)	(46.9678%)
(+/-)	-108.802	-52.6615	-33.6442	-2.0465	+4.2268

Table 5.6 shows $\hat{C}$ declines much faster in large cities than in small ones. Similar to the data in Table 5.5, the values of "% decrease" in Table 5.6 are all different. Compared with Table 4.7, Table 5.6 tends to underestimate most NO_2 pollution levels except for areas 10 km from the center of large cities. When the centrality is 5 km or 10 km, the difference between the estimates of Tables 4.7 and Column 5.6 is within 10 mol/m^2.

In order to find out the effect of background NO_2, we calculate the difference of A and the difference of B when calculating R in 2 ways. Tables 5.4 and 5.5 show the differences using scatter plots.

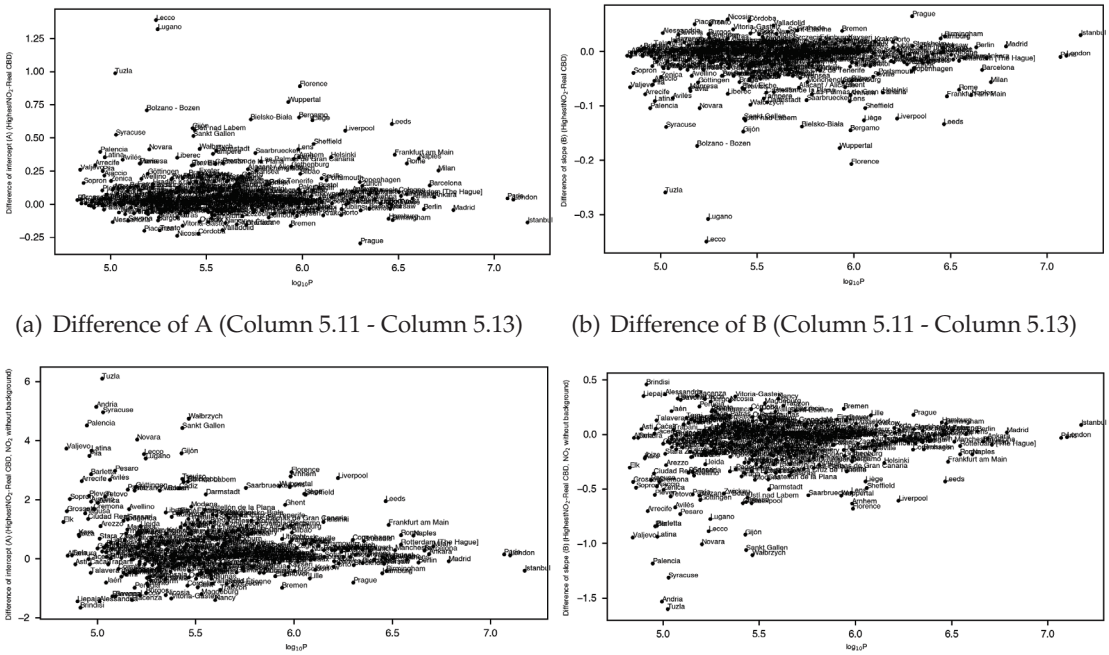

(a) Difference of A (Column 5.11 - Column 5.13)

(b) Difference of B (Column 5.11 - Column 5.13)

(c) Difference of A (Column 5.12 - Column 5.14)

(d) Difference of B (Column 5.12 - Column 5.14)

Figure 5.4: Differences of A or B of Table 5.3

Figures 5.4(a) and 5.4(b) show the majority of data points fluctuate around the line of Y = 0. The outliers in Figures 5.4(a) and 5.4(b) show no evident relationship with $\log_{10}$P. The offset between the city center and the location of the highest NO_2 is independent of city size. This means that the location of city center chosen when calculating centrality does not affect the impact of city size on centrality. Lemoy and Caruso (2018) proposed similar views.

In Figures 5.4(c) and 5.4(d), the groups of points near the line of Y = 0 are less concentrated than the ones in Figures 5.4(a) and 5.4(b). The outliers of small cities tend to drift further than the ones of larger cities. It shows the NO_2 levels in small cities are more susceptible to background NO_2 than the NO_2 levels in large cities. This means large cities create conditions for high NO_2 levels, such as anthropogenic activities (Section 1.1.3) and the interaction between UHI and NO_2 (Section 1.1.4) in built environment.

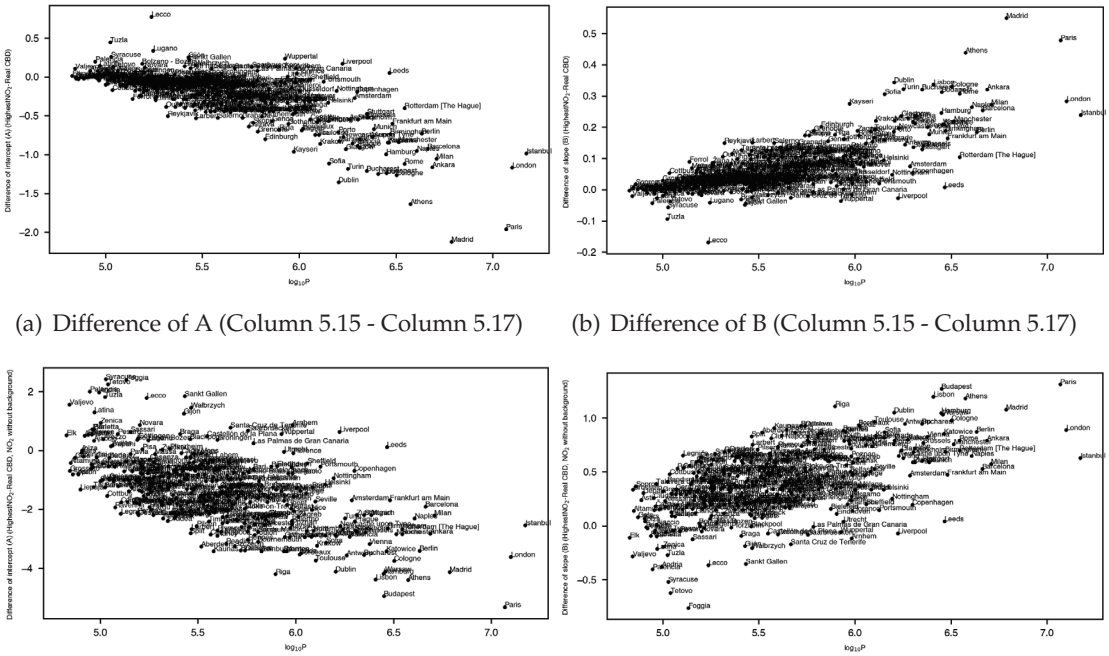

(a) Difference of A (Column 5.15 - Column 5.17) (b) Difference of B (Column 5.15 - Column 5.17)

(c) Difference of A (Column 5.16 - Column 5.18) (d) Difference of B (Column 5.16 - Column 5.18)

Figure 5.5: Differences of A or B of Table 5.4

Figure 5.5 shows that R is not suitable to be used as an independent variable in finding the population size effect on centrality. This is because the points in Figure 5.5 show heteroscedasticity (i.e. the standard deviations of Y values increase with $\log_{10}$P).

5.4 Limitations

The methods used in this chapter have some drawbacks. First, RMSC cannot describe the impact of population size on centrality, partly because the spatial distribution of NO_2 is much more complex than the distribution of artificial land use studied by Lemoy and Caruso (2018). We hope that future studies can improve RMSC by adding scaling factors related to wind speed and neighborhood analysis etc. Second, due to limited time, unlike Lemoy and Caruso (2021), our 2-step linear regression does not consider the use of nonlinear regression to explore the effect of population size on centrality. We think that the use of non-linear regression can improve, for example, the overestimation or underestimation in Tables 5.5 and 5.6 to some extent as Lemoy and Caruso (ibid.) proposed similar views.

5.5 Suggestions for urban planners

Our results of RMSC find that the relationship between NO_2 concentration and centrality cannot be explained solely by population size. Factors such as neighboring large cities and wind speed influence the NO_2 levels inside the city, and in some cases, the intra-urban NO_2 levels of the city are even almost irrelevant to centrality if the NO_2 pollution levels of the neighboring city are high enough (e.g. Brescia). Therefore, while NO_2 is generally considered to be a local pollutant (Colvile et al. 2001), however, if urban planners want to reduce the NO_2 levels in one city, then the NO_2 levels in neighboring large cities must also be controlled.

Our results of 2-step linear regression suggest that large cities are less affected by background NO_2 than smaller cities, because large cities have conditions to generate extremely high NO_2 levels (e.g. large populations, built environment). Therefore, urban planners should use some measures to improve the built environment of city centers and prevent excessive NO_2 pollution levels. Because the NO_2 levels in large cities decrease faster with centrality than in small cities, therefore, urban planners can develop Bus Rapid Transit (BRT) or subways that connect the city center to the outskirts of the city in order to reduce citizens' NO_2 exposure.

5.6 Code availability

Code link for calculating minimum NO_2 column of each FUA of 378 FUAs:
github.com/WeiYufei/PHD_Thesis_University_of_Luxembourg/blob/main/CaculateminFUA_for1kmResolutionRaster_ALLCITIES.py.

Code link for Equation 5.7:
github.com/WeiYufei/PHD_Thesis_University_of_Luxembourg/blob/main/rmsceqa.py.

Code links for Table 5.3:
1st column (Equation 5.9, α_0, α_1) - github.com/WeiYufei/PHD_Thesis_University_of_Luxembourg/blob/main/C41_AlgP.py,
1st column (Equation 5.10, β_0, β_1) - github.com/WeiYufei/PHD_Thesis_University_of_Luxembourg/blob/main/C41_BlgP.py,
2nd column (Equation 5.9, α_0, α_1) - github.com/WeiYufei/PHD_Thesis_University_of_Luxembourg/blob/main/C42_AlgP.py,
2nd column (Equation 5.10, β_0, β_1) - github.com/WeiYufei/PHD_Thesis_University_of_Luxembourg/blob/main/C42_BlgP.py,
3rd column (Equation 5.9, α_0, α_1) - github.com/WeiYufei/

PHD_Thesis_University_of_Luxembourg/blob/main/C43_AlgP.py,
3rd column (Equation 5.10, β_0, β_1) - github.com/WeiYufei/
PHD_Thesis_University_of_Luxembourg/blob/main/C43_BlgP.py,
4th column (Equation 5.9, α_0, α_1) - github.com/WeiYufei/
PHD_Thesis_University_of_Luxembourg/blob/main/C44_AlgP.py,
4th column (Equation 5.10, β_0, β_1) - github.com/WeiYufei/
PHD_Thesis_University_of_Luxembourg/blob/main/C44_BlgP.py.

Code links for Table 5.4:
1st column (Equation 5.9, α_0, α_1) - github.com/WeiYufei/
PHD_Thesis_University_of_Luxembourg/blob/main/C41_AlgPR.py,
1st column (Equation 5.10, β_0, β_1) - github.com/WeiYufei/
PHD_Thesis_University_of_Luxembourg/blob/main/C41_BlgPR.py,
2nd column (Equation 5.9, α_0, α_1) - github.com/WeiYufei/
PHD_Thesis_University_of_Luxembourg/blob/main/C42_AlgPR.py,
2nd column (Equation 5.10, β_0, β_1) - github.com/WeiYufei/
PHD_Thesis_University_of_Luxembourg/blob/main/C42_BlgPR.py,
3rd column (Equation 5.9, α_0, α_1) - github.com/WeiYufei/
PHD_Thesis_University_of_Luxembourg/blob/main/C43_AlgPR.py,
3rd column (Equation 5.10, β_0, β_1) - github.com/WeiYufei/
PHD_Thesis_University_of_Luxembourg/blob/main/C43_BlgPR.py,
4th column (Equation 5.9, α_0, α_1) - github.com/WeiYufei/
PHD_Thesis_University_of_Luxembourg/blob/main/C44_AlgPR.py,
4th column (Equation 5.10, β_0, β_1) - github.com/WeiYufei/
PHD_Thesis_University_of_Luxembourg/blob/main/C44_BlgPR.py.

Code links for Table 5.5:
github.com/WeiYufei/PHD_Thesis_University_of_Luxembourg/
blob/main/attenNO_logR.py,

Code links for Table 5.6:
github.com/WeiYufei/PHD_Thesis_University_of_Luxembourg/
blob/main/attenNO_logRR.py,

Code link for Figure 5.2(a):
github.com/WeiYufei/PHD_Thesis_University_of_Luxembourg/
blob/main/rmscSelectedcitiesUSC.py.

Code link for Figure 5.2(b):
github.com/WeiYufei/PHD_Thesis_University_of_Luxembourg/blob/main/rmscSelectedcities.py.

Code link for Figure 5.2(c):
github.com/WeiYufei/PHD_Thesis_University_of_Luxembourg/blob/main/rmscAllcitiesUSC.py.

Code link for Figure 5.2(d):
github.com/WeiYufei/PHD_Thesis_University_of_Luxembourg/blob/main/rmscAllcities.py.

Code link for Figure 5.4(a):
github.com/WeiYufei/PHD_Thesis_University_of_Luxembourg/blob/main/interceptDif.py.

Code link for Figure 5.4(b):
github.com/WeiYufei/PHD_Thesis_University_of_Luxembourg/blob/main/slopeDif.py.

Code link for Figure 5.4(c):
github.com/WeiYufei/PHD_Thesis_University_of_Luxembourg/blob/main/interceptDif_extractedNO2.py.

Code link for Figure 5.4(d):
github.com/WeiYufei/PHD_Thesis_University_of_Luxembourg/blob/main/slopeDif_extractedNO2.py.

Code link for Figure 5.5(a):
github.com/WeiYufei/PHD_Thesis_University_of_Luxembourg/blob/main/interceptDifR.py.

Code link for Figure 5.5(b):
github.com/WeiYufei/PHD_Thesis_University_of_Luxembourg/blob/main/SlopeDifR.py.

Code link for Figure 5.5(c):
github.com/WeiYufei/PHD_Thesis_University_of_Luxembourg/blob/main/interceptDif_extractedNO2R.py.

Code link for Figure 5.5(d):
github.com/WeiYufei/PHD_Thesis_University_of_Luxembourg/
blob/main/slopeDif_extractedNO2R.py.

6 Conclusions

Today, over half of the world's population lives in urban areas (UN 2013). The number of people in a city determines the amount of infrastructure and public transportation used, while the distribution of the population within the city determines how infrastructure and transportation are allocated in the city. At the same time, we also note that anthropogenic activities in cities, including the use of private cars, can lead to a series of environmental problems. For example, the construction of city infrastructure and housing requires the conversion of soil into impermeable surfaces, which can absorb a large amount of solar radiation and heat during the day and release them at night (John et al. 2013; Ndiaye et al. 2018), forming UHI that causes temperatures in urban areas to be much higher than in surrounding rural areas (U.S. EPA 2023). Private cars driven by fossil fuels emit large amounts of toxic gases, with NO_2 being the most prominent toxic exhaust gas (Seddiek and Elgohary 2014). UHI threatens citizen's health (Havenith 2005; Robine et al. 2008; UNEP 2004), while NO_2 damages residents' respiratory and cardiovascular systems (Andersen et al. 2012; Gauderman et al. 2005; Kelly and Fussell 2011; Schindler et al. 1998). UHI and NO_2 can interact with each other and exacerbate each other's destructive effect (Clark 2020; Constantin et al. 2015). Therefore, this thesis includes a meta-analysis on UHI and NO_2. However, due to time constraints and the similarity of causes and mitigation strategies for UHI and NO_2 (Section 1.1.4), this thesis chooses NO_2 as the sole urban environmental problem in empirical analysis.

Due to the complex relationship between a city's economic level and environmental problems, some recent studies attempted to compare cities to living organisms and used power laws based on the allometric theory to describe the relationship between population size and socioeconomic features or environmental problems (Batty 2013; Ramaswami et al. 2018). Power laws can answer questions such as whether the development of a city increases or decreases its emissions or not (Louf and Barthelemy 2014b). We find some articles that used power laws to describe how the effect of population size affects UHI or NO_2 levels, but these articles used different measurement methods and indicators when measuring UHI or NO_2 (Section 1.3). Therefore, we perform a qualitative synthesis and a meta-analysis to summarize the effect of population on UHI or NO_2 levels in published works (Chapter 2).

In Chapter 2, we conduct a qualitative synthesis and a meta-analysis based on the PRISMA guideline. PRISMA has four steps. In general, first, we identify the resources that make up the corpus using a series of keywords and remove duplicate records from Scopus and Google Scholar. Then, in the second and third steps, we filter the titles and full-text contents of the articles to ensure that either the data related to UHI intensity (i.e. ΔT) or NO_2 concentrations and population size are included in the articles, or the relationship between UHI intensity or NO_2 concentrations and population size are clearly stated. Finally, in the fourth step, we conduct qualitative synthesis and meta-analysis of these papers. It is worth noting that although we initially find 287 and 192 non-duplicate UHI and NO_2 records at the initial stage of PRISMA, only 13 UHI and 9 NO_2 articles are suitable for qualitative and quantitative analyses after the third step. Meanwhile, we add 6 articles to the corpus that describe the relationship between NO_2 concentrations and population size under the IPAT framework, as the keywords we use in PRISMA cannot find relevant literature under the IPAT framework. We carry out the qualitative synthesis by reading the full-text contents of the articles in the corpus. We perform meta-analysis using ANOVA test and linear regression. We add dummy variables representing different articles to the linear regression.

The qualitative synthesis of UHI shows car traverse was a popular way to measure ΔT until the early 21^{st} century but now climate models, monitoring stations and remote sensing are the main ways to gain ΔT. Remote sensing measures land surface ΔT while other ways retrieve aerial ΔT. 8 papers show ΔT is positively correlated with P, but whether ΔT is significantly correlated with D remains inconclusive due to the conflicting conclusions. The 2 studies quantifying mean aerial ΔT by car traverse show the coefficients of $\log_{10}$P are 1.93 and 1.33. The studies quantifying max aerial ΔT by car traverse reveal the coefficients of $\log_{10}$P range from 1.42 to 2.96. The studies quantifying max land surface ΔT by remote sensing reveal the coefficients of $\log_{10}$P range from 2.38 to 3.53. Studies using climate models and monitoring stations both illustrate the positive relationship between aerial ΔT and P but neither give quantitative equations.

The qualitative synthesis of NO_2 shows only 2 studies using handy samplers measure NO_2 in barely 4 cities. The only study using data from emission inventory covers NO_2 pollution across 8,032 cities around the world but ignores cities with less than 50,000 residents. It is difficult to find a consolidated NO_2 metric in evaluating the effect of city size on NO_2 across cities because different forms of equations and metrics are found among the studies. 4 out of 15 papers do not give corresponding conclusions as they target for other aims. 7 out of 8 articles providing liner regression say non-log/$\log_{10}$/ln NO_2 is positively correlated with $\log_{10}$P/lnP, but they use different metrics or form of relationship. Only 3 articles point to a relationship between NO_2 and D, but the conclusions are inconsistent.

We then group studies having the same combination of environmental and population variables and carry out ANOVA test for each group. The ANOVA test shows the regression of max ΔT with $\log_{10}$P, $\log_{10}$(max ΔT) with $\log_{10}$P, and $\log_{10}$(mean NO2) with $\log_{10}$P pass the test of significance at the level of 0.1%. Thus these 3 kinds of relationships are used in the linear regression. The results of linear regression show $\log_{10}$-$\log_{10}$(max ΔT) is better than $\log_{10}$-max ΔT relationship in showing the population effect on UHI. $\log_{10}$P can explain 75% of $\log_{10}$(max ΔT) and in this case the coefficient of $\log_{10}$P is 0.1489. We find that even small cities of 10,000 inhabitants are likely to have a 4.5°C difference to their surroundings, and this difference can increase to 12°C for a city having 10 million residents. For the meta-analysis of NO_2, around half of the data points are above the WHO annual mean limit in 2000 (i.e. 40 $\mu g/m^3$), and all the points are above the WHO annual mean limit in 2021 (i.e. 10 $\mu g/m^3$). Our results suggest that people should change their dependence on fossil fuels in transportation, as so far no city has an annual mean NO_2 surface concentration that meets the 2021 annual mean limit of WHO (WHO 2021). We find that $\log_{10}$P can explain nearly 90% of $\log_{10}$(mean NO2) and in this case the coefficient of $\log_{10}$P is 0.1587. In Chapter 4, we test rationality of the coefficient of $\log_{10}$P derived from the meta-analysis using empirical data of annual mean NO_2 surface concentrations and annual mean NO_2 columns. The coefficient of $\log_{10}$P is 0.1911 when using monitoring station data, and the coefficient of $\log_{10}$P is 0.1354 when using satellite data. **Our meta-analysis and empirical analysis results confirm Hypothesis 1 (Section 1.4), that the relationship between UHI or NO_2 and population size follows a power law, and larger cities have higher levels of UHI or NO_2.**

In urban economics, Alonso (1964) proposed the bid-rent curve, which suggests that population density and land prices decrease with centrality. Schindler et al. (2017) pointed out that residents relocate to areas farther away from the city center to reduce the exposure of traffic-related pollution. The canyon effect in the city center exacerbates air pollution and UHI (Karimimoshaver et al. 2021), and theoretical models suggest that improving the built environment in the city center can significantly improve air quality (Schindler and Caruso 2014). The single-city studies we find show that the NO_2 pollution level in the city center is significantly higher than that in the surrounding areas (Kirby et al. 1998; Nicholas Hewitt 1991; Vintar Mally and Ogrin 2015). The multi-city studies we find either focus on qualitative descriptions without quantitative analysis (Wang et al. 2020c), or do not consider population size (Borck and Schrauth 2021). Therefore, in Chapter 4, we use empirical data from monitoring stations and satellites to describe the impacts of population size and centrality on NO_2 levels, and compare the relative importance of population size and centrality. Specifically, we regress $\log_{10}$G or $\log_{10}$C on $\log_{10}$R and $\log_{10}$P respectively and together. We include dummy variables showing the backgrounds

of NO_2 monitoring stations when regressing land surface NO_2. We consider $\log_{10}C_{min}$ when regressing tropospheric NO_2.

The results of Chapter 4 show that $\log_{10}P$ is always positively correlated with $\log_{10}G$ or $\log_{10}C$, while $\log_{10}R$ is always negatively correlated with $\log_{10}G$ or $\log_{10}C$. **Our empirical analysis results confirm Hypothesis 2 (Section 1.4), that the NO_2 emissions within cities are negatively correlated with centrality**. $\log_{10}P$ is always relatively more important than $\log_{10}R$. When dummy variables or $\log_{10}C_{min}$ appears in linear regression, then dummy variables or $\log_{10}C_{min}$ is the most important factor in deciding the NO_2 levels. We compare measured NO_2 columns with predicted NO_2 columns obtained through linear regression using 3 sets of population data, each set consisting of 38 cities, and find that the predicted values are fairly close to the measured values. However, the predicted values tend to underestimate the NO_2 levels in the city center of large cities (e.g. Paris) and overestimate the NO_2 levels in the city center of small cities (e.g. Nuremberg). We think that this may be related to the built environment in city centers and the effect of population size.

Therefore, in Chapter 5, we use annual mean NO_2 columns to investigate the impact of population size on centrality. Due to the characteristic of decreasing NO_2 levels with centrality within cities, we use a radial analysis in this chapter, which involves analyzing geographic phenomena within concentric circles starting from a point or area. We find some studies using radial analysis to study land use or UHI, however, they either use urban core area as the start (Irwin and Bockstael 2007; Schneider and Woodcock 2008; Zhou et al. 2015), or aggregate land use data within the circles (Seto and Fragkias 2005), or use complicated functions (Jiao 2015).

Because NO_2 is a local air pollutant (Colvile et al. 2001), thus the radial analysis we use is similar to the one used by Lemoy and Caruso (2018). Lemoy and Caruso (ibid.) calculated R from the location of city center (rather than the area of urban core), and continuously described how NO_2 levels change along with centrality. Lemoy and Caruso (ibid.) used 0.5 as the scaling exponent and built scaling factors for centrality and artificial land use share based on the scaling exponent, population size, and the maximum population size. Lemoy and Caruso (ibid.) found that the artificial land use share is largely related to centrality, and population size has a very small impact on artificial land use share, thus proving the homotheticity of spatial distribution of artificial land use share. Lemoy and Caruso (ibid.) used a method called SNR, to test the rationality of using 0.5 as the scaling exponent. Therefore, we use RMSC, which is similar to SNR, to find the scaling exponents for centrality and NO_2 levels to test whether the relationship between NO_2 levels and centrality conforms to homotheticity (i.e. population size has a very small impact). We find the scaling exponent of centrality is 0.45, and the scaling exponent of NO_2 levels is 0.95. However, RMSC does not reveal the homotheticity of spatial distribution of NO_2 levels within cities, as NO_2 concentrations are affected by factors such as wind speed,

climate, and the NO_2 levels from neighboring large cities. For a small city near a large city, the feature of decreasing NO_2 levels along centrality may not be shown.

Lemoy and Caruso (2021) proposed another way to find scaling exponent by using a 2-step linear regression. Lemoy and Caruso (ibid.) regressed artificial land use share on centrality to get the value of characteristic distance, and then regressed characteristic distance on population size. Lemoy and Caruso (ibid.) used both linear regression and nonlinear regression to perform 2-step regression separately, and in both cases the scaling exponent of population size is close to 0.5. Inspired by Lemoy and Caruso (ibid.) we also try a 2-step linear regression to find the coefficients showing the impact of population size on centrality. In the first step, for each city we regress $\log_{10}C$ on $\log_{10}R$ and get the values of slope and intercept of the regression. In the second step, we regress the slope values of all the cities on $\log_{10}P$, and regress the intercept values of all the cities on $\log_{10}P$. We also consider 1) NO_2 levels without background effect; 2) calculate R from the pixel having the highest NO_2 value; 3) replace $\log_{10}R$ with R. Our results indicate that: 1) The NO_2 pollution levels in small cities are more affected by background NO_2 than in large cities. 2) NO_2 levels decrease faster along centrality in large cities than in small cities. 3) Changing the starting point of calculating centrality does not alter the decreasing trend of NO_2 levels along centrality. 4) The coefficients of $\log_{10}P$ we derived (i.e. 0.8330 and 0.2728) are close to that of $\log_{10}P$ in Chapter 4 (i.e. 0.2161). **Our results thus answer the question in Section 1.4, that the variation of NO_2 with centrality is influenced by population size, and NO_2 levels decrease faster along centrality in large cities than in small cities**.

To sum up, we show that both NO_2 surface concentrations and tropospheric NO_2 columns are reliable and useful tools for exploring urban NO_2 levels. Monitoring stations are close to the emission sources, therefore they are suitable for describing changes in NO_2 concentrations over short distances, while NO_2 columns are suitable for describing the extent of NO_2 in the whole city. Larger cities have higher UHI and NO_2 levels. We have not found the turning point of environmental Kuznets curve of NO_2 and UHI, which means urban planners cannot only count on economic or population growth to gain reduced NO_2 levels and heat waves. However, different cities have different climate types, different average wind speeds, different proximity to the nearest large city, thus population size is not the only factor that can decide the NO_2 levels inside the city. So if urban planners want to reduce the NO_2 levels in one city, then climate factors should be considered and the NO_2 levels in neighboring large cities must be controlled. Large cities have conditions to generate extremely high NO_2 levels, and the NO_2 levels in large cities decrease faster with centrality than in small cities. Therefore, urban planners can develop BRT or subways that connect the city center to the outskirts of the city in order to reduce citizens' NO_2 exposure.

6.1 Limitations and future works

However, this thesis has some limitations and many future works can be carried out based on the content of this thesis.

We performed the the qualitative synthesis and meta-analysis in 2019 but I started to write this thesis in 2022. Therefore, papers showing the relationship between UHI or NO_2 with urban population published during the past 3 years are not included. Given that only 13 UHI and 15 NO_2 studies are included in the qualitative synthesis and meta-analysis in Chapter 2, and only the data from 4 UHI and 5 NO_2 papers show statistical significance in ANOVA test, inclusion of newly published articles would enable researchers to more accurately assess the UHI and NO_2 pollution incurred by urban population. Furthermore, in Chapter 2, we use Google Scholar and Scopus as the data sources to construct a corpus based on the PRISMA guideline. However, in the future, we can explore searching in more databases such as Web of Science and Microsoft Bing. Scopus was launched in 2004 (Elsevier 2019), while Web of Science was launched in 1900 (Winter et al. 2014), so we may find more historical literature in Web of Science. The Journal Citation Reports (JCR) provided by Web of Science (Clarivate 2023) contains an evaluation of the impact of journals. So in the future, the literature can be screened according to the evaluation of the journals recommended by JCR, which can improve the accuracy and credibility of the results of qualitative synthesis and meta-analysis. The reason why we suggest to use Microsoft Bing is that different search engines have different search algorithms (Shahzad et al. 2018), so using Bing may help to discover literature that we cannot find when using Google Scholar. Another limitation of Chapter 2 is that, the articles in qualitative synthesis and meta-analysis study UHI and NO_2 in Asia, Europe, North America, and Oceania, but other regions of the world such as Africa, Latin America, and the Caribbean are not included in the investigation. Therefore, in the future, we can include studies on more countries and regions by changing the keywords or optimizing the data sources when searching.

Another drawback in Chapter 2 is that we use different articles as dummy variables because we do not have specific coordinates for the study area in each article. Therefore, we cannot use geographical conditions or climate types of study areas as dummy variables.

In our empirical studies of Chapters 4 and 5, we only focus on NO_2 and do not consider UHI. Although we explain in Section 1.1.4 of this thesis that it is reasonable for us to study NO_2, UHI and NO_2 are different types of pollution (i.e. the former is a temperature difference, and the latter is toxic gas). Therefore, empirical studies on the effects of population and centrality on UHI intensity, whether UHI intensity is related to centrality, and how population size affects the relationship between centrality and UHI intensity would provide intuitive support for urban planners in planning urban green spaces and optimizing roof materials. Or, we can regress UHI

intensity on the areas of green spaces and water to find out the effects of green spaces and water bodies on UHI intensity. We can also investigate whether increasing the areas of green spaces and water bodies alone can lead to a continuous decrease in UHI intensity, and whether the rate of decrease is gradually increasing or decreasing.

For the empirical study of NO_2, although we have explained in Section 1.2.6 why we do not consider population density and built-up areas in this thesis, we can carry out empirical studies on the effect of population density on NO_2 levels and the effect of built-up area on NO_2 levels in the future. Considering that we found in Section 1.2.6 that different definitions of population density and built-up areas can affect conclusions, our future empirical studies should be conducted from two spatial scales: the entire city and local neighborhoods.

In our empirical studies of Chapters 4 and 5, we use FUAs as the definition of cities. FUAs are defined by the employment and commuting patterns of residents (Simeonova 2019). However, this definition has drawbacks. For example, as we discussed in Section 3.2.8, FUA may ignore 3 possible factories around Kiel (Figure 3.20(b)), leading to an underestimation of the NO_2 levels of this FUA. Therefore, in the future, we suggest to design a unified definition of cities when exploring the relationship between environmental problems and population. This definition should not only consider the employment and commuting patterns of residents, but also take into account the emission sources of pollutants and their proximity to the city center. Then we can use this newly designed definition of cities for studying the relationship between NO_2 and population in countries outside Europe.

The independent variables we use in Chapters 4 and 5 also need improvement. We use population, centrality and background NO_2 as the independent variables and the background of monitoring station as the dummy variable. However, these variables are not sufficient to explain the spatial distribution of NO_2 inside some cities (e.g. Lecco in Figure 5.2(d)). Therefore, in the future, we can add the following variables: distance to the coast, wind speed and direction, distance to nearby large cities, and distance to transportation hubs (e.g. airports (Zhang et al. 2021b)).

We include logarithmic variables in this thesis, but because of the undefined *log(0)*, so the monitoring stations situated close to the city center and the NO_2 columns overlapped with the city center should be examined separately to find out the NO_2 concentrations at the exact point of the city center, which shows that there are some difficulties in using power laws to predict real-world air pollution.

Due to limited time, we don't include nonlinear regression in our 2-step linear regression analysis in Chapter 5. According to Lemoy and Caruso (2021), the results derived by nonlinear regression may be more satisfactory because of their lower values of SEs and higher values of R^2. Also because of limited time, in this thesis we don't consider predicted surface concentration

values from satellite columns. Predicted NO_2 surface concentrations come from climate models such as GEOS-Chem and EAC4. In climate models, tropospheric NO_2 columns are converted to NO_2 surface concentrations by considering anthropogenic emissions, biomass burning emissions, and assimilated trace gases retrievals, etc (Johnson et al. 2016). There are some advantages in using predicted NO_2 surface concentrations from satellites. First, for instance, the spatial resolution of GEOS-Chem can reach to 12.5 km x 12.5 km, which is higher than most NO_2 satellites except Sentinel-5P (Hu et al. 2018). Second, climate models provide comprehensive chemistry of atmosphere through a combination of model systems, users can customize the choice of the models, and can customize and predict the influence of weather on ground surface NO_2 for specific scenarios (Inness et al. 2019). The predicted NO_2 is positively correlated with measured NO_2 surface concentration, and the coefficient of determination can reach to 86% in analyzing spring and winter data (Lamsal et al. 2008). Therefore in the future, we can perform linear regression and time-series studies for predicted NO_2 surface concentrations, for example, in different seasons. Seasonal analysis can overcome the limitation of using annual mean NO_2 levels because the annual mean value ignores the impact of seasonal differences in anthropogenic activities on NO_2 levels (e.g. cooling and heating).

Bibliography

Abdel-Rahman, Hesham and Masahisa Fujita (1990). "Product variety, Marshallian externalities, and city sizes". In: *Journal of Regional Science* vol. 30.2, pp. 165–183.

Aboelata, Amir and Sahar Sodoudi (2020). "Evaluating the effect of trees on UHI mitigation and reduction of energy usage in different built up areas in Cairo". In: *Building and Environment* vol. 168, p. 106490.

Adinna, E. N., Ifeanyi Christian Enete, and Arch. Tony Okolie (2009). "Assessment of urban heat island and possible adaptations in Enugu urban using landsat-ETM". In: *Journal of Geography and Regional Planning* vol. 2.2, pp. 30–36.

Aflaki, Ardalan et al. (2017). "Urban heat island mitigation strategies: A state-of-the-art review on Kuala Lumpur, Singapore and Hong Kong". In: *Cities* vol. 62, pp. 131–145.

Agarwal, Manju and Abhinav Tandon (2010). "Modeling of the urban heat island in the form of mesoscale wind and of its effect on air pollution dispersal". In: *Applied Mathematical Modelling* vol. 34.9, pp. 2520–2530.

Aguilera, Inmaculada et al. (2015). "Land use regression models for crustal and traffic-related $PM_{2.5}$ constituents in four areas of the SAPALDIA study". In: *Environmental Research* vol. 140, pp. 377–384.

Ahmad, Shaharuddin and Noorazuan Md Hashim (2007). "Effects of soil moisture on urban heat island occurrences: Case of Selangor, Malaysia". In: *Humanity & Social Sciences Journal* vol. 2.2, pp. 132–138.

Ahmad, Sheikh Saeed and Neelam Aziz (2013). "Spatial and temporal analysis of ground level ozone and nitrogen dioxide concentration across the twin cities of Pakistan". In: *Environmental Monitoring and Assessment* vol. 185.4, pp. 3133–3147.

Ahmad, Sohail, Giovanni Baiocchi, and Felix Creutzig (2015). "CO_2 emissions from direct energy use of urban households in India". In: *Environmental Science & Technology* vol. 49.19, pp. 11312–11320.

Alberti, Marina (1999). "Urban patterns and environmental performance: What do we know?" In: *Journal of Planning Education and Research* vol. 19.2, pp. 151–163.

— (2005). "The effects of urban patterns on ecosystem function". In: *International Regional Science Review* vol. 28.2, pp. 168–192.

Alcoforado, Maria João and Henrique Andrade (2008). "Global warming and the urban heat island". In: *Urban ecology: An international perspective on the interaction between humans and nature*. Ed. by John M. Marzluff et al. Boston, MA: Springer US, pp. 249–262.

Allen, Alistair, Dejan Milenic, and Paul Sikora (2003). "Shallow gravel aquifers and the urban 'heat island' effect: A source of low enthalpy geothermal energy". In: *Geothermics* vol. 32.4, pp. 569–578.

Allen, L., F. Lindberg, and C.S.B. Grimmond (2011). "Global to city scale urban anthropogenic heat flux: Model and variability". In: *International Journal of Climatology* vol. 31.13, pp. 1990–2005.

Alonso, M. S., J. L. Labajo, and M. R. Fidalgo (2003). "Characteristics of the urban heat island in the city of Salamanca, Spain". In: *Atmósfera* vol. 16, pp. 137–148.

Alonso, William (1964). *Location and land use: Toward a general theory of land rent*. Harvard University Press.

Alrashed, Farajallah and Muhammad Asif (2014). "Trends in residential energy consumption in Saudi Arabia with particular reference to the Eastern Province". In: *Journal of Sustainable Development of Energy, Water and Environment Systems* vol. 2.4, pp. 376–387.

Andersen, Zorana J. et al. (2012). "Stroke and long-term exposure to outdoor air pollution from nitrogen dioxide". In: *Stroke* vol. 43.2, pp. 320–325.

Andrews, Clinton J. (2008). "Greenhouse gas emissions along the rural-urban gradient". In: *Journal of Environmental Planning and Management* vol. 51.6, pp. 847–870.

Anttila, Pia, Juha-Pekka Tuovinen, and Jarkko V. Niemi (2011). "Primary NO_2 emissions and their role in the development of NO_2 concentrations in a traffic environment". In: *Atmospheric Environment* vol. 45.4, pp. 986–992.

APIS (2023). *Nitrogen deposition*. Accessed March 23, 2023. URL: https://www.apis.ac.uk/overview/pollutants/overview_n_deposition.htm.

AQEG (2013). *Linking emission inventories and ambient measurements*. Tech. rep. Accessed October 3, 2022. Air Quality Expert Group. URL: hhttps://uk-air.defra.gov.uk/assets/documents/reports/cat11/1508060906_DEF-PB14106_Linking_Emissions_Inventories_And_Ambient_Measurements_Final.pdf.

Araujo, Ricardo Vieira et al. (2015). "São Paulo urban heat islands have a higher incidence of dengue than other urban areas". In: *The Brazilian Journal of Infectious Diseases* vol. 19.2, pp. 146–155.

Arifwidodo, Sigit D. and Takahiro Tanaka (2015). "The characteristics of urban heat island in Bangkok, Thailand". In: *Procedia-Social and Behavioral Sciences* vol. 195, pp. 423–428.

Arifwidodo, Sigit and Orana Chandrasiri (2015). "Urban heat island and household energy consumption in Bangkok, Thailand". In: *Energy Procedia* vol. 79, pp. 189–194.

Arsanjani, Jamal Jokar, Marco Helbich, and Eric de Noronha Vaz (2013). "Spatiotemporal simulation of urban growth patterns using agent-based modeling: The case of Tehran". In: *Cities* vol. 32, pp. 33–42.

Artun, Gülzade Küçükaçl et al. (2017). "An integrative approach for determination of air pollution and its health effects in a coal fired power plant area by passive sampling". In: *Atmospheric Environment* vol. 150, pp. 331–345.

Atkinson, B.W. (2003). "Numerical modelling of urban heat-island intensity". In: *Boundary-Layer Meteorology* vol. 109.3, pp. 285–310.

Balakrishnan, K et al. (2011). "Part 1. Short-term effects of air pollution on mortality: Results from a time-series analysis in Chennai, India". In: *Research Report Health Effects Institute* 157, pp. 7–44.

Bares, Ryan et al. (2018). "The wintertime covariation of CO_2 and criteria pollutants in an urban valley of the western United States". In: *Journal of Geophysical Research: Atmospheres* vol. 123.5, pp. 2684–2703.

Baró, Francesc et al. (2015). "Mismatches between ecosystem services supply and demand in urban areas: A quantitative assessment in five European cities". In: *Ecological Indicators* vol. 55, pp. 146–158.

Baró, Francesc et al. (2016). "Mapping ecosystem service capacity, flow and demand for landscape and urban planning: A case study in the Barcelona metropolitan region". In: *Land Use Policy* vol. 57, pp. 405–417.

Bartlett, Randall (1998). *The crisis of America's cities: Solutions for the future, lessons from the past*. Routledge.

Basahi, JM, IM Ismail, and IA Hassan (2014). "A global challenge of air pollution and public health: A mini review". In: *Advances in Environmental Biology*, pp. 281–289.

Bassett, Richard et al. (2019). "Semi-idealized urban heat advection simulations using the Weather Research and Forecasting mesoscale model". In: *International Journal of Climatology* vol. 39.3, pp. 1345–1358.

Batty, Michael (2008). "The size, scale, and shape of cities". In: *Science* vol. 319.5864, pp. 769–771.

— (2013). *The new science of cities*. Mit Press.

Bechle, Matthew J., Dylan B. Millet, and Julian D. Marshall (2011). "Effects of income and urban form on urban NO_2: Global evidence from satellites". In: *Environmental Science & Technology* vol. 45.11, pp. 4914–4919.

— (2013). "Remote sensing of exposure to NO_2: Satellite versus ground-based measurement in a large urban area". In: *Atmospheric Environment* vol. 69, pp. 345–353.

Bechtel, Benjamin and Katharina Johanna Schmidt (2011). "Floristic mapping data as a proxy for the mean urban heat island". In: *Climate Research* vol. 49.1, pp. 45–58.

Beck, Hylke E. et al. (2018). "Present and future Köppen-Geiger climate classification maps at 1-km resolution". In: *Scientific Data* 1, p. 180214.

Beelen, Rob et al. (2009). "Mapping of background air pollution at a fine spatial scale across the European Union". In: *Science of the Total Environment* vol. 407.6, pp. 1852–1867.

Beelen, Rob et al. (2010). "Comparison of the performances of land use regression modelling and dispersion modelling in estimating small-scale variations in long-term air pollution concentrations in a Dutch urban area". In: *Atmospheric Environment* vol. 44.36, pp. 4614–4621.

Behera, Sailesh N. et al. (2011). "Development of GIS-aided emission inventory of air pollutants for an urban environment". In: *Advanced air pollution*. Ed. by Farhad Nejadkoorki. Rijeka: IntechOpen. Chap. 16.

Beirle, S. et al. (2003). "Weekly cycle of NO_2 by GOME measurements: A signature of anthropogenic sources". In: *Atmospheric Chemistry and Physics* vol. 3.6, pp. 2225–2232.

Beirle, Steffen et al. (2011). "Megacity emissions and lifetimes of nitrogen oxides probed from space". In: *Science* vol. 333.6050, pp. 1737–1739.

Bekele, A. et al. (2003). "Comparative evaluation of spatial prediction methods in a field experiment for mapping soil potassium". In: *Soil Science* vol. 168.1.

Bellander, T. et al. (2001). "Using geographic information systems to assess individual historical exposure to air pollution from traffic and house heating in Stockholm". In: *Environmental Health Perspectives* vol. 109.6, pp. 633–639.

Benkovitz, C.M. (1983). "Characteristics of oxidant precursor emissions from anthropogenic sources in the United States". In: *Environment International* vol. 9.6, pp. 429–445.

Benz, Susanne A., Peter Bayer, and Philipp Blum (2017). "Identifying anthropogenic anomalies in air, surface and groundwater temperatures in Germany". In: *Science of the Total Environment* vol. 584-585, pp. 145–153.

Bereitschaft, Bradley and Keith Debbage (2013). "Urban form, air pollution, and CO_2 emissions in large U.S. metropolitan areas". In: *The Professional Geographer* vol. 65.4, pp. 612–635.

Bermejo-Orduna, R. et al. (2014). "Biomonitoring of traffic-related nitrogen pollution using Letharia vulpina (L.) Hue in the Sierra Nevada, California". In: *Science of the Total Environment* vol. 490, pp. 205–212.

Bettencourt, Luís M. A. (2013). "The origins of scaling in cities". In: *Science* vol. 340.6139, pp. 1438–1441.

Bettencourt, Luís M. A. et al. (2007). "Growth, innovation, scaling, and the pace of life in cities". In: *Proceedings of the National Academy of Sciences* vol. 104.17, pp. 7301–7306.

Bey, Isabelle et al. (2001). "Global modeling of tropospheric chemistry with assimilated meteorology: Model description and evaluation". In: *Journal of Geophysical Research: Atmospheres* vol. 106.D19, pp. 23073–23095.

Blazejczyk, Krzysztof, Monika Bakowska, and Miroslaw Wieclaw (2006). "Urban heat island in large and small cities". In: *6th International Conference on Urban Climate, Göteborg, Sweden, June 12-16*. Vol. 2006, pp. 94–797.

Blond, N. et al. (2007). "Intercomparison of SCIAMACHY nitrogen dioxide observations, in situ measurements and air quality modeling results over Western Europe". In: *Journal of Geophysical Research: Atmospheres* vol. 112.D10.

Bogo, H et al. (2001). "Traffic pollution in a downtown site of Buenos Aires City". In: *Atmospheric Environment* vol. 35.10, pp. 1717–1727.

Böhm, Reinhard (1998). "Urban bias in temperature time series-A case study for the City of Vienna, Austria". In: *Climatic Change* vol. 38.1, pp. 113–128.

Bokaie, Mehdi et al. (2016). "Assessment of urban heat island based on the relationship between land surface temperature and land use/land cover in Tehran". In: *Sustainable Cities and Society* vol. 23, pp. 94–104.

Borck, Rainald and Philipp Schrauth (2021). "Population density and urban air quality". In: *Regional Science and Urban Economics* vol. 86, p. 103596.

Bornstein, Marc and Helen Bornstein (1976). "The pace of life". In: *Nature* vol. 259.5544, pp. 557–559.

Borrego, C. et al. (2006). "How urban structure can affect city sustainability from an air quality perspective". In: *Environmental Modelling & Software* vol. 21.4, pp. 461–467.

Bosch-Cano, Floriane et al. (2011). "Human exposure to allergenic pollens: A comparison between urban and rural areas". In: *Environmental Research* vol. 111.5, pp. 619–625.

Bose, Probir Kumar and Dines Maji (2009). "An experimental investigation on engine performance and emissions of a single cylinder diesel engine using hydrogen as inducted fuel and diesel as injected fuel with exhaust gas recirculation". In: *International Journal of Hydrogen Energy* vol. 34.11. 2nd International Workshop on Hydrogen, pp. 4847–4854.

Boyne, George (1995). "Population size and economies of scale in local government". In: *Policy & Politics* vol. 23.3, pp. 213–222.

Brandsma, Theo and Dirk Wolters (2012). "Measurement and statistical modeling of the urban heat island of the city of Utrecht (the Netherlands)". In: *Journal of Applied Meteorology and Climatology* vol. 51.6, pp. 1046–1060.

Branis, Martin and Martina Linhartova (2012). "Association between unemployment, income, education level, population size and air pollution in Czech cities: Evidence for environmental inequality? A pilot national scale analysis". In: *Health & Place* vol. 18.5, pp. 1110–1114.

Broersma, Lourens and Jouke van Dijk (2007). "The effect of congestion and agglomeration on multifactor productivity growth in Dutch regions". In: *Journal of Economic Geography* vol. 8.2, pp. 181–209.

Butler, TM et al. (2008). "The representation of emissions from megacities in global emission inventories". In: *Atmospheric Environment* vol. 42.4, pp. 703–719.

Butryn, Ryan S., Donna L. Parrish, and Donna M. Rizzo (2013). "Summer stream temperature metrics for predicting brook trout (Salvelinus fontinalis) distribution in streams". In: *Hydrobiologia* vol. 703.1, pp. 47–57.

Butu, Ioana Maria et al. (2012). "Evaluation of air pollution with NO_2 in Bucharest Area". In: *Revista de Chimie -Bucharest-Original Edition* vol. 63.3, pp. 330–333.

Cahuana-Bartra, Marc Josep et al. (2022). "Maternal short-term exposure to NO_2 during pregnancy and its relationship with Doppler markers of placental function". In: *Environmental Research* vol. 214, p. 113813.

Cai, Guoyin, Mingyi Du, and Yang Gao (2019). "City block-based assessment of land cover components′ impacts on the urban thermal environment". In: *Remote Sensing Applications: Society and Environment* vol. 13, pp. 85–96.

Cai, Guoyin, Yang Liu, and Mingyi Du (2017). "Impact of the 2008 Olympic Games on urban thermal environment in Beijing, China from satellite images". In: *Sustainable Cities and Society* vol. 32, pp. 212–225.

Cakmak, Sabit et al. (2011). "The risk of dying on days of higher air pollution among the socially disadvantaged elderly". In: *Environmental Research* vol. 111.3, pp. 388–393.

Caldwell, John Charles (1990). "The soft underbelly of development - demographic transition in conditions of limited economic change". In: *The World Bank Economic Review* vol. 4, pp. 207–253.

Camilloni, Inés and Vicente Barros (1997). "On the urban heat island effect dependence on temperature trends". In: *Climatic Change* vol. 37.4, pp. 665–681.

Camilloni, Inés and Mariana Barrucand (2012). "Temporal variability of the Buenos Aires, Argentina, urban heat island". In: *Theoretical and Applied Climatology* vol. 107.1, pp. 47–58.

Campbell, G.W, J.R Stedman, and K Stevenson (1994). "A survey of nitrogen dioxide concentrations in the United Kingdom using diffusion tubes, July-December 1991". In: *Atmospheric Environment* vol. 28.3, pp. 477–486.

Capello, Roberta and Roberto Camagni (2000). "Beyond optimal city size: An evaluation of alternative urban growth patterns". In: *Urban Studies* vol. 37.9, pp. 1479–1496.

Cardelino, C. A. and W. L. Chameides (1990). "Natural hydrocarbons, urbanization, and urban ozone". In: *Journal of Geophysical Research: Atmospheres* vol. 95.D9, pp. 13971–13979.

Carnahan, Walter H. and Robert C. Larson (1990). "An analysis of an urban heat sink". In: *Remote Sensing of Environment* vol. 33.1, pp. 65–71.

Carslaw, David C. et al. (2006). "Detecting and quantifying aircraft and other on-airport contributions to ambient nitrogen oxides in the vicinity of a large international airport". In: *Atmospheric Environment* vol. 40.28, pp. 5424–5434.

Ceplová, Natálie, Veronika Kalusová, and Zdenka Lososová (2017). "Effects of settlement size, urban heat island and habitat type on urban plant biodiversity". In: *Landscape and Urban Planning* vol. 159, pp. 15–22.

Cesaroni, Giulia et al. (2012). "Nitrogen dioxide levels estimated from land use regression models several years apart and association with mortality in a large cohort study". In: *Environmental Health: A Global Access Science Source* vol. 11, pp. 48–48.

Chan, Kam Wing and Xueqiang Xu (1985). "Urban population growth and urbanization in China since 1949: Reconstructing a baseline". In: *The China Quarterly* 104, pp. 583–613.

Chance, K. (2002). *OMI algorithm theoretical basis document - Volume IV*. Accessed June 30, 2022. URL: https://ozoneaq.gsfc.nasa.gov/media/docs/ATBD-OMI-04.pdf.

Chance, Kelly V. and Robert J.D. Spurr (1997). "Ring effect studies: Rayleigh scattering, including molecular parameters for rotational Raman scattering, and the Fraunhofer spectrum". In: *Applied Optics* vol. 36.21, pp. 5224–5230.

Chang, Huawei et al. (2016). "Study on the thermal performance and wind environment in a residential community". In: *International Journal of Hydrogen Energy* vol. 41.35, pp. 15868–15878.

Changnon, Stanley A. (1999). "A rare long record of deep soil temperatures defines temporal temperature changes and an urban heat island". In: *Climatic Change* vol. 42.3, pp. 531–538.

Chaube, Abha, Anil K. Baveja, and V. K. Gupta (February 1984). "A sensitive method for the determination of nitrogen dioxide in air using solvent extraction". In: *Journal of Indian Chemical Society* vol. Vol. 61.Feb. 1984, pp. 157–158.

Che Ani, Adi Irfan et al. (2009). "Mitigating the urban heat island effect: Some points without altering existing city planning". In: *European Journal of Scientific Research* vol. 35.2, pp. 204–216.

Cheela, V. R. Sankar et al. (2021). "Combating urban heat island effect - A review of reflective pavements and tree shading strategies". In: *Buildings* vol. 11.3.

Chen, Li et al. (2010). "A land use regression for predicting NO_2 and PM_{10} concentrations in different seasons in Tianjin region, China". In: *Journal of Environmental Sciences* vol. 22.9, pp. 1364–1373.

Chen, Li et al. (2012). "A land use regression model incorporating data on industrial point source pollution". In: *Journal of Environmental Sciences* vol. 24.7, pp. 1251–1258.

Chen, Qian et al. (2018). "Spatially explicit assessment of heat health risk by using multi-sensor remote sensing images and socioeconomic data in Yangtze River Delta, China". In: *International Journal of Health Geographics* vol. 17.1, p. 15.

Chen, Xiao-Ling et al. (2006). "Remote sensing image-based analysis of the relationship between urban heat island and land use/cover changes". In: *Remote Sensing of Environment* vol. 104.2, pp. 133–146.

Cheng, Jianquan and Ian Masser (2003). "Urban growth pattern modeling: A case study of Wuhan City, PR China". In: *Landscape and Urban Planning* vol. 62.4, pp. 199–217.

Chertow, Marian R. (2000). "The IPAT equation and its variants". In: *Journal of Industrial Ecology* vol. 4, pp. 13–29.

Cheval, S. and A. Dumitrescu (2009). "The July urban heat island of Bucharest as derived from MODIS images". In: *Theoretical and Applied Climatology* vol. 96.1, pp. 145–153.

Chiesa, M. et al. (2009). "A target-oriented risk assessment for air pollution in Milan: Preliminary results". In: *GIMT - Giornale Italiano delle Malattie del Torace* vol. 63.6, pp. 439–446.

Chipperfield, M. P. et al. (1994). "A two-dimensional model study of the QBO signal in SAGE II NO_2 and O_3". In: *Geophysical Research Letters* vol. 21.7, pp. 589–592.

Choi, Giehae, Seulkee Heo, and Jong-Tae Lee (2016). "Assessment of environmental injustice in Korea using synthetic air quality index and multiple indicators of socioeconomic status: A cross-sectional study". In: *Journal of the Air & Waste Management Association* vol. 66.1, pp. 28–37.

Choi, Jaeyeon, Uran Chung, and Jin I. Yun (2003). "Urban-effect correction to improve accuracy of spatially interpolated temperature estimates in Korea". In: *Journal of Applied Meteorology* vol. 42.12, pp. 1711–1719.

Chow, Winston T. L. and Matthias Roth (2006). "Temporal dynamics of the urban heat island of Singapore". In: *International Journal of Climatology* vol. 26.15, pp. 2243–2260.

Chow, Winston T.L. et al. (2014). "A multi-method and multi-scale approach for estimating city-wide anthropogenic heat fluxes". In: *Atmospheric Environment* vol. 99, pp. 64–76.

Clarivate (2023). *Journal Citation Reports - Clarivate*. Accessed April 20, 2023. URL: https://access.clarivate.com/login?app=jcr&referrer=target%3Dhttps:%2F%2Fjcr.clarivate.com%2Fjcr%2Fhome&alternative=true&shibShireURL=https:%2F%2Flogin.incites.clarivate.com%2F%3FDestApp%3DIC2JCR%26amp;auth%3DShibboleth&shibReturnURL=https:%2F%2Flogin.incites.clarivate.com%2F.

Clark, Jim (2020). *The thermal stability of the nitrates and carbonates*. Accessed 9 March, 2023. URL: https://chem.libretexts.org/Bookshelves/Inorganic_Chemistry/Supplemental_Modules_and_Websites_(Inorganic_Chemistry)/Descriptive_Chemistry/Elements_Organized_by_Block/1_s-Block_Elements/Group__2_Elements%3A_The_Alkaline_Earth_Metals/1Group_2%3A_Chemical_Reactions_of_Alkali_Earth_Metals/The_Thermal_Stability_of_the_Nitrates_and_Carbonates.

Clark, Lara P., Dylan B. Millet, and Julian D. Marshall (2011). "Air quality and urban form in U.S. urban areas: Evidence from regulatory monitors". In: *Environmental Science & Technology* vol. 45.16, pp. 7028–7035.

Clay, Roger et al. (2016). "Urban heat island traverses in the city of Adelaide, South Australia". In: *Urban Climate* vol. 17, pp. 89–101.

Clougherty, Jane E., E. Andres Houseman, and Jonathan I. Levy (2009). "Examining intra-urban variation in fine particle mass constituents using GIS and constrained factor analysis". In: *Atmospheric Environment* vol. 43.34, pp. 5545–5555.

Clougherty, Jane E. et al. (2007). "Synergistic effects of traffic-related air pollution and exposure to violence on urban asthma etiology". In: *Environmental Health Perspectives* vol. 115.8, pp. 1140–1146.

Clougherty, Jane E. et al. (2008). "Land use regression modeling of intra-urban residential variability in multiple traffic-related air pollutants". In: *Environmental Health* vol. 7.1, p. 17.

Clougherty, Jane E. et al. (2013). "Intra-urban spatial variability in wintertime street-level concentrations of multiple combustion-related air pollutants: The New York City Community Air Survey (NYCCAS)". In: *Journal of Exposure Science & Environmental Epidemiology* vol. 23.3, pp. 232–240.

Cohen, Matthew (2017). "A systematic review of urban sustainability assessment literature". In: *Sustainability* vol. 9.11, p. 2048.

Colvile, R.N et al. (2001). "The transport sector as a source of air pollution". In: *Atmospheric Environment* vol. 35.9, pp. 1537–1565.

Constantin, Daniel-Eduard et al. (2015). "Study of solar variability impact on nitrogen dioxide: 2004-2013". In: *EGU General Assembly Conference Abstracts*. EGU General Assembly Conference Abstracts, p. 542.

Coppalle, A., V. Delmas, and M. Bobbia (2001). "Variability of NO_x and NO_2 concentrations observed at pedestrian level in the city centre of a medium sized urban area". In: *Atmospheric Environment* vol. 35.31, pp. 5361–5369.

Costanzo, V., G. Evola, and L. Marletta (2016). "Energy savings in buildings or UHI mitigation? Comparison between green roofs and cool roofs". In: *Energy and Buildings* vol. 114. SI: Countermeasures to Urban Heat Island, pp. 247–255.

Cowie, Christine T. et al. (2019). "Comparison of model estimates from an intra-city land use regression model with a national satellite-LUR and a regional Bayesian Maximum Entropy model, in estimating NO_2 for a birth cohort in Sydney, Australia". In: *Environmental Research* vol. 174, pp. 24–34.

Craig, John and John Haskey (1978). "The relationships between the population, area, and density of urban areas". In: *Urban Studies* vol. 15.1, pp. 101–107.

Crouse, Dan L. et al. (2018). "Associations between living near water and risk of mortality among urban Canadians". In: *Environmental Health Perspectives* vol. 126.7, p. 077008.

Crouse, Dan L et al. (2017). "Urban greenness and mortality in Canada's largest cities: A national cohort study". In: *The Lancet Planetary Health* vol. 1.7, e289–e297.

Cui, Linli, Jun Shi, and Zhiqiang Gao (2007). "Urban heat island in Shanghai, China". In: *Remote Sensing and Modeling of Ecosystems for Sustainability IV*. Ed. by Wei Gao and Susan L. Ustin. Vol. 6679. International Society for Optics and Photonics. SPIE, pp. 327–335.

Cui, Yuanzheng et al. (2019). "Evaluation of China's environmental pressures based on satellite NO_2 observation and the extended STIRPAT model". In: *International Journal of Environmental Research and Public Health* vol. 16.9.

Cusack, Stephen (2014). "Increased tornado hazard in large metropolitan areas". In: *Atmospheric Research* vol. 149, pp. 255–262.

Cyrys, Josef et al. (2012). "Variation of NO_2 and NO_x concentrations between and within 36 European study areas: Results from the ESCAPE study". In: *Atmospheric Environment* vol. 62, pp. 374–390.

Dahlhausen, Jens et al. (2018). "Urban climate modifies tree growth in Berlin". In: *International Journal of Biometeorology* vol. 62.5, pp. 795–808.

Dale, Adam G. and Steven D. Frank (2014). "Urban warming trumps natural enemy regulation of herbivorous pests". In: *Ecological Applications* vol. 24.7, pp. 1596–1607.

Danciulescu, Valeriu et al. (2015). "Correlations between noise level and pollutants concentration in order to assess the level of air pollution induced by heavy traffic". In: *Journal of Environmental Protection and Ecology* vol. 16.3, pp. 815–823.

Danzlger, Sheldon (1976). "Explaining urban crime rates". In: *Criminology* vol. 14.2, pp. 291–296.

De Redder, Koen et al. (2015). "The impact of model resolution on simulated ambient air quality and associated human exposure". In: *Atmósfera* vol. 27.4, pp. 403–410.

Debbage, Neil and J. Marshall Shepherd (2015). "The urban heat island effect and city contiguity". In: *Computers, Environment and Urban Systems* vol. 54, pp. 181–194.

Dedele, Audrius and Aukse Miskinyte (2016). "Seasonal variation of indoor and outdoor air quality of nitrogen dioxide in homes with gas and electric stoves". In: *Environmental Science and Pollution Research* vol. 23.17, pp. 17784–17792.

Degraeuwe, Bart et al. (2016). "Impact of passenger car NO_x emissions and NO_2 fractions on urban NO_2 pollution - Scenario analysis for the city of Antwerp, Belgium". In: *Atmospheric Environment* vol. 126, pp. 218–224.

Deilami, Kaveh and Md. Kamruzzaman (2017). "Modelling the urban heat island effect of smart growth policy scenarios in Brisbane". In: *Land Use Policy* vol. 64, pp. 38–55.

Deilami, Kaveh, Md. Kamruzzaman, and John Francis Hayes (2016). "Correlation or causality between land cover patterns and the urban heat island effect? Evidence from Brisbane, Australia". In: *Remote Sensing* vol. 8.9.

Delaney, Conor and Paul Dowding (1998). "The relationship between extreme nitrogen oxide (NOx) concentrations in Dublin's atmosphere and meteorological conditions". In: *Environmental Monitoring and Assessment* vol. 52.1, pp. 159–172.

Denby, Bruce et al. (2011). "Sub-grid variability and its impact on European wide air quality exposure assessment". In: *Atmospheric Environment* vol. 45.25, pp. 4220–4229.

Devadas, Monsingh D and AL Rose (2009). "Urban factors and the intensity of heat island in the city of Chennai". In: *The Seventh International Conference on Urban Climate*. Vol. 29.

Diao, Beidi et al. (2018). "The spatial-temporal characteristics and influential factors of NO_x emissions in China: A spatial econometric analysis". In: *International Journal of Environmental Research and Public Health* vol. 15.7.

Dietz, Thomas and Eugene A. Rosa (1997). "Effects of population and affluence on CO_2 emissions". In: *Proceedings of the National Academy of Sciences* vol. 94.1, pp. 175–179.

Dieudonne, E. et al. (2013). "Linking NO_2 surface concentration and integrated content in the urban developed atmospheric boundary layer". In: *Geophysical Research Letters* vol. 40.6, pp. 1247–1251.

Dihkan, Mustafa et al. (2018). "Evaluation of urban heat island effect in Turkey". In: *Arabian Journal of Geosciences* vol. 11.8, p. 186.

Dijkstra, Lewis, Hugo Poelman, and Paolo Veneri (2019). *The EU-OECD definition of a functional urban area*. OECD.

Ding, Chengri and Xingshuo Zhao (2011). "Assessment of urban spatial-growth patterns in China during rapid urbanization". In: *The Chinese Economy* vol. 44.1, pp. 46–71.

Dixon, P. Grady and Thomas L. Mote (2003). "Patterns and causes of Atlanta's urban heat island-initiated precipitation". In: *Journal of Applied Meteorology* vol. 42.9, pp. 1273–1284.

Domingo, Alcaraz-Segura, Di Bella Carlos Marcelo, and Straschnoy Julieta Veronica (2013). *Earth observation of ecosystem services*. Florida: CRC Press.

Dong, Weihua et al. (2014). "Assessing heat health risk for sustainability in Beijing′s urban heat island". In: *Sustainability* vol. 6.10, pp. 7334–7357.

Donnelly, Aoife, Bruce Misstear, and Brian Broderick (2011). "Application of nonparametric regression methods to study the relationship between NO2 concentrations and local wind direction and speed at background sites". In: *Science of The Total Environment* vol. 409.6, pp. 1134–1144.

Douglas, Ashley N.J., Peter J. Irga, and Fraser R. Torpy (2019). "Determining broad scale associations between air pollutants and urban forestry: A novel multifaceted methodological approach". In: *Environmental Pollution* vol. 247, pp. 474–481.

Dragomir, Carmelia Mariana et al. (2015). "Modeling results of atmospheric dispersion of NO_2 in an urban area using METILIS and comparison with coincident mobile DOAS measurements". In: *Atmospheric Pollution Research* vol. 6.3, pp. 503–510.

Du, Hongyu et al. (2016). "Influences of land cover types, meteorological conditions, anthropogenic heat and urban area on surface urban heat island in the Yangtze River Delta Urban Agglomeration". In: *Science of the Total Environment* vol. 571, pp. 461–470.

Du, Yin et al. (2007). "Impact of urban expansion on regional temperature change in the Yangtze River Delta". In: *Journal of Geographical Sciences* vol. 17.4, pp. 387–398.

Duarte, Denise H.S. et al. (2015). "The impact of vegetation on urban microclimate to counterbalance built density in a subtropical changing climate". In: *Urban Climate* vol. 14, pp. 224–239.

Duncan, Bryan N. et al. (2016). "A space-based, high-resolution view of notable changes in urban NO_x pollution around the world (2005-2014)". In: *Journal of Geophysical Research: Atmospheres* vol. 121.2, pp. 976–996.

Dütemeyer, Dirk et al. (2014). "Measures against heat stress in the city of Gelsenkirchen, Germany". In: *DIE ERDE Journal of the Geographical Society of Berlin* vol. 144.3-4, pp. 181–201.

Dwivedi, Aparna and Mohan V. Khire (2018). "Application of split- window algorithm to study Urban Heat Island effect in Mumbai through land surface temperature approach". In: *Sustainable Cities and Society*.

Eberts, Randall W et al. (1986). *Estimating the contribution of urban public infrastructure to regional growth*. Vol. 8610. Federal Reserve Bank of Cleveland Cleveland, OH.

Echevarría Icaza, Leyre and Franklin Van der Hoeven (2017). "Regionalist principles to reduce the urban heat island effect". In: *Sustainability* vol. 9.5.

ECMWF (2023). *CAMS global reanalysis (EAC4)*. Accessed 9 March, 2023. URL: https://www.ecmwf.int/en/forecasts/dataset/cams-global-reanalysis.

EEA (2016). *Air quality in Europe - 2016 report*. EEA.

— (2018a). *Air quality in Europe - 2018 report*. EEA.

— (2018b). *AQ e-Reporting products on EEA data service*. Accessed June 27, 2022. URL: https://www.eea.europa.eu/data-and-maps/data/aqereporting-8/aq-ereporting-products.

— (2023). *About Air Quality e-reporting*. Accessed March 17, 2023. URL: https://eeadmz1-cws-wp-air02.azurewebsites.net/index.php/european-air-quality-portal/about-reporting/.

Eeftens, Marloes et al. (2011). "Stability of measured and modelled spatial contrasts in NO_2 over time". In: *Occupational & Environmental Medicine* vol. 68.10, pp. 765–770.

Eeftens, Marloes et al. (2019). "Modelling the vertical gradient of nitrogen dioxide in an urban area". In: *Science of the Total Environment* vol. 650, pp. 452–458.

Eggleston, Simon et al. (2006). *2006 IPCC guidelines for national greenhouse gas inventories*. Vol. 4. Institute for Global Environmental Strategies Hayama, Japan. URL: https://www.ipcc-nggip.iges.or.jp/public/2006gl/pdf/4_Volume4/V4_09_Ch9_Other_Land.pdf.

Elansky, Nikolai F et al. (2016). "Trace gases in the atmosphere over Russian cities". In: *Atmospheric Environment* vol. 143, pp. 108–119.

Eliasson, Ingegärd (1996). "Urban nocturnal temperatures, street geometry and land use". In: *Atmospheric Environment* vol. 30.3, pp. 379–392.

Elsayed, Ilham SM (2012). "Effects of population density and land management on the intensity of urban heat islands: A case study on the city of Kuala Lumpur, Malaysia". In: *Application of geographic information systems*, pp. 267–283.

Elsevier (2019). *Search for an author profile*. https://www.scopus.com/freelookup/form/author.uri. Accessed December 16, 2019.

Endlicher, Wilfried et al. (2008). "Heat waves, urban climate and human health". In: *Urban ecology: An international perspective on the interaction between humans and nature*. Ed. by John M. Marzluff et al. Boston, MA: Springer US, pp. 269–278.

Endreny, Theodore (2008). "Naturalizing urban watershed hydrology to mitigate urban heat-island effects". In: *Hydrological Processes* vol. 22.3, pp. 461–463.

Erell, Evyatar, David Pearlmutter, and Terence Williamson (2012). *Urban microclimate: Designing the spaces between buildings*. Routledge.

ESA (2020). *Nitrogen dioxide concentrations over Europe*. https://www.esa.int/ESA_Multimedia/Images/2020/04/Nitrogen_dioxide_concentrations_over_Europe. Accessed March 25, 2023.

— (2021). *Sentinel-5P pre-operations data hub*. Accessed June 27, 2022. URL: https://s5phub.copernicus.eu/dhus/#/home.

— (2022). *Level - 2 algorithms - DOAS*. Accessed June 5, 2022. URL: https://sentinels.copernicus.eu/web/sentinel/technical-guides/sentinel-5p/level-2/doas-method.

— (2023a). *Cal/Val activities - calibration*. Accessed March 17, 2023. URL: https://sentinels.copernicus.eu/web/sentinel/technical-guides/sentinel-5p/calibration.

— (2023b). *Sentinel-5P*. Accessed 9 March, 2023. URL: https://sentinels.copernicus.eu/web/sentinel/missions/sentinel-5p.

— (2023c). *SNAP download*. Accessed March 17, 2023. URL: https://step.esa.int/main/download/snap-download/.

Esau, Igor and Victoria Miles (2018). "Exogenous drivers of surface urban heat islands in northern west Siberia". In: *Geography, Environment, Sustainability* vol. 11.3, pp. 83–99.

Escudero, M et al. (2014). "Urban influence on increasing ozone concentrations in a characteristic Mediterranean agglomeration". In: *Atmospheric Environment* vol. 99, pp. 322–332.

Eskes, Henk and K.-U. Eichmann (2021). *S5P mission performance centre nitrogen dioxide [L2__NO2___] readme*. Tech. rep. Accessed June 28, 2022. European Space Agency. URL:

https://sentinels.copernicus.eu/documents/247904/3541451/Sentinel-5P-Nitrogen-Dioxide-Level-2-Product-Readme-File.

Eskes, Henk et al. (2019). *Sentinel-5 precursor/TROPOMI level 2 product user manual nitrogen dioxide*. Tech. rep. Accessed June 28, 2022. Royal Netherlands Meteorological Institute. URL: http://www.tropomi.eu/sites/default/files/files/publicSentinel-5P-Level-2-Product-User-Manual-Nitrogen-Dioxide.pdf.

Esplugues, A. et al. (2010). "Indoor and outdoor concentrations and determinants of NO_2 in a cohort of 1-year-old children in Valencia, Spain". In: *Indoor Air* vol. 20.3, pp. 213–223.

Estoque, Ronald C. and Yuji Murayama (2017). "Monitoring surface urban heat island formation in a tropical mountain city using Landsat data (19872015)". In: *ISPRS Journal of Photogrammetry and Remote Sensing* vol. 133, pp. 18–29.

Estoque, Ronald C., Yuji Murayama, and Soe W. Myint (2017). "Effects of landscape composition and pattern on land surface temperature: An urban heat island study in the megacities of Southeast Asia". In: *Science of the Total Environment* vol. 577, pp. 349–359.

EU (2008). "Directive 2008/50/EC of the European Parliament and of the Council of 21 May 2008 on ambient air quality and cleaner air for Europe". In: *Official Journal of the European Union*, pp. 1–44.

European Comission (2019). *GHSL-OECD Functional Urban Areas*. Accessed 18 March, 2023. URL: https://ghsl.jrc.ec.europa.eu/documents/GHSL_FUA_2019.pdf?t=1583246033.

European Commission (2010). *Guidance on air quality assessment around point sources under the EU Air Quality Directive 2008/50/EC*. Tech. rep. Accessed June 28, 2022. European Commission. URL: https://ec.europa.eu/environment/air/quality/legislation/pdf/Guidance%20on%20assessment%20around%20point%20sources%20AQCincluded_final.pdf.

European Committee for Standardization (2005). *Ambient air quality - Standard method for the measurement of the concentration of nitrogen dioxide and nitrogen monoxide by chemiluminescence*. Accessed June 5, 2022. URL: https://standards.iteh.ai/catalog/standards/cen/181f3d8d-a64c-46fb-b90a-7affd10c7c0b/en-14211-2005.

European Court of Auditors (2022). *Our activities in 2021 - annual activity report of the European Court of Auditors*. Tech. rep. Accessed March 17, 2023. European Court of Auditors. URL: https://www.eca.europa.eu/Lists/ECADocuments/AAR21/AAR21_EN.pdf.

Eurostat (2018a). *Glossary: City*. Accessed June 27, 2022. URL: https://ec.europa.eu/eurostat/statistics-explained/index.php/Glossary:City.

— (2018b). *Glossary: Commuting zone*. Accessed June 27, 2022. URL: https://ec.europa.eu/eurostat/statistics-explained/index.php?title=Glossary:Commuting_zone.

Ewing, Reid and Fang Rong (2008). "The impact of urban form on U.S. residential energy use". In: *Housing Policy Debate* vol. 19.1, pp. 1–30.

Fabrizi, Roberto, Stefania Bonafoni, and Riccardo Biondi (2010). "Satellite and ground-based sensors for the urban heat island analysis in the city of Rome". In: *Remote Sensing* vol. 2.5, pp. 1400–1415.

Fahy, Benjamin et al. (2019). "Spatial analysis of urban flooding and extreme heat hazard potential in Portland, OR". In: *International Journal of Disaster Risk Reduction* vol. 39, p. 101117.

Fallmann, Joachim, Renate Forkel, and Stefan Emeis (2016). "Secondary effects of urban heat island mitigation measures on air quality". In: *Atmospheric Environment* vol. 125, pp. 199–211.

Fan, Chao et al. (2017). "Understanding the impact of urbanization on surface urban heat islands-A longitudinal analysis of the oasis effect in subtropical desert cities". In: *Remote Sensing* vol. 9.7, p. 672.

Farhana, Khandaker Mursheda, Syed Ajijur Rahman, and Mahfuzur Rahman (2012). "Factors of migration in urban Bangladesh: An empirical study of poor migrants in rahshahi city". In: *Bangladesh E-Journal of Sociology* vol. 9, pp. 105–117.

Fecht, Daniela et al. (2015). "Associations between air pollution and socioeconomic characteristics, ethnicity and age profile of neighbourhoods in England and the Netherlands". In: *Environmental Pollution* vol. 198, pp. 201–210.

Ferguson, Grant and Allan D. Woodbury (2007). "Urban heat island in the subsurface". In: *Geophysical Research Letters* vol. 34.23, p. L23713.

Fischer-Kowalski, Marina (1998). "Society's metabolism". In: *Journal of Industrial Ecology* vol. 2.1, pp. 61–78.

Fleck, Alan da Silveira et al. (2014). "A comparison of the human buccal cell assay and the pollen abortion assay in assessing genotoxicity in an urban-rural gradient". In: *International journal of environmental research and public health* vol. 11.9, pp. 8825–8838.

Fluschnik, Till et al. (2016). "The size distribution, scaling properties and spatial organization of urban clusters: A global and regional percolation perspective". In: *ISPRS International Journal of Geo-Information* vol. 5.7.

Foraster, Maria et al. (2011). "Local determinants of road traffic noise levels versus determinants of air pollution levels in a Mediterranean city". In: *Environmental Research* vol. 111.1, pp. 177–183.

Fortuniak, K., K. Kysik, and J. Wibig (2006). "Urban-rural contrasts of meteorological parameters in ód". In: *Theoretical and Applied Climatology* vol. 84.1, pp. 91–101.

Founda, Dimitra and Mattheos Santamouris (2017). "Synergies between urban heat island and heat waves in Athens (Greece), during an extremely hot summer (2012)". In: *Scientific reports* vol. 7.1, pp. 10973–10973.

Frank, Lawrence D et al. (2006). "Many pathways from land use to health: Associations between neighborhood walkability and active transportation, body mass index, and air quality". In: *Journal of the American Planning Association* vol. 72.1, pp. 75–87.

Franklin, Meredith et al. (2012). "Predictors of intra-community variation in air quality". In: *Journal of Exposure Science & Environmental Epidemiology* vol. 22.2, pp. 135–147.

Fuertes, E. et al. (2016). "Residential greenness is differentially associated with childhood allergic rhinitis and aeroallergen sensitization in seven birth cohorts". In: *Allergy* vol. 71.10, pp. 1461–1471.

Fujibe, Fumiaki (2009). "Detection of urban warming in recent temperature trends in Japan". In: *International Journal of Climatology* vol. 29.12, pp. 1811–1822.

— (2011). "Urban warming in Japanese cities and its relation to climate change monitoring". In: *International Journal of Climatology* vol. 31.2, pp. 162–173.

— (2012). "Dependence of long-term temperature trends on wind and precipitation at urban stations in Japan". In: *Journal of the Meteorological Society of Japan. Ser. II* vol. 90.4, pp. 525–534.

Fujita, Eric M. et al. (1992). "Comparison of emission inventory and ambient concentration ratios of CO, NMOG, and NO_x in California's south coast air basin". In: *Journal of the Air & Waste Management Association* vol. 42.3, pp. 264–276.

Gabaix, Xavier (1999). "Zipf's law for cities: An explanation". In: *The Quarterly Journal of Economics* vol. 114.3, pp. 739–767.

Gaffin, S.R. et al. (2008). "Variations in New York City′s urban heat island strength over time and space". In: *Theoretical and Applied Climatology* vol. 94.1, pp. 1–11.

Gaga, Eftade O. et al. (2012). "Evaluation of air quality by passive and active sampling in an urban city in Turkey: Current status and spatial analysis of air pollution exposure". In: *Environmental Science and Pollution Research* vol. 19.8, pp. 3579–3596.

Gagné, Sara A et al. (2016). "The effect of human population size on the breeding bird diversity of urban regions". In: *Biodiversity and Conservation* vol. 25.4, pp. 653–671.

Gainsborough, Juliet F. (2002). "Slow growth and urban sprawl: Support for a new regional agenda?" In: *Urban Affairs Review* vol. 37.5, pp. 728–744.

Gallo, K.P. et al. (1993). "The use of NOAA AVHRR data for assessment of the urban heat island effect". In: *Journal of Applied Meteorology* vol. 32.5, pp. 899–908.

Gallo, K.P. et al. (1995). "Assessment of urban heat islands: A satellite perspective". In: *Atmospheric Research* vol. 37.1, pp. 37–43.

Gallo, Kevin P. and Timothy W. Owen (1999). "Satellite-based adjustments for the urban heat island temperature bias". In: *Journal of Applied Meteorology* vol. 38.6, pp. 806–813.

Ganeshan, Manisha, Raghu Murtugudde, and Marc L. Imhoff (2013). "A multi-city analysis of the UHI-influence on warm season rainfall". In: *Urban Climate* vol. 6, pp. 1–23.

Gariazzo, Claudio, Armando Pelliccioni, and Andrea Bolignano (2016). "A dynamic urban air pollution population exposure assessment study using model and population density data derived by mobile phone traffic". In: *Atmospheric Environment* vol. 131, pp. 289–300.

Gauderman, W. James et al. (2005). "Childhood asthma and exposure to traffic and nitrogen dioxide". In: *Epidemiology* vol. 16.6, pp. 737–743.

Gaur, Abhishek, Markus Kalev Eichenbaum, and Slobodan P. Simonovic (2018). "Analysis and modelling of surface urban heat island in 20 Canadian cities under climate and land-cover change". In: *Journal of Environmental Management* vol. 206, pp. 145–157.

Gazal, Rico et al. (2008). "GLOBE students, teachers, and scientists demonstrate variable differences between urban and rural leaf phenology". In: *Global Change Biology* vol. 14.7, pp. 1568–1580.

Geffen, J.H.G.M. van et al. (2015). "Improved spectral fitting of nitrogen dioxide from OMI in the 405465 nm window". In: *Atmospheric Measurement Techniques* vol. 8.4, pp. 1685–1699.

Geffen, Jos van et al. (2019). *TROPOMI ATBD of the total and tropospheric NO_2 data products*. Accessed June 5, 2022. URL: https://sentinel.esa.int/documents/247904/2476257/Sentinel-5P-TROPOMI-ATBD-NO2-data-products.pdf/7a4fdde7-516e-48e7-bf44-da60c62b1e4d?version=1.4.

Geffen, Jos van et al. (2020). "S5p tropomi NO_2 slant column retrieval: Method, stability, uncertainties and comparisons with OMI". In: *Atmospheric Measurement Techniques* vol. 13, pp. 1315–1335.

Geng, G. et al. (2017). "Impact of spatial proxies on the representation of bottom-up emission inventories: A satellite-based analysis". In: *Atmospheric Chemistry and Physics* vol. 17.6, pp. 4131–4145.

Ghude, Sachin D. et al. (2008). "Detection of surface emission hot spots, trends, and seasonal cycle from satellite-retrieved NO_2 over India". In: *Journal of Geophysical Research: Atmospheres* vol. 113.D20, p. D20305.

Ghude, Sachin D. et al. (2020). "What is driving the diurnal variation in tropospheric NO_2 columns over a cluster of high emission thermal power plants in India?" In: *Atmospheric Environment: X* vol. 5, p. 100058.

Gibbons, Charlie (2011). *Why the Breusch-Pagan test fails if I set the intercept to zero?* https://stats.stackexchange.com/questions/15477/why-the-breusch-pagan-test-fails-if-i-set-the-intercept-to-zero. Accessed January 1, 2020.

Gilabert, Joan et al. (2021). "Abating heat waves in a coastal Mediterranean city: What can cool roofs and vegetation contribute?" In: *Urban Climate* vol. 37, p. 100863.

Gilbert, Nicolas L. et al. (2003). "Ambient nitrogen dioxide and distance from a major highway". In: *Science of the Total Environment* vol. 312.1, pp. 43–46.

Gilbert, Nicolas L. et al. (2005). "Assessing spatial variability of ambient nitrogen dioxide in Montréal, Canada, with a land-use regression model". In: *Journal of the Air & Waste Management Association* vol. 55.8, pp. 1059–1063.

Global Modeling and Assimilation Office (2021). *MERRA-2*. Accessed June 11, 2022. URL: http://wiki.seas.harvard.edu/geos-chem/index.php/MERRA-2.

Goggins, Gary Daniel (2009). *Impacts of city size and vegetation coverage on the urban heat island using Landsat satellite imagery*. Mississippi State University.

Goggins, William B. et al. (2012). "Effect modification of the association between short-term meteorological factors and mortality by urban heat islands in Hong Kong". In: *PLOS ONE* vol. 7.6, pp. 1–6.

Goldberg, Daniel L. et al. (2019). "Enhanced capabilities of TROPOMI NO_2: Estimating NO_X from North American cities and power plants". In: *Environmental Science & Technology* vol. 53.21, pp. 12594–12601.

Golroudbary, Vahid Rahimpour et al. (2018). "Urban impacts on air temperature and precipitation over the Netherlands". In: *Climate Research* vol. 75.2, pp. 95–109.

Gómez-Baggethun, Erik and David N. Barton (2013). "Classifying and valuing ecosystem services for urban planning". In: *Ecological Economics* vol. 86, pp. 235–245.

Goodridge, James D. (1992). "Urban bias influences on long-term California air temperature trends". In: *Atmospheric Environment. Part B. Urban Atmosphere* vol. 26.1, pp. 1–7.

Gorshelev, V. et al. (2014). "High spectral resolution ozone absorption cross-sections - Part 1: Measurements, data analysis and comparison with previous measurements around 293 K". In: *Atmospheric Measurement Techniques* vol. 7.2, pp. 609–624.

Goulding, K. W. T. et al. (1998). "Nitrogen deposition and its contribution to nitrogen cycling and associated soil processes". In: *The New Phytologist* vol. 139.1, pp. 49–58.

Goward, Samuel N. (1981). "Thermal behavior of urban landscapes and the urban heat island". In: *Physical Geography* vol. 2.1, pp. 19–33.

Grajales, John Freddy and Astrid Baquero-Berna (2014). "Inference of surface concentrations of nitrogen dioxide (NO_2) in Colombia from tropospheric columns of the ozone measurement instrument (OMI)". In: *Atmosfera* vol. 27, pp. 193–214.

Greenaway-McGrevy, Ryan and James Allan Jones (2022). "Agglomeration, congestion, and the effects of rapid transit improvements on cities". In: URL: https://cdn.auckland.ac.nz/assets/auckland/business/our-research/docs/economic-policy-centre/Agglomeration,%20Congestion,%20and%20the%20Effects%20of%20Rapid.pdf.

Grekousis, George (2019). "Artificial neural networks and deep learning in urban geography: A systematic review and meta-analysis". In: *Computers, Environment and Urban Systems* vol. 74, pp. 244–256.

Grice, Susannah et al. (2009). "Recent trends and projections of primary NO_2 emissions in Europe". In: *Atmospheric Environment* vol. 43.13, pp. 2154–2167.

Grimm, Nancy B. et al. (2008). "Global change and the ecology of cities". In: *Science* vol. 319.5864, pp. 756–760.

Grossman, Gene (1993). *Pollution and growth: What do we know?* CEPR Discussion Papers 848. C.E.P.R. Discussion Papers. URL: https://ideas.repec.org/p/cpr/ceprdp/848.html.

Grossman, Gene M. and Alan B. Krueger (1994). *Economic Growth and the Environment*. NBER Working Papers 4634. National Bureau of Economic Research, Inc. URL: https://ideas.repec.org/p/nbr/nberwo/4634.html.

Grover, Aakriti and Ram Babu Singh (2015). "Analysis of urban heat island (UHI) in relation to normalized difference vegetation index (NDVI): A comparative study of Delhi and Mumbai". In: *Environments* vol. 2.2, pp. 125–138.

Grundstrom, M. et al. (2015). "Variation and co-variation of PM_{10}, particle number concentration, NO_x and NO_2 in the urban air - Relationships with wind speed, vertical temperature gradient and weather type". In: *Atmospheric Environment* vol. 120, pp. 317–327.

Guertal, E.A. (2009). "Slow-release nitrogen fertilizers in vegetable production: A review". In: *HortTechnology hortte* vol. 19.1, pp. 16–19.

Guhathakurta, Subhrajit and Patricia Gober (2010). "Residential land use, the urban heat island, and water use in Phoenix: A path analysis". In: *Journal of Planning Education and Research* vol. 30.1, pp. 40–51.

Gunawardena, K.R., M.J. Wells, and T. Kershaw (2017). "Utilising green and bluespace to mitigate urban heat island intensity". In: *Science of the Total Environment* vol. 584-585, pp. 1040–1055.

Gupta, AK et al. (2008). "Spatio-temporal characteristics of gaseous and particulate pollutants in an urban region of Kolkata, India". In: *Atmospheric Research* vol. 87.2, pp. 103–115.

Gupta, Rupesh (2012). "Temporal and spatial variations of urban heat island effect in Jaipur City using satellite data". In: *Environment and Urbanization ASIA* vol. 3.2, pp. 359–374.

Gurjar, B.R. et al. (2008). "Evaluation of emissions and air quality in megacities". In: *Atmospheric Environment* vol. 42.7, pp. 1593–1606.

Hamdi, Rafiq (2010). "Estimating urban heat island effects on the temperature series of uccle (Brussels, Belgium) using remote sensing data and a land surface scheme". In: *Remote Sensing* vol. 2.12, pp. 2773–2784.

Hamra, Ghassan B. et al. (2015). "Lung cancer and exposure to nitrogen dioxide and traffic: A systematic review and meta-analysis". In: *Environmental Health Perspectives* vol. 123.11, pp. 1107–1112.

Han, Cheng-Yu, Zhao-Lin Gu, and Hexiang Yang (2022). "Investigate the effects of industrial agglomeration on nitrogen dioxide pollution using spatial panel durbin and panel threshold models". In: *Frontiers in Environmental Science* vol. 10.

Han, Chengyu, Zhaolin Gu, and Hexiang Yang (2021). "EKC test of the relationship between nitrogen dioxide pollution and economic Growth-A spatial econometric analysis based on Chinese city data". In: *International Journal of Environmental Research and Public Health* vol. 18.18.

Han, Lijian et al. (2016). "An optimum city size? The scaling relationship for urban population and fine particulate ($PM_{2.5}$) concentration". In: *Environmental Pollution* vol. 208, pp. 96–101.

Han, Lijian et al. (2018). "Multicontaminant air pollution in Chinese cities". In: *Bulletin of the World Health Organization* vol. 96.4, 233–242E.

Hao, Yufang and Shaodong Xie (2018). "Optimal redistribution of an urban air quality monitoring network using atmospheric dispersion model and genetic algorithm". In: *Atmospheric Environment* vol. 177, pp. 222–233.

Hardin, A.W. et al. (2018). "Urban heat island intensity and spatial variability by synoptic weather type in the northeast U.S." In: *Urban Climate* vol. 24, pp. 747–762.

Harkey, Monica et al. (2015). "An evaluation of CMAQ NO2 using observed chemistry-meteorology correlations". In: *Journal of Geophysical Research: Atmospheres* vol. 120.22, pp. 11775–11797.

Harper, Susan (2018). *What is urban encroachment?* Accessed 15 March, 2023. URL: https://sciencing.com/info-8758278-urban-encroachment.html.

Hart, Jaime E. et al. (2009). "Spatial modeling of PM_{10} and NO_2 in the continental United States, 1985-2000". In: *Environmental Health Perspectives* vol. 117.11, pp. 1690–1696.

Harvard University (2023). *GEOS-Chem*. Accessed 9 March, 2023. URL: https://geos-chem.seas.harvard.edu/.

Hass, Alisa L. et al. (2016). "Heat and humidity in the city: Neighborhood heat index variability in a mid-sized city in the Southeastern United States". In: *International journal of environmental research and public health* vol. 13.1, p. 117.

Hassan, Ibrahim A et al. (2013). "Spatial distribution and temporal variation in ambient ozone and its associated NO_x in the atmosphere of Jeddah City, Saudi Arabia". In: *Aerosol and Air Quality Research* vol. 13.6, pp. 1712–1722.

El-Hattab, M., Amany S.M., and Lamia G.E. (2018). "Monitoring and assessment of urban heat islands over the Southern region of Cairo Governorate, Egypt". In: *The Egyptian Journal of Remote Sensing and Space Science* vol. 21.3, pp. 311–323.

Havenith, George (2005). "Temperature regulation, heat balance and climatic stress". In: *Extreme weather events and public health responses*. Ed. by Wilhelm Kirch, Roberto Bertollini, and Bettina Menne. Berlin, Heidelberg: Springer Berlin Heidelberg, pp. 69–80.

He, Bao-Jie (2018). "Potentials of meteorological characteristics and synoptic conditions to mitigate urban heat island effects". In: *Urban Climate* vol. 24, pp. 26–33.

Heaviside, Clare, Helen Macintyre, and Sotiris Vardoulakis (2017). "The urban heat island: Implications for health in a changing environment". In: *Current Environmental Health Reports* vol. 4.3, pp. 296–305.

Heaviside, Clare, Sotiris Vardoulakis, and Xiao-Ming Cai (2016). "Attribution of mortality to the urban heat island during heatwaves in the West Midlands, UK". In: *Environmental Health* vol. 15 Suppl 1, pp. 27–27.

Heinl, Michael et al. (2015). "Determinants of urban-rural land surface temperature differences-A landscape scale perspective". In: *Landscape and Urban Planning* vol. 134, pp. 33–42.

Heisler, Gordon M and Anthony J Brazel (2010). "The urban physical environment: Temperature and urban heat islands". In: *Urban ecosystem ecology agronomy monograph 55*. Ed. by Jacqueline Aitkenhead-Peterson and Astrid Volder. American Society of Agronomy, Crop Science Society of America, Soil Science Society of America. Chap. 2, pp. 29–56.

Henderson, J. Vernon (1983). "Industrial bases and city sizes". In: *The American Economic Review* vol. 73.2, pp. 164–168.

Henry, Jamesa et al. (1989). "Comparison of satellite, ground-based, and modeling techniques for analyzing the urban heat island". In: *Photogrammetric Engineering and Remote Sensing* vol. 55.1, pp. 69–76.

Herndon, Scott C. et al. (2004). "NO and NO_2 emission ratios measured from in-use commercial aircraft during taxi and takeoff". In: *Environmental Science & Technology* vol. 38.22, pp. 6078–6084.

Hess, Paul (2014). "Density, urban". In: *Encyclopedia of quality of life and well-being research*. Ed. by Alex C. Michalos. Dordrecht: Springer Netherlands, pp. 1554–1557.

Heuss, Jon M. and William A. Glasson (1968). "Hydrocarbon reactivity and eye irritation". In: *Environmental Science & Technology* vol. 2.12, pp. 1109–1116.

Hey, Jonathan (2023). *Sketchplanation - The square-cube law*. Accessed 13 April, 2022. URL: https://sketchplanations.com/the-square-cube-law.

Hidalgo, J., G. Pigeon, and V. Masson (2008). "Urban-breeze circulation during the CAPITOUL experiment: Observational data analysis approach". In: *Meteorology and Atmospheric Physics* vol. 102.3, pp. 223–241.

Hidalgo, Julia, Valéry Masson, and Luis Gimeno (2010). "Scaling the daytime urban heat island and urban-breeze circulation". In: *Journal of Applied Meteorology and Climatology* vol. 49.5, pp. 889–901.

Hien, P.D. et al. (2014). "Concentrations of NO_2, SO_2, and benzene across Hanoi measured by passive diffusion samplers". In: *Atmospheric Environment* vol. 88, pp. 66–73.

Hien, P.D. et al. (2020). "Impact of urban expansion on the air pollution landscape: A case study of Hanoi, Vietnam". In: *Science of The Total Environment* vol. 702, p. 134635.

Higashino, Makoto and Heinz G. Stefan (2014). "Hydro-climatic change in Japan (1906-2005): Impacts of global warming and urbanization". In: *Air, Soil and Water Research* vol. 7, ASWR.S13632.

Hilboll, A., A. Richter, and J.P. Burrows (2013). "Long-term changes of tropospheric NO_2 over megacities derived from multiple satellite instruments". In: *Atmospheric Chemistry and Physics* vol. 13.8, pp. 4145–4169.

Hilgers, Michael and Wilfried Achenbach (2021). "The exhaust system". In: *The diesel engine*. Berlin, Heidelberg: Springer Berlin Heidelberg, pp. 31–42.

Hinkel, Kenneth M. et al. (2003). "The urban heat island in winter at Barrow, Alaska". In: *International Journal of Climatology* vol. 23.15, pp. 1889–1905.

Hoch, Irving and Judith Drake (1974). "Wages, climate, and the quality of life". In: *Journal of Environmental Economics and Management* vol. 1.4, pp. 268–295.

Hoek, Gerard et al. (2008). "A review of land-use regression models to assess spatial variation of outdoor air pollution". In: *Atmospheric Environment* vol. 42.33, pp. 7561–7578.

Hoek, Gerard et al. (2015). "Satellite NO_2 data improve national land use regression models for ambient NO_2 in a small densely populated country". In: *Atmospheric Environment* vol. 105, pp. 173–180.

Hoffmann, Peter, Oliver Krueger, and K. Heinke Schlünzen (2012). "A statistical model for the urban heat island and its application to a climate change scenario". In: *International Journal of Climatology* vol. 32.8, pp. 1238–1248.

Hoffmann, Peter and K. Heinke Schlünzen (2013). "Weather pattern classification to represent the urban heat island in present and future climate". In: *Journal of Applied Meteorology and Climatology* vol. 52.12, pp. 2699–2714.

Holdren, John P. and Paul R. Ehrlich (1974). "Human population and the global environment: Population growth, rising per capita material consumption, and disruptive technologies have made civilization a global ecological force". In: *American Scientist* vol. 62.3, pp. 282–292.

Holland, Elisabeth A. et al. (2005). "Nitrogen deposition onto the united states and western europe: Synthesis of observations and models". In: *Ecological Applications* vol. 15.1, pp. 38–57.

Holt, James B., C.P. Lo, and Thomas W. Hodler (2004). "Dasymetric estimation of population density and areal interpolation of census data". In: *Cartography and Geographic Information Science* vol. 31.2, pp. 103–121.

Hondula, David M. and Adrian G. Barnett (2014). "Heat-related morbidity in Brisbane, Australia: Spatial variation and area-level predictors". In: *Environmental health perspectives* vol. 122.8, pp. 831–836.

Hong, Hyunkee et al. (2017). "Investigation of simultaneous effects of aerosol properties and aerosol peak height on the air mass factors for space-borne NO_2 retrievals". In: *Remote Sensing* vol. 9.3.

Honninger, G., C. von Friedeburg, and U. Platt (2004). "Multi axis differential optical absorption spectroscopy (MAX-DOAS)". In: *Atmospheric Chemistry and Physics* vol. 4.1, pp. 231–254. URL: https://acp.copernicus.org/articles/4/231/2004/.

Honsberg, Christiana and Stuart Bowden (2023). *Air Mass*. Accessed 9 March, 2023. URL: https://www.pveducation.org/pvcdrom/properties-of-sunlight/air-mass.

Hosein, H. Roland, Charles A. Mitchell, and Arend Bouhuys (1977). "Evaluation of outdoor air quality in rural and urban communities". In: *Archives of Environmental Health: An International Journal* vol. 32.1, pp. 4–13.

Houck, Max M. and Jay A. Siegel (2015). "Chapter 18 - Fires and explosions". In: *Fundamentals of forensic science (Third Edition)*. Ed. by Max M. Houck and Jay A. Siegel. San Diego: Academic Press, pp. 451–490.

Howard, Luke (1833). *The climate of London: Deduced from meteorological observations made at different places in the neighbourhood of the metropolis. Volume I*. International Association for Urban Climate.

Hu, L. et al. (2018). "Global simulation of tropospheric chemistry at 12.5 km resolution: performance and evaluation of the GEOS-Chem chemical module (v10-1) within the NASA GEOS Earth system model (GEOS-5 ESM)". In: *Geoscientific Model Development* vol. 11.11, pp. 4603–4620.

Hu, Leiqiu, Olga V. Wilhelmi, and Christopher Uejio (2019a). "Assessment of heat exposure in cities: Combining the dynamics of temperature and population". In: *Science of the Total Environment* vol. 655, pp. 1–12.

Hu, Xiaofang et al. (2017). "Urban expansion and local land-cover change both significantly contribute to urban warming, but their relative importance changes over time". In: *Landscape Ecology* vol. 32.4, pp. 763–780.

Hu, Yonghong et al. (2019b). "Comparison of surface and canopy urban heat islands within megacities of eastern China". In: *ISPRS Journal of Photogrammetry and Remote Sensing* vol. 156, pp. 160–168.

Huang, Lei, Can Zhang, and Jun Bi (2017). "Development of land use regression models for $PM_{2.5}$, SO_2, NO_2 and O_3 in Nanjing, China". In: *Environmental Research* vol. 158, pp. 542–552.

Huang, Qunfang and Yuqi Lu (2015). "The effect of urban heat island on climate warming in the Yangtze River Delta urban agglomeration in China". In: *International Journal of Environmental Research and Public Health* vol. 12.8, pp. 8773–8789.

Hui, Sam C.M (2001). "Low energy building design in high density urban cities". In: *Renewable Energy* vol. 24.3, pp. 627–640.

IBM (2021). *Carbon footprint calculations*. Accessed 19 August, 2022. URL: https://www.ibm.com/docs/en/tririga/10.6.0?topic=impact-carbon-footprint-calculations.

Imhoff, Marc L. et al. (2010). "Remote sensing of the urban heat island effect across biomes in the continental USA". In: *Remote Sensing of Environment* vol. 114.3, pp. 504–513.

Inness, A. et al. (2015). "Data assimilation of satellite-retrieved ozone, carbon monoxide and nitrogen dioxide with ECMWF's Composition-IFS". In: *Atmospheric Chemistry and Physics* vol. 15.9, pp. 5275–5303.

Inness, A. et al. (2019). "The CAMS reanalysis of atmospheric composition". In: *Atmospheric Chemistry and Physics* vol. 19.6, pp. 3515–3556.

Irga, P.J., M.D. Burchett, and F.R. Torpy (2015). "Does urban forestry have a quantitative effect on ambient air quality in an urban environment?" In: *Atmospheric Environment* vol. 120, pp. 173–181.

Iroh Tam, P. Y. et al. (2017). "Spatial variation of pneumonia hospitalization risk in Twin Cities metro area, Minnesota". In: *Epidemiology and infection* vol. 145.15, pp. 3274–3283.

Irwin, Elena G. and Nancy E. Bockstael (2007). "The evolution of urban sprawl: Evidence of spatial heterogeneity and increasing land fragmentation". In: *Proceedings of the National Academy of Sciences* vol. 104.52, pp. 20672–20677.

Irwin, J.G. and M.L. Williams (1988). "Acid rain: Chemistry and transport". In: *Environmental Pollution* vol. 50.1. Toxic Substance in the Environment, pp. 29–59.

Ivajni, Danijel, Mitja Kaligari, and Igor iberna (2014). "Geographically weighted regression of the urban heat island of a small city". In: *Applied Geography* vol. 53, pp. 341–353.

Jackson, Trisha L et al. (2010). "Parameterization of urban characteristics for global climate modeling". In: *Annals of the Association of American Geographers* vol. 100.4, pp. 848–865.

Jacob, Daniel J (1999). *Introduction to atmospheric chemistry*. Princeton University Press.

James, Peter et al. (2017). "Interrelationships between walkability, air pollution, greenness, and body mass index". In: *Epidemiology* vol. 28.6, pp. 780–788.

Jeffrey, Simon and Kathrin Enenkel (2020). *The importance of city centres to the national economy*. Accessed 21 August, 2022. URL: https://www.centreforcities.org/reader/getting-moving/the-importance-of-city-centres-to-the-national-economy/.

Jenerette, G. Darrel et al. (2007). "Regional relationships between surface temperature, vegetation, and human settlement in a rapidly urbanizing ecosystem". In: *Landscape Ecology* vol. 22.3, pp. 353–365.

Jeong, Ukkyo and Hyunkee Hong (2021). "Assessment of tropospheric concentrations of NO_2 from the tropomi/sentinel-5 precursor for the estimation of long-term exposure to surface NO_2 over South Korea". In: *Remote Sensing* vol. 13.10.

Jerrett, M. et al. (2007). "Modeling the intraurban variability of ambient traffic pollution in Toronto, Canada". In: *Journal of Toxicology and Environmental Health, Part A* vol. 70, pp. 200–212.

Jerrett, Michael et al. (2005). "A review and evaluation of intraurban air pollution exposure models". In: *Journal of Exposure Science & Environmental Epidemiology* vol. 15.2, pp. 185–204.

Jiang, Lei et al. (2021). "Identifying the driving factors of NO_2 pollution of One Belt One Road countries: Satellite observation technique and dynamic spatial panel data analysis". In: *Environmental Science and Pollution Research* vol. 28.16, pp. 20393–20407.

Jiang, Yunfang et al. (2018). "Spatial zoning strategy of urbanization based on urban climate co-movement: A case study in Shanghai mainland area". In: *Sustainability* vol. 10.8.

Jiao, Limin (2015). "Urban land density function: A new method to characterize urban expansion". In: *Landscape and Urban Planning* vol. 139, pp. 26–39.

Jin, Lan et al. (2019). "A land use regression model of nitrogen dioxide and fine particulate matter in a complex urban core in Lanzhou, China". In: *Environmental Research* vol. 177, p. 108597.

Jin, Menglin, Robert E. Dickinson, and Da Zhang (2005a). "The footprint of urban areas on global climate as characterized by MODIS". In: *Journal of Climate* vol. 18.10, pp. 1551–1565.

Jin, Menglin, J. Marshall Shepherd, and Michael D. King (2005b). "Urban aerosols and their variations with clouds and rainfall: A case study for New York and Houston". In: *Journal of Geophysical Research: Atmospheres* vol. 110.D10, D10S20.

Jin, Mengun and J. Marshall Shepherd (2005). "Inclusion of urban landscape in a climate model: How can satellite data help?" In: *Bulletin of the American Meteorological Society* vol. 86.5, pp. 681–690.

John, Emerson, Micah Hale, and Panneer Selvam (2013). "Concrete as a thermal energy storage medium for thermocline solar energy storage systems". In: *Solar Energy* vol. 96, pp. 194–204.

Johnson, B. T. et al. (2016). "Evaluation of biomass burning aerosols in the HadGEM3 climate model with observations from the SAMBBA field campaign". In: *Atmospheric Chemistry and Physics* vol. 16.22, pp. 14657–14685.

Johnson, Daniel P. and Jeffrey S. Wilson (2009). "The socio-spatial dynamics of extreme urban heat events: The case of heat-related deaths in Philadelphia". In: *Applied Geography* vol. 29.3, pp. 419–434.

Jordanova, Diana, Neli Jordanova, and Petar Petrov (2014). "Magnetic susceptibility of road deposited sediments at a national scale-Relation to population size and urban pollution". In: *Environmental Pollution* vol. 189, pp. 239–251.

Kabano, Peter, Sarah Lindley, and Angela Harris (2021). "Evidence of urban heat island impacts on the vegetation growing season length in a tropical city". In: *Landscape & Urban Planning* vol. 206, p. 103989.

Kammuang-Lue, Niti et al. (2015). "Influences of population, building, and traffic densities on urban heat island intensity in Chiang Mai City, Thailand". In: *Thermal Science* vol. 19.Suppl. 2, pp. 445–455.

Kao, Lillian S. and Charles E. Green (2008). "Analysis of variance: Is there a difference in means and what does it mean?" In: *Journal of Surgical Research* vol. 144.1, pp. 158–170.

Karaca, M., Ü. Antepliolu, and H. Karsan (1995). "Detection of urban heat island in Istanbul, Turkey". In: *Il Nuovo Cimento C* vol. 18.1, pp. 49–55.

Karambelas, Alexandra et al. (2018). "Constraining the uncertainty in emissions over India with a regional air quality model evaluation". In: *Atmospheric Environment* vol. 174, pp. 194–203.

Karimimoshaver, Mehrdad, Rezvan Khalvandi, and Mohammad Khalvandi (2021). "The effect of urban morphology on heat accumulation in urban street canyons and mitigation approach". In: *Sustainable Cities and Society* vol. 73, p. 103127.

Karr, Catherine J. et al. (2009). "Influence of ambient air pollutant sources on clinical encounters for infant bronchiolitis". In: *American Journal of Respiratory & Critical Care Medicine* vol. 180.10, pp. 995–1001.

Kasmaee, Sara and Francesco Tinti (2018). "A method to evaluate the impact of urbanization on ground temperature evolution at regional scale". In: *Rudarsko-geoloko-naftni zbornik* vol. 33.5, pp. 1–12.

Kato, M.S.A et al. (1999). "Fire-free alternatives to slash-and-burn for shifting cultivation in the eastern Amazon region: The role of fertilizers". In: *Field Crops Research* vol. 62.2, pp. 225–237.

Kaufmann, Robert K. et al. (2007). "Climate response to rapid urban growth: Evidence of a human-induced precipitation deficit". In: *Journal of Climate* vol. 20.10, pp. 2299–2306.

Kaufmann, Talia et al. (2022). "Scaling of urban amenities: Generative statistics and implications for urban planning". In: *EPJ Data Science* vol. 11.1, p. 50.

Kaya, Sinasi et al. (2012). "Assessment of urban heat islands using remotely sensed data". In: *Ekoloji* vol. 21.84, pp. 107–113.

Kaye, Jason P. et al. (2006). "A distinct urban biogeochemistry?" In: *Trends in Ecology & Evolution* vol. 21.4, pp. 192–199.

Kelley, Allen C. (1988). "Economic consequences of population change in the third world". In: *Journal of Economic Literature* vol. 26.4, pp. 1685–1728.

Kelly, F. J. and J. C. Fussell (2011). "Air pollution and airway disease". In: *Clinical & Experimental Allergy* vol. 41.8, pp. 1059–1071.

Kershaw, Suzanne E. and Andrew A. Millward (2012). "A spatio-temporal index for heat vulnerability assessment". In: *Environmental Monitoring and Assessment* vol. 184.12, pp. 7329–7342.

Khaikine, M. N. et al. (2006). "Investigation of temporal - spatial parameters of an urban heat island on the basis of passive microwave remote sensing". In: *Theoretical and Applied Climatology* vol. 84.1, pp. 161–169.

Kifle, Bisrat (2003). "Urban heat island and its feature in Addis Ababa (a case study)". In: *Fifth International Conference on Urban Climate*, pp. 1–5.

Kim, Ik Ki (1994). "The environmental problems in urban communities and the protection of the environment in Korea". In: *Korea Journal of Population and Development*, pp. 63–76.

Kim, J., C. Chu, and S. Shin (2014). "ISSAQ: An integrated sensing systems for real-time indoor air quality monitoring". In: *IEEE Sensors Journal* vol. 14.12, pp. 4230–4244.

Kim, Myounghee, Okhee Yi, and Ho Kim (2012). "The role of differences in individual and community attributes in perceived air quality". In: *Science of the Total Environment* vol. 425, pp. 20–26.

Kim, Y.-H. and J.-J. Baik (2004). "Daily maximum urban heat island intensity in large cities of Korea". In: *Theoretical and Applied Climatology* vol. 79.3, pp. 151–164.

Kim, Yeon-Hee and Jong-Jin Baik (2005). "Spatial and temporal structure of the urban heat island in Seoul". In: *Journal of Applied Meteorology* vol. 44.5, pp. 591–605.

King, Lesliel J. (1967). "Discriminatory analysis of urban growth patterns in Ontario and Quebec, 1951-1961". In: *Annals of the Association of American Geographers* vol. 57.3, pp. 566–578.

Kirby, C., A. Greig, and T. Drye (1998). "Temporal and spatial variations in nitrogen dioxide concentrations across an urban landscape: Cambridge, UK". In: *Urban air quality: Monitoring and modelling*. Ed. by Ranjeet S. Sokhi. Dordrecht: Springer, pp. 65–82.

Kleiber, William, Richard W. Katz, and Balaji Rajagopalan (2012). "Daily spatiotemporal precipitation simulation using latent and transformed Gaussian processes". In: *Water Resources Research* vol. 48.1.

Kleipool, Q. et al. (2018). "Pre-launch calibration results of the TROPOMI payload on-board the Sentinel-5 Precursor satellite". In: *Atmospheric Measurement Techniques* vol. 11.12, pp. 6439–6479.

Koch, Natália Mossmann et al. (2019). "Selecting lichen functional traits as ecological indicators of the effects of urban environment". In: *Science of the Total Environment* vol. 654, pp. 705–713.

Kok, Herman and Zoltan Kovacs (1999). "The process of suburbanization in the agglomeration of Budapest". In: *Netherlands Journal of Housing and the Built Environment* vol. 14.2, pp. 119–141.

Kolokotroni, Maria et al. (2012). "London's urban heat island: Impact on current and future energy consumption in office buildings". In: *Energy and Buildings* vol. 47, pp. 302–311.

Kopec, Richard J. (1970). "Further observations of the urban heat island in a small city". In: *Bulletin of the American Meteorological Society* vol. 51.7, pp. 602–607.

Koralegedara, Suranjith Bandara et al. (2016). "Estimation of anthropogenic heat emissions in urban Taiwan and their spatial patterns". In: *Environmental Pollution* vol. 215, pp. 84–95.

Kotak, Y et al. (2014). "Installation of roof-top solar PV modules and their impact on building cooling load". In: *Building Services Engineering Research and Technology* vol. 35.6, pp. 613–633.

Kotharkar, Rajashree and Meenal Surawar (2016). "Land use, land cover, and population density impact on the formation of canopy urban heat islands through traverse survey in the Nagpur urban area, India". In: *Journal of Urban Planning and Development* vol. 142.1, p. 04015003.

Kousa, Anu et al. (2002). "A model for evaluating the population exposure to ambient air pollution in an urban area". In: *Atmospheric Environment* vol. 36.13, pp. 2109–2119.

Krieve, Walter F. and David M. Mason (1961). "Heat transfer in reacting systems: Heat transfer to nitrogen dioxide gas under turbulent pipe flow conditions". In: *AIChE Journal* vol. 7.2, pp. 277–281.

Kumar, Awkash et al. (2016). "Air quality mapping using GIS and economic evaluation of health impact for Mumbai City, India". In: *Journal of the Air & Waste Management Association* vol. 66.5, pp. 470–481.

Kummu, Matti and Olli Varis (2011). "The world by latitudes: A global analysis of human population, development level and environment across the northsouth axis over the past half century". In: *Applied Geography* vol. 31.2, pp. 495–507.

L., Berry Brian J., Simmons James W., and Tennant Robert J. (1963). "Urban population densities: Structure and change". In: *Geographical Review* vol. 53.3, pp. 389–405.

Laffray, Xavier, Christophe Rose, and Jean-Pierre Garrec (2010). "Biomonitoring of traffic-related nitrogen oxides in the Maurienne valley (Savoie, France), using purple moor grass growth parameters and leaf 15N/14N ratio". In: *Environmental Pollution* vol. 158.5, pp. 1652–1660.

Lai, Li-Wei and Wan-Li Cheng (2009). "Air quality influenced by urban heat island coupled with synoptic weather patterns". In: *Science of the Total Environment* vol. 407.8, pp. 2724–2733.

Lamsal, L. N. et al. (2013). "Scaling relationship for NO_2 pollution and urban population size: A satellite perspective". In: *Environmental Science & Technology* vol. 47.14, pp. 7855–7861.

Lamsal, L. N. et al. (2014). "Evaluation of OMI operational standard NO_2 column retrievals using in situ and surface-based NO_2 observations". In: *Atmospheric Chemistry and Physics* vol. 14.21, pp. 11587–11609.

Lamsal, L.N. et al. (2008). "Ground-level nitrogen dioxide concentrations inferred from the satellite-borne Ozone Monitoring Instrument". In: *Journal of Geophysical Research: Atmospheres* vol. 113.D16, p. D16308.

Lamsal, L.N. et al. (2010). "Indirect validation of tropospheric nitrogen dioxide retrieved from the OMI satellite instrument: Insight into the seasonal variation of nitrogen oxides at northern midlatitudes". In: *Journal of Geophysical Research: Atmospheres* vol. 115.D5, p. D05302.

Larkin, Andrew et al. (2016). "Relationships between changes in urban characteristics and air quality in East Asia from 2000 to 2010". In: *Environmental Science & Technology* vol. 50.17, pp. 9142–9149.

Lee, Derek O. (1992). "Urban warming? - An analysis of recent trends in London′s heat island". In: *Weather* vol. 47.2, pp. 50–56.

Lee, Hyoun-Young (1993). "An application of NOAA AVHRR thermal data to the study of urban heat islands". In: *Atmospheric Environment. Part B. Urban Atmosphere* vol. 27.1, pp. 1–13.

Lee, Jui-Huan et al. (2014a). "Land use regression models for estimating individual NO_x and NO_2 exposures in a metropolis with a high density of traffic roads and population". In: *Science of the Total Environment* vol. 472, pp. 1163–1171.

Lee, K et al. (1992). "Wind velocity effects on sampling rate of NO_2 badge". In: *Journal of Exposure Analysis and Environmental Epidemiology* vol. 2.2, pp. 207–219.

Lee, Sang-Hyun and Jong-Jin Baik (2010). "Statistical and dynamical characteristics of the urban heat island intensity in Seoul". In: *Theoretical and Applied Climatology* vol. 100.1, pp. 227–237.

Lee, Sungwon and Bumsoo Lee (2014). "The influence of urban form on GHG emissions in the U.S. household sector". In: *Energy Policy* vol. 68, pp. 534–549.

Lee, T.-W., Heung S. Choi, and Jinoh Lee (2014b). "Generalized scaling of urban heat island effect and its applications for energy consumption and renewable energy". In: *Advances in Meteorology* vol. 2014, p. 5.

Lee, Yee-Yong et al. (2017). "Overview of urban heat island (UHI) phenomenon towards human thermal comfort". In: *Environmental Engineering & Management Journal (EEMJ)* vol. 16.9.

Lemonsu, A. et al. (2015). "Vulnerability to heat waves: Impact of urban expansion scenarios on urban heat island and heat stress in Paris (France)". In: *Urban Climate* vol. 14, pp. 586–605.

Lemoy, Rémi and Geoffrey Caruso (2018). "Evidence for the homothetic scaling of urban forms". In: *Environment and Planning B: Urban Analytics and City Science* vol. 0.0, p. 2399808318810532.

— (2021). "Radial analysis and scaling of urban land use". In: *Scientific Reports* vol. 11.1, p. 22044.

Lertxundi-Manterola, Aitana and Marc Saez (2009). "Modelling of nitrogen dioxide (NO_2) and fine particulate matter (PM_{10}) air pollution in the metropolitan areas of Barcelona and Bilbao, Spain". In: *Environmetrics* vol. 20.5, pp. 477–493.

Levinson, Herbert S. and F. Houston Wynn (1963). "Effects of density on urban transportation requirements". In: *Highway Research Record* 2, pp. 38–64.

Li, Bing et al. (2018). "Comparative analysis of urban heat island intensities in Chinese, Russian, and DPRK regions across the transnational urban agglomeration of the Tumen River in Northeast Asia". In: *Sustainability* vol. 10.8.

Li, Congyuan and Ning Zhang (2021). "Analysis of the daytime urban heat island mechanism in East China". In: *Journal of Geophysical Research: Atmospheres* vol. 126.12, e2020JD034066.

Li, Jinghui et al. (2017a). "Correlations between socioeconomic drivers and indicators of urban expansion: Evidence from the heavily urbanised Shanghai Metropolitan Area, China". In: *Sustainability* vol. 9.7.

Li, Junxiang et al. (2011). "Impacts of landscape structure on surface urban heat islands: A case study of Shanghai, China". In: *Remote Sensing of Environment* vol. 115.12, pp. 3249–3263.

Li, Lianfa et al. (2017b). "Constrained mixed-effect models with ensemble learning for prediction of nitrogen oxides concentrations at high spatiotemporal resolution". In: *Environmental Science & Technology* vol. 51.17, pp. 9920–9929.

Li, Lin et al. (2014). "Impact of land cover and population density on land surface temperature: Case study in Wuhan, China". In: *Journal of Applied Remote Sensing* vol. 8.1, pp. 1–20.

Li, Meng et al. (2017c). "Anthropogenic emission inventories in China: A review". In: *National Science Review* vol. 4.6, pp. 834–866.

Li, Q. et al. (2004). "Urban heat island effect on annual mean temperature during the last 50 years in China". In: *Theoretical and Applied Climatology* vol. 79.3, pp. 165–174.

Li, Weifeng et al. (2017d). "Linking potential heat source and sink to urban heat island: Heterogeneous effects of landscape pattern on land surface temperature". In: *Science of the Total Environment* vol. 586, pp. 457–465.

Li, Xiaoma et al. (2017e). "The surface urban heat island response to urban expansion: A panel analysis for the conterminous United States". In: *Science of the Total Environment* vol. 605-606, pp. 426–435.

Li, Ying-ying, Hao Zhang, and Wolfgang Kainz (2012). "Monitoring patterns of urban heat islands of the fast-growing Shanghai metropolis, China: Using time-series of Landsat TM/ETM+ data". In: *International Journal of Applied Earth Observation and Geoinformation* vol. 19, pp. 127–138.

Liang, Jinyou et al. (1998). "Seasonal budgets of reactive nitrogen species and ozone over the United States, and export fluxes to the global atmosphere". In: *Journal of Geophysical Research: Atmospheres* vol. 103.D11, pp. 13435–13450.

Lin, Chuan-Yao et al. (2008). "Urban heat island effect and its impact on boundary layer development and land-sea circulation over northern Taiwan". In: *Atmospheric Environment* vol. 42.22, pp. 5635–5649.

Lin, Chuan-Yao et al. (2011). "Impact of the urban heat island effect on precipitation over a complex geographic environment in Northern Taiwan". In: *Journal of Applied Meteorology and Climatology* vol. 50.2, pp. 339–353.

Lin, George C.S. (2007). "Chinese urbanism in question: State, society, and the reproduction of urban spaces". In: *Urban Geography* vol. 28.1, pp. 7–29.

Lin, Pingying et al. (2017). "Effects of urban planning indicators on urban heat island: A case study of pocket parks in high-rise high-density environment". In: *Landscape and Urban Planning* vol. 168, pp. 48–60.

Lin, Shu-Hua and Chung-Ming Liu (2013). "Data assimilation of Island climate observations with large-scale re-analysis data to high-resolution grids". In: *International Journal of Climatology* vol. 33.5, pp. 1228–1236.

Lin, Wen-Zer et al. (2005). "The subtropical urban heat island effect revealed in eight major cities of Taiwan". In: *WSEAS Transactions on Environment and Development* vol. 1.2, pp. 14–20.

Liu, Chao et al. (2016). "A land use regression application into assessing spatial variation of intra-urban fine particulate matter ($PM_{2.5}$) and nitrogen dioxide (NO_2) concentrations in City of Shanghai, China". In: *Science of the Total Environment* vol. 565, pp. 607–615.

Liu, W. et al. (2007). "Temporal characteristics of the Beijing urban heat island". In: *Theoretical and Applied Climatology* vol. 87.1, pp. 213–221.

Liu, Yupeng, Jianguo Wu, and Deyong Yu (2018a). "Disentangling the complex effects of socioeconomic, climatic, and urban form factors on air pollution: A case study of China". In: *Sustainability* vol. 10.3.

Liu, Yupeng et al. (2018b). "The relationship between urban form and air pollution depends on seasonality and city size". In: *Environmental Science and Pollution Research* vol. 25.16, pp. 15554–15567.

Long, Lawrence C., Vincent D'Amico, and Steven D. Frank (2019). "Urban forest fragments buffer trees from warming and pests". In: *Science of the Total Environment* vol. 658, pp. 1523–1530.

Lorente, A. et al. (2017). "Structural uncertainty in air mass factor calculation for NO_2 and HCHO satellite retrievals". In: *Atmospheric Measurement Techniques* vol. 10.3, pp. 759–782.

Louf, Rémi and Marc Barthelemy (2014a). "How congestion shapes cities: From mobility patterns to scaling". In: *Scientific Reports* vol. 4.1, p. 5561.

— (2014b). "Scaling: Lost in the smog". In: *Environment and Planning B: Planning and Design* vol. 41.5, pp. 767–769.

Loughner, Christopher P. et al. (2012). "Roles of urban tree canopy and buildings in urban heat island effects: Parameterization and preliminary results". In: *Journal of Applied Meteorology and Climatology* vol. 51.10, pp. 1775–1793.

Lövblad, G. et al. (1997). *Position paper on air quality: Nitrogen dioxide*. Tech. rep. Accessed June 28, 2022. European Commission. URL: https://ec.europa.eu/environment/archives/air/pdf/pp_no2.pdf.

Lu, Jie et al. (1997). "A laboratory study of the urban heat island in a calm and stably stratified environment. Part I: Temperature Field". In: *Journal of Applied Meteorology* vol. 36.10, pp. 1377–1391.

Lu, Juan et al. (2021). "Expansion of city scale, traffic modes, traffic congestion, and air pollution". In: *Cities* vol. 108, p. 102974. URL: https://www.sciencedirect.com/science/article/pii/S0264275120313226.

Lu, Jun et al. (2017). "A micro-climatic study on cooling effect of an urban park in a hot and humid climate". In: *Sustainable Cities and Society* vol. 32, pp. 513–522.

Lu, W.Z. and X.K. Wang (2004). "Interaction patterns of major air pollutants in Hong Kong territory". In: *Science of the Total Environment* vol. 324.1, pp. 247–259.

Lundgren, Karin and Tord Kjellstrom (2013). "Sustainability challenges from climate change and air conditioning use in urban areas". In: *Sustainability* vol. 5.7, pp. 3116–3128.

Luo, Zhi et al. (2018). "Urban pollution and road infrastructure: A case study of China". In: *China Economic Review* vol. 49, pp. 171–183.

Madsen, Christian et al. (2007). "Modeling the intra-urban variability of outdoor traffic pollution in Oslo, Norway-A GA^{2}LEN project". In: *Atmospheric Environment* vol. 41.35, pp. 7500–7511.

Madsen, Christian et al. (2011). "Comparison of land-use regression models for predicting spatial NO_x contrasts over a three year period in Oslo, Norway". In: *Atmospheric Environment* vol. 45.21, pp. 3576–3583.

Magee, N., J. Curtis, and G. Wendler (1999). "The urban heat island effect at Fairbanks, Alaska". In: *Theoretical and Applied Climatology* vol. 64.1, pp. 39–47.

Mallick, Javed and Atiqur Rahman (2012). "Impact of population density on the surface temperature and micro-climate of Delhi". In: *Current Science* vol. 102.12, pp. 1708–1713.

Markovic, Marko et al. (2008). "An evaluation of the surface radiation budget over North America for a suite of regional climate models against surface station observations". In: *Climate Dynamics* vol. 31.7, pp. 779–794.

Marshall, Julian D, Elizabeth Nethery, and Michael Brauer (2008). "Within-urban variability in ambient air pollution: Comparison of estimation methods". In: *Atmospheric Environment* vol. 42.6, pp. 1359–1369.

Martenies, Sheena E. et al. (2017). "Disease and health inequalities attributable to air pollutant exposure in Detroit, Michigan". In: *International Journal of Environmental Research and Public Health* vol. 14.10, p. 1243.

Martilli, Alberto (2014). "An idealized study of city structure, urban climate, energy consumption, and air quality". In: *Urban Climate* vol. 10, pp. 430–446.

Martín-Martín, Alberto et al. (2018). "Google Scholar, Web of Science, and Scopus: A systematic comparison of citations in 252 subject categories". In: *Journal of Informetrics* vol. 12.4, pp. 1160–1177.

Martin-Vide, Javier, Pablo Sarricolea, and M. Carmen Moreno-García (2015). "On the definition of urban heat island intensity: The rural reference". In: *Frontiers in Earth Science* vol. 3, p. 24.

Martin, Charles G. and Paul A. Games (1977). "Anova tests for homogeneity of variance: Nonnormality and unequal samples". In: *Journal of Educational Statistics* vol. 2.3, pp. 187–206.

Martin, Frank P and Grace L Powell (1977). "The urban heat island in Akron, Ohio". In: *Proceedings of the Conference on Metropolitan Physical Environment*. Vol. 25, pp. 94–97.

Martinson, Holly M. and Michael J. Raupp (2013). "A meta-analysis of the effects of urbanization on ground beetle communities". In: *Ecosphere* vol. 4.5, art60.

Masey, Nicola et al. (2017). "Influence of wind-speed on short-duration NO_2 measurements using Palmes and Ogawa passive diffusion samplers". In: *Atmospheric Environment* vol. 160, pp. 70–76.

Masiol, Mauro et al. (2013). "Seasonal trends and spatial variations of PM_{10}-bounded polycyclic aromatic hydrocarbons in Veneto Region, Northeast Italy". In: *Atmospheric Environment* vol. 79, pp. 811–821.

Matte, Thomas D. et al. (2013). "Monitoring intraurban spatial patterns of multiple combustion air pollutants in New York City: Design and implementation". In: *Journal of Exposure Science & Environmental Epidemiology* vol. 23.3, pp. 223–231.

Matthews, Tony and Dirk van der Kamp (2017). *Canyon effect in Australian cities*. Tech. rep. Accessed March 13, 2023. Griffith University. URL: https://medium.com/the-machinery-of-government/canyon-effect-in-australian-cities-ce496190c760.

Maurya, J.B. et al. (2018). "A silicon-black phosphorous based surface plasmon resonance sensor for the detection of NO_2 gas". In: *Optik* vol. 160, pp. 428–433.

McCarty, Joshua and Nikhil Kaza (2015). "Urban form and air quality in the United States". In: *Landscape and Urban Planning* vol. 139, pp. 168–179.

McPhearson, Timon et al. (2021). "Radical changes are needed for transformations to a good Anthropocene". In: *npj Urban Sustainability* vol. 1.

McPherson, E Gregory (1994). "Cooling urban heat islands with sustainable landscapes". In: *The ecological city: Preserving and restoring urban biodiversity*. Ed. by Rutherford H. Platt, Rowan A. Rowntree, and Pamela C. Muick. Amherst, MA: University of Massachusetts Press, pp. 151–171.

Mei, Shuo-Jun et al. (2018). "Thermal buoyancy driven canyon airflows inside the compact urban blocks saturated with very weak synoptic wind: Plume merging mechanism". In: *Building and Environment* vol. 131, pp. 32–43.

Melhuish, Edward and Mike Pedder (1998). "Observing an urban heat island by bicycle". In: *Weather* vol. 53.4, pp. 121–128.

Memon, Rizwan Ahmed et al. (2011). "Urban heat island and its effect on the cooling and heating demands in urban and suburban areas of Hong Kong". In: *Theoretical and Applied Climatology* vol. 103.3, pp. 441–450.

Menberg, Kathrin et al. (2013a). "Long-term evolution of anthropogenic heat fluxes into a subsurface urban heat island". In: *Environmental Science & Technology* vol. 47.17, pp. 9747–9755.

Menberg, Kathrin et al. (2013b). "Subsurface urban heat islands in German cities". In: *Science of the Total Environment* vol. 442, pp. 123–133.

Meng, F. and M. Liu (2013). "Remote-sensing image-based analysis of the patterns of urban heat islands in rapidly urbanizing Jinan, China". In: *International Journal of Remote Sensing* vol. 34.24, pp. 8838–8853.

Meng, Xia et al. (2015). "A land use regression model for estimating the NO_2 concentration in Shanghai, China". In: *Environmental Research* vol. 137, pp. 308–315.

Meteorological Office (2023). *The heatwave of 2003*. Accessed 18 March, 2023. URL: https://www.metoffice.gov.uk/weather/learn-about/weather/case-studies/heatwave#:~:text=More%20than%2020%2C000%20people%20died,countries%20experienced%20their%20highest%20temperatures..

Milan, Blanca Fernandez and Felix Creutzig (2015). "Reducing urban heat wave risk in the 21st century". In: *Current Opinion in Environmental Sustainability* vol. 14, pp. 221–231.

Miller, Marvin E. (1967). "A note on comparison of statistical and analytical results for calculating oxides of nitrogen concentrations". In: *Journal of the Air Pollution Control Association* vol. 17.4, pp. 232–234.

Miller, Roberta Balstad and Christopher Small (2003). "Cities from space: Potential applications of remote sensing in urban environmental research and policy". In: *Environmental Science & Policy* vol. 6.2, pp. 129–137.

Mills, Edwin S. (1972). "Welfare aspects of national policy toward city sizes". In: *Urban Studies* vol. 9.1, pp. 117–124.

Min, Min, Hongbo Zhao, and Changhong Miao (2018). "Spatio-temporal evolution analysis of the urban heat island: A case study of Zhengzhou City, China". In: *Sustainability* vol. 10.6.

Mirzaei, Parham A. and Fariborz Haghighat (2010). "A novel approach to enhance outdoor air quality: Pedestrian ventilation system". In: *Building and Environment* vol. 45.7, pp. 1582–1593.

Moeletsi, Mokhele Edmond and Mphethe Isaac Tongwane (2015). "2004 methane and nitrous oxide emissions from manure management in South Africa". In: *Animals* vol. 5.2, pp. 193–205.

Mohan, Manju et al. (2012). "Urban heat island assessment for a tropical urban airshed in India". In: *Atmospheric and Climate Sciences* vol. 2.2, pp. 127–138.

Mohan, Manju et al. (2013). "Assessment of urban heat island effect for different land use-land cover from micrometeorological measurements and remote sensing data for megacity Delhi". In: *Theoretical and Applied Climatology* vol. 112.3, pp. 647–658.

Moher, David et al. (2009). "Preferred reporting items for systematic reviews and meta-analyses: The PRISMA statement". In: *Annals of Internal Medicine* vol. 151.4, pp. 264–269.

Mohr, Franz X. (2018). *Heteroskedasticity robust standard errors in R*. Accessed June 27, 2022. URL: https://www.r-econometrics.com/methods/hcrobusterrors/.

Montávez, Juan Pedro, Jesús Fidel González-Rouco, and Francisco Valero (2008). "A simple model for estimating the maximum intensity of nocturnal urban heat Island". In: *International Journal of Climatology* vol. 28.2, pp. 235–242.

Montero-Montoya, Regina, Rocío López-Vargas, and Omar Arellano-Aguilar (2018). "Volatile organic compounds in air: Sources, distribution, exposure and associated illnesses in children". In: *Annals of Global Health* vol. 84.2, pp. 225–238.

Moore, Melinda, Philip Gould, and Barbara S. Keary (2003). "Global urbanization and impact on health". In: *International Journal of Hygiene and Environmental Health* vol. 206.4, pp. 269–278.

Morabito, Marco et al. (2016). "The impact of built-up surfaces on land surface temperatures in Italian urban areas". In: *Science of the Total Environment* vol. 551-552, pp. 317–326.

Morgenstern, V. et al. (2007). "Respiratory health and individual estimated exposure to traffic-related air pollutants in a cohort of young children". In: *Occupational and Environmental Medicine* vol. 64.1, pp. 8–16.

Morris, C.J.G., I. Simmonds, and N. Plummer (2001). "Quantification of the influences of wind and cloud on the nocturnal urban heat island of a large city". In: *Journal of Applied Meteorology* vol. 40.2, pp. 169–182.

Mukerjee, Shaibal et al. (2009). "Spatial analysis and land use regression of VOCs and NO_2 from school-based urban air monitoring in Detroit/Dearborn, USA". In: *Science of the Total Environment* vol. 407.16, pp. 4642–4651.

Mutiibwa, Denis, Scotty Strachan, and Thomas Albright (2015). "Land surface temperature and surface air temperature in complex terrain". In: *IEEE Journal of Selected Topics in Applied Earth Observations and Remote Sensing* vol. 8.10, pp. 4762–4774.

Mutlu, Servet (1989). "Urban concentration and primacy revisited: An analysis and some policy conclusions". In: *Economic Development and Cultural Change* vol. 37.3, pp. 611–639.

Nadal, Martí et al. (2011). "Health risk map of a petrochemical complex through GIS-fuzzy integration of air pollution monitoring data". In: *Human and Ecological Risk Assessment: An International Journal* vol. 17.4, pp. 873–891.

Nakagawa, Kiyotaka (1996). "Recent trends of urban climatological studies in Japan, with special emphasis on the thermal environments of urban areas". In: *Geographical review of Japan, Series B* vol. 69.2, pp. 206–224.

NASA (2019a). *MODIS*. https://aqua.nasa.gov/modis. Accessed October 28, 2019.

— (2019b). *MODIS*. https://modis.gsfc.nasa.gov/about/specifications.php. Accessed October 28, 2019.

— (2020). *Global nitrogen dioxide monitoring news - FAQs*. Accessed June 27, 2022. URL: https://so2.gsfc.nasa.gov/no2/FAQs.htm#:~:text=Can%20satellites%20measure%20%22nose%2Dlevel,the%20pollutant%20in%20the%20atmosphere.

— (2022). *Land surface temperature*. Accessed 29 October, 2022. URL: https://earthobservatory.nasa.gov/global-maps/MOD_LSTD_M.

— (2023a). *Ozone Monitoring Instrument (OMI)*. Accessed 9 March, 2023. URL: https://aura.gsfc.nasa.gov/omi.html.

— (2023b). *Tropospheric monitoring instrument (TROPOMI)*. Accessed March 17, 2023. URL: hhttps://www.earthdata.nasa.gov/sensors/tropomi.

Ndiaye, Khadim, Stéphane Ginestet, and Martin Cyr (2018). "Thermal energy storage based on cementitious materials: A review". In: *AIMS Energy* vol. 6.1, pp. 97–120.

Ng, Mee Kam and Wing-Shing Tang (1999). "Urban system planning in China: A case study of the Pearl River Delta". In: *Urban Geography* vol. 20.7, pp. 591–616.

Ngarambe, Jack et al. (2021). "Exploring the relationship between particulate matter, CO, SO_2, NO_2, O_3 and urban heat island in Seoul, Korea". In: *Journal of Hazardous Materials* vol. 403, p. 123615.

Nguyen, Hang Thi and Ki-Hyun Kim (2006). "Comparison of spatiotemporal distribution patterns of NO_2 between four different types of air quality monitoring stations". In: *Chemosphere* vol. 65.2, pp. 201–212.

Nguyen, Hoa Q. et al. (2018). "Urban heat island effect on cicada densities in metropolitan Seoul". In: *PeerJ* vol. 6, e4238.

Nguyen, Hoa Quynh et al. (2019). "Characterization of polymorphic loci for two cicada species: Cryptotympana atrata and Hyalessa fuscata (Hemiptera: Cicadoidae)". In: *Molecular Biology Reports* vol. 46.2, pp. 1555–1561.

Nicholas Hewitt, C. (1991). "Spatial variations in nitrogen dioxide concentrations in an urban area". In: *Atmospheric Environment. Part B. Urban Atmosphere* vol. 25.3, pp. 429–434.

Nieuwenhuijsen, Mark J. (2016). "Urban and transport planning, environmental exposures and health-new concepts, methods and tools to improve health in cities". In: *Environmental Health : A Global Access Science Source* vol. 15 Suppl 1.Suppl 1, pp. 38–38.

Nonomura, Atsuko, Mutsuko Kitahara, and Takuro Masuda (2009). "Impact of land use and land cover changes on the ambient temperature in a middle scale city, Takamatsu, in Southwest Japan". In: *Journal of Environmental Management* vol. 90.11, pp. 3297–3304.

Nordbeck, Stig (1971). "Urban allometric growth". In: *Geografiska Annaler. Series B, Human Geography* vol. 53.1, pp. 54–67.

Norris, Gary and Timothy Larson (1999). "Spatial and temporal measurements of NO_2 in an urban area using continuous mobile monitoring and passive samplers". In: *Journal of Exposure Science & Environmental Epidemiology* vol. 9.6, pp. 586–593.

Novotny, Eric V. et al. (2011). "National satellite-based land-use regression: NO_2 in the United States". In: *Environmental Science & Technology* vol. 45.10, pp. 4407–4414.

Nowak, David J., Daniel E. Crane, and Jack C. Stevens (2006a). "Air pollution removal by urban trees and shrubs in the United States". In: *Urban Forestry & Urban Greening* vol. 4.3, pp. 115–123.

Nowak, David J et al. (2006b). "Assessing urban forest effects and values, Minneapolis' urban forest". In: *Resour. Bull. NE-166. Newtown Square, PA: US Department of Agriculture, Forest Service, Northeastern Research Station. 20 p.* Vol. 166, pp. 1–22.

— (2006c). "Assessing urban forest effects and values, Washington, DC's urban forest". In: *Resour. Bull. NRS-1. Newtown Square, PA: US Department of Agriculture, Forest Service, Northern Research Station. 24 p.* Vol. 1, pp. 1–24.

Nowak, David J et al. (2007a). "Assessing urban forest effects and values, New York City's urban forest". In: *Resour. Bull. NRS-9. Newtown Square, PA: US Department of Agriculture, Forest Service, Northern Research Station. 22 p.* Vol. 9, pp. 1–22.

— (2007b). "Assessing urban forest effects and values, San Francisco's urban forest". In: *Resour. Bull. NRS-37. Newtown Square, PA: U.S. Department of Agriculture, Forest Service, Northern Research Station. 22 p.* Vol. 7, pp. 1–22.

Nowak, David J et al. (2010). "Assessing urban forest effects and values, Chicago's urban forest". In: *Resour. Bull. NRS-37. Newtown Square, PA: US Department of Agriculture, Forest Service, Northern Research Station. 27 p.* Vol. 37, pp. 1–27.

O'Sullivan, Arthur (2012). *Urban economics*. McGraw-Hill.

OECD & European Commission (June 2020). *Cities in the world: A new perspective on urbanisation*. Paris: OECD Publishing.

Oke, T. R. (1981). "Canyon geometry and the nocturnal urban heat island: Comparison of scale model and field observations". In: *Journal of Climatology* vol. 1.3, pp. 237–254.

— (2011). "Urban heat island". In: *Handbook of urban ecology*. Ed. by Ian Douglas et al. Taylor and Francis. Chap. 11, pp. 120–131.

— (1973). "City size and the urban heat island". In: *Atmospheric Environment (1967)* vol. 7.8, pp. 769–779.

— (1976). "The distinction between canopy and boundary-layer urban heat islands". In: *Atmosphere* vol. 14.4, pp. 268–277.

— (1982). "The energetic basis of the urban heat island". In: *Quarterly Journal of the Royal Meteorological Society* vol. 108.455, pp. 1–24.

— (1995). "The heat island of the urban boundary layer: Characteristics, causes and effects". In: *Wind climate in cities*. Ed. by Jack E. Cermak et al. Dordrecht: Springer Netherlands, pp. 81–107.

Oke, T.R. and G.B. Maxwell (1975). "Urban heat island dynamics in Montreal and Vancouver". In: *Atmospheric Environment (1967)* vol. 9.2, pp. 191–200.

Oke, T.R. et al. (1991). "Simulation of surface urban heat islands under 'ideal' conditions at night part 2: Diagnosis of causation". In: *Boundary-Layer Meteorology* vol. 56.4, pp. 339–358.

Oleson, K. W. et al. (2008). "An urban parameterization for a global climate model. Part II: Sensitivity to input parameters and the simulated urban heat island in offline simulations". In: *Journal of Applied Meteorology and Climatology* vol. 47.4, pp. 1061–1076.

Oliver, J.Eric (2000). "City size and civic involvement in Metropolitan America". In: *The American Political Science Review* vol. 94.2, pp. 361–373.

Olvera-García, Miguel Ángel et al. (2016). "Air quality assessment using a weighted Fuzzy Inference System". In: *Ecological Informatics* vol. 33, pp. 57–74.

Ongoma, Victor, John Nzioka Muthama, and Wilson Gitau (2013). "Evaluation of urbanization influences on urban temperature of Nairobi City, Kenya". In: *Global Meteorology* vol. 2.1, e1.

Oxford University Press (2023). *Rank-size rule*. Accessed 12 March, 2023. URL: https://www.oxfordreference.com/display/10.1093/oi/authority.20110803100404250;jsessionid=6FA34E90E09E62F96A3877DD73AC4472.

Padam, Sudarsanam and Sanjay Kumar Singh (2004). "Urbanization and urban transport in India: The search for a policy". In: *European Transport/Trasporti Europei* vol. 27, pp. 27–44.

Pamfilos, Paris (2021). *Homotheties and similarities*. Tech. rep. Accessed April 11, 2023. Geometrikon. URL: http://users.math.uoc.gr/~pamfilos/eGallery/problems/Similarities.pdf.

Paraschiv, Spiru et al. (2017). "OMI and ground-based in-situ tropospheric nitrogen dioxide observations over several important European cities during 2005–2014". In: *International Journal of Environmental Research and Public Health* vol. 14.11.

Park, Hayoung et al. (2021). "An assessment of emission characteristics of Northern Hemisphere cities using spaceborne observations of CO_2, CO, and NO_2". In: *Remote Sensing of Environment* vol. 254, p. 112246.

Park, Hye-Sook (1987). "City size and urban heat island intensity for Japanese and Korean cities". In: *Geographical Review of Japa,. Ser. A, Chirigaku Hyoron* vol. 60.4, pp. 238–250.

Parker, Danny and Nick Drake (2018). *Energy-efficient lighting for Florida homes*. Tech. rep. Accessed March 8, 2023. Florida Solar Energy Center. URL: https://stars.library.ucf.edu/fsec/846.

Parrish, D.F. and J.C. Derber (1992). "The National Meteorological Centers spectral statistical-interpolation analysis scheme". In: *Monthly Weather Review* vol. 120, pp. 1747–1763.

Parrish, David D. and Tong Zhu (2009). "Clean air for megacities". In: *Science* vol. 326.5953, pp. 674–675.

Peach, W. J. et al. (2008). "Reproductive success of house sparrows along an urban gradient". In: *Animal Conservation* vol. 11.6, pp. 493–503.

Peach, Will J. et al. (2018). "Depleted suburban house sparrow *Passer domesticus* population not limited by food availability". In: *Urban Ecosystems* vol. 21.6, pp. 1053–1065.

Pedersen, Marie et al. (2013). "Does consideration of larger study areas yield more accurate estimates of air pollution health effects? An illustration of the bias-variance trade-off in air pollution epidemiology". In: *Environment International* vol. 60, pp. 23–30.

Pekey, Beyhan and Hande Ylmaz (2011). "The use of passive sampling to monitor spatial trends of volatile organic compounds (VOCs) at an industrial city of Turkey". In: *Microchemical Journal* vol. 97.2, pp. 213–219.

Peng, Chaoyang et al. (2002). "Urban air quality and health in China". In: *Urban Studies* vol. 39.12, pp. 2283–2299.

Peng, Shijia et al. (2019). "Spatial-temporal pattern of, and driving forces for, urban heat island in China". In: *Ecological Indicators* vol. 96, pp. 127–132.

Peng, Shushi et al. (2012). "Surface urban heat island across 419 global big cities". In: *Environmental Science & Technology* vol. 46.2, pp. 696–703.

Pham, Thi-Thanh-Hien et al. (2013). "Predictors of the distribution of street and backyard vegetation in Montreal, Canada". In: *Urban Forestry & Urban Greening* vol. 12.1, pp. 18–27.

Pickett, S.T.A. et al. (2001). "Urban ecological systems: Linking terrestrial ecological, physical, and socioeconomic components of metropolitan areas". In: *Annual Review of Ecology and Systematics* vol. 32.1, pp. 127–157.

Pickett, S.T.A. et al. (2011). "Urban ecological systems: Scientific foundations and a decade of progress". In: *Journal of Environmental Management* vol. 92.3, pp. 331–362.

Pistocchi, Plberto (2015). *European monthly wind speed (MAPPE model)*. Accessed 21 August, 2022. URL: https://data.jrc.ec.europa.eu/dataset/jrc-mappe-europe-setup-d-11-wind-speed.

Platt, Ulrich and Jochen Stutz (2008). *Differential optical absorption spectroscopy*. Springer Berlin.

Polycarpou, Lakis (2010). *No more pavement! The problem of impervious surfaces*. URL: https://blogs.ei.columbia.edu/2010/07/13/no-more-pavement-the-problem-of-impervious-surfaces/.

Pope, Robin M. and Edward S. Fry (1997). "Absorption spectrum (380–700 nm) of pure water. II. Integrating cavity measurements". In: *Applied Optics* vol. 36.33, pp. 8710–8723.

Poplawski, Karla et al. (2009). "Intercity transferability of land use regression models for estimating ambient concentrations of nitrogen dioxide". In: *Journal of Exposure Science & Environmental Epidemiology* vol. 19.1, pp. 107–117.

Portman, David A. (1993). "Identifying and correcting urban bias in regional time series: Surface temperature in China's northern plains". In: *Journal of Climate* vol. 6.12, pp. 2298–2308.

Preston, Samuel H. (1979). "Urban growth in developing countries: A demographic reappraisal". In: *Population and Development Review* vol. 5.2, pp. 195–215.

Puliafito, S. Enrique et al. (2017). "High-resolution atmospheric emission inventory of the argentine energy sector. Comparison with edgar global emission database". In: *Heliyon* vol. 3.12, e00489–e00489.

Pulselli, R et al. (2008). "Computing urban mobile landscapes through monitoring population density based on cellphone chatting". In: *International Journal of Design & Nature and Ecodynamics* vol. 3.2, pp. 121–134.

Puppim de Oliveira, J.A. et al. (2011). "Cities and biodiversity: Perspectives and governance challenges for implementing the convention on biological diversity (CBD) at the city level". In: *Biological Conservation* vol. 144.5, pp. 1302–1313.

Qiao, Zhi, Guangjin Tian, and Lin Xiao (2013). "Diurnal and seasonal impacts of urbanization on the urban thermal environment: A case study of Beijing using MODIS data". In: *Isprs Journal of Photogrammetry and Remote Sensing* vol. 85, pp. 93–101.

Qiao, Zhi et al. (2014). "Influences of urban expansion on urban heat island in Beijing during 1989 - 2010". In: *Advances in Meteorology* vol. 2014.

Qiu, Peipei et al. (2014). "An elaborate high resolution emission inventory of primary air pollutants for the Central Plain Urban Agglomeration of China". In: *Atmospheric Environment* vol. 86, pp. 93–101.

Quah, Anne K.L. and Matthias Roth (2012). "Diurnal and weekly variation of anthropogenic heat emissions in a tropical city, Singapore". In: *Atmospheric Environment* vol. 46, pp. 92–103.

Raan, Anthony F. J. van, Gerwin van der Meulen, and Willem Goedhart (2016). "Urban scaling of cities in the Netherlands". In: *PLOS ONE* vol. 11.1, pp. 1–16. URL: https://doi.org/10.1371/journal.pone.0146775.

Raaschou-nielsen, Ole et al. (2000). "An air pollution model for use in epidemiological studies: Evaluation with measured levels of nitrogen dioxide and benzene". In: *Journal of Exposure Science & Environmental Epidemiology* vol. 10.1, pp. 4–14.

Raciti, Steve M., Lucy R. Hutyra, and Jared D. Newell (2014). "Mapping carbon storage in urban trees with multi-source remote sensing data: Relationships between biomass, land use, and demographics in Boston neighborhoods". In: *Science of the Total Environment* vol. 500-501, pp. 72–83.

Rahman, Muhammad Tauhidur (2018). "Examining and modelling the determinants of the rising land surface temperatures in Arabian desert cities: An example from Riyadh, Saudi Arabia". In: *Journal of Settlements and Spatial Planning* vol. 9.1, pp. 1–10.

Ramaswami, Anu et al. (2018). "Sustainable urban systems: Articulating a long-term convergence research agenda". In: *Washington DC USA: National Science Foundation*. URL: https://www.nsf.gov/ere/ereweb/ac-ere/sustainable-urban-systems.pdf.

Ranagalage, Manjula et al. (2018). "Spatial changes of urban heat island formation in the Colombo District, Sri Lanka: Implications for sustainability planning". In: *Sustainability* vol. 10.5.

Rank, Mark R and Thomas A Hirschl (1988). "A rural-urban comparison of welfare exits: The importance of population density". In: *Rural Sociology* vol. 53.2, pp. 190–206.

Rao, Meenakshi et al. (2014). "Assessing the relationship among urban trees, nitrogen dioxide, and respiratory health". In: *Environmental Pollution* vol. 194, pp. 96–104.

Restrepo, Carlos E. (2021). "Nitrogen dioxide, greenhouse gas emissions and transportation in urban areas: Lessons from the covid-19 pandemic". In: *Frontiers in Environmental Science* vol. 9, p. 204.

Reutov, VP et al. (2012). "The possible role of nitrogen dioxide produced in the field of bifurcation of vessels, in the processes of their damage in hemorrhagic strokes, and the formation of atherosclerotic plaques". In: *Uspekhi Fiziologicheskikh Nauk* vol. 43.4, pp. 73–93.

Rivera, Erika et al. (2017). "Spatiotemporal analysis of the atmospheric and surface urban heat islands of the Metropolitan Area of Toluca, Mexico". In: *Environmental Earth Sciences* vol. 76.5, p. 225.

Rizwan, Ahmed Memon, Leung Y.C. Dennis, and Chunho Liu (2008). "A review on the generation, determination and mitigation of urban heat island". In: *Journal of Environmental Sciences* vol. 20.1, pp. 120–128.

Robine, Jean-Marie et al. (2008). "Death toll exceeded 70,000 in Europe during the summer of 2003". In: *Comptes Rendus Biologies* vol. 331.2, pp. 171–178.

Robinson, James A. and T.N. Srinivasan (1997). "Chapter 21 Long-term consequences of population growth: Technological change, natural resources, and the environment". In: vol. 1. Handbook of population and family economics. Elsevier, pp. 1175–1298.

Robson, Brian T (2012). *Urban growth: An approach*. Routledge.

Rodríguez, Miguel Cárdenas, Laura Dupont-Courtade, and Walid Oueslati (2016). "Air pollution and urban structure linkages: Evidence from European cities". In: *Renewable and Sustainable Energy Reviews* vol. 53, pp. 1–9.

Roman, Kibria K. et al. (2016). "Simulating the effects of cool roof and PCM (phase change materials) based roof to mitigate UHI (urban heat island) in prominent US cities". In: *Energy* vol. 96, pp. 103–117.

Roorda-Knape, Mirjam C et al. (1998). "Air pollution from traffic in city districts near major motorways". In: *Atmospheric Environment* vol. 32.11, pp. 1921–1930.

Rosenlund, Mats et al. (2008). "Comparison of regression models with land-use and emissions data to predict the spatial distribution of traffic-related air pollution in Rome". In: *Journal of Exposure Science & Environmental Epidemiology* vol. 18.2, pp. 192–199.

Rosenzweig, Cynthia et al. (2005). "Characterizing the urban heat island in current and future climates in New Jersey". In: *Global Environmental Change Part B: Environmental Hazards* vol. 6.1, pp. 51–62.

Roth, Matthias and Winston T.L. Chow (2012). "A historical review and assessment of urban heat island research in Singapore". In: *Singapore Journal of Tropical Geography* vol. 33.3, pp. 381–397.

Rozenfeld, Hernán D. et al. (2008). "Laws of population growth". In: *Proceedings of the National Academy of Sciences* vol. 105.48, pp. 18702–18707.

Rozenfeld, Hernán D. et al. (2011). "The area and population of cities: New insights from a different perspective on cities". In: *American Economic Review* vol. 101.5, pp. 2205–25.

Rubel, Franz and Markus Kottek (2010). "Observed and projected climate shifts 1901-2100 depicted by world maps of the Koppen-Geiger climate classification". In: *Meteorologische Zeitschrift* vol. 19.2, pp. 135–141.

Ruthirako, Poonyanuch, Rotchanatch Darnsawasdi, and Wichien Chatupote (2015). "Intensity and pattern of land surface temperature in Hat Yai City, Thailand". In: *Walailak Journal of Science and Technology (WJST)* vol. 12.1, pp. 83–94.

Rybski, Diego et al. (2017). "Cities as nuclei of sustainability?" In: *Environment and Planning B: Urban Analytics and City Science* vol. 44.3, pp. 425–440.

Safirova, Elena (2002). "Telecommuting, traffic congestion, and agglomeration: A general equilibrium model". In: *Journal of Urban Economics* vol. 52.1, pp. 26–52.

Sagris, V. and M. Sepp (2017). "Landsat-8 TIRS data for assessing urban heat island effect and its impact on human health". In: *IEEE Geoscience and Remote Sensing Letters* vol. 14.12, pp. 2385–2389.

Sahashi, K (1983). "Errors in the air temperature observation by traveling method with the automobiles: Effects of the automobiles". In: *Tenki* vol. 30, pp. 509–514.

Sahsuvaroglu, Talar et al. (2006). "A land use regression model for predicting ambient concentrations of nitrogen dioxide in Hamilton, Ontario, Canada". In: *Journal of the Air & Waste Management Association* vol. 56.8, pp. 1059–1069.

Sailor, David J. (2011). "A review of methods for estimating anthropogenic heat and moisture emissions in the urban environment". In: *International Journal of Climatology* vol. 31.2, pp. 189–199.

Sakakibara, Yasushi and Emi Matsui (2005). "Relation between heat island intensity and city size indices/urban canopy characteristics in settlements of Nagano Basin, Japan". In: *Geographical Review of Japan* vol. 78.12, pp. 812–824.

Samoli, E et al. (2019). "Spatial variability in air pollution exposure in relation to socioeconomic indicators in nine European metropolitan areas: A study on environmental inequality". In: *Environmental Pollution* vol. 249, pp. 345–353.

Santamouris, M. (2015). "Analyzing the heat island magnitude and characteristics in one hundred Asian and Australian cities and regions". In: *Science of the Total Environment* vol. 512-513, pp. 582–598.

Santamouris, M. et al. (2015). "On the impact of urban heat island and global warming on the power demand and electricity consumption of buildings: A review". In: *Energy and Buildings* vol. 98, pp. 119–124.

Santos, Ana Paula Milla dos et al. (2014). "A support tool for air pollution health risk management in emerging countries: A case in Brazil". In: *Human and Ecological Risk Assessment: An International Journal* vol. 20.5, pp. 1406–1424.

Sarrat, C. et al. (2006). "Impact of urban heat island on regional atmospheric pollution". In: *Atmospheric Environment* vol. 40.10, pp. 1743–1758.

Sarzynski, Andrea (2012). "Bigger is not always better: A comparative analysis of cities and their air pollution impact". In: *Urban Studies* vol. 49.14, pp. 3121–3138.

Saucy, Apolline et al. (2018). "Land use regression modelling of outdoor NO_2 and $PM_{2.5}$ concentrations in three low income areas in the Western Cape Province, South Africa". In: *International Journal of Environmental Research and Public Health* vol. 15.7, p. 1452.

Scalenghe, Riccardo and Franco Ajmone Marsan (2009). "The anthropogenic sealing of soils in urban areas". In: *Landscape and Urban Planning* vol. 90.1, pp. 1–10.

Schatz, Jason and Christopher J Kucharik (2015). "Urban climate effects on extreme temperatures in Madison, Wisconsin, USA". In: *Environmental Research Letters* vol. 10.9, p. 094024.

Schaub, D. et al. (2007). "SCIAMACHY tropospheric NO_2 over Switzerland: Estimates of NO_x lifetimes and impact of the complex Alpine topography on the retrieval". In: *Atmospheric Chemistry and Physics* vol. 7.23, pp. 5971–5987.

Schiavina, M. et al. (2019). *GHSL-OECD functional urban areas*. Accessed June 27, 2022. URL: https://jeodpp.jrc.ec.europa.eu/ftp/jrc-opendata/GHSL/GHS_FUA_UCDB2015_GLOBE_R2019A/V1-0/GHS_FUA_UCDB2015_GLOBE_R2019A_54009_1K_V1_0.zip.

Schiller, Frank (2016). "Urban transitions: scaling complex cities down to human size". In: *Journal of Cleaner Production* vol. 112, pp. 4273–4282.

Schindler, Christian et al. (1998). "Associations between lung function and estimated average exposure to NO_2 in eight areas of Switzerland". In: *Epidemiology* vol. 9.4, pp. 405–411.

Schindler, Mirjam and Geoffrey Caruso (2014). "Urban compactness and the trade-off between air pollution emission and exposure: Lessons from a spatially explicit theoretical model". In: *Computers, Environment and Urban Systems* vol. 45, pp. 13–23.

Schindler, Mirjam, Geoffrey Caruso, and Pierre Picard (2017). "Equilibrium and first-best city with endogenous exposure to local air pollution from traffic". In: *Regional Science & Urban Economics* vol. 62, pp. 12–23.

Schmid, Paul E. and Dev Niyogi (2013). "Impact of city size on precipitation-modifying potential". In: *Geophysical Research Letters* vol. 40.19, pp. 5263–5267.

Schneider, Annemarie and Curtis E. Woodcock (2008). "Compact, dispersed, fragmented, extensive? A comparison of urban growth in twenty-five global cities using remotely sensed data, pattern metrics and census information". In: *Urban Studies* vol. 45.3, pp. 659–692.

Schulze, P.C. (2002). "I=PBAT". In: *Ecological Economics* vol. 40, pp. 149–150.

Schwarz, Nina (2012). "Comment on "Surface urban heat island across 419 global big cities"". In: *Environmental Science & Technology* vol. 46.12, pp. 6888–6888.

Schwarz, Nina et al. (2012). "Relationship of land surface and air temperatures and its implications for quantifying urban heat island indicators - An application for the city of Leipzig (Germany)". In: *Ecological Indicators* vol. 18, pp. 693–704.

SCIAVALIG (2023). *SCIAMACHY*. Accessed 9 March, 2023. URL: https://www.sciamachy.org/.

Scoggins, Amanda and Gavin Fisher (2002). "Air pollution exposure index for New Zealand". In: *New Zealand Geographer* vol. 58.2, pp. 56–64.

Scott, Alister, Alana Gilbert, and Ayele Gelan (2007). *The urban-rural divide: Myth or reality?* Macaulay Institute.

Seddiek, Ibrahim S. and Mohamed M. Elgohary (2014). "Eco-friendly selection of ship emissions reduction strategies with emphasis on SO_x and NO_x emissions". In: *International Journal of Naval Architecture & Ocean Engineering* vol. 6.3, pp. 737–748.

Serdyuchenko, A. et al. (2014). "High spectral resolution ozone absorption cross-sections - Part 2: Temperature dependence". In: *Atmospheric Measurement Techniques* vol. 7.2, pp. 625–636.

Seto, Karen C. and Michail Fragkias (2005). "Quantifying spatiotemporal patterns of urban land-use change in four cities of China with time series landscape metrics". In: *Landscape Ecology* vol. 20.7, pp. 871–888.

Shah, V. et al. (2020). "Effect of changing NO_x lifetime on the seasonality and long-term trends of satellite-observed tropospheric NO_2 columns over China". In: *Atmospheric Chemistry and Physics* vol. 20.3, pp. 1483–1495.

Shahmohamadi, P. et al. (2010). "Reducing urban heat island effects: A systematic review to achieve energy consumption balance". In: *International Journal of Physical Sciences* vol. 5.6, pp. 626–636.

Shahzad, Asim et al. (2018). "Search engine optimization techniques for malaysian university websites: A comparative analysis on google and bing search engine". In: *International Journal on Advanced Science Engineering Information Technology* vol. 8.4, pp. 1262–1269.

Shao, Min et al. (2006). "City clusters in China: Air and surface water pollution". In: *Frontiers in Ecology and the Environment* vol. 4.7, pp. 353–361.

Sharma, Disha and U.C. Kulshrestha (2014). "Spatial and temporal patterns of air pollutants in rural and urban areas of India". In: *Environmental Pollution* vol. 195, pp. 276–281.

Shazia, Pervaiz et al. (2019). "Spatial analysis of vegetation cover in urban green space under new government agenda of clean and green Pakistan to tackle climate change". In: *Journal of Ecological Engineering* vol. 20, pp. 245–255.

Shen, Lidu, Jianning Sun, and Renmin Yuan (2018). "Idealized large-eddy simulation study of interaction between urban heat island and sea breeze circulations". In: *Atmospheric Research* vol. 214, pp. 338–347.

Sheng, Li, Dengsheng Lu, and Jingfeng Huang (2015). "Impacts of land-cover types on an urban heat island in Hangzhou, China". In: *International Journal of Remote Sensing* vol. 36.6, pp. 1584–1603.

Sheng, Li et al. (2017). "Comparison of the urban heat island intensity quantified by using air temperature and Landsat land surface temperature in Hangzhou, China". In: *Ecological Indicators* vol. 72, pp. 738–746.

Sheppard, Eric (1982). "City size distributions and spatial economic change". In: *International Regional Science Review* vol. 7.2, pp. 127–151.

Sheridan, Charlotte E. et al. (2019). "Inequalities in exposure to nitrogen dioxide in parks and playgrounds in Greater London". In: *International Journal of Environmental Research and Public Health* vol. 16.17.

Sheshinski, Eytan (1973). "Congestion and the optimum city size". In: *The American Economic Review* vol. 63.2, pp. 61–66.

Shi, Bin et al. (2012). "Observation and analysis of the urban heat island effect on soil in Nanjing, China". In: *Environmental Earth Sciences* vol. 67.1, pp. 215–229.

Shirani-bidabadi, Niloufar et al. (2019). "Evaluating the spatial distribution and the intensity of urban heat island using remote sensing, case study of Isfahan city in Iran". In: *Sustainable Cities and Society* vol. 45, pp. 686–692.

Shishegar, Nastaran (2014). "The impact of green areas on mitigating urban heat island effect: A review". In: *International Journal of Environmental Sustainability* vol. 9, pp. 119–130.

Shmool, Jessie L.C. et al. (2015). "Area-level socioeconomic deprivation, nitrogen dioxide exposure, and term birth weight in New York City". In: *Environmental Research* vol. 142, pp. 624–632.

Shrestha, Kundan Lal et al. (2009). "Numerical simulation of urban heat island using gridded urban configuration and anthropogenic heat data generated by a simplified method". In: *Proceedings of the 7th Conference on Urban Climate*.

Silveira Fleck, Alan da et al. (2017). "The use of tree barks and human fingernails for monitoring metal levels in urban areas of different population densities of Porto Alegre, Brazil". In: *Environmental Science and Pollution Research* vol. 24.3, pp. 2433–2441.

Simeonova, V.S. (2019). *Functionality in metropolitan areas: Transnational brief*. Luxembourg: ESPON.

Singh, Nidhi, Saumya Singh, and R.K. Mall (2020). "Chapter 17 - Urban ecology and human health: Implications of urban heat island, air pollution and climate change nexus". In: *Urban ecology*. Ed. by Pramit Verma et al. Elsevier, pp. 317–334.

Singh, Prafull, Noyingbeni Kikon, and Pradipika Verma (2017). "Impact of land use change and urbanization on urban heat island in Lucknow city, Central India. A remote sensing based estimate". In: *Sustainable Cities and Society* vol. 32, pp. 100–114.

Singh, Saumya and U. C. Kulshrestha (2014). "Rural versus urban gaseous inorganic reactive nitrogen in the Indo-Gangetic plains (IGP) of India". In: *Environmental Research Letters* vol. 9.12, p. 125004.

Siu, Leong Wai and Melissa A. Hart (2013). "Quantifying urban heat island intensity in Hong Kong SAR, China". In: *Environmental Monitoring and Assessment* vol. 185.5, pp. 4383–4398.

Skene, Katherine J. et al. (2010). "Modeling effects of traffic and landscape characteristics on ambient nitrogen dioxide levels in Connecticut". In: *Atmospheric environment (Oxford, England : 1994)* vol. 44.39, pp. 5156–5164.

Skoulika, Fotini et al. (2014). "On the thermal characteristics and the mitigation potential of a medium size urban park in Athens, Greece". In: *Landscape and Urban Planning* vol. 123, pp. 73–86.

Skouloudis, A. N. and D. G. Rickerby (2016). "Verifiable emission reductions in European urban areas with air-quality models". In: *Faraday Discuss.* Vol. 189 (0), pp. 617–633.

Slama, Rémy et al. (2007). "Traffic-related atmospheric pollutants levels during pregnancy and offspring's term birth weight: A study relying on a land-use regression exposure model". In: *Environmental Health Perspectives* vol. 115.9, pp. 1283–1292.

Sobrino, José A. et al. (2013). "Evaluation of the surface urban heat island effect in the city of Madrid by thermal remote sensing". In: *International Journal of Remote Sensing* vol. 34.9-10, pp. 3177–3192.

Solomon, S. et al. (1999). "On the role of nitrogen dioxide in the absorption of solar radiation". In: *Journal of Geophysical Research: Atmospheres* vol. 104.D10, pp. 12047–12058.

Soltanzadeh, I et al. (2011). "Study of local winds over Tehran using WRF in ideal conditions". In: *Iranian Journal of Physics Research* vol. 11.2, pp. 199–213.

Song, Congbo et al. (2018). "Heavy-duty diesel vehicles dominate vehicle emissions in a tunnel study in northern China". In: *Science of the Total Environment* vol. 637-638, pp. 431–442.

Song, Fei et al. (2011). "Relationships among the springtime groundlevel NO_x, O_3 and NO_3 in the vicinity of highways in the US East Coast". In: *Atmospheric Pollution Research* vol. 2.3, pp. 374–383.

Soriano, Luis Rivas and Fernando de Pablo (2002). "Effect of small urban areas in central Spain on the enhancement of cloud-to-ground lightning activity". In: *Atmospheric Environment* vol. 36.17, pp. 2809–2816.

South Australia EPA (2004). *Photochemical smog - What it means for us*. Accessed June 19, 2022. URL: https://www.epa.sa.gov.au/files/8238_info_photosmog.pdf.

Squalli, Jay (2010). "An empirical assessment of U.S. state-level immigration and environmental emissions". In: *Ecological Economics* vol. 69.5, pp. 1170–1175.

Stallins, J. Anthony (2004). "Characteristics of urban lightning hazards for Atlanta, Georgia". In: *Climatic Change* vol. 66.1, pp. 137–150.

Stauber, Christine et al. (2018). "Measuring the impact of environment on the health of large cities". In: *International Journal of Environmental Research and Public Health* vol. 15.6, p. 1216.

Stead, Dominic and Stephen Marshall (2001). "The relationships between urban form and travel patterns. An international review and evaluation". In: *European Journal of Transport and Infrastructure Research* vol. 1.2, pp. 113–141.

Steeneveld, G. J. et al. (2011). "Quantifying urban heat island effects and human comfort for cities of variable size and urban morphology in the Netherlands". In: *Journal of Geophysical Research: Atmospheres* vol. 116.D20129.

Steeneveld, G.J. et al. (2014). "Refreshing the role of open water surfaces on mitigating the maximum urban heat island effect". In: *Landscape and Urban Planning* vol. 121, pp. 92–96.

Stewart, I.D. and T.R. Oke (2012). "Local climate zones for urban temperature studies". In: *Bulletin of the American Meteorological Society* vol. 93.12, pp. 1879–1900.

Stewart, I.D. and Tim Oke (2009). "Classifying urban climate field sites by "local climate zones": The case of Nagano, Japan". In: *Seventh International Conference on Urban Climate*. Vol. 29.

Stewart, Ian Douglas (2007). "Landscape representation and the urban-rural dichotomy in empirical urban heat island literature, 1950 - 2006". In: *Acta Climatologica et Chorologica* vol. 40.41, pp. 111–121.

Stone Jr, Brian (2007). "Urban and rural temperature trends in proximity to large US cities: 19512000". In: *International Journal of Climatology* vol. 27.13, pp. 1801–1807.

— (2008). "Urban sprawl and air quality in large US cities". In: *Journal of Environmental Management* vol. 86.4, pp. 688–698.

Stone Jr, Brian and Michael O Rodgers (2001). "Urban form and thermal efficiency: How the design of cities influences the urban heat island effect". In: *Journal of the American Planning Association* vol. 67.2, pp. 186–198.

Stone, Brian and John M. Norman (2006). "Land use planning and surface heat island formation: A parcel-based radiation flux approach". In: *Atmospheric Environment* vol. 40.19, pp. 3561–3573.

Streutker, D.R. (2002). "A remote sensing study of the urban heat island of Houston, Texas". In: *International Journal of Remote Sensing* vol. 23.13, pp. 2595–2608.

Streutker, David R (2003a). "Satellite-measured growth of the urban heat island of Houston, Texas". In: *Remote Sensing of Environment* vol. 85.3, pp. 282–289.

Streutker, David Richard (2003b). "A study of the urban heat island of Houston, Texas". Ph.D. dissertation. Rice Univeristy.

Strohbach, Michael W. et al. (2019). "The hidden urbanization: Trends of impervious surface in low-density housing developments and resulting impacts on the water balance". In: *Frontiers in Environmental Science* vol. 7.29, pp. 1–10.

Su, J.G., M. Brauer, and M. Buzzelli (2008). "Estimating urban morphometry at the neighborhood scale for improvement in modeling long-term average air pollution concentrations". In: *Atmospheric Environment* vol. 42.34, pp. 7884–7893.

Su, Yuan-Fong, Giles M. Foody, and Ke-Sheng Cheng (2012). "Spatial non-stationarity in the relationships between land cover and surface temperature in an urban heat island and its impacts on thermally sensitive populations". In: *Landscape and Urban Planning* vol. 107.2, pp. 172–180.

Suomi, Juuso, Jan Hjort, and Jukka Käyhkö (2012). "Effects of scale on modelling the urban heat island in Turku, SW Finland". In: *Climate Research* vol. 55.2, pp. 105–118.

Suomi, Juuso and Jukka Käyhkö (2012). "The impact of environmental factors on urban temperature variability in the coastal city of Turku, SW Finland". In: *International Journal of Climatology* vol. 32.3, pp. 451–463.

Susaya, Janice et al. (2013). "Demonstration of long-term increases in tropospheric O_3 levels: Causes and potential impacts". In: *Chemosphere* vol. 92.11, pp. 1520–1528.

Sveikauskas, Leo, John Gowdy, and Michael Funk (1988). "Urban productivity: City size or industry size". In: *Journal of Regional Science* vol. 28.2, pp. 185–202.

Sweeney, John (1987). "The urban heat island of Dublin City". In: *Irish Geography* vol. 20.1, pp. 1–10.

Swinney, Paul (2011). *Statsblog: What role do city centres play in local economic growth?* Accessed 21 August, 2022. URL: https://www.theguardian.com/local-government-network/statsblog/2011/nov/09/statsblog-role-of-city-centres.

Szegedi, Sándor and Andrea Kircsi (2003). "The development of the urban heat island under various weather conditions in Debrecen, Hungary". In: *Proceedings of the Fifth International Conference on Urban Climate*.

Tainio, Marko et al. (2014). "Intake fraction variability between air pollution emission sources inside an urban area". In: *Risk Analysis* vol. 34.11, pp. 2021–2034.

Taj, Tahir et al. (2017). "Short-term associations between air pollution concentrations and respiratory health-Comparing primary health care visits, hospital admissions, and emergency department visits in a multi-municipality study". In: *International journal of environmental research and public health* vol. 14.6, p. 587.

Tam, Benita Y., William A. Gough, and Tanzina Mohsin (2015). "The impact of urbanization and the urban heat island effect on day to day temperature variation". In: *Urban Climate* vol. 12, pp. 1–10.

Tan, Jianguo et al. (2010). "The urban heat island and its impact on heat waves and human health in Shanghai". In: *International Journal of Biometeorology* vol. 54.1, pp. 75–84.

Tan, Minghong and Xiubin Li (2015). "Quantifying the effects of settlement size on urban heat islands in fairly uniform geographic areas". In: *Habitat International* vol. 49, pp. 100–106.

Tan, Zheng, Kevin Ka-Lun Lau, and Edward Ng (2016). "Urban tree design approaches for mitigating daytime urban heat island effects in a high-density urban environment". In: *Energy and Buildings* vol. 114, pp. 265–274.

Tang, Junmei et al. (2017). "Impacts of land use and socioeconomic patterns on urban heat Island". In: *International Journal of Remote Sensing* vol. 38.11, pp. 3445–3465.

Tang, U. Wa and Zhishi Wang (2006). "Determining gaseous emission factors and drivers particle exposures during traffic congestion by vehicle-following measurement techniques". In: *Journal of the Air & Waste Management Association* vol. 56.11, pp. 1532–1539.

Taylor, O.C. (1969). "Importance of peroxyacetyl nitrate (PAN) as a phytotoxic air pollutant". In: *Journal of the Air Pollution Control Association* vol. 19.5, pp. 347–351.

Temple, P.J. and O.C. Taylor (1983). "World-wide ambient measurements of peroxyacetyl nitrate (PAN) and implications for plant injury". In: *Atmospheric Environment (1967)* vol. 17.8, pp. 1583–1587.

Tenailleau, Quentin M. et al. (2016). "Do outdoor environmental noise and atmospheric NO_2 levels spatially overlap in urban areas?" In: *Environmental Pollution* vol. 214, pp. 767–775.

Thalman, Ryan and Rainer Volkamer (2013). "Temperature dependent absorption cross-sections of O_2-O_2 collision pairs between 340 and 630 nm and at atmospherically relevant pressure". In: *Physical Chemistry Chemical Physics* vol. 15 (37), pp. 15371–15381.

Theeuwes, Natalie E. et al. (2017). "A diagnostic equation for the daily maximum urban heat island effect for cities in Northwestern Europe". In: *International Journal of Climatology* vol. 37.1, pp. 443–454.

Thomas, G and EJ Zachariah (2011). "Urban heat island in a tropical city interlaced by wetlands". In: *Indian Journal of Environmental Health* vol. 5, pp. 234–240.

Tian, Liu et al. (2021). "Review on urban heat island in China: Methods, its impact on buildings energy demand and mitigation strategies". In: *Sustainability* vol. 13.2.

Tie, X., G. Brasseur, and Z. Ying (2010). "Impact of model resolution on chemical ozone formation in Mexico City: Application of the WRF-Chem model". In: *Atmospheric Chemistry and Physics* vol. 10.18, pp. 8983–8995.

Timmermans, R.M.A. et al. (2013). "Quantification of the urban air pollution increment and its dependency on the use of down-scaled and bottom-up city emission inventories". In: *Urban Climate* vol. 6, pp. 44–62.

Tomlinson, Charlie J. et al. (2011). "Including the urban heat island in spatial heat health risk assessment strategies: A case study for Birmingham, UK". In: *International Journal of Health Geographics* vol. 10.1, p. 42.

Ton, Danique et al. (2017). "How do people cycle in Amsterdam, Netherlands?: Estimating cyclists route choice determinants with GPS data from an urban area". In: *Transportation Research Record* vol. 2662.1, pp. 75–82.

Tonne, C et al. (2008). "Air pollution and mortality benefits of the London Congestion Charge: spatial and socioeconomic inequalities". In: *Occupational and Environmental Medicine* vol. 65.9, pp. 620–627.

Tormoehlen, L.M., K.J. Tekulve, and K.A. Nañagas (2014). "Hydrocarbon toxicity: A review". In: *Clinical Toxicology* vol. 52.5, pp. 479–489.

Torok, Simon J et al. (2001). "Urban heat island features of southeast Australian towns". In: *Australian Meteorological Magazine* vol. 50.1, pp. 1–13.

Tran, Hung et al. (2006). "Assessment with satellite data of the urban heat island effects in Asian mega cities". In: *International Journal of Applied Earth Observation and Geoinformation* vol. 8.1, pp. 34–48.

Trangmar, B.B., R.S. Yost, and G. Uehara (1986). "Application of geostatistics to spatial studies of soil properties". In: ed. by N.C. Brady. Vol. 38. Advances in agronomy. Academic Press, pp. 45–94.

Trlica, A. et al. (2017). "Albedo, land cover, and daytime surface temperature variation across an urbanized landscape". In: *Earth's Future* vol. 5.11, pp. 1084–1101.

Tsan, M. (2006). "Oxygen toxicity". In: *Encyclopedia of respiratory medicine*. Ed. by Geoffrey J. Laurent and Steven D. Shapiro. Oxford: Academic Press, pp. 282–289.

Tschoeke, Helmut et al. (2010). "Diesel engine exhaust emissions". In: *Handbook of diesel engines*. Ed. by Klaus Mollenhauer and Helmut Tschöke. Berlin, Heidelberg: Springer Berlin Heidelberg, pp. 417–485.

Tseng, Chong-Yu et al. (2016). "Characteristics of atmospheric $PM_{2.5}$ in a densely populated city with multi-emission sources". In: *Aerosol and Air Quality Research* vol. 16.9, pp. 2145–2158.

Tu, Jun et al. (2007). "Impact of urban sprawl on water quality in Eastern Massachusetts, USA". In: *Environmental Management* vol. 40.2, pp. 183–200.

Turner, Barry (2003). *The Statesman's yearbook 2004: The politics, cultures and economies of the world*. Springer.

Tzavali, Anna et al. (2015). "Urban heat island intensity: A literature review". In: *Fresenius Environmental Bulletin* vol. 24.12b, pp. 4537–4554.

U.S. EPA (1999). *Technical bulletin: Nitrogen oxides (NO_x), why and how they are controlled*. Tech. rep. Accessed June 28, 2022. U.S. EPA. URL: https://nepis.epa.gov/Exe/ZyNET.exe/000037B0.TXT?ZyActionD=ZyDocument&Client=EPA&Index=1995+Thru+1999&Docs=&Query=&Time=&EndTime=&SearchMethod=1&TocRestrict=n&Toc=&TocEntry=&QField=&QFieldYear=&QFieldMonth=&QFieldDay=&IntQFieldOp=0&ExtQFieldOp=0&XmlQuery=&File=D%3A%5Czyfiles%5CIndex%20Data%5C95thru99%5CTxt%5C00000013%5C000037B0.txt&User=ANONYMOUS&Password=anonymous&SortMethod=h%7C-&MaximumDocuments=1&FuzzyDegree=0&ImageQuality=r75g8/r75g8/x150y150g16/i425&Display=hpfr&DefSeekPage=x&SearchBack=ZyActionL&Back=ZyActionS&BackDesc=Results%20page&MaximumPages=1&ZyEntry=1&SeekPage=x&ZyPURL.

— (2022a). *Basic information of air emissions factors and quantification*. Accessed 9 March, 2023. URL: https://www.epa.gov/air-emissions-factors-and-quantification/basic-information-air-emissions-factors-and-quantification.

— (2022b). *Managing air quality - Emissions inventories*. Accessed 21 August, 2022. URL: https://www.epa.gov/air-quality-management-process/managing-air-quality-emissions-inventories#:~:text=An%20emissions%20inventory%20is%20a,year%20or%20other%20time%20period.

— (2023). *Heat island effect*. Accessed April 1, 2023. URL: https://www.epa.gov/heatislands.

U.S. National University Library (2023). *One-way ANOVA*. https://resources.nu.edu/statsresources/One-WayANOVA. Accessed April 4, 2023.

UN (2013). *World population prospects- Volume I: Comprehensive tables (2015 revision)*. https://population.un.org/wpp/Publications/Files/WPP2015_Volume-I_Comprehensive-Tables.pdf. Accessed October 28, 2019.

UNEP (2004). *Impacts of summer 2003 heat wave in Europe*. Tech. rep. Accessed June 28, 2022. UNEP. URL: https://www.unisdr.org/files/1145_ewheatwave.en.pdf.

Unger, János et al. (2000). "Urban heat island development affected by urban surface factors". In: *IDJÁRÁS/Quarterly Journal of the Hungarian Meteorological Service* vol. 104, pp. 253–268.

University of Bremen (2018). *Tropospheric NO2 from SCIAMACHY measurements*. Accessed March 17, 2023. URL: https://www.iup.uni-bremen.de/doas/no2_tropos_from_scia.htm.

Upadhyay, Abhishek et al. (2014). "Development of a fuzzy pattern recognition model for air quality assessment of Howrah City". In: *Aerosol and Air Quality Research* vol. 14.6, pp. 1639–1652.

Urban, Ale, Hana Davídkovová, and Jan Kyselý (2014). "Heat- and cold-stress effects on cardiovascular mortality and morbidity among urban and rural populations in the Czech Republic". In: *International Journal of Biometeorology* vol. 58.6, pp. 1057–1068.

US Census Bureau (2020). *Indianapolis city (balance), Indiana*. https://www.census.gov/quickfacts/indianapoliscitybalanceindiana. Accessed March 25, 2023.

Valin, L.C., A.R. Russell, and R.C. Cohen (2013). "Variations of OH radical in an urban plume inferred from NO_2 column measurements". In: *Geophysical Research Letters* vol. 40.9, pp. 1856–1860.

Van Der Zee, Saskia C. et al. (1998). "Characterization of particulate air pollution in urban and non-urban areas in the Netherlands". In: *Atmospheric Environment* vol. 32.21, pp. 3717–3729.

Van Hove, LWA et al. (2011). *Exploring the urban heat island intensity of Dutch cities: Assessment based on a literature review, recent meteorological observation and datasets provide by hobby meteorologists*. Tech. rep. Alterra.

Vandaele, A.C. et al. (2015). *Measurement of absorption cross sections and spectroscopic molecular parameters*. Accessed June 27, 2022. URL: http://spectrolab.aeronomie.be/no2.htm.

Verbavatz, Vincent and Marc Barthelemy (2019). "Critical factors for mitigating car traffic in cities". In: *PLOS ONE* vol. 14.7, pp. 1–16.

Vienneau, Danielle et al. (2013). "Western European land use regression incorporating satellite- and ground-based measurements of NO_2 and PM_{10}". In: *Environmental Science & Technology* vol. 47.23, pp. 13555–13564.

Vinken, G. C. M. et al. (2014). "Constraints on ship NO_x emissions in Europe using GEOS-Chem and OMI satellite NO_2 observations". In: *Atmospheric Chemistry and Physics* vol. 14.3, pp. 1353–1369.

Vintar Mally, Katja and Matej Ogrin (2015). "Spatial variations in nitrogen dioxide concentrations in urban Ljubljana, Slovenia". In: *Moravian Geographical Reports* vol. 23.3, pp. 27–35.

Vizcaino, Pilar and Carlo Lavalle (2018). "Development of European NO_2 land use regression model for present and future exposure assessment: Implications for policy analysis". In: *Environmental Pollution* vol. 240, pp. 140–154.

Voogt, James (2007). "How researchers measure urban heat islands". In: *United States Environmental Protection Agency (EPA), State and Local Climate and Energy Program, Heat Island Effect, Urban Heat Island Webcasts and Conference Calls*.

Vujovic, Svetlana et al. (2021). "Urban heat island: Causes, consequences, and mitigation measures with emphasis on reflective and permeable pavements". In: *CivilEng* vol. 2.2, pp. 459–484.

Vyskocil, Adolf, Claude Viau, and Serge Lamy (1998). "Peroxyacetyl nitrate: Review of toxicity". In: *Human & Experimental Toxicology* vol. 17.4, pp. 212–220.

Walker, Sara Louise (2011). "Building mounted wind turbines and their suitability for the urban scaleA review of methods of estimating urban wind resource". In: *Energy and Buildings* vol. 43.8, pp. 1852–1862.

Wallace, Julie and Pavlos Kanaroglou (2009). "The sensitivity of OMI-derived nitrogen dioxide to boundary layer temperature inversions". In: *Atmospheric Environment* vol. 43.22, pp. 3596–3604.

Wang, Chunjiao et al. (2020a). "Comparison and validation of TROPOMI and OMI NO_2 observations over China". In: *Atmosphere* vol. 11.6.

Wang, Fahui and Yixing Zhou (1999). "Modelling urban population densities in Beijing 1982-90: Suburbanisation and its causes". In: *Urban Studies* vol. 36.2, pp. 271–287.

Wang, Fang et al. (2018). "Evolution of the commercial blocks in ancient Beijing city from the street network perspective". In: *Journal of Geographical Sciences* vol. 28.6, pp. 845–868.

Wang, Jifeng, Huapu Lu, and Hu Peng (2008). "System dynamics model of urban transportation system and its application". In: *Journal of Transportation Systems Engineering and Information Technology* vol. 8.3, pp. 83–89.

Wang, Juan et al. (2015). "Spatiotemporal variation in surface urban heat island intensity and associated determinants across major Chinese cities". In: *Remote Sensing* vol. 7.4, pp. 3670–3689.

Wang, Juan et al. (2016). "Response of urban heat island to future urban expansion over the Beijing-Tianjin-Hebei metropolitan area". In: *Applied Geography* vol. 70, pp. 26–36.

Wang, Meng et al. (2014). "Performance of multi-city land use regression models for nitrogen dioxide and fine particles". In: *Environmental Health Perspectives* vol. 122.8, pp. 843–849.

Wang, Y., Daniel J. Jacob, and Jennifer A. Logan (1998). "Global simulation of tropospheric O_3-NO_x-hydrocarbon chemistry: 3. Origin of tropospheric ozone and effects of nonmethane hydrocarbons". In: *Journal of Geophysical Research: Atmospheres* vol. 103.D9, pp. 10757–10767.

Wang, Y. et al. (2020b). "Evaluation of the CAMS global atmospheric trace gas reanalysis 2003–2016 using aircraft campaign observations". In: *Atmospheric Chemistry and Physics* vol. 20.7, pp. 4493–4521.

Wang, Yuzhou et al. (2020c). "Spatial decomposition analysis of NO_2 and $PM_{2.5}$ air pollution in the United States". In: *Atmospheric Environment* vol. 241, p. 117470.

Wania, Annett et al. (2014). "Mapping recent built-up area changes in the city of Harare with high resolution satellite imagery". In: *Applied Geography* vol. 46, pp. 35–44.

Ward, Kathrin et al. (2016). "Heat waves and urban heat islands in Europe: A review of relevant drivers". In: *Science of the Total Environment* vol. 569-570, pp. 527–539.

Webb, J. and T.H. Misselbrook (2004). "A mass-flow model of ammonia emissions from UK livestock production". In: *Atmospheric Environment* vol. 38.14, pp. 2163–2176.

Wei, Peng et al. (2011). "Environmental process and convergence belt of atmospheric NO2 pollution in North China". In: *Acta Meteorologica Sinica* vol. 25.6, pp. 797–811.

Weng, Qihao and Shihong Yang (2004). "Managing the adverse thermal effects of urban development in a densely populated Chinese city". In: *Journal of Environmental Management* vol. 70.2, pp. 145–156.

Wheeler, Amanda J. et al. (2008). "Intra-urban variability of air pollution in Windsor, Ontario - Measurement and modeling for human exposure assessment". In: *Environmental Research* vol. 106.1, pp. 7–16.

WHO (1977). *Environmental health criteria 4 oxide of nitrogen*. Tech. rep. Accessed June 28, 2022. WHO. URL: https://apps.who.int/iris/bitstream/handle/10665/39555/9241540648-eng.pdf.

— (2000). *Air quality guidelines for Europe - Second edition*. WHO.

— (2005). *Air quality guidelines: Global update 2005: Particulate matter, ozone, nitrogen dioxide, and sulfur dioxide*. WHO.

— (2021). *WHO global air quality guidelines: Particulate matter ($PM_{2.5}$ and PM_{10}), ozone, nitrogen dioxide, sulfur dioxide and carbon monoxide*. WHO.

— (2022). *Ambient (outdoor) air pollution*. Accessed 3 October, 2022. URL: https://www.who.int/news-room/fact-sheets/detail/ambient-(outdoor)-air-quality-and-health.

— (2023). *Air pollution - Impact*. Accessed mARCH 4, 2023. URL: https://www.who.int/health-topics/air-pollution#tab=tab_2.

Wilson, A. G. (1970). *Entropy in urban and regional modelling*. London: Pion.

Wilson, Will (2011). *Constructed climates: A primer on urban environments*. University of Chicago Press.

Winter, Joost C. F. de, Amir A. Zadpoor, and Dimitra Dodou (2014). "The expansion of Google Scholar versus Web of Science: A longitudinal study". In: *Scientometrics* vol. 98.2, pp. 1547–1565.

Wolters, Dirk and Theo Brandsma (2012). "Estimating the urban heat island in residential areas in the Netherlands using observations by weather amateurs". In: *Journal of Applied Meteorology and Climatology* vol. 51.4, pp. 711–721.

Wong, Kaufui V., Andrew Paddon, and Alfredo Jimenez (2013). "Review of world urban heat islands: many linked to increased mortality". In: *Journal of Energy Resources Technology* vol. 135.2.

Wong, Man Sing and Janet E. Nichol (2013). "Spatial variability of frontal area index and its relationship with urban heat island intensity". In: *International Journal of Remote Sensing* vol. 34.3, pp. 885–896.

Wong, Man Sing et al. (2010a). "A simple method for designation of urban ventilation corridors and its application to urban heat island analysis". In: *Building and Environment* vol. 45.8, pp. 1880–1889.

Wong, MS, A Shaker, and KH Lee (2010b). "Integrating biophysical and socioeconomic data to support land surface temperature analysis: An example in Hong Kong". In: *International Journal of Geoinformatics* vol. 6.1, pp. 1–10.

World Bank (2020). *Analysis of heat waves and urban heat island effects in central European cities and implications for urban planning*. Tech. rep. Accessed June 28, 2022. World Bank. URL: https://openknowledge.worldbank.org/bitstream/handle/10986/34335/Analysis-of-Heat-Waves-and-Urban-Heat-Island-Effects-in-Central-European-Cities-and-Implications-for-Urban-Planning.pdf?sequence=1&isAllowed=y.

Xian, George, Mike Crane, and Junshan Su (2007). "An analysis of urban development and its environmental impact on the Tampa Bay watershed". In: *Journal of Environmental Management* vol. 85.4, pp. 965–976.

Xiao, Rongbo et al. (2002). "Detecting and analyzing urban heat island patterns in Beijing, China". In: *Research Center for Eco-Environmental Sciences. Chinese Acad. Sci., Beijing* vol. 100085.

Xiao, Rongbo et al. (2008). "Land surface temperature variation and major factors in Beijing, China". In: *Photogrammetric Engineering & Remote Sensing* vol. 74.4, pp. 451–461.

Xie, Yichun and Frank J. Costa (1993). "Urban planning in socialist China: Theory and practice". In: *Cities* vol. 10.2, pp. 103–114.

Xu, Jianhui et al. (2021). "Estimating the spatial and temporal variability of the ground-level NO_2 concentration in China during 2005-2019 based on satellite remote sensing". In: *Atmospheric Pollution Research* vol. 12.2, pp. 57–67.

Xu, Lixia et al. (2017). "An ecological study of the association between area-level green space and adult mortality in Hong Kong". In: *Climate* vol. 5.3.

Xu, Meimei et al. (2019). "Local variation of $PM_{2.5}$ and NO_2 concentrations within metropolitan Beijing". In: *Atmospheric Environment* vol. 200, pp. 254–263.

Yalcin, Tolga and Omer Yetemen (2009). "Local warming of groundwaters caused by the urban heat island effect in Istanbul, Turkey". In: *Hydrogeology Journal* vol. 17.5, pp. 1247–1255.

Yamagata, Yoshiki and Hajime Seya (2013). "Simulating a future smart city: An integrated land use-energy model". In: *Applied Energy* vol. 112, pp. 1466–1474.

Yamashita, Shuji and Kiyoshi Sekine (1990). "Some studies on the earth's surface conditions relating to the urban heat island". In: *Energy and Buildings* vol. 15.1, pp. 279–288.

Yan, Zhaogui et al. (2019). "Impervious surface area is a key predictor for urban plant diversity in a city undergone rapid urbanization". In: *Science of the Total Environment* vol. 650, pp. 335–342.

Yandle, Bruce, Maya Vijayaraghavan, and Madhusudan Bhattarai (2014). *The environmental Kuznets curve: A primer*. Tech. rep. Accessed March 12, 2023. Property and Environment Research Center. URL: https://www.perc.org/2002/12/01/the-environmental-kuznets-curve/.

Yang, Jiachuan, Zhi-Hua Wang, and Kamil E Kaloush (2015). "Environmental impacts of reflective materials: Is high albedo a silver bullet for mitigating urban heat island?" In: *Renewable and Sustainable Energy Reviews* vol. 47, pp. 830–843.

Yang, Li et al. (2016). "Research on urban heat-island effect". In: *Procedia Engineering* vol. 169, pp. 11–18.

Yang, Ping, Guoyu Ren, and Wei Hou (2019). "Impact of daytime precipitation duration on urban heat island intensity over Beijing city". In: *Urban Climate* vol. 28, p. 100463.

Yang, Wangming, Bing Chen, and Xuefeng Cui (2014). "High-resolution mapping of anthropogenic heat in China from 1992 to 2010". In: *International journal of environmental research and public health* vol. 11.4, pp. 4066–4077.

Yang, Bo-Yi et al. (2018). "Overweight modifies the association between long-term ambient air pollution and prehypertension in Chinese adults: The 33 communities Chinese health study". In: *Environmental Health : A Global Access Science Source* vol. 17.1, p. 57.

Yeh, Anthony Gar-On and Xueqiang Xu (1984). "Provincial variation of urbanization and urban primacy in China". In: *The Annals of Regional Science* vol. 18.3, pp. 1–20.

Yokobori, Takuya and Shunji Ohta (2009). "Effect of land cover on air temperatures involved in the development of an intra-urban heat island". In: *Climate Research* vol. 39.1, pp. 61–73.

Young, S. Stanley and Warren B. Kindzierski (2019). "Evaluation of a meta-analysis of air quality and heart attacks, a case study". In: *Critical Reviews in Toxicology* vol. 49.1, pp. 85–94.

Yu, K.N et al. (2004). "Identifying the impact of large urban airports on local air quality by nonparametric regression". In: *Atmospheric Environment* vol. 38.27, pp. 4501–4507.

Yu, Shaocai et al. (2006). "New unbiased symmetric metrics for evaluation of air quality models". In: *Atmospheric Science Letters* vol. 7.1, pp. 26–34.

Yu, Tsann-Wang and Norman K. Wagner (1975). "Numerical study of the nocturnal urban boundary layer". In: *Boundary-Layer Meteorology* vol. 9.2, pp. 143–162.

Yue, Wenze et al. (2012). "Assessing spatial pattern of urban thermal environment in Shanghai, China". In: *Stochastic Environmental Research and Risk Assessment* vol. 26.7, pp. 899–911.

Zander, Kerstin K et al. (2018). "Perceived heat stress increases with population density in urban Philippines". In: *Environmental Research Letters* vol. 13.8, p. 084009.

Zee, S van der et al. (1999). "Acute effects of urban air pollution on respiratory health of children with and without chronic respiratory symptoms." In: *Occupational and Environmental Medicine* vol. 56.12, pp. 802–812.

Zeileis, Achim et al. (2021). *Package sandwich*. Accessed June 27, 2022. URL: https://cran.r-project.org/web/packages/sandwich/sandwich.pdf.

Zeka, A., A. Zanobetti, and J. Schwartz (2005). "Short term effects of particulate matter on cause specific mortality: Effects of lags and modification by city characteristics". In: *Occupational and Environmental Medicine* vol. 62.10, pp. 718–725.

Zhang, Hao et al. (2013). "Analysis of land use/land cover change, population shift, and their effects on spatiotemporal patterns of urban heat islands in metropolitan Shanghai, China". In: *Applied Geography* vol. 44, pp. 121–133.

Zhang, Jinqu and Yunpeng Wang (2008). "Study of the relationships between the spatial extent of surface urban heat islands and urban characteristic factors based on Landsat ETM+ data". In: *Sensors* vol. 8.11, pp. 7453–7468.

Zhang, Kaixuan et al. (2010a). "Temporal and spatial characteristics of the urban heat island during rapid urbanization in Shanghai, China". In: *Environmental Monitoring and Assessment* vol. 169.1, pp. 101–112.

Zhang, Lina et al. (2021a). "A satellite-based land use regression model of ambient NO_2 with high spatial resolution in a Chinese city". In: *Remote Sensing* vol. 13.3.

Zhang, Da-Lin et al. (2011a). "Impact of upstream urbanization on the urban heat island effects along the Washington - Baltimore Corridor". In: *Journal of Applied Meteorology and Climatology* vol. 50.10, pp. 2012–2029.

Zhang, Ning, Lianfang Zhu, and Yan Zhu (2011b). "Urban heat island and boundary layer structures under hot weather synoptic conditions: A case study of Suzhou City, China". In: *Advances in Atmospheric Sciences* vol. 28.4, p. 855.

Zhang, Ping et al. (2010b). "Characterizing urban heat islands of global settlements using MODIS and nighttime lights products". In: *Canadian Journal of Remote Sensing* vol. 36.3, pp. 185–196.

Zhang, Xinmin, Ronald C. Estoque, and Yuji Murayama (2017). "An urban heat island study in Nanchang City, China based on land surface temperature and social-ecological variables". In: *Sustainable Cities and Society* vol. 32, pp. 557–568.

Zhang, Xueying et al. (2021b). "A hybrid approach to predict daily NO_2 concentrations at city block scale". In: *Science of the Total Environment* vol. 761, p. 143279.

Zhang, Yajuan et al. (2012). "The spatial characteristics of ambient particulate matter and daily mortality in the urban area of Beijing, China". In: *Science of the Total Environment* vol. 435-436, pp. 14–20.

Zhang, Ying and Lixin Sun (2019). "Spatial-temporal impacts of urban land use land cover on land surface temperature: Case studies of two Canadian urban areas". In: *International Journal of Applied Earth Observation and Geoinformation* vol. 75, pp. 171–181.

Zhang, Yongping and Zhifu Mi (2018). "Environmental benefits of bike sharing: A big data-based analysis". In: *Applied Energy* vol. 220, pp. 296–301.

Zhao, Hongbo, Zhibin Ren, and Juntao Tan (2018a). "The spatial patterns of land surface temperature and its impact factors: Spatial non-stationarity and scale effects based on a geographically-weighted regression model". In: *Sustainability* vol. 10.7.

Zhao, Jian-Liang et al. (2013). "Evaluation of triclosan and triclocarban at river basin scale using monitoring and modeling tools: Implications for controlling of urban domestic sewage discharge". In: *Water Research* vol. 47.1, pp. 395–405.

Zhao, Lei et al. (2014). "Strong contributions of local background climate to urban heat islands". In: *Nature* vol. 511, pp. 216–219.

Zhao, Shuang et al. (2018b). "Temporal dynamics of SO_2 and NO_X pollution and contributions of driving forces in urban areas in China". In: *Environmental Pollution* vol. 242, pp. 239–248.

Zhao, X. et al. (2020). "Assessment of the quality of TROPOMI high-spatial-resolution NO_2 data products in the Greater Toronto Area". In: *Atmospheric Measurement Techniques* vol. 13.4, pp. 2131–2159.

Zhao, Y. et al. (2015). "Advantages of a city-scale emission inventory for urban air quality research and policy: The case of Nanjing, a typical industrial city in the Yangtze River Delta, China". In: *Atmospheric Chemistry and Physics* vol. 15.21, pp. 12623–12644.

Zhou, Anhua and Jun Li (2021). "Analysis of the spatial effect of outward foreign direct investment on air pollution: Evidence from China". In: *Environmental Science and Pollution Research* vol. 28.37, pp. 50983–51002.

Zhou, B., D. Rybski, and J. P. Kropp (2013). "On the statistics of urban heat island intensity". In: *Geophysical Research Letters* vol. 40.20, pp. 5486–5491.

Zhou, Bin, Diego Rybski, and Jürgen P. Kropp (2017). "The role of city size and urban form in the surface urban heat island". In: *Scientific Reports* vol. 7.1, p. 4791.

Zhou, Decheng et al. (2015). "The footprint of urban heat island effect in China". In: *Scientific Reports* vol. 5, p. 11160.

Zhou, Decheng et al. (2018). "Remote sensing of the urban heat island effect in a highly populated urban agglomeration area in East China". In: *Science of the Total Environment* vol. 628-629, pp. 415–429.

Zhou, Ying and Jonathan I. Levy (2008). "The impact of urban street canyons on population exposure to traffic-related primary pollutants". In: *Atmospheric Environment* vol. 42.13, pp. 3087–3098.

Zhou, Yixing and Laurence J.C. Ma (2000). "Economic restructuring and suburbanization in China". In: *Urban Geography* vol. 21.3, pp. 205–236.

Zhu, Ke et al. (2010). "The geothermal potential of urban heat islands". In: *Environmental Research Letters* vol. 5.4, p. 044002.

Zhu, Wen-Xing and Li-Dong Zhang (2012). "Friction coefficient and radius of curvature effects upon traffic flow on a curved Road". In: *Physica A: Statistical Mechanics and its Applications* vol. 391.20, pp. 4597–4605.

Zhu, Xiaoliang et al. (2017). "An idealized LES study of urban modification of moist convection". In: *Quarterly Journal of the Royal Meteorological Society* vol. 143.709, pp. 3228–3243.

Zhu, Xinyue et al. (2014). "The role of rapid urbanization in surface warming over Eastern China". In: *International Journal of Remote Sensing* vol. 35.24, pp. 8295–8308.

Zhu, Xiudi et al. (2019). "Impact of urbanization on hourly precipitation in Beijing, China: Spatiotemporal patterns and causes". In: *Global and Planetary Change* vol. 172, pp. 307–324.

Zou, Bin et al. (2009). "Spatially differentiated and source-specific population exposure to ambient urban air pollution". In: *Atmospheric Environment* vol. 43.26, pp. 3981–3988.

Appendices

A Literature identification in Scopus and Google Scholar

A.1 Search term for finding UHI studies in Scopus

TITLE (("city size" OR "urban size" OR "population size" OR "population density") AND (urban OR city) AND ("urban heat island" OR UHI)) OR ABS (("city size" OR "urban size" OR "population size" OR "population density") AND (urban OR city) AND ("urban heat island" OR UHI)) OR KEY (("city size" OR "urban size" OR "population size" OR "population density") AND (urban OR city) AND ("urban heat island" OR UHI)) AND (LIMIT-TO (SRCTYPE , "j")) AND (LIMIT-TO (DOCTYPE , "ar")) AND (LIMIT-TO (LANGUAGE , "English"))

A.2 Search term for finding UHI studies in Google Scholar

(city size OR urban size OR population size OR population density) AND (urban OR city) AND (urban heat island OR UHI)

A.3 Search term for finding NO_2 studies in Scopus

TITLE (("city size" OR "urban size" OR "population size" OR "population density") AND (urban OR city) AND ("nitrogen dioxide" OR no2 OR nox)) OR ABS (("city size" OR "urban size" OR "population size" OR "population density") AND (urban OR city) AND ("nitrogen dioxide" OR no2 OR nox)) OR KEY (("city size" OR "urban size" OR "population size" OR "population density") AND (urban OR city) AND ("nitrogen dioxide" OR no2 OR nox)) AND (LIMIT-TO (SRCTYPE , "j")) AND (LIMIT-TO (DOCTYPE , "ar")) AND (LIMIT-TO (LANGUAGE , "English"))

A.4 Search term for finding NO_2 studies in Google Scholar

(city size OR urban size OR population size OR population density) AND (urban OR city) AND (nitrogen dioxide OR no2 OR nox)

B Excluded records in screening [1]

B.1 Excluded UHI records for the 1st criterion

Aflaki, Ardalan et al. (2017). "Urban heat island mitigation strategies: A state-of-the-art review on Kuala Lumpur, Singapore and Hong Kong". In: *Cities* vol. 62, pp. 131–145.

Alcoforado, Maria João and Henrique Andrade (2008). "Global warming and the urban heat island". In: *Urban ecology: An international perspective on the interaction between humans and nature*. Ed. by John M. Marzluff et al. Boston, MA: Springer US, pp. 249–262.

Blazejczyk, Krzysztof, Monika Bakowska, and Miroslaw Wieclaw (2006). "Urban heat island in large and small cities". In: *6th International Conference on Urban Climate, Göteborg, Sweden, June 12-16*. Vol. 2006, pp. 94–797.

Che Ani, Adi Irfan et al. (2009). "Mitigating the urban heat island effect: Some points without altering existing city planning". In: *European Journal of Scientific Research* vol. 35.2, pp. 204–216.

Echevarría Icaza, Leyre and Franklin Van der Hoeven (2017). "Regionalist principles to reduce the urban heat island effect". In: *Sustainability* vol. 9.5.

Endlicher, Wilfried et al. (2008). "Heat waves, urban climate and human health". In: *Urban ecology: An international perspective on the interaction between humans and nature*. Ed. by John M. Marzluff et al. Boston, MA: Springer US, pp. 269–278.

Fujibe, Fumiaki (2011). "Urban warming in Japanese cities and its relation to climate change monitoring". In: *International Journal of Climatology* vol. 31.2, pp. 162–173.

[1] Excluded records or articles may be excluded based on more than 1 criterion, the same below.

Gallo, K.P. et al. (1995). "Assessment of urban heat islands: A satellite perspective". In: *Atmospheric Research* vol. 37.1, pp. 37–43.

Goggins, Gary Daniel (2009). *Impacts of city size and vegetation coverage on the urban heat island using Landsat satellite imagery*. Mississippi State University.

Gunawardena, K.R., M.J. Wells, and T. Kershaw (2017). "Utilising green and bluespace to mitigate urban heat island intensity". In: *Science of the Total Environment* vol. 584-585, pp. 1040–1055.

He, Bao-Jie (2018). "Potentials of meteorological characteristics and synoptic conditions to mitigate urban heat island effects". In: *Urban Climate* vol. 24, pp. 26–33.

Heaviside, Clare, Helen Macintyre, and Sotiris Vardoulakis (2017). "The urban heat island: Implications for health in a changing environment". In: *Current Environmental Health Reports* vol. 4.3, pp. 296–305.

Heisler, Gordon M and Anthony J Brazel (2010). "The urban physical environment: Temperature and urban heat islands". In: *Urban ecosystem ecology agronomy monograph 55*. Ed. by Jacqueline Aitkenhead-Peterson and Astrid Volder. American Society of Agronomy, Crop Science Society of America, Soil Science Society of America. Chap. 2, pp. 29–56.

Jin, Mengun and J. Marshall Shepherd (2005). "Inclusion of urban landscape in a climate model: How can satellite data help?" In: *Bulletin of the American Meteorological Society* vol. 86.5, pp. 681–690.

Lee, Yee-Yong et al. (2017). "Overview of urban heat island (UHI) phenomenon towards human thermal comfort". In: *Environmental Engineering & Management Journal (EEMJ)* vol. 16.9.

Lin, Wen-Zer et al. (2005). "The subtropical urban heat island effect revealed in eight major cities of Taiwan". In: *WSEAS Transactions on Environment and Development* vol. 1.2, pp. 14–20.

McPherson, E Gregory (1994). "Cooling urban heat islands with sustainable landscapes". In: *The ecological city: Preserving and restoring urban biodiversity*. Ed. by Rutherford H. Platt, Rowan A. Rowntree, and Pamela C. Muick. Amherst, MA: University of Massachusetts Press, pp. 151–171.

Nakagawa, Kiyotaka (1996). "Recent trends of urban climatological studies in Japan, with special emphasis on the thermal environments of urban areas". In: *Geographical review of Japan, Series B* vol. 69.2, pp. 206–224.

Oke, T. R. (2011). "Urban heat island". In: *Handbook of urban ecology*. Ed. by Ian Douglas et al. Taylor and Francis. Chap. 11, pp. 120–131.

Park, Hye-Sook (1987). "City size and urban heat island intensity for Japanese and Korean cities". In: *Geographical Review of Japa,. Ser. A, Chirigaku Hyoron* vol. 60.4, pp. 238–250.

Pickett, S.T.A. et al. (2001). "Urban ecological systems: Linking terrestrial ecological, physical, and socioeconomic components of metropolitan areas". In: *Annual Review of Ecology and Systematics* vol. 32.1, pp. 127–157.

Rizwan, Ahmed Memon, Leung Y.C. Dennis, and Chunho Liu (2008). "A review on the generation, determination and mitigation of urban heat island". In: *Journal of Environmental Sciences* vol. 20.1, pp. 120–128.

Santamouris, M. (2015). "Analyzing the heat island magnitude and characteristics in one hundred Asian and Australian cities and regions". In: *Science of the Total Environment* vol. 512-513, pp. 582–598.

Schwarz, Nina (2012). "Comment on "Surface urban heat island across 419 global big cities"". In: *Environmental Science & Technology* vol. 46.12, pp. 6888–6888.

Shahmohamadi, P. et al. (2010). "Reducing urban heat island effects: A systematic review to achieve energy consumption balance". In: *International Journal of Physical Sciences* vol. 5.6, pp. 626–636.

Stewart, Ian Douglas (2007). "Landscape representation and the urban-rural dichotomy in empirical urban heat island literature, 1950 - 2006". In: *Acta Climatologica et Chorologica* vol. 40.41, pp. 111–121.

Tzavali, Anna et al. (2015). "Urban heat island intensity: A literature review". In: *Fresenius Environmental Bulletin* vol. 24.12b, pp. 4537–4554.

Van Hove, LWA et al. (2011). *Exploring the urban heat island intensity of Dutch cities: Assessment based on a literature review, recent meteorological observation and datasets provide by hobby meteorologists*. Tech. rep. Alterra.

Voogt, James (2007). "How researchers measure urban heat islands". In: *United States Environmental Protection Agency (EPA), State and Local Climate and Energy Program, Heat Island Effect, Urban Heat Island Webcasts and Conference Calls*.

Wilson, Will (2011). *Constructed climates: A primer on urban environments*. University of Chicago Press.

Yamashita, Shuji and Kiyoshi Sekine (1990). "Some studies on the earth′s surface conditions relating to the urban heat island". In: *Energy and Buildings* vol. 15.1, pp. 279–288.

B.2 Excluded UHI records for the 2nd criterion

Adinna, E. N., Ifeanyi Christian Enete, and Arch. Tony Okolie (2009). "Assessment of urban heat island and possible adaptations in Enugu urban using landsat-ETM". In: *Journal of Geography and Regional Planning* vol. 2.2, pp. 30–36.

Ahmad, Shaharuddin and Noorazuan Md Hashim (2007). "Effects of soil moisture on urban heat island occurrences: Case of Selangor, Malaysia". In: *Humanity & Social Sciences Journal* vol. 2.2, pp. 132–138.

Ahmad, Sohail, Giovanni Baiocchi, and Felix Creutzig (2015). "CO_2 emissions from direct energy use of urban households in India". In: *Environmental Science & Technology* vol. 49.19, pp. 11312–11320.

Allen, Alistair, Dejan Milenic, and Paul Sikora (2003). "Shallow gravel aquifers and the urban 'heat island' effect: A source of low enthalpy geothermal energy". In: *Geothermics* vol. 32.4, pp. 569–578.

Allen, L., F. Lindberg, and C.S.B. Grimmond (2011). "Global to city scale urban anthropogenic heat flux: Model and variability". In: *International Journal of Climatology* vol. 31.13, pp. 1990–2005.

Alonso, M. S., J. L. Labajo, and M. R. Fidalgo (2003). "Characteristics of the urban heat island in the city of Salamanca, Spain". In: *Atmósfera* vol. 16, pp. 137–148.

Araujo, Ricardo Vieira et al. (2015). "São Paulo urban heat islands have a higher incidence of dengue than other urban areas". In: *The Brazilian Journal of Infectious Diseases* vol. 19.2, pp. 146–155.

Arifwidodo, Sigit D. and Takahiro Tanaka (2015). "The characteristics of urban heat island in Bangkok, Thailand". In: *Procedia-Social and Behavioral Sciences* vol. 195, pp. 423–428.

Arifwidodo, Sigit and Orana Chandrasiri (2015). "Urban heat island and household energy consumption in Bangkok, Thailand". In: *Energy Procedia* vol. 79, pp. 189–194.

Bechtel, Benjamin and Katharina Johanna Schmidt (2011). "Floristic mapping data as a proxy for the mean urban heat island". In: *Climate Research* vol. 49.1, pp. 45–58.

Böhm, Reinhard (1998). "Urban bias in temperature time series-A case study for the City of Vienna, Austria". In: *Climatic Change* vol. 38.1, pp. 113–128.

Bokaie, Mehdi et al. (2016). "Assessment of urban heat island based on the relationship between land surface temperature and land use/land cover in Tehran". In: *Sustainable Cities and Society* vol. 23, pp. 94–104.

Brandsma, Theo and Dirk Wolters (2012). "Measurement and statistical modeling of the urban heat island of the city of Utrecht (the Netherlands)". In: *Journal of Applied Meteorology and Climatology* vol. 51.6, pp. 1046–1060.

Cai, Guoyin, Yang Liu, and Mingyi Du (2017). "Impact of the 2008 Olympic Games on urban thermal environment in Beijing, China from satellite images". In: *Sustainable Cities and Society* vol. 32, pp. 212–225.

Camilloni, Inés and Mariana Barrucand (2012). "Temporal variability of the Buenos Aires, Argentina, urban heat island". In: *Theoretical and Applied Climatology* vol. 107.1, pp. 47–58.

Carnahan, Walter H. and Robert C. Larson (1990). "An analysis of an urban heat sink". In: *Remote Sensing of Environment* vol. 33.1, pp. 65–71.

Ceplová, Natálie, Veronika Kalusová, and Zdenka Lososová (2017). "Effects of settlement size, urban heat island and habitat type on urban plant biodiversity". In: *Landscape and Urban Planning* vol. 159, pp. 15–22.

Changnon, Stanley A. (1999). "A rare long record of deep soil temperatures defines temporal temperature changes and an urban heat island". In: *Climatic Change* vol. 42.3, pp. 531–538.

Chen, Xiao-Ling et al. (2006). "Remote sensing image-based analysis of the relationship between urban heat island and land use/cover changes". In: *Remote Sensing of Environment* vol. 104.2, pp. 133–146.

Cheval, S. and A. Dumitrescu (2009). "The July urban heat island of Bucharest as derived from MODIS images". In: *Theoretical and Applied Climatology* vol. 96.1, pp. 145–153.

Choi, Jaeyeon, Uran Chung, and Jin I. Yun (2003). "Urban-effect correction to improve accuracy of spatially interpolated temperature estimates in Korea". In: *Journal of Applied Meteorology* vol. 42.12, pp. 1711–1719.

Chow, Winston T. L. and Matthias Roth (2006). "Temporal dynamics of the urban heat island of Singapore". In: *International Journal of Climatology* vol. 26.15, pp. 2243–2260.

Chow, Winston T.L. et al. (2014). "A multi-method and multi-scale approach for estimating city-wide anthropogenic heat fluxes". In: *Atmospheric Environment* vol. 99, pp. 64–76.

Cui, Linli, Jun Shi, and Zhiqiang Gao (2007). "Urban heat island in Shanghai, China". In: *Remote Sensing and Modeling of Ecosystems for Sustainability IV*. Ed. by Wei Gao and Susan L. Ustin. Vol. 6679. International Society for Optics and Photonics. SPIE, pp. 327–335.

Cusack, Stephen (2014). "Increased tornado hazard in large metropolitan areas". In: *Atmospheric Research* vol. 149, pp. 255–262.

Dale, Adam G. and Steven D. Frank (2014). "Urban warming trumps natural enemy regulation of herbivorous pests". In: *Ecological Applications* vol. 24.7, pp. 1596–1607.

Deilami, Kaveh and Md. Kamruzzaman (2017). "Modelling the urban heat island effect of smart growth policy scenarios in Brisbane". In: *Land Use Policy* vol. 64, pp. 38–55.

Deilami, Kaveh, Md. Kamruzzaman, and John Francis Hayes (2016). "Correlation or causality between land cover patterns and the urban heat island effect? Evidence from Brisbane, Australia". In: *Remote Sensing* vol. 8.9.

Devadas, Monsingh D and AL Rose (2009). "Urban factors and the intensity of heat island in the city of Chennai". In: *The Seventh International Conference on Urban Climate*. Vol. 29.

Dixon, P. Grady and Thomas L. Mote (2003). "Patterns and causes of Atlanta's urban heat island-initiated precipitation". In: *Journal of Applied Meteorology* vol. 42.9, pp. 1273–1284.

Dong, Weihua et al. (2014). "Assessing heat health risk for sustainability in Beijing′s urban heat island". In: *Sustainability* vol. 6.10, pp. 7334–7357.

Duarte, Denise H.S. et al. (2015). "The impact of vegetation on urban microclimate to counterbalance built density in a subtropical changing climate". In: *Urban Climate* vol. 14, pp. 224–239.

Dütemeyer, Dirk et al. (2014). "Measures against heat stress in the city of Gelsenkirchen, Germany". In: *DIE ERDE Journal of the Geographical Society of Berlin* vol. 144.3-4, pp. 181–201.

Eliasson, Ingegärd (1996). "Urban nocturnal temperatures, street geometry and land use". In: *Atmospheric Environment* vol. 30.3, pp. 379–392.

Elsayed, Ilham SM (2012). "Effects of population density and land management on the intensity of urban heat islands: A case study on the city of Kuala Lumpur, Malaysia". In: *Application of geographic information systems*, pp. 267–283.

Endreny, Theodore (2008). "Naturalizing urban watershed hydrology to mitigate urban heat-island effects". In: *Hydrological Processes* vol. 22.3, pp. 461–463.

Erell, Evyatar, David Pearlmutter, and Terence Williamson (2012). *Urban microclimate: Designing the spaces between buildings*. Routledge.

Estoque, Ronald C. and Yuji Murayama (2017). "Monitoring surface urban heat island formation in a tropical mountain city using Landsat data (19872015)". In: *ISPRS Journal of Photogrammetry and Remote Sensing* vol. 133, pp. 18–29.

Ewing, Reid and Fang Rong (2008). "The impact of urban form on U.S. residential energy use". In: *Housing Policy Debate* vol. 19.1, pp. 1–30.

Fabrizi, Roberto, Stefania Bonafoni, and Riccardo Biondi (2010). "Satellite and ground-based sensors for the urban heat island analysis in the city of Rome". In: *Remote Sensing* vol. 2.5, pp. 1400–1415.

Fahy, Benjamin et al. (2019). "Spatial analysis of urban flooding and extreme heat hazard potential in Portland, OR". In: *International Journal of Disaster Risk Reduction* vol. 39, p. 101117.

Fan, Chao et al. (2017). "Understanding the impact of urbanization on surface urban heat islands-A longitudinal analysis of the oasis effect in subtropical desert cities". In: *Remote Sensing* vol. 9.7, p. 672.

Ferguson, Grant and Allan D. Woodbury (2007). "Urban heat island in the subsurface". In: *Geophysical Research Letters* vol. 34.23, p. L23713.

Fortuniak, K., K. Kysik, and J. Wibig (2006). "Urban-rural contrasts of meteorological parameters in ód". In: *Theoretical and Applied Climatology* vol. 84.1, pp. 91–101.

Founda, Dimitra and Mattheos Santamouris (2017). "Synergies between urban heat island and heat waves in Athens (Greece), during an extremely hot summer (2012)". In: *Scientific reports* vol. 7.1, pp. 10973–10973.

Gaffin, S.R. et al. (2008). "Variations in New York City′s urban heat island strength over time and space". In: *Theoretical and Applied Climatology* vol. 94.1, pp. 1–11.

Gazal, Rico et al. (2008). "GLOBE students, teachers, and scientists demonstrate variable differences between urban and rural leaf phenology". In: *Global Change Biology* vol. 14.7, pp. 1568–1580.

Gupta, Rupesh (2012). "Temporal and spatial variations of urban heat island effect in Jaipur City using satellite data". In: *Environment and Urbanization ASIA* vol. 3.2, pp. 359–374.

Hass, Alisa L. et al. (2016). "Heat and humidity in the city: Neighborhood heat index variability in a mid-sized city in the Southeastern United States". In: *International journal of environmental research and public health* vol. 13.1, p. 117.

Henry, Jamesa et al. (1989). "Comparison of satellite, ground-based, and modeling techniques for analyzing the urban heat island". In: *Photogrammetric Engineering and Remote Sensing* vol. 55.1, pp. 69–76.

Hidalgo, J., G. Pigeon, and V. Masson (2008). "Urban-breeze circulation during the CAPITOUL experiment: Observational data analysis approach". In: *Meteorology and Atmospheric Physics* vol. 102.3, pp. 223–241.

Hidalgo, Julia, Valéry Masson, and Luis Gimeno (2010). "Scaling the daytime urban heat island and urban-breeze circulation". In: *Journal of Applied Meteorology and Climatology* vol. 49.5, pp. 889–901.

Hinkel, Kenneth M. et al. (2003). "The urban heat island in winter at Barrow, Alaska". In: *International Journal of Climatology* vol. 23.15, pp. 1889–1905.

Hoch, Irving and Judith Drake (1974). "Wages, climate, and the quality of life". In: *Journal of Environmental Economics and Management* vol. 1.4, pp. 268–295.

Hoffmann, Peter, Oliver Krueger, and K. Heinke Schlünzen (2012). "A statistical model for the urban heat island and its application to a climate change scenario". In: *International Journal of Climatology* vol. 32.8, pp. 1238–1248.

Hoffmann, Peter and K. Heinke Schlünzen (2013). "Weather pattern classification to represent the urban heat island in present and future climate". In: *Journal of Applied Meteorology and Climatology* vol. 52.12, pp. 2699–2714.

Hondula, David M. and Adrian G. Barnett (2014). "Heat-related morbidity in Brisbane, Australia: Spatial variation and area-level predictors". In: *Environmental health perspectives* vol. 122.8, pp. 831–836.

Hu, Leiqiu, Olga V. Wilhelmi, and Christopher Uejio (2019a). "Assessment of heat exposure in cities: Combining the dynamics of temperature and population". In: *Science of the Total Environment* vol. 655, pp. 1–12.

Hu, Xiaofang et al. (2017). "Urban expansion and local land-cover change both significantly contribute to urban warming, but their relative importance changes over time". In: *Landscape Ecology* vol. 32.4, pp. 763–780.

Ivajni, Danijel, Mitja Kaligari, and Igor iberna (2014). "Geographically weighted regression of the urban heat island of a small city". In: *Applied Geography* vol. 53, pp. 341–353.

Jenerette, G. Darrel et al. (2007). "Regional relationships between surface temperature, vegetation, and human settlement in a rapidly urbanizing ecosystem". In: *Landscape Ecology* vol. 22.3, pp. 353–365.

Jiang, Yunfang et al. (2018). "Spatial zoning strategy of urbanization based on urban climate co-movement: A case study in Shanghai mainland area". In: *Sustainability* vol. 10.8.

Jin, Menglin, J. Marshall Shepherd, and Michael D. King (2005b). "Urban aerosols and their variations with clouds and rainfall: A case study for New York and Houston". In: *Journal of Geophysical Research: Atmospheres* vol. 110.D10, D10S20.

Johnson, Daniel P. and Jeffrey S. Wilson (2009). "The socio-spatial dynamics of extreme urban heat events: The case of heat-related deaths in Philadelphia". In: *Applied Geography* vol. 29.3, pp. 419–434.

Kammuang-Lue, Niti et al. (2015). "Influences of population, building, and traffic densities on urban heat island intensity in Chiang Mai City, Thailand". In: *Thermal Science* vol. 19.Suppl. 2, pp. 445–455.

Karaca, M., Ü. Antepliolu, and H. Karsan (1995). "Detection of urban heat island in Istanbul, Turkey". In: *Il Nuovo Cimento C* vol. 18.1, pp. 49–55.

Kasmaee, Sara and Francesco Tinti (2018). "A method to evaluate the impact of urbanization on ground temperature evolution at regional scale". In: *Rudarsko-geoloko-naftni zbornik* vol. 33.5, pp. 1–12.

Kaufmann, Robert K. et al. (2007). "Climate response to rapid urban growth: Evidence of a human-induced precipitation deficit". In: *Journal of Climate* vol. 20.10, pp. 2299–2306.

Kaya, Sinasi et al. (2012). "Assessment of urban heat islands using remotely sensed data". In: *Ekoloji* vol. 21.84, pp. 107–113.

Kershaw, Suzanne E. and Andrew A. Millward (2012). "A spatio-temporal index for heat vulnerability assessment". In: *Environmental Monitoring and Assessment* vol. 184.12, pp. 7329–7342.

Khaikine, M. N. et al. (2006). "Investigation of temporal - spatial parameters of an urban heat island on the basis of passive microwave remote sensing". In: *Theoretical and Applied Climatology* vol. 84.1, pp. 161–169.

Kifle, Bisrat (2003). "Urban heat island and its feature in Addis Ababa (a case study)". In: *Fifth International Conference on Urban Climate*, pp. 1–5.

Kim, Yeon-Hee and Jong-Jin Baik (2005). "Spatial and temporal structure of the urban heat island in Seoul". In: *Journal of Applied Meteorology* vol. 44.5, pp. 591–605.

Koch, Natália Mossmann et al. (2019). "Selecting lichen functional traits as ecological indicators of the effects of urban environment". In: *Science of the Total Environment* vol. 654, pp. 705–713.

Kopec, Richard J. (1970). "Further observations of the urban heat island in a small city". In: *Bulletin of the American Meteorological Society* vol. 51.7, pp. 602–607.

Kotak, Y et al. (2014). "Installation of roof-top solar PV modules and their impact on building cooling load". In: *Building Services Engineering Research and Technology* vol. 35.6, pp. 613–633.

Kotharkar, Rajashree and Meenal Surawar (2016). "Land use, land cover, and population density impact on the formation of canopy urban heat islands through traverse survey in the Nagpur urban area, India". In: *Journal of Urban Planning and Development* vol. 142.1, p. 04015003.

Lee, Derek O. (1992). "Urban warming? - An analysis of recent trends in London's heat island". In: *Weather* vol. 47.2, pp. 50–56.

Lee, Sang-Hyun and Jong-Jin Baik (2010). "Statistical and dynamical characteristics of the urban heat island intensity in Seoul". In: *Theoretical and Applied Climatology* vol. 100.1, pp. 227–237.

Lee, Sungwon and Bumsoo Lee (2014). "The influence of urban form on GHG emissions in the U.S. household sector". In: *Energy Policy* vol. 68, pp. 534–549.

Lemonsu, A. et al. (2015). "Vulnerability to heat waves: Impact of urban expansion scenarios on urban heat island and heat stress in Paris (France)". In: *Urban Climate* vol. 14, pp. 586–605.

Li, Jinghui et al. (2017a). "Correlations between socioeconomic drivers and indicators of urban expansion: Evidence from the heavily urbanised Shanghai Metropolitan Area, China". In: *Sustainability* vol. 9.7.

Li, Lin et al. (2014). "Impact of land cover and population density on land surface temperature: Case study in Wuhan, China". In: *Journal of Applied Remote Sensing* vol. 8.1, pp. 1–20.

Li, Weifeng et al. (2017d). "Linking potential heat source and sink to urban heat island: Heterogeneous effects of landscape pattern on land surface temperature". In: *Science of the Total Environment* vol. 586, pp. 457–465.

Li, Ying-ying, Hao Zhang, and Wolfgang Kainz (2012). "Monitoring patterns of urban heat islands of the fast-growing Shanghai metropolis, China: Using time-series of Landsat TM/ETM+ data". In: *International Journal of Applied Earth Observation and Geoinformation* vol. 19, pp. 127–138.

Lin, Pingying et al. (2017). "Effects of urban planning indicators on urban heat island: A case study of pocket parks in high-rise high-density environment". In: *Landscape and Urban Planning* vol. 168, pp. 48–60.

Liu, W. et al. (2007). "Temporal characteristics of the Beijing urban heat island". In: *Theoretical and Applied Climatology* vol. 87.1, pp. 213–221.

Long, Lawrence C., Vincent D′Amico, and Steven D. Frank (2019). "Urban forest fragments buffer trees from warming and pests". In: *Science of the Total Environment* vol. 658, pp. 1523–1530.

Loughner, Christopher P. et al. (2012). "Roles of urban tree canopy and buildings in urban heat island effects: Parameterization and preliminary results". In: *Journal of Applied Meteorology and Climatology* vol. 51.10, pp. 1775–1793.

Magee, N., J. Curtis, and G. Wendler (1999). "The urban heat island effect at Fairbanks, Alaska". In: *Theoretical and Applied Climatology* vol. 64.1, pp. 39–47.

Mallick, Javed and Atiqur Rahman (2012). "Impact of population density on the surface temperature and micro-climate of Delhi". In: *Current Science* vol. 102.12, pp. 1708–1713.

Martin, Frank P and Grace L Powell (1977). "The urban heat island in Akron, Ohio". In: *Proceedings of the Conference on Metropolitan Physical Environment*. Vol. 25, pp. 94–97.

Martinson, Holly M. and Michael J. Raupp (2013). "A meta-analysis of the effects of urbanization on ground beetle communities". In: *Ecosphere* vol. 4.5, art60.

Melhuish, Edward and Mike Pedder (1998). "Observing an urban heat island by bicycle". In: *Weather* vol. 53.4, pp. 121–128.

Memon, Rizwan Ahmed et al. (2011). "Urban heat island and its effect on the cooling and heating demands in urban and suburban areas of Hong Kong". In: *Theoretical and Applied Climatology* vol. 103.3, pp. 441–450.

Menberg, Kathrin et al. (2013a). "Long-term evolution of anthropogenic heat fluxes into a subsurface urban heat island". In: *Environmental Science & Technology* vol. 47.17, pp. 9747–9755.

Menberg, Kathrin et al. (2013b). "Subsurface urban heat islands in German cities". In: *Science of the Total Environment* vol. 442, pp. 123–133.

Meng, F. and M. Liu (2013). "Remote-sensing image-based analysis of the patterns of urban heat islands in rapidly urbanizing Jinan, China". In: *International Journal of Remote Sensing* vol. 34.24, pp. 8838–8853.

Min, Min, Hongbo Zhao, and Changhong Miao (2018). "Spatio-temporal evolution analysis of the urban heat island: A case study of Zhengzhou City, China". In: *Sustainability* vol. 10.6.

Mirzaei, Parham A. and Fariborz Haghighat (2010). "A novel approach to enhance outdoor air quality: Pedestrian ventilation system". In: *Building and Environment* vol. 45.7, pp. 1582–1593.

Mohan, Manju et al. (2012). "Urban heat island assessment for a tropical urban airshed in India". In: *Atmospheric and Climate Sciences* vol. 2.2, pp. 127–138.

Mohan, Manju et al. (2013). "Assessment of urban heat island effect for different land use-land cover from micrometeorological measurements and remote sensing data for megacity Delhi". In: *Theoretical and Applied Climatology* vol. 112.3, pp. 647–658.

Morris, C.J.G., I. Simmonds, and N. Plummer (2001). "Quantification of the influences of wind and cloud on the nocturnal urban heat island of a large city". In: *Journal of Applied Meteorology* vol. 40.2, pp. 169–182.

Nguyen, Hoa Q. et al. (2018). "Urban heat island effect on cicada densities in metropolitan Seoul". In: *PeerJ* vol. 6, e4238.

Nguyen, Hoa Quynh et al. (2019). "Characterization of polymorphic loci for two cicada species: Cryptotympana atrata and Hyalessa fuscata (Hemiptera: Cicadoidae)". In: *Molecular Biology Reports* vol. 46.2, pp. 1555–1561.

Nonomura, Atsuko, Mutsuko Kitahara, and Takuro Masuda (2009). "Impact of land use and land cover changes on the ambient temperature in a middle scale city, Takamatsu, in Southwest Japan". In: *Journal of Environmental Management* vol. 90.11, pp. 3297–3304.

Oke, T.R. (1976). "The distinction between canopy and boundary-layer urban heat islands". In: *Atmosphere* vol. 14.4, pp. 268–277.

— (1982). "The energetic basis of the urban heat island". In: *Quarterly Journal of the Royal Meteorological Society* vol. 108.455, pp. 1–24.

— (1995). "The heat island of the urban boundary layer: Characteristics, causes and effects". In: *Wind climate in cities*. Ed. by Jack E. Cermak et al. Dordrecht: Springer Netherlands, pp. 81–107.

Ongoma, Victor, John Nzioka Muthama, and Wilson Gitau (2013). "Evaluation of urbanization influences on urban temperature of Nairobi City, Kenya". In: *Global Meteorology* vol. 2.1, e1.

Pham, Thi-Thanh-Hien et al. (2013). "Predictors of the distribution of street and backyard vegetation in Montreal, Canada". In: *Urban Forestry & Urban Greening* vol. 12.1, pp. 18–27.

Qiao, Zhi et al. (2014). "Influences of urban expansion on urban heat island in Beijing during 1989 - 2010". In: *Advances in Meteorology* vol. 2014.

Quah, Anne K.L. and Matthias Roth (2012). "Diurnal and weekly variation of anthropogenic heat emissions in a tropical city, Singapore". In: *Atmospheric Environment* vol. 46, pp. 92–103.

Raciti, Steve M., Lucy R. Hutyra, and Jared D. Newell (2014). "Mapping carbon storage in urban trees with multi-source remote sensing data: Relationships between biomass, land use, and demographics in Boston neighborhoods". In: *Science of the Total Environment* vol. 500-501, pp. 72–83.

Rahman, Muhammad Tauhidur (2018). "Examining and modelling the determinants of the rising land surface temperatures in Arabian desert cities: An example from Riyadh, Saudi Arabia". In: *Journal of Settlements and Spatial Planning* vol. 9.1, pp. 1–10.

Rivera, Erika et al. (2017). "Spatiotemporal analysis of the atmospheric and surface urban heat islands of the Metropolitan Area of Toluca, Mexico". In: *Environmental Earth Sciences* vol. 76.5, p. 225.

Ruthirako, Poonyanuch, Rotchanatch Darnsawasdi, and Wichien Chatupote (2015). "Intensity and pattern of land surface temperature in Hat Yai City, Thailand". In: *Walailak Journal of Science and Technology (WJST)* vol. 12.1, pp. 83–94.

Sagris, V. and M. Sepp (2017). "Landsat-8 TIRS data for assessing urban heat island effect and its impact on human health". In: *IEEE Geoscience and Remote Sensing Letters* vol. 14.12, pp. 2385–2389.

Scalenghe, Riccardo and Franco Ajmone Marsan (2009). "The anthropogenic sealing of soils in urban areas". In: *Landscape and Urban Planning* vol. 90.1, pp. 1–10.

Schatz, Jason and Christopher J Kucharik (2015). "Urban climate effects on extreme temperatures in Madison, Wisconsin, USA". In: *Environmental Research Letters* vol. 10.9, p. 094024.

Schwarz, Nina et al. (2012). "Relationship of land surface and air temperatures and its implications for quantifying urban heat island indicators - An application for the city of Leipzig (Germany)". In: *Ecological Indicators* vol. 18, pp. 693–704.

Sheng, Li, Dengsheng Lu, and Jingfeng Huang (2015). "Impacts of land-cover types on an urban heat island in Hangzhou, China". In: *International Journal of Remote Sensing* vol. 36.6, pp. 1584–1603.

Sheng, Li et al. (2017). "Comparison of the urban heat island intensity quantified by using air temperature and Landsat land surface temperature in Hangzhou, China". In: *Ecological Indicators* vol. 72, pp. 738–746.

Shi, Bin et al. (2012). "Observation and analysis of the urban heat island effect on soil in Nanjing, China". In: *Environmental Earth Sciences* vol. 67.1, pp. 215–229.

Shrestha, Kundan Lal et al. (2009). "Numerical simulation of urban heat island using gridded urban configuration and anthropogenic heat data generated by a simplified method". In: *Proceedings of the 7th Conference on Urban Climate*.

Singh, Prafull, Noyingbeni Kikon, and Pradipika Verma (2017). "Impact of land use change and urbanization on urban heat island in Lucknow city, Central India. A remote sensing based estimate". In: *Sustainable Cities and Society* vol. 32, pp. 100–114.

Siu, Leong Wai and Melissa A. Hart (2013). "Quantifying urban heat island intensity in Hong Kong SAR, China". In: *Environmental Monitoring and Assessment* vol. 185.5, pp. 4383–4398.

Skoulika, Fotini et al. (2014). "On the thermal characteristics and the mitigation potential of a medium size urban park in Athens, Greece". In: *Landscape and Urban Planning* vol. 123, pp. 73–86.

Sobrino, José A. et al. (2013). "Evaluation of the surface urban heat island effect in the city of Madrid by thermal remote sensing". In: *International Journal of Remote Sensing* vol. 34.9-10, pp. 3177–3192.

Soltanzadeh, I et al. (2011). "Study of local winds over Tehran using WRF in ideal conditions". In: *Iranian Journal of Physics Research* vol. 11.2, pp. 199–213.

Soriano, Luis Rivas and Fernando de Pablo (2002). "Effect of small urban areas in central Spain on the enhancement of cloud-to-ground lightning activity". In: *Atmospheric Environment* vol. 36.17, pp. 2809–2816.

Stallins, J. Anthony (2004). "Characteristics of urban lightning hazards for Atlanta, Georgia". In: *Climatic Change* vol. 66.1, pp. 137–150.

Stauber, Christine et al. (2018). "Measuring the impact of environment on the health of large cities". In: *International Journal of Environmental Research and Public Health* vol. 15.6, p. 1216.

Steeneveld, G.J. et al. (2014). "Refreshing the role of open water surfaces on mitigating the maximum urban heat island effect". In: *Landscape and Urban Planning* vol. 121, pp. 92–96.

Stewart, I.D. and T.R. Oke (2012). "Local climate zones for urban temperature studies". In: *Bulletin of the American Meteorological Society* vol. 93.12, pp. 1879–1900.

Stewart, I.D. and Tim Oke (2009). "Classifying urban climate field sites by "local climate zones": The case of Nagano, Japan". In: *Seventh International Conference on Urban Climate*. Vol. 29.

Stone Jr, Brian and Michael O Rodgers (2001). "Urban form and thermal efficiency: How the design of cities influences the urban heat island effect". In: *Journal of the American Planning Association* vol. 67.2, pp. 186–198.

Stone, Brian and John M. Norman (2006). "Land use planning and surface heat island formation: A parcel-based radiation flux approach". In: *Atmospheric Environment* vol. 40.19, pp. 3561–3573.

Streutker, David R (2003a). "Satellite-measured growth of the urban heat island of Houston, Texas". In: *Remote Sensing of Environment* vol. 85.3, pp. 282–289.

Streutker, David Richard (2003b). "A study of the urban heat island of Houston, Texas". Ph.D. dissertation. Rice Univeristy.

Su, Yuan-Fong, Giles M. Foody, and Ke-Sheng Cheng (2012). "Spatial non-stationarity in the relationships between land cover and surface temperature in an urban heat island and its impacts on thermally sensitive populations". In: *Landscape and Urban Planning* vol. 107.2, pp. 172–180.

Suomi, Juuso, Jan Hjort, and Jukka Käyhkö (2012). "Effects of scale on modelling the urban heat island in Turku, SW Finland". In: *Climate Research* vol. 55.2, pp. 105–118.

Suomi, Juuso and Jukka Käyhkö (2012). "The impact of environmental factors on urban temperature variability in the coastal city of Turku, SW Finland". In: *International Journal of Climatology* vol. 32.3, pp. 451–463.

Sweeney, John (1987). "The urban heat island of Dublin City". In: *Irish Geography* vol. 20.1, pp. 1–10.

Szegedi, Sándor and Andrea Kircsi (2003). "The development of the urban heat island under various weather conditions in Debrecen, Hungary". In: *Proceedings of the Fifth International Conference on Urban Climate*.

Tan, Jianguo et al. (2010). "The urban heat island and its impact on heat waves and human health in Shanghai". In: *International Journal of Biometeorology* vol. 54.1, pp. 75–84.

Tan, Zheng, Kevin Ka-Lun Lau, and Edward Ng (2016). "Urban tree design approaches for mitigating daytime urban heat island effects in a high-density urban environment". In: *Energy and Buildings* vol. 114, pp. 265–274.

Tang, Junmei et al. (2017). "Impacts of land use and socioeconomic patterns on urban heat Island". In: *International Journal of Remote Sensing* vol. 38.11, pp. 3445–3465.

Thomas, G and EJ Zachariah (2011). "Urban heat island in a tropical city interlaced by wetlands". In: *Indian Journal of Environmental Health* vol. 5, pp. 234–240.

Tomlinson, Charlie J. et al. (2011). "Including the urban heat island in spatial heat health risk assessment strategies: A case study for Birmingham, UK". In: *International Journal of Health Geographics* vol. 10.1, p. 42.

Trlica, A. et al. (2017). "Albedo, land cover, and daytime surface temperature variation across an urbanized landscape". In: *Earth's Future* vol. 5.11, pp. 1084–1101.

Unger, János et al. (2000). "Urban heat island development affected by urban surface factors". In: *IDJÁRÁS/Quarterly Journal of the Hungarian Meteorological Service* vol. 104, pp. 253–268.

Urban, Ale, Hana Davídkovová, and Jan Kyselý (2014). "Heat- and cold-stress effects on cardiovascular mortality and morbidity among urban and rural populations in the Czech Republic". In: *International Journal of Biometeorology* vol. 58.6, pp. 1057–1068.

Weng, Qihao and Shihong Yang (2004). "Managing the adverse thermal effects of urban development in a densely populated Chinese city". In: *Journal of Environmental Management* vol. 70.2, pp. 145–156.

Wong, Man Sing and Janet E. Nichol (2013). "Spatial variability of frontal area index and its relationship with urban heat island intensity". In: *International Journal of Remote Sensing* vol. 34.3, pp. 885–896.

Wong, MS, A Shaker, and KH Lee (2010b). "Integrating biophysical and socioeconomic data to support land surface temperature analysis: An example in Hong Kong". In: *International Journal of Geoinformatics* vol. 6.1, pp. 1–10.

Xiao, Rongbo et al. (2002). "Detecting and analyzing urban heat island patterns in Beijing, China". In: *Research Center for Eco-Environmental Sciences. Chinese Acad. Sci., Beijing* vol. 100085.

Xiao, Rongbo et al. (2008). "Land surface temperature variation and major factors in Beijing, China". In: *Photogrammetric Engineering & Remote Sensing* vol. 74.4, pp. 451–461.

Xu, Lixia et al. (2017). "An ecological study of the association between area-level green space and adult mortality in Hong Kong". In: *Climate* vol. 5.3.

Yalcin, Tolga and Omer Yetemen (2009). "Local warming of groundwaters caused by the urban heat island effect in Istanbul, Turkey". In: *Hydrogeology Journal* vol. 17.5, pp. 1247–1255.

Yokobori, Takuya and Shunji Ohta (2009). "Effect of land cover on air temperatures involved in the development of an intra-urban heat island". In: *Climate Research* vol. 39.1, pp. 61–73.

Yue, Wenze et al. (2012). "Assessing spatial pattern of urban thermal environment in Shanghai, China". In: *Stochastic Environmental Research and Risk Assessment* vol. 26.7, pp. 899–911.

Zhang, Hao et al. (2013). "Analysis of land use/land cover change, population shift, and their effects on spatiotemporal patterns of urban heat islands in metropolitan Shanghai, China". In: *Applied Geography* vol. 44, pp. 121–133.

Zhang, Kaixuan et al. (2010a). "Temporal and spatial characteristics of the urban heat island during rapid urbanization in Shanghai, China". In: *Environmental Monitoring and Assessment* vol. 169.1, pp. 101–112.

Zhang, Da-Lin et al. (2011a). "Impact of upstream urbanization on the urban heat island effects along the Washington - Baltimore Corridor". In: *Journal of Applied Meteorology and Climatology* vol. 50.10, pp. 2012–2029.

Zhang, Ning, Lianfang Zhu, and Yan Zhu (2011b). "Urban heat island and boundary layer structures under hot weather synoptic conditions: A case study of Suzhou City, China". In: *Advances in Atmospheric Sciences* vol. 28.4, p. 855.

Zhang, Xinmin, Ronald C. Estoque, and Yuji Murayama (2017). "An urban heat island study in Nanchang City, China based on land surface temperature and social-ecological variables". In: *Sustainable Cities and Society* vol. 32, pp. 557–568.

Zhao, Hongbo, Zhibin Ren, and Juntao Tan (2018a). "The spatial patterns of land surface temperature and its impact factors: Spatial non-stationarity and scale effects based on a geographically-weighted regression model". In: *Sustainability* vol. 10.7.

Zhu, Ke et al. (2010). "The geothermal potential of urban heat islands". In: *Environmental Research Letters* vol. 5.4, p. 044002.

Zhu, Xiudi et al. (2019). "Impact of urbanization on hourly precipitation in Beijing, China: Spatiotemporal patterns and causes". In: *Global and Planetary Change* vol. 172, pp. 307–324.

B.3 Excluded UHI records for the 3rd criterion

Atkinson, B.W. (2003). "Numerical modelling of urban heat-island intensity". In: *Boundary-Layer Meteorology* vol. 109.3, pp. 285–310.

Bassett, Richard et al. (2019). "Semi-idealized urban heat advection simulations using the Weather Research and Forecasting mesoscale model". In: *International Journal of Climatology* vol. 39.3, pp. 1345–1358.

Lu, Jie et al. (1997). "A laboratory study of the urban heat island in a calm and stably stratified environment. Part I: Temperature Field". In: *Journal of Applied Meteorology* vol. 36.10, pp. 1377–1391.

Martilli, Alberto (2014). "An idealized study of city structure, urban climate, energy consumption, and air quality". In: *Urban Climate* vol. 10, pp. 430–446.

Mei, Shuo-Jun et al. (2018). "Thermal buoyancy driven canyon airflows inside the compact urban blocks saturated with very weak synoptic wind: Plume merging mechanism". In: *Building and Environment* vol. 131, pp. 32–43.

Oke, T. R. (1981). "Canyon geometry and the nocturnal urban heat island: Comparison of scale model and field observations". In: *Journal of Climatology* vol. 1.3, pp. 237–254.

Oke, T.R. et al. (1991). "Simulation of surface urban heat islands under 'ideal' conditions at night part 2: Diagnosis of causation". In: *Boundary-Layer Meteorology* vol. 56.4, pp. 339–358.

Schmid, Paul E. and Dev Niyogi (2013). "Impact of city size on precipitation-modifying potential". In: *Geophysical Research Letters* vol. 40.19, pp. 5263–5267.

Shen, Lidu, Jianning Sun, and Renmin Yuan (2018). "Idealized large-eddy simulation study of interaction between urban heat island and sea breeze circulations". In: *Atmospheric Research* vol. 214, pp. 338–347.

Yamagata, Yoshiki and Hajime Seya (2013). "Simulating a future smart city: An integrated land use-energy model". In: *Applied Energy* vol. 112, pp. 1466–1474.

Yu, Tsann-Wang and Norman K. Wagner (1975). "Numerical study of the nocturnal urban boundary layer". In: *Boundary-Layer Meteorology* vol. 9.2, pp. 143–162.

Zander, Kerstin K et al. (2018). "Perceived heat stress increases with population density in urban Philippines". In: *Environmental Research Letters* vol. 13.8, p. 084009.

Zhu, Xiaoliang et al. (2017). "An idealized LES study of urban modification of moist convection". In: *Quarterly Journal of the Royal Meteorological Society* vol. 143.709, pp. 3228–3243.

B.4 Excluded NO_2 records for the 1^{st} criterion

Alberti, Marina (1999). "Urban patterns and environmental performance: What do we know?" In: *Journal of Planning Education and Research* vol. 19.2, pp. 151–163.

Basahi, JM, IM Ismail, and IA Hassan (2014). "A global challenge of air pollution and public health: A mini review". In: *Advances in Environmental Biology*, pp. 281–289.

Capello, Roberta and Roberto Camagni (2000). "Beyond optimal city size: An evaluation of alternative urban growth patterns". In: *Urban Studies* vol. 37.9, pp. 1479–1496.

Gómez-Baggethun, Erik and David N. Barton (2013). "Classifying and valuing ecosystem services for urban planning". In: *Ecological Economics* vol. 86, pp. 235–245.

Nieuwenhuijsen, Mark J. (2016). "Urban and transport planning, environmental exposures and health-new concepts, methods and tools to improve health in cities". In: *Environmental Health : A Global Access Science Source* vol. 15 Suppl 1.Suppl 1, pp. 38–38.

Parrish, David D. and Tong Zhu (2009). "Clean air for megacities". In: *Science* vol. 326.5953, pp. 674–675.

Robson, Brian T (2012). *Urban growth: An approach*. Routledge.

Scott, Alister, Alana Gilbert, and Ayele Gelan (2007). *The urban-rural divide: Myth or reality?* Macaulay Institute.

Shao, Min et al. (2006). "City clusters in China: Air and surface water pollution". In: *Frontiers in Ecology and the Environment* vol. 4.7, pp. 353–361.

Stead, Dominic and Stephen Marshall (2001). "The relationships between urban form and travel patterns. An international review and evaluation". In: *European Journal of Transport and Infrastructure Research* vol. 1.2, pp. 113–141.

B.5 Excluded NO_2 records for the 2^{nd} criterion

Abdel-Rahman, Hesham and Masahisa Fujita (1990). "Product variety, Marshallian externalities, and city sizes". In: *Journal of Regional Science* vol. 30.2, pp. 165–183.

Artun, Gülzade Küçükaçl et al. (2017). "An integrative approach for determination of air pollution and its health effects in a coal fired power plant area by passive sampling". In: *Atmospheric Environment* vol. 150, pp. 331–345.

Balakrishnan, K et al. (2011). "Part 1. Short-term effects of air pollution on mortality: Results from a time-series analysis in Chennai, India". In: *Research Report Health Effects Institute* 157, pp. 7–44.

Baró, Francesc et al. (2016). "Mapping ecosystem service capacity, flow and demand for landscape and urban planning: A case study in the Barcelona metropolitan region". In: *Land Use Policy* vol. 57, pp. 405–417.

Beelen, Rob et al. (2010). "Comparison of the performances of land use regression modelling and dispersion modelling in estimating small-scale variations in long-term air pollution concentrations in a Dutch urban area". In: *Atmospheric Environment* vol. 44.36, pp. 4614–4621.

Bogo, H et al. (2001). "Traffic pollution in a downtown site of Buenos Aires City". In: *Atmospheric Environment* vol. 35.10, pp. 1717–1727.

Bosch-Cano, Floriane et al. (2011). "Human exposure to allergenic pollens: A comparison between urban and rural areas". In: *Environmental Research* vol. 111.5, pp. 619–625.

Boyne, George (1995). "Population size and economies of scale in local government". In: *Policy & Politics* vol. 23.3, pp. 213–222.

Butu, Ioana Maria et al. (2012). "Evaluation of air pollution with NO_2 in Bucharest Area". In: *Revista de Chimie -Bucharest-Original Edition* vol. 63.3, pp. 330–333.

Cardelino, C. A. and W. L. Chameides (1990). "Natural hydrocarbons, urbanization, and urban ozone". In: *Journal of Geophysical Research: Atmospheres* vol. 95.D9, pp. 13971–13979.

Chan, Kam Wing and Xueqiang Xu (1985). "Urban population growth and urbanization in China since 1949: Reconstructing a baseline". In: *The China Quarterly* 104, pp. 583–613.

Chen, Li et al. (2010). "A land use regression for predicting NO_2 and PM_{10} concentrations in different seasons in Tianjin region, China". In: *Journal of Environmental Sciences* vol. 22.9, pp. 1364–1373.

Chen, Li et al. (2012). "A land use regression model incorporating data on industrial point source pollution". In: *Journal of Environmental Sciences* vol. 24.7, pp. 1251–1258.

Cheng, Jianquan and Ian Masser (2003). "Urban growth pattern modeling: A case study of Wuhan City, PR China". In: *Landscape and Urban Planning* vol. 62.4, pp. 199–217.

Chiesa, M. et al. (2009). "A target-oriented risk assessment for air pollution in Milan: Preliminary results". In: *GIMT - Giornale Italiano delle Malattie del Torace* vol. 63.6, pp. 439–446.

Choi, Giehae, Seulkee Heo, and Jong-Tae Lee (2016). "Assessment of environmental injustice in Korea using synthetic air quality index and multiple indicators of socioeconomic status: A

cross-sectional study". In: *Journal of the Air & Waste Management Association* vol. 66.1, pp. 28–37.

Clougherty, Jane E., E. Andres Houseman, and Jonathan I. Levy (2009). "Examining intra-urban variation in fine particle mass constituents using GIS and constrained factor analysis". In: *Atmospheric Environment* vol. 43.34, pp. 5545–5555.

Clougherty, Jane E. et al. (2007). "Synergistic effects of traffic-related air pollution and exposure to violence on urban asthma etiology". In: *Environmental Health Perspectives* vol. 115.8, pp. 1140–1146.

Clougherty, Jane E. et al. (2008). "Land use regression modeling of intra-urban residential variability in multiple traffic-related air pollutants". In: *Environmental Health* vol. 7.1, p. 17.

Clougherty, Jane E. et al. (2013). "Intra-urban spatial variability in wintertime street-level concentrations of multiple combustion-related air pollutants: The New York City Community Air Survey (NYCCAS)". In: *Journal of Exposure Science & Environmental Epidemiology* vol. 23.3, pp. 232–240.

Cowie, Christine T. et al. (2019). "Comparison of model estimates from an intra-city land use regression model with a national satellite-LUR and a regional Bayesian Maximum Entropy model, in estimating NO_2 for a birth cohort in Sydney, Australia". In: *Environmental Research* vol. 174, pp. 24–34.

Crouse, Dan L. et al. (2018). "Associations between living near water and risk of mortality among urban Canadians". In: *Environmental Health Perspectives* vol. 126.7, p. 077008.

Crouse, Dan L et al. (2017). "Urban greenness and mortality in Canada's largest cities: A national cohort study". In: *The Lancet Planetary Health* vol. 1.7, e289–e297.

Danciulescu, Valeriu et al. (2015). "Correlations between noise level and pollutants concentration in order to assess the level of air pollution induced by heavy traffic". In: *Journal of Environmental Protection and Ecology* vol. 16.3, pp. 815–823.

Danzlger, Sheldon (1976). "Explaining urban crime rates". In: *Criminology* vol. 14.2, pp. 291–296.

De Redder, Koen et al. (2015). "The impact of model resolution on simulated ambient air quality and associated human exposure". In: *Atmósfera* vol. 27.4, pp. 403–410.

Ding, Chengri and Xingshuo Zhao (2011). "Assessment of urban spatial-growth patterns in China during rapid urbanization". In: *The Chinese Economy* vol. 44.1, pp. 46–71.

Douglas, Ashley N.J., Peter J. Irga, and Fraser R. Torpy (2019). "Determining broad scale associations between air pollutants and urban forestry: A novel multifaceted methodological approach". In: *Environmental Pollution* vol. 247, pp. 474–481.

Eberts, Randall W et al. (1986). *Estimating the contribution of urban public infrastructure to regional growth*. Vol. 8610. Federal Reserve Bank of Cleveland Cleveland, OH.

Eeftens, Marloes et al. (2019). "Modelling the vertical gradient of nitrogen dioxide in an urban area". In: *Science of the Total Environment* vol. 650, pp. 452–458.

Escudero, M et al. (2014). "Urban influence on increasing ozone concentrations in a characteristic Mediterranean agglomeration". In: *Atmospheric Environment* vol. 99, pp. 322–332.

Esplugues, A. et al. (2010). "Indoor and outdoor concentrations and determinants of NO_2 in a cohort of 1-year-old children in Valencia, Spain". In: *Indoor Air* vol. 20.3, pp. 213–223.

Fleck, Alan da Silveira et al. (2014). "A comparison of the human buccal cell assay and the pollen abortion assay in assessing genotoxicity in an urban-rural gradient". In: *International journal of environmental research and public health* vol. 11.9, pp. 8825–8838.

Fuertes, E. et al. (2016). "Residential greenness is differentially associated with childhood allergic rhinitis and aeroallergen sensitization in seven birth cohorts". In: *Allergy* vol. 71.10, pp. 1461–1471.

Gaga, Eftade O. et al. (2012). "Evaluation of air quality by passive and active sampling in an urban city in Turkey: Current status and spatial analysis of air pollution exposure". In: *Environmental Science and Pollution Research* vol. 19.8, pp. 3579–3596.

Gagné, Sara A et al. (2016). "The effect of human population size on the breeding bird diversity of urban regions". In: *Biodiversity and Conservation* vol. 25.4, pp. 653–671.

Gariazzo, Claudio, Armando Pelliccioni, and Andrea Bolignano (2016). "A dynamic urban air pollution population exposure assessment study using model and population density data derived by mobile phone traffic". In: *Atmospheric Environment* vol. 131, pp. 289–300.

Gilbert, Nicolas L. et al. (2005). "Assessing spatial variability of ambient nitrogen dioxide in Montréal, Canada, with a land-use regression model". In: *Journal of the Air & Waste Management Association* vol. 55.8, pp. 1059–1063.

Gupta, AK et al. (2008). "Spatio-temporal characteristics of gaseous and particulate pollutants in an urban region of Kolkata, India". In: *Atmospheric Research* vol. 87.2, pp. 103–115.

Han, Lijian et al. (2016). "An optimum city size? The scaling relationship for urban population and fine particulate ($PM_{2.5}$) concentration". In: *Environmental Pollution* vol. 208, pp. 96–101.

Hao, Yufang and Shaodong Xie (2018). "Optimal redistribution of an urban air quality monitoring network using atmospheric dispersion model and genetic algorithm". In: *Atmospheric Environment* vol. 177, pp. 222–233.

Hassan, Ibrahim A et al. (2013). "Spatial distribution and temporal variation in ambient ozone and its associated NO_x in the atmosphere of Jeddah City, Saudi Arabia". In: *Aerosol and Air Quality Research* vol. 13.6, pp. 1712–1722.

Henderson, J. Vernon (1983). "Industrial bases and city sizes". In: *The American Economic Review* vol. 73.2, pp. 164–168.

Hien, P.D. et al. (2014). "Concentrations of NO_2, SO_2, and benzene across Hanoi measured by passive diffusion samplers". In: *Atmospheric Environment* vol. 88, pp. 66–73.

Holt, James B., C.P. Lo, and Thomas W. Hodler (2004). "Dasymetric estimation of population density and areal interpolation of census data". In: *Cartography and Geographic Information Science* vol. 31.2, pp. 103–121.

Huang, Lei, Can Zhang, and Jun Bi (2017). "Development of land use regression models for $PM_{2.5}$, SO_2, NO_2 and O_3 in Nanjing, China". In: *Environmental Research* vol. 158, pp. 542–552.

Irga, P.J., M.D. Burchett, and F.R. Torpy (2015). "Does urban forestry have a quantitative effect on ambient air quality in an urban environment?" In: *Atmospheric Environment* vol. 120, pp. 173–181.

Iroh Tam, P. Y. et al. (2017). "Spatial variation of pneumonia hospitalization risk in Twin Cities metro area, Minnesota". In: *Epidemiology and infection* vol. 145.15, pp. 3274–3283.

James, Peter et al. (2017). "Interrelationships between walkability, air pollution, greenness, and body mass index". In: *Epidemiology* vol. 28.6, pp. 780–788.

Jerrett, M. et al. (2007). "Modeling the intraurban variability of ambient traffic pollution in Toronto, Canada". In: *Journal of Toxicology and Environmental Health, Part A* vol. 70, pp. 200–212.

Jordanova, Diana, Neli Jordanova, and Petar Petrov (2014). "Magnetic susceptibility of road deposited sediments at a national scale-Relation to population size and urban pollution". In: *Environmental Pollution* vol. 189, pp. 239–251.

Kim, Ik Ki (1994). "The environmental problems in urban communities and the protection of the environment in Korea". In: *Korea Journal of Population and Development*, pp. 63–76.

Kim, J., C. Chu, and S. Shin (2014). "ISSAQ: An integrated sensing systems for real-time indoor air quality monitoring". In: *IEEE Sensors Journal* vol. 14.12, pp. 4230–4244.

Kim, Myounghee, Okhee Yi, and Ho Kim (2012). "The role of differences in individual and community attributes in perceived air quality". In: *Science of the Total Environment* vol. 425, pp. 20–26.

King, Lesliel J. (1967). "Discriminatory analysis of urban growth patterns in Ontario and Quebec, 1951-1961". In: *Annals of the Association of American Geographers* vol. 57.3, pp. 566–578.

Kousa, Anu et al. (2002). "A model for evaluating the population exposure to ambient air pollution in an urban area". In: *Atmospheric Environment* vol. 36.13, pp. 2109–2119.

L., Berry Brian J., Simmons James W., and Tennant Robert J. (1963). "Urban population densities: Structure and change". In: *Geographical Review* vol. 53.3, pp. 389–405.

Levinson, Herbert S. and F. Houston Wynn (1963). "Effects of density on urban transportation requirements". In: *Highway Research Record* 2, pp. 38–64.

Lin, George C.S. (2007). "Chinese urbanism in question: State, society, and the reproduction of urban spaces". In: *Urban Geography* vol. 28.1, pp. 7–29.

Liu, Chao et al. (2016). "A land use regression application into assessing spatial variation of intra-urban fine particulate matter ($PM_{2.5}$) and nitrogen dioxide (NO_2) concentrations in City of Shanghai, China". In: *Science of the Total Environment* vol. 565, pp. 607–615.

Lu, W.Z. and X.K. Wang (2004). "Interaction patterns of major air pollutants in Hong Kong territory". In: *Science of the Total Environment* vol. 324.1, pp. 247–259.

Madsen, Christian et al. (2007). "Modeling the intra-urban variability of outdoor traffic pollution in Oslo, Norway-A GA^2LEN project". In: *Atmospheric Environment* vol. 41.35, pp. 7500–7511.

Marshall, Julian D, Elizabeth Nethery, and Michael Brauer (2008). "Within-urban variability in ambient air pollution: Comparison of estimation methods". In: *Atmospheric Environment* vol. 42.6, pp. 1359–1369.

Martenies, Sheena E. et al. (2017). "Disease and health inequalities attributable to air pollutant exposure in Detroit, Michigan". In: *International Journal of Environmental Research and Public Health* vol. 14.10, p. 1243.

Matte, Thomas D. et al. (2013). "Monitoring intraurban spatial patterns of multiple combustion air pollutants in New York City: Design and implementation". In: *Journal of Exposure Science & Environmental Epidemiology* vol. 23.3, pp. 223–231.

Meng, Xia et al. (2015). "A land use regression model for estimating the NO_2 concentration in Shanghai, China". In: *Environmental Research* vol. 137, pp. 308–315.

Mills, Edwin S. (1972). "Welfare aspects of national policy toward city sizes". In: *Urban Studies* vol. 9.1, pp. 117–124.

Morgenstern, V. et al. (2007). "Respiratory health and individual estimated exposure to traffic-related air pollutants in a cohort of young children". In: *Occupational and Environmental Medicine* vol. 64.1, pp. 8–16.

Mutlu, Servet (1989). "Urban concentration and primacy revisited: An analysis and some policy conclusions". In: *Economic Development and Cultural Change* vol. 37.3, pp. 611–639.

Nadal, Martí et al. (2011). "Health risk map of a petrochemical complex through GIS-fuzzy integration of air pollution monitoring data". In: *Human and Ecological Risk Assessment: An International Journal* vol. 17.4, pp. 873–891.

Ng, Mee Kam and Wing-Shing Tang (1999). "Urban system planning in China: A case study of the Pearl River Delta". In: *Urban Geography* vol. 20.7, pp. 591–616.

Norris, Gary and Timothy Larson (1999). "Spatial and temporal measurements of NO_2 in an urban area using continuous mobile monitoring and passive samplers". In: *Journal of Exposure Science & Environmental Epidemiology* vol. 9.6, pp. 586–593.

Nowak, David J., Daniel E. Crane, and Jack C. Stevens (2006a). "Air pollution removal by urban trees and shrubs in the United States". In: *Urban Forestry & Urban Greening* vol. 4.3, pp. 115–123.

Nowak, David J et al. (2006b). "Assessing urban forest effects and values, Minneapolis' urban forest". In: *Resour. Bull. NE-166. Newtown Square, PA: US Department of Agriculture, Forest Service, Northeastern Research Station. 20 p.* Vol. 166, pp. 1–22.

Nowak, David J et al. (2006c). "Assessing urban forest effects and values, Washington, DC′s urban forest". In: *Resour. Bull. NRS-1. Newtown Square, PA: US Department of Agriculture, Forest Service, Northern Research Station. 24 p.* Vol. 1, pp. 1–24.

— (2007a). "Assessing urban forest effects and values, New York City′s urban forest". In: *Resour. Bull. NRS-9. Newtown Square, PA: US Department of Agriculture, Forest Service, Northern Research Station. 22 p.* Vol. 9, pp. 1–22.

— (2007b). "Assessing urban forest effects and values, San Francisco′s urban forest". In: *Resour. Bull. NRS-37. Newtown Square, PA: U.S. Department of Agriculture, Forest Service, Northern Research Station. 22 p.* Vol. 7, pp. 1–22.

Nowak, David J et al. (2010). "Assessing urban forest effects and values, Chicago′s urban forest". In: *Resour. Bull. NRS-37. Newtown Square, PA: US Department of Agriculture, Forest Service, Northern Research Station. 27 p.* Vol. 37, pp. 1–27.

Oliver, J.Eric (2000). "City size and civic involvement in Metropolitan America". In: *The American Political Science Review* vol. 94.2, pp. 361–373.

Olvera-García, Miguel Ángel et al. (2016). "Air quality assessment using a weighted Fuzzy Inference System". In: *Ecological Informatics* vol. 33, pp. 57–74.

Padam, Sudarsanam and Sanjay Kumar Singh (2004). "Urbanization and urban transport in India: The search for a policy". In: *European Transport/Trasporti Europei* vol. 27, pp. 27–44.

Peach, W. J. et al. (2008). "Reproductive success of house sparrows along an urban gradient". In: *Animal Conservation* vol. 11.6, pp. 493–503.

Peach, Will J. et al. (2018). "Depleted suburban house sparrow *Passer domesticus* population not limited by food availability". In: *Urban Ecosystems* vol. 21.6, pp. 1053–1065.

Pedersen, Marie et al. (2013). "Does consideration of larger study areas yield more accurate estimates of air pollution health effects? An illustration of the bias-variance trade-off in air pollution epidemiology". In: *Environment International* vol. 60, pp. 23–30.

Pekey, Beyhan and Hande Ylmaz (2011). "The use of passive sampling to monitor spatial trends of volatile organic compounds (VOCs) at an industrial city of Turkey". In: *Microchemical Journal* vol. 97.2, pp. 213–219.

Peng, Chaoyang et al. (2002). "Urban air quality and health in China". In: *Urban Studies* vol. 39.12, pp. 2283–2299.

Preston, Samuel H. (1979). "Urban growth in developing countries: A demographic reappraisal". In: *Population and Development Review* vol. 5.2, pp. 195–215.

Pulselli, R et al. (2008). "Computing urban mobile landscapes through monitoring population density based on cellphone chatting". In: *International Journal of Design & Nature and Ecodynamics* vol. 3.2, pp. 121–134.

Raaschou-nielsen, Ole et al. (2000). "An air pollution model for use in epidemiological studies: Evaluation with measured levels of nitrogen dioxide and benzene". In: *Journal of Exposure Science & Environmental Epidemiology* vol. 10.1, pp. 4–14.

Rank, Mark R and Thomas A Hirschl (1988). "A rural-urban comparison of welfare exits: The importance of population density". In: *Rural Sociology* vol. 53.2, pp. 190–206.

Rao, Meenakshi et al. (2014). "Assessing the relationship among urban trees, nitrogen dioxide, and respiratory health". In: *Environmental Pollution* vol. 194, pp. 96–104.

Rosenlund, Mats et al. (2008). "Comparison of regression models with land-use and emissions data to predict the spatial distribution of traffic-related air pollution in Rome". In: *Journal of Exposure Science & Environmental Epidemiology* vol. 18.2, pp. 192–199.

Sahsuvaroglu, Talar et al. (2006). "A land use regression model for predicting ambient concentrations of nitrogen dioxide in Hamilton, Ontario, Canada". In: *Journal of the Air & Waste Management Association* vol. 56.8, pp. 1059–1069.

Santos, Ana Paula Milla dos et al. (2014). "A support tool for air pollution health risk management in emerging countries: A case in Brazil". In: *Human and Ecological Risk Assessment: An International Journal* vol. 20.5, pp. 1406–1424.

Sheppard, Eric (1982). "City size distributions and spatial economic change". In: *International Regional Science Review* vol. 7.2, pp. 127–151.

Sheshinski, Eytan (1973). "Congestion and the optimum city size". In: *The American Economic Review* vol. 63.2, pp. 61–66.

Silveira Fleck, Alan da et al. (2017). "The use of tree barks and human fingernails for monitoring metal levels in urban areas of different population densities of Porto Alegre, Brazil". In: *Environmental Science and Pollution Research* vol. 24.3, pp. 2433–2441.

Slama, Rémy et al. (2007). "Traffic-related atmospheric pollutants levels during pregnancy and offspring's term birth weight: A study relying on a land-use regression exposure model". In: *Environmental Health Perspectives* vol. 115.9, pp. 1283–1292.

Song, Congbo et al. (2018). "Heavy-duty diesel vehicles dominate vehicle emissions in a tunnel study in northern China". In: *Science of the Total Environment* vol. 637-638, pp. 431–442.

Stone Jr, Brian and Michael O Rodgers (2001). "Urban form and thermal efficiency: How the design of cities influences the urban heat island effect". In: *Journal of the American Planning Association* vol. 67.2, pp. 186–198.

Su, J.G., M. Brauer, and M. Buzzelli (2008). "Estimating urban morphometry at the neighborhood scale for improvement in modeling long-term average air pollution concentrations". In: *Atmospheric Environment* vol. 42.34, pp. 7884–7893.

Susaya, Janice et al. (2013). "Demonstration of long-term increases in tropospheric O_3 levels: Causes and potential impacts". In: *Chemosphere* vol. 92.11, pp. 1520–1528.

Sveikauskas, Leo, John Gowdy, and Michael Funk (1988). "Urban productivity: City size or industry size". In: *Journal of Regional Science* vol. 28.2, pp. 185–202.

Tainio, Marko et al. (2014). "Intake fraction variability between air pollution emission sources inside an urban area". In: *Risk Analysis* vol. 34.11, pp. 2021–2034.

Taj, Tahir et al. (2017). "Short-term associations between air pollution concentrations and respiratory health-Comparing primary health care visits, hospital admissions, and emergency department visits in a multi-municipality study". In: *International journal of environmental research and public health* vol. 14.6, p. 587.

Tang, U. Wa and Zhishi Wang (2006). "Determining gaseous emission factors and drivers particle exposures during traffic congestion by vehicle-following measurement techniques". In: *Journal of the Air & Waste Management Association* vol. 56.11, pp. 1532–1539.

Tenailleau, Quentin M. et al. (2016). "Do outdoor environmental noise and atmospheric NO_2 levels spatially overlap in urban areas?" In: *Environmental Pollution* vol. 214, pp. 767–775.

Tie, X., G. Brasseur, and Z. Ying (2010). "Impact of model resolution on chemical ozone formation in Mexico City: Application of the WRF-Chem model". In: *Atmospheric Chemistry and Physics* vol. 10.18, pp. 8983–8995.

Timmermans, R.M.A. et al. (2013). "Quantification of the urban air pollution increment and its dependency on the use of down-scaled and bottom-up city emission inventories". In: *Urban Climate* vol. 6, pp. 44–62.

Tseng, Chong-Yu et al. (2016). "Characteristics of atmospheric $PM_{2.5}$ in a densely populated city with multi-emission sources". In: *Aerosol and Air Quality Research* vol. 16.9, pp. 2145–2158.

Tu, Jun et al. (2007). "Impact of urban sprawl on water quality in Eastern Massachusetts, USA". In: *Environmental Management* vol. 40.2, pp. 183–200.

Upadhyay, Abhishek et al. (2014). "Development of a fuzzy pattern recognition model for air quality assessment of Howrah City". In: *Aerosol and Air Quality Research* vol. 14.6, pp. 1639–1652.

Wang, Fahui and Yixing Zhou (1999). "Modelling urban population densities in Beijing 1982-90: Suburbanisation and its causes". In: *Urban Studies* vol. 36.2, pp. 271–287.

Wang, Jifeng, Huapu Lu, and Hu Peng (2008). "System dynamics model of urban transportation system and its application". In: *Journal of Transportation Systems Engineering and Information Technology* vol. 8.3, pp. 83–89.

Wheeler, Amanda J. et al. (2008). "Intra-urban variability of air pollution in Windsor, Ontario - Measurement and modeling for human exposure assessment". In: *Environmental Research* vol. 106.1, pp. 7–16.

Xian, George, Mike Crane, and Junshan Su (2007). "An analysis of urban development and its environmental impact on the Tampa Bay watershed". In: *Journal of Environmental Management* vol. 85.4, pp. 965–976.

Xie, Yichun and Frank J. Costa (1993). "Urban planning in socialist China: Theory and practice". In: *Cities* vol. 10.2, pp. 103–114.

Xu, Meimei et al. (2019). "Local variation of $PM_{2.5}$ and NO_2 concentrations within metropolitan Beijing". In: *Atmospheric Environment* vol. 200, pp. 254–263.

Yang, Bo-Yi et al. (2018). "Overweight modifies the association between long-term ambient air pollution and prehypertension in Chinese adults: The 33 communities Chinese health study". In: *Environmental Health : A Global Access Science Source* vol. 17.1, p. 57.

Yeh, Anthony Gar-On and Xueqiang Xu (1984). "Provincial variation of urbanization and urban primacy in China". In: *The Annals of Regional Science* vol. 18.3, pp. 1–20.

Zee, S van der et al. (1999). "Acute effects of urban air pollution on respiratory health of children with and without chronic respiratory symptoms." In: *Occupational and Environmental Medicine* vol. 56.12, pp. 802–812.

Zeka, A., A. Zanobetti, and J. Schwartz (2005). "Short term effects of particulate matter on cause specific mortality: Effects of lags and modification by city characteristics". In: *Occupational and Environmental Medicine* vol. 62.10, pp. 718–725.

Zhang, Yajuan et al. (2012). "The spatial characteristics of ambient particulate matter and daily mortality in the urban area of Beijing, China". In: *Science of the Total Environment* vol. 435-436, pp. 14–20.

Zhang, Yongping and Zhifu Mi (2018). "Environmental benefits of bike sharing: A big data-based analysis". In: *Applied Energy* vol. 220, pp. 296–301.

Zhao, Jian-Liang et al. (2013). "Evaluation of triclosan and triclocarban at river basin scale using monitoring and modeling tools: Implications for controlling of urban domestic sewage discharge". In: *Water Research* vol. 47.1, pp. 395–405.

Zhou, Ying and Jonathan I. Levy (2008). "The impact of urban street canyons on population exposure to traffic-related primary pollutants". In: *Atmospheric Environment* vol. 42.13, pp. 3087–3098.

B.6 Excluded NO_2 records for the 3^{rd} criterion

Borrego, C. et al. (2006). "How urban structure can affect city sustainability from an air quality perspective". In: *Environmental Modelling & Software* vol. 21.4, pp. 461–467.

B.7 Excluded NO_2 records for the 4^{th} criterion

Cakmak, Sabit et al. (2011). "The risk of dying on days of higher air pollution among the socially disadvantaged elderly". In: *Environmental Research* vol. 111.3, pp. 388–393.

C Excluded articles in eligibility

C.1 Excluded UHI articles based on the 1st criterion

Cai, Guoyin, Mingyi Du, and Yang Gao (2019). "City block-based assessment of land cover components' impacts on the urban thermal environment". In: *Remote Sensing Applications: Society and Environment* vol. 13, pp. 85–96.

Lin, Chuan-Yao et al. (2008). "Urban heat island effect and its impact on boundary layer development and land-sea circulation over northern Taiwan". In: *Atmospheric Environment* vol. 42.22, pp. 5635–5649.

Montávez, Juan Pedro, Jesús Fidel González-Rouco, and Francisco Valero (2008). "A simple model for estimating the maximum intensity of nocturnal urban heat Island". In: *International Journal of Climatology* vol. 28.2, pp. 235–242.

Oleson, K. W. et al. (2008). "An urban parameterization for a global climate model. Part II: Sensitivity to input parameters and the simulated urban heat island in offline simulations". In: *Journal of Applied Meteorology and Climatology* vol. 47.4, pp. 1061–1076.

Yang, Li et al. (2016). "Research on urban heat-island effect". In: *Procedia Engineering* vol. 169, pp. 11–18.

C.2 Excluded UHI articles based on the 2nd criterion

Benz, Susanne A., Peter Bayer, and Philipp Blum (2017). "Identifying anthropogenic anomalies in air, surface and groundwater temperatures in Germany". In: *Science of the Total Environment* vol. 584-585, pp. 145–153.

Estoque, Ronald C., Yuji Murayama, and Soe W. Myint (2017). "Effects of landscape composition and pattern on land surface temperature: An urban heat island study in the megacities of Southeast Asia". In: *Science of the Total Environment* vol. 577, pp. 349–359.

Grover, Aakriti and Ram Babu Singh (2015). "Analysis of urban heat island (UHI) in relation to normalized difference vegetation index (NDVI): A comparative study of Delhi and Mumbai". In: *Environments* vol. 2.2, pp. 125–138.

Higashino, Makoto and Heinz G. Stefan (2014). "Hydro-climatic change in Japan (1906-2005): Impacts of global warming and urbanization". In: *Air, Soil and Water Research* vol. 7, ASWR.S13632.

Lin, Chuan-Yao et al. (2011). "Impact of the urban heat island effect on precipitation over a complex geographic environment in Northern Taiwan". In: *Journal of Applied Meteorology and Climatology* vol. 50.2, pp. 339–353.

Rosenzweig, Cynthia et al. (2005). "Characterizing the urban heat island in current and future climates in New Jersey". In: *Global Environmental Change Part B: Environmental Hazards* vol. 6.1, pp. 51–62.

Yang, Wangming, Bing Chen, and Xuefeng Cui (2014). "High-resolution mapping of anthropogenic heat in China from 1992 to 2010". In: *International journal of environmental research and public health* vol. 11.4, pp. 4066–4077.

C.3 Excluded UHI articles based on the 4^{th} criterion

Andrews, Clinton J. (2008). "Greenhouse gas emissions along the rural-urban gradient". In: *Journal of Environmental Planning and Management* vol. 51.6, pp. 847–870.

Camilloni, Inés and Vicente Barros (1997). "On the urban heat island effect dependence on temperature trends". In: *Climatic Change* vol. 37.4, pp. 665–681.

Chen, Qian et al. (2018). "Spatially explicit assessment of heat health risk by using multi-sensor remote sensing images and socioeconomic data in Yangtze River Delta, China". In: *International Journal of Health Geographics* vol. 17.1, p. 15.

Du, Yin et al. (2007). "Impact of urban expansion on regional temperature change in the Yangtze River Delta". In: *Journal of Geographical Sciences* vol. 17.4, pp. 387–398.

Gallo, K.P. et al. (1993). "The use of NOAA AVHRR data for assessment of the urban heat island effect". In: *Journal of Applied Meteorology* vol. 32.5, pp. 899–908.

Gallo, Kevin P. and Timothy W. Owen (1999). "Satellite-based adjustments for the urban heat island temperature bias". In: *Journal of Applied Meteorology* vol. 38.6, pp. 806–813.

Gaur, Abhishek, Markus Kalev Eichenbaum, and Slobodan P. Simonovic (2018). "Analysis and modelling of surface urban heat island in 20 Canadian cities under climate and land-cover change". In: *Journal of Environmental Management* vol. 206, pp. 145–157.

Goodridge, James D. (1992). "Urban bias influences on long-term California air temperature trends". In: *Atmospheric Environment. Part B. Urban Atmosphere* vol. 26.1, pp. 1–7.

Goward, Samuel N. (1981). "Thermal behavior of urban landscapes and the urban heat island". In: *Physical Geography* vol. 2.1, pp. 19–33.

El-Hattab, M., Amany S.M., and Lamia G.E. (2018). "Monitoring and assessment of urban heat islands over the Southern region of Cairo Governorate, Egypt". In: *The Egyptian Journal of Remote Sensing and Space Science* vol. 21.3, pp. 311–323.

Heaviside, Clare, Sotiris Vardoulakis, and Xiao-Ming Cai (2016). "Attribution of mortality to the urban heat island during heatwaves in the West Midlands, UK". In: *Environmental Health* vol. 15 Suppl 1, pp. 27–27.

Heinl, Michael et al. (2015). "Determinants of urban-rural land surface temperature differences-A landscape scale perspective". In: *Landscape and Urban Planning* vol. 134, pp. 33–42.

Huang, Qunfang and Yuqi Lu (2015). "The effect of urban heat island on climate warming in the Yangtze River Delta urban agglomeration in China". In: *International Journal of Environmental Research and Public Health* vol. 12.8, pp. 8773–8789.

Imhoff, Marc L. et al. (2010). "Remote sensing of the urban heat island effect across biomes in the continental USA". In: *Remote Sensing of Environment* vol. 114.3, pp. 504–513.

Jin, Menglin, Robert E. Dickinson, and Da Zhang (2005a). "The footprint of urban areas on global climate as characterized by MODIS". In: *Journal of Climate* vol. 18.10, pp. 1551–1565.

Kim, Y.-H. and J.-J. Baik (2004). "Daily maximum urban heat island intensity in large cities of Korea". In: *Theoretical and Applied Climatology* vol. 79.3, pp. 151–164.

Li, Q. et al. (2004). "Urban heat island effect on annual mean temperature during the last 50 years in China". In: *Theoretical and Applied Climatology* vol. 79.3, pp. 165–174.

Li, Xiaoma et al. (2017e). "The surface urban heat island response to urban expansion: A panel analysis for the conterminous United States". In: *Science of the Total Environment* vol. 605-606, pp. 426–435.

Morabito, Marco et al. (2016). "The impact of built-up surfaces on land surface temperatures in Italian urban areas". In: *Science of the Total Environment* vol. 551-552, pp. 317–326.

Peng, Shushi et al. (2012). "Surface urban heat island across 419 global big cities". In: *Environmental Science & Technology* vol. 46.2, pp. 696–703.

Portman, David A. (1993). "Identifying and correcting urban bias in regional time series: Surface temperature in China′s northern plains". In: *Journal of Climate* vol. 6.12, pp. 2298–2308.

Ranagalage, Manjula et al. (2018). "Spatial changes of urban heat island formation in the Colombo District, Sri Lanka: Implications for sustainability planning". In: *Sustainability* vol. 10.5.

Stone Jr, Brian (2007). "Urban and rural temperature trends in proximity to large US cities: 19512000". In: *International Journal of Climatology* vol. 27.13, pp. 1801–1807.

— (2008). "Urban sprawl and air quality in large US cities". In: *Journal of Environmental Management* vol. 86.4, pp. 688–698.

Tam, Benita Y., William A. Gough, and Tanzina Mohsin (2015). "The impact of urbanization and the urban heat island effect on day to day temperature variation". In: *Urban Climate* vol. 12, pp. 1–10.

Tan, Minghong and Xiubin Li (2015). "Quantifying the effects of settlement size on urban heat islands in fairly uniform geographic areas". In: *Habitat International* vol. 49, pp. 100–106.

Theeuwes, Natalie E. et al. (2017). "A diagnostic equation for the daily maximum urban heat island effect for cities in Northwestern Europe". In: *International Journal of Climatology* vol. 37.1, pp. 443–454.

Wang, Juan et al. (2015). "Spatiotemporal variation in surface urban heat island intensity and associated determinants across major Chinese cities". In: *Remote Sensing* vol. 7.4, pp. 3670–3689.

Zhang, Jinqu and Yunpeng Wang (2008). "Study of the relationships between the spatial extent of surface urban heat islands and urban characteristic factors based on Landsat ETM+ data". In: *Sensors* vol. 8.11, pp. 7453–7468.

Zhang, Ping et al. (2010b). "Characterizing urban heat islands of global settlements using MODIS and nighttime lights products". In: *Canadian Journal of Remote Sensing* vol. 36.3, pp. 185–196.

Zhang, Ying and Lixin Sun (2019). "Spatial-temporal impacts of urban land use land cover on land surface temperature: Case studies of two Canadian urban areas". In: *International Journal of Applied Earth Observation and Geoinformation* vol. 75, pp. 171–181.

Zhou, B., D. Rybski, and J. P. Kropp (2013). "On the statistics of urban heat island intensity". In: *Geophysical Research Letters* vol. 40.20, pp. 5486–5491.

Zhou, Bin, Diego Rybski, and Jürgen P. Kropp (2017). "The role of city size and urban form in the surface urban heat island". In: *Scientific Reports* vol. 7.1, p. 4791.

Zhou, Decheng et al. (2015). "The footprint of urban heat island effect in China". In: *Scientific Reports* vol. 5, p. 11160.

Zhu, Xinyue et al. (2014). "The role of rapid urbanization in surface warming over Eastern China". In: *International Journal of Remote Sensing* vol. 35.24, pp. 8295–8308.

C.4 Excluded UHI articles based on the 5^{th} criterion

Dihkan, Mustafa et al. (2018). "Evaluation of urban heat island effect in Turkey". In: *Arabian Journal of Geosciences* vol. 11.8, p. 186.

Fujibe, Fumiaki (2009). "Detection of urban warming in recent temperature trends in Japan". In: *International Journal of Climatology* vol. 29.12, pp. 1811–1822.

— (2012). "Dependence of long-term temperature trends on wind and precipitation at urban stations in Japan". In: *Journal of the Meteorological Society of Japan. Ser. II* vol. 90.4, pp. 525–534.

Golroudbary, Vahid Rahimpour et al. (2018). "Urban impacts on air temperature and precipitation over the Netherlands". In: *Climate Research* vol. 75.2, pp. 95–109.

Jackson, Trisha L et al. (2010). "Parameterization of urban characteristics for global climate modeling". In: *Annals of the Association of American Geographers* vol. 100.4, pp. 848–865.

Li, Bing et al. (2018). "Comparative analysis of urban heat island intensities in Chinese, Russian, and DPRK regions across the transnational urban agglomeration of the Tumen River in Northeast Asia". In: *Sustainability* vol. 10.8.

Lin, Shu-Hua and Chung-Ming Liu (2013). "Data assimilation of Island climate observations with large-scale re-analysis data to high-resolution grids". In: *International Journal of Climatology* vol. 33.5, pp. 1228–1236.

Peng, Shijia et al. (2019). "Spatial-temporal pattern of, and driving forces for, urban heat island in China". In: *Ecological Indicators* vol. 96, pp. 127–132.

Steeneveld, G. J. et al. (2011). "Quantifying urban heat island effects and human comfort for cities of variable size and urban morphology in the Netherlands". In: *Journal of Geophysical Research: Atmospheres* vol. 116.D20129.

Wolters, Dirk and Theo Brandsma (2012). "Estimating the urban heat island in residential areas in the Netherlands using observations by weather amateurs". In: *Journal of Applied Meteorology and Climatology* vol. 51.4, pp. 711–721.

C.5 Excluded UHI articles based on the 6^{th} criterion

Esau, Igor and Victoria Miles (2018). "Exogenous drivers of surface urban heat islands in northern west Siberia". In: *Geography, Environment, Sustainability* vol. 11.3, pp. 83–99.

Lee, T.-W., Heung S. Choi, and Jinoh Lee (2014b). "Generalized scaling of urban heat island effect and its applications for energy consumption and renewable energy". In: *Advances in Meteorology* vol. 2014, p. 5.

C.6 Excluded NO_2 articles based on the 1^{st} criterion

Cesaroni, Giulia et al. (2012). "Nitrogen dioxide levels estimated from land use regression models several years apart and association with mortality in a large cohort study". In: *Environmental Health: A Global Access Science Source* vol. 11, pp. 48–48.

Fecht, Daniela et al. (2015). "Associations between air pollution and socioeconomic characteristics, ethnicity and age profile of neighbourhoods in England and the Netherlands". In: *Environmental Pollution* vol. 198, pp. 201–210.

Puliafito, S. Enrique et al. (2017). "High-resolution atmospheric emission inventory of the argentine energy sector. Comparison with edgar global emission database". In: *Heliyon* vol. 3.12, e00489–e00489.

C.7 Excluded NO_2 articles based on the 2^{nd} criterion

Geng, G. et al. (2017). "Impact of spatial proxies on the representation of bottom-up emission inventories: A satellite-based analysis". In: *Atmospheric Chemistry and Physics* vol. 17.6, pp. 4131–4145.

Larkin, Andrew et al. (2016). "Relationships between changes in urban characteristics and air quality in East Asia from 2000 to 2010". In: *Environmental Science & Technology* vol. 50.17, pp. 9142–9149.

C.8 Excluded NO_2 articles based on the 3^{rd} criterion

Clark, Lara P., Dylan B. Millet, and Julian D. Marshall (2011). "Air quality and urban form in U.S. urban areas: Evidence from regulatory monitors". In: *Environmental Science & Technology* vol. 45.16, pp. 7028–7035.

Samoli, E et al. (2019). "Spatial variability in air pollution exposure in relation to socioeconomic indicators in nine European metropolitan areas: A study on environmental inequality". In: *Environmental Pollution* vol. 249, pp. 345–353.

C.9 Excluded NO_2 articles based on the 4^{th} criterion

Bereitschaft, Bradley and Keith Debbage (2013). "Urban form, air pollution, and CO_2 emissions in large U.S. metropolitan areas". In: *The Professional Geographer* vol. 65.4, pp. 612–635.

Butler, TM et al. (2008). "The representation of emissions from megacities in global emission inventories". In: *Atmospheric Environment* vol. 42.4, pp. 703–719.

Campbell, G.W, J.R Stedman, and K Stevenson (1994). "A survey of nitrogen dioxide concentrations in the United Kingdom using diffusion tubes, July-December 1991". In: *Atmospheric Environment* vol. 28.3, pp. 477–486.

Duncan, Bryan N. et al. (2016). "A space-based, high-resolution view of notable changes in urban NO_x pollution around the world (2005-2014)". In: *Journal of Geophysical Research: Atmospheres* vol. 121.2, pp. 976–996.

Elansky, Nikolai F et al. (2016). "Trace gases in the atmosphere over Russian cities". In: *Atmospheric Environment* vol. 143, pp. 108–119.

Ghude, Sachin D. et al. (2008). "Detection of surface emission hot spots, trends, and seasonal cycle from satellite-retrieved NO_2 over India". In: *Journal of Geophysical Research: Atmospheres* vol. 113.D20, p. D20305.

Gurjar, B.R. et al. (2008). "Evaluation of emissions and air quality in megacities". In: *Atmospheric Environment* vol. 42.7, pp. 1593–1606.

Han, Lijian et al. (2018). "Multicontaminant air pollution in Chinese cities". In: *Bulletin of the World Health Organization* vol. 96.4, 233–242E.

Hilboll, A., A. Richter, and J.P. Burrows (2013). "Long-term changes of tropospheric NO_2 over megacities derived from multiple satellite instruments". In: *Atmospheric Chemistry and Physics* vol. 13.8, pp. 4145–4169.

Holland, Elisabeth A. et al. (2005). "Nitrogen deposition onto the united states and western europe: Synthesis of observations and models". In: *Ecological Applications* vol. 15.1, pp. 38–57.

Karambelas, Alexandra et al. (2018). "Constraining the uncertainty in emissions over India with a regional air quality model evaluation". In: *Atmospheric Environment* vol. 174, pp. 194–203.

Koralegedara, Suranjith Bandara et al. (2016). "Estimation of anthropogenic heat emissions in urban Taiwan and their spatial patterns". In: *Environmental Pollution* vol. 215, pp. 84–95.

Liu, Yupeng, Jianguo Wu, and Deyong Yu (2018a). "Disentangling the complex effects of socioeconomic, climatic, and urban form factors on air pollution: A case study of China". In: *Sustainability* vol. 10.3.

McCarty, Joshua and Nikhil Kaza (2015). "Urban form and air quality in the United States". In: *Landscape and Urban Planning* vol. 139, pp. 168–179.

Miller, Marvin E. (1967). "A note on comparison of statistical and analytical results for calculating oxides of nitrogen concentrations". In: *Journal of the Air Pollution Control Association* vol. 17.4, pp. 232–234.

Rodríguez, Miguel Cárdenas, Laura Dupont-Courtade, and Walid Oueslati (2016). "Air pollution and urban structure linkages: Evidence from European cities". In: *Renewable and Sustainable Energy Reviews* vol. 53, pp. 1–9.

Scoggins, Amanda and Gavin Fisher (2002). "Air pollution exposure index for New Zealand". In: *New Zealand Geographer* vol. 58.2, pp. 56–64.

Sharma, Disha and U.C. Kulshrestha (2014). "Spatial and temporal patterns of air pollutants in rural and urban areas of India". In: *Environmental Pollution* vol. 195, pp. 276–281.

Skouloudis, A. N. and D. G. Rickerby (2016). "Verifiable emission reductions in European urban areas with air-quality models". In: *Faraday Discuss.* Vol. 189 (0), pp. 617–633.

Van Der Zee, Saskia C. et al. (1998). "Characterization of particulate air pollution in urban and non-urban areas in the Netherlands". In: *Atmospheric Environment* vol. 32.21, pp. 3717–3729.

Zhao, Shuang et al. (2018b). "Temporal dynamics of SO_2 and NO_X pollution and contributions of driving forces in urban areas in China". In: *Environmental Pollution* vol. 242, pp. 239–248.

C.10 Excluded NO_2 articles based on the 5^{th} criterion

Aguilera, Inmaculada et al. (2015). "Land use regression models for crustal and traffic-related $PM_{2.5}$ constituents in four areas of the SAPALDIA study". In: *Environmental Research* vol. 140, pp. 377–384.

Beelen, Rob et al. (2009). "Mapping of background air pollution at a fine spatial scale across the European Union". In: *Science of the Total Environment* vol. 407.6, pp. 1852–1867.

Benkovitz, C.M. (1983). "Characteristics of oxidant precursor emissions from anthropogenic sources in the United States". In: *Environment International* vol. 9.6, pp. 429–445.

Denby, Bruce et al. (2011). "Sub-grid variability and its impact on European wide air quality exposure assessment". In: *Atmospheric Environment* vol. 45.25, pp. 4220–4229.

Franklin, Meredith et al. (2012). "Predictors of intra-community variation in air quality". In: *Journal of Exposure Science & Environmental Epidemiology* vol. 22.2, pp. 135–147.

Hart, Jaime E. et al. (2009). "Spatial modeling of PM_{10} and NO_2 in the continental United States, 1985-2000". In: *Environmental Health Perspectives* vol. 117.11, pp. 1690–1696.

Hoek, Gerard et al. (2015). "Satellite NO_2 data improve national land use regression models for ambient NO_2 in a small densely populated country". In: *Atmospheric Environment* vol. 105, pp. 173–180.

Lee, Jui-Huan et al. (2014a). "Land use regression models for estimating individual NO_x and NO_2 exposures in a metropolis with a high density of traffic roads and population". In: *Science of the Total Environment* vol. 472, pp. 1163–1171.

Li, Lianfa et al. (2017b). "Constrained mixed-effect models with ensemble learning for prediction of nitrogen oxides concentrations at high spatiotemporal resolution". In: *Environmental Science & Technology* vol. 51.17, pp. 9920–9929.

Mukerjee, Shaibal et al. (2009). "Spatial analysis and land use regression of VOCs and NO_2 from school-based urban air monitoring in Detroit/Dearborn, USA". In: *Science of the Total Environment* vol. 407.16, pp. 4642–4651.

Novotny, Eric V. et al. (2011). "National satellite-based land-use regression: NO_2 in the United States". In: *Environmental Science & Technology* vol. 45.10, pp. 4407–4414.

Poplawski, Karla et al. (2009). "Intercity transferability of land use regression models for estimating ambient concentrations of nitrogen dioxide". In: *Journal of Exposure Science & Environmental Epidemiology* vol. 19.1, pp. 107–117.

Qiu, Peipei et al. (2014). "An elaborate high resolution emission inventory of primary air pollutants for the Central Plain Urban Agglomeration of China". In: *Atmospheric Environment* vol. 86, pp. 93–101.

Saucy, Apolline et al. (2018). "Land use regression modelling of outdoor NO_2 and $PM_{2.5}$ concentrations in three low income areas in the Western Cape Province, South Africa". In: *International Journal of Environmental Research and Public Health* vol. 15.7, p. 1452.

Vienneau, Danielle et al. (2013). "Western European land use regression incorporating satellite- and ground-based measurements of NO_2 and PM_{10}". In: *Environmental Science & Technology* vol. 47.23, pp. 13555–13564.

Wang, Meng et al. (2014). "Performance of multi-city land use regression models for nitrogen dioxide and fine particles". In: *Environmental Health Perspectives* vol. 122.8, pp. 843–849.

Zou, Bin et al. (2009). "Spatially differentiated and source-specific population exposure to ambient urban air pollution". In: *Atmospheric Environment* vol. 43.26, pp. 3981–3988.

D Data for ANOVA and linear regression

D.1 Data for max ΔT with $\log_{10}$P and $\log_{10}$(max ΔT) with $\log_{10}$P

Table D.1: Data for max ΔT with $\log_{10}$P and $\log_{10}$(max ΔT) with $\log_{10}$P

Study	City	Country	P	max ΔT (°C)

continued on the next page

continued from the previous page

Oke (1973)	Montreal	Canada	2000000	12
Oke (ibid.)	St. Hyacinthe	Canada	23600	6.6
Oke (ibid.)	St. Hubert	Canada	18200	6.3
Oke (ibid.)	Chambly	Canada	12000	5.1
Oke (ibid.)	Marieville	Canada	4250	5.2
Oke (ibid.)	Saint-Basile-le-Grand	Canada	4000	3.7
Oke (ibid.)	St. Cesaire	Canada	2400	4.3
Oke (ibid.)	St.Pie	Canada	1550	3.3
Oke (ibid.)	Ste. Angele-de-Monnoir	Canada	1150	2.7
Oke (ibid.)	Ste. Madeleine	Canada	1100	1.8
Oke (ibid.)	Vancouver	Canada	1000000	10.2
Oke (ibid.)	San Francisco	USA	784000	11.1
Oke (ibid.)	Winnipeg	Canada	534000	11.6
Oke (ibid.)	Edmonton	Canada	401000	11.5
Oke (ibid.)	Hamilton	Canada	300000	9.5
Oke (ibid.)	San Jose	USA	101000	7.7
Oke (ibid.)	Palo Alto	USA	33000	6.9
Oke (ibid.)	Corvallis	USA	21000	6.1
Oke (ibid.)	London	UK	8500000	10
Oke (ibid.)	Berlin	Germany	4200000	10
Oke (ibid.)	Vienna	Austria	1870000	8
Oke (ibid.)	Munich	Germany	822000	7
Oke (ibid.)	Sheffield	UK	500000	8
Oke (ibid.)	Utrecht	Netherlands	278000	6
Oke (ibid.)	Malmo	Sweden	275000	7.4
Oke (ibid.)	Karlsruhe	Germany	160000	7
Oke (ibid.)	Reading	UK	120000	4.4
Oke (ibid.)	Uppsala	Sweden	63000	6.5
Oke (ibid.)	Lund	Sweden	50000	5.8
Oke and Maxwell (1975)	Vancouver	Canada	1100000	11.6
Torok et al. (2001)	Camperdown	Australia	3315	2.7

continued on the next page

continued from the previous page

Torok et al. (2001)	Cobden	Australia	1477	2.6
Torok et al. (ibid.)	Colac	Australia	9171	2.8
Torok et al. (ibid.)	Hamilton	Australia	9753	5.4
Torok et al. (ibid.)	Melbourne (1993)	Australia	3022157	7.1
Torok et al. (ibid.)	Melbourne (1972)	Australia	2500000	6.8
Torok et al. (ibid.)	Hobart	Australia	130000	5.7
Torok et al. (ibid.)	Adelaide	Australia	870000	4.4
Sakakibara and Matsui (2005)	Nagano (2001)	Japan	364000	8
Sakakibara and Matsui (ibid.)	Nagano (1983)	Japan	325000	3
Sakakibara and Matsui (ibid.)	Obuse (2001)	Japan	11800	4.8
Sakakibara and Matsui (ibid.)	Obuse (1996)	Japan	11800	5.4
Sakakibara and Matsui (ibid.)	Suzaka	Japan	54100	5.7
Sakakibara and Matsui (ibid.)	Toyono	Japan	10200	4.4
Sakakibara and Matsui (ibid.)	Wakahowatauchi	Japan	6100	2.5
Sakakibara and Matsui (ibid.)	Wakahokawada	Japan	3500	2.1
Sakakibara and Matsui (ibid.)	Asahikawa	Japan	362000	9
Sakakibara and Matsui (ibid.)	Koshigaya	Japan	292000	5.5
Sakakibara and Matsui (ibid.)	Matsumoto	Japan	208000	6.1
Sakakibara and Matsui (ibid.)	Nozawa & Nakagome	Japan	23300	3.8
Sakakibara and Matsui (ibid.)	Iwamurada	Japan	13000	5
Sakakibara and Matsui (ibid.)	Hakuba	Japan	9600	4.1
Sakakibara and Matsui (ibid.)	Asashina	Japan	3500	2.7
Sakakibara and Matsui (ibid.)	Akaiwa &Tokida	Japan	2200	2.6
Sakakibara and Matsui (ibid.)	Tomono	Japan	1200	1.7
Sakakibara and Matsui (ibid.)	Koundai	Japan	800	3.2

D.2 Data for $\log_{10}$(mean NO2) with $\log_{10}$P

Table D.2: Data for $\log_{10}$(mean NO2) with $\log_{10}$P

Study	City	Country	P	mean NO2 ($\mu g/m^3$)
Nguyen and Kim (2006) urban bg.	Seoul	Korea	9895217	65.31
Nguyen and Kim (ibid.) urban bg.	Busan	Korea	3662884	47.61

continued on the next page

continued from the previous page

Nguyen and Kim (2006) urban bg.	Daegu	Korea	2480578	50.81
Nguyen and Kim (ibid.) urban bg.	Incheon	Korea	2475139	50.81
Nguyen and Kim (ibid.) urban bg.	Gwangju	Korea	1352797	38.58
Nguyen and Kim (ibid.) urban bg.	Daejeon	Korea	1368207	40.27
Nguyen and Kim (ibid.) urban bg.	Ulsan	Korea	1014428	36.89
Nguyen and Kim (ibid.) traffic bg.	Seoul	Korea	9895217	102.76
Nguyen and Kim (ibid.) traffic bg.	Busan	Korea	3662884	62.29
Nguyen and Kim (ibid.) traffic bg.	Daegu	Korea	2480578	69.82
Nguyen and Kim (ibid.) traffic bg.	Incheon	Korea	2475139	85.44
Nguyen and Kim (ibid.) traffic bg.	Gwangju	Korea	1352797	46.67
Nguyen and Kim (ibid.) traffic bg.	Daejeon	Korea	1368207	49.68
Nguyen and Kim (ibid.) traffic bg.	Ulsan	Korea	1014428	52.88
Lertxundi-Manterola and Saez (2009)	Barcelona	Spain	2377703	43.65
Lertxundi-Manterola and Saez (ibid.)	Bilbao	Spain	801770	39.24
Masiol et al. (2013) urban bg.	Belluno	Italy	37000	24
Masiol et al. (ibid.) urban bg.	Treviso	Italy	84000	37
Masiol et al. (ibid.) urban bg.	Vicenza	Italy	116000	38.5
Masiol et al. (ibid.) urban bg.	Schio	Italy	40000	24
Masiol et al. (ibid.) urban bg.	Legnago	Italy	25000	25
Masiol et al. (ibid.) urban bg.	Verona	Italy	264000	41
Masiol et al. (ibid.) urban bg.	Padova	Italy	215000	32
Masiol et al. (ibid.) urban bg.	Venice	Italy	271000	36
Masiol et al. (ibid.) urban bg.	Rovigo	Italy	53000	26
Masiol et al. (ibid.) traffic bg.	Vicenza	Italy	116000	49
Masiol et al. (ibid.) traffic bg.	Verona	Italy	264000	45
Masiol et al. (ibid.) traffic bg.	Padova	Italy	215000	43.7
Masiol et al. (ibid.) traffic bg.	Venice	Italy	271000	48
Masiol et al. (ibid.) traffic bg.	Rovigo	Italy	53000	38
Singh and Kulshrestha (2014)	Okhla	India	98415	24.4
Singh and Kulshrestha (ibid.)	Mai	India	5997	18.8
Singh and Kulshrestha (ibid.) winter	Okhla	India	98415	39.6

continued on the next page

continued from the previous page

Singh and Kulshrestha (2014) winter	Mai	India	5997	27.5
Singh and Kulshrestha (ibid.) summer	Okhla	India	98415	24.5
Singh and Kulshrestha (ibid.) summer	Mai	India	5997	17.2
Baró et al. (2015)	Barcelona	Spain	1615908	53.78
Baró et al. (ibid.)	Berlin	Germany	3431675	53.38
Baró et al. (ibid.)	Stockholm	Sweden	810120	38.5
Baró et al. (ibid.)	Rotterdam	the Netherlands	582951	48.66
Baró et al. (ibid.)	Salzburg	Austria	147169	45.21

D.3 Data for $\log_{10}$(mean NO2) with $\log_{10}$D

Table D.3: Data for $\log_{10}$(mean NO2) with $\log_{10}$D

Study	City	Country	P	Area (km^2)	mean NO2 ($\mu g/m^3$)
Nguyen and Kim (2006) urban bg.	Seoul	Korea	9895217	606	65.31
Nguyen and Kim (ibid.) urban bg.	Busan	Korea	3662884	760	47.61
Nguyen and Kim (ibid.) urban bg.	Daegu	Korea	2480578	886	50.81
Nguyen and Kim (ibid.) urban bg.	Incheon	Korea	2475139	965	50.81
Nguyen and Kim (ibid.) urban bg.	Gwangju	Korea	1352797	501	38.58
Nguyen and Kim (ibid.) urban bg.	Daejeon	Korea	1368207	540	40.27
Nguyen and Kim (ibid.) urban bg.	Ulsan	Korea	1014428	1056	36.89
Nguyen and Kim (ibid.) traffic bg.	Seoul	Korea	9895217	606	102.76
Nguyen and Kim (ibid.) traffic bg.	Busan	Korea	3662884	760	62.29
Nguyen and Kim (ibid.) traffic bg.	Daegu	Korea	2480578	886	69.82
Nguyen and Kim (ibid.) traffic bg.	Incheon	Korea	2475139	965	85.44
Nguyen and Kim (ibid.) traffic bg.	Gwangju	Korea	1352797	501	46.67
Nguyen and Kim (ibid.) traffic bg.	Daejeon	Korea	1368207	540	49.68
Nguyen and Kim (ibid.) traffic bg.	Ulsan	Korea	1014428	1056	52.88
Lertxundi-Manterola and Saez (2009)	Barcelona	Spain	2377703	230	43.65
Lertxundi-Manterola and Saez (ibid.)	Bilbao	Spain	801770	208	39.24

continued on the next page

continued from the previous page

Singh and Kulshrestha (2014)	Okhla	India	98415	9	24.4
Singh and Kulshrestha (ibid.)	Mai	India	5997	6.17	18.8
Singh and Kulshrestha (ibid.) winter	Okhla	India	98415	9	39.6
Singh and Kulshrestha (ibid.) winter	Mai	India	5997	6.17	27.5
Singh and Kulshrestha (ibid.) summer	Okhla	India	98415	9	24.5
Singh and Kulshrestha (ibid.) summer	Mai	India	5997	6.17	17.2
Baró et al. (2015)	Barcelona	Spain	1615908	101.6	53.78
Baró et al. (ibid.)	Berlin	Germany	3431675	891.1	53.38
Baró et al. (ibid.)	Stockholm	Sweden	810120	215.8	38.5
Baró et al. (ibid.)	Rotterdam	the Netherlands	582951	277.4	48.66
Baró et al. (ibid.)	Salzburg	Austria	147169	65.7	45.21

D.4 Data for $\log_{10}$(max NO2) with $\log_{10}$P and max NO2 with $\log_{10}$D

Table D.4: Data for $\log_{10}$(max NO2) with $\log_{10}$P and $\log_{10}$(max NO2) with $\log_{10}$D

Study	City	Country	P	Area (km^2)	max NO2 ($\mu g/m^3$)
Lertxundi-Manterola and Saez (2009)	Barcelona	Spain	2377703	230	148
Lertxundi-Manterola and Saez (ibid.)	Bilbao	Spain	801770	208	199
Singh and Kulshrestha (2014)	Okhla	India	98415	9	63.7
Singh and Kulshrestha (ibid.)	Mai	India	5997	6.17	40.6

E Principle of chemiluminescence

The principle of chemiluminescence in this section is based on the reference measurement method EN 14211:2005 of the European Commission (European Committee for Standardization 2005).

The concentration of NO in the sampled air is determined by the reaction of NO with O_3. To do this, the sampled air is mixed with excessive O_3 as a way to get excited NO_2 (Equation E.1).

The excited NO_2 then decomposes into NO_2 and emits near-infrared lights (Equation E.2). The radiation is converted into electrical signals by a photomultiplier or a photodiode. The volume of the lights is proportional to the concentration of NO in the sampled air.

$$NO + O_3 \longrightarrow NO_2{}^* + O_2 \tag{E.1}$$

$$NO_2{}^* \longrightarrow NO_2 + hv \tag{E.2}$$

$$NO_2 \xrightarrow{\text{converter (catalyst)}} NO \tag{E.3}$$

The sampled air also goes through a converter where all the NO_2 in it is reduced to NO (Equation E.3). The NO then reacts with the excessive O_3 in the same way (i.e. Equations E.1 and E.2). The volume of the emitted lights in this step is proportional to the sum of the concentration of NO in the sampled air and the concentration of NO converted from NO_2. The subtraction of these two NO concentrations can determine how much NO was converted from NO_2, and thus we can get the NO_2 concentration in the sampled air.

F Retrieval of tropospheric NO_2 vertical columns

This section is mainly based on the works of Chance (2002) and Geffen et al. (2019, 2020). To generate the tropospheric NO_2 vertical columns, the steps are

1. get total NO_2 slant columns using the method of DOAS. In this case, the main idea is to obtain slant column of NO_2 by comparing modeled and observed reflectance spectra. DOAS is introduced in Appendix G,
2. separate the total NO_2 slant columns into tropospheric NO_2 slant columns and stratospheric NO_2 slant columns using a data assimilation system of the global 3D chemistry transport model (e.g. TM5-MP CTM), and
3. subtract the stratospheric NO_2 slant columns from the total NO_2 slant columns to get the tropospheric NO_2 slant columns. The tropospheric NO_2 vertical columns are then gained

by converting the tropospheric NO_2 slant columns to tropospheric NO_2 vertical columns. The parameters of the conversion come from pre-calculated AMF look-up tables.

G General principle of DOAS

This section is mainly based on the works of Chance (2002), ESA (2022), Geffen et al. (2019, 2020), and Platt and Stutz (2008). This section focuses on how DOAS is used in the latest NO_2 sensor - TROPOMI. The earlier-launched sensor OMI uses the same principle with slightly different parameters (Chance 2002).

Suppose a reflectance spectrum at the wavelength λ observed by TROPOMI is denoted as $R_{meas}(\lambda)$, and is defined as Equation G.1,

$$R_{meas}(\lambda) = \frac{\pi * I(\lambda)}{\mu_0 * E_0(\lambda)} \tag{G.1}$$

where $I(\lambda)$ is the radiance at the top of the atmosphere, μ_0 is the cosine of the solar zenith angle, $E_0(\lambda)$ is the extraterrestrial solar irradiance which is measured once every day.

The reflectance spectrum at the wavelength λ modeled by TROPOMI is denoted as $R_{mod}(\lambda)$, and is defined as Equation G.2,

$$R_{mod}(\lambda) = P(\lambda) * exp\left[-\sum_{k=1}^{N_k} \sigma_k(\lambda) * N_{s,k}\right] * \left(1 + C_{ring} * \frac{I_{ring}(\lambda)}{E_0(\lambda)}\right) \tag{G.2}$$

where

$$P(\lambda) = \sum_{m=1}^{N_p} a_k * \lambda^m \tag{G.3}$$

In Equations G.2 and G.3, $P(\lambda)$ represents the scattering and absorbing of molecular, the scattering of aerosol, and the effects of surface albedo. For TROPOMI, usually N_p equals 5. a_m is the coefficient of this polynomial.

The sum in the square brackets of Equation G.2 represents the intensity of lights absorbed by the specific gas (in this case, NO_2) and secondary trace gases as the lights exits the sun, travels through the atmosphere, and are finally captured by TROPOMI. TROPOMI observes NO_2 by the channel of visible light with wavelength ranges from 440 nm to 496 nm. In this range, O_3, water

vapor (H_2O_{vap}), collisions between two oxygen molecules (O_2-O_2), and liquid water (H_2O_{liq}) are found to have ability of absorb the lights as well, so O_3, H_2O_{vap}, O_2-O_2, and H_2O_{liq} are the secondary trace gases in this case. The $\sigma_k(\lambda)$ values of the specific gas and the secondary trace gases are collected from published literature (e.g. Geffen et al. 2015; Gorshelev et al. 2014; Pope and Fry 1997; Serdyuchenko et al. 2014; Thalman and Volkamer 2013; Vandaele, A.C. et al. 2015) and are substituted to G.2. k is the amount of molecule.

The formula in the brackets of Equation G.2 accounts for the Ring spectrum effects, which are caused by the inelastic Raman scattering of incoming sunlight. C_{ring} is the coefficient. The value of $I_{ring}(\lambda)$ is collected from Chance and Spurr (1997).

To get the values of a_m, $N_{s.k}$ (i.e. the slant column amount of molecule k=1,..., N_k), and C_{ring}, $R_{mod}(\lambda)$ and $R_{meas}(\lambda)$ are compared by the minimization of a chi-square function (Equation G.4) or Root Mean Square (RMS) Equation G.5. The routine of Optimal Estimation (OE) is used in this step,

$$\chi^2 = \sum_{i=1}^{N_\lambda} \left(\frac{R_{meas}(\lambda_i) - R_{mod}(\lambda_i)}{\Delta R_{meas}(\lambda_i)} \right)^2 \tag{G.4}$$

where $\Delta R_{meas}(\lambda_i)$ is the precision of the measurements decided by TROPOMI.

$$R_{RMS} = \sqrt{\frac{1}{N_\lambda} \sum_{i=1}^{N_\lambda} (R_{meas}(\lambda_i) - R_{mod}(\lambda_i))^2} \tag{G.5}$$

H Inferring NO_2 surface concentrations using 3D atmospheric models

Popular 3D atmospheric models including EAC4 and GEOS-Chem. In this section they are briefly introduced. Please refer to other works (e.g. Bey et al. 2001; Inness et al. 2019; Wang et al. 1998) for the details of GEOS-Chem and EAC4.

EAC4 is a global reanalysis dataset of atmospheric composition developed from Eruopean Center for Medium-Range Weather Forecasts (ECMWF). Until 2016, its horizontal resolution is 40 km and it divides the vertical space from the surface to the atmospheric pressure of 0.1 hPa into 60 model layers. It contains 3 model systems: MACCRA, CIRA, and CAMSRA. Each model system considers components such as anthropogenic emissions, biomass burning emissions,

biogenic emissions and assimilated trace gases retrievals. It provides results of analyses and forecasts at the temporal resolution ranges from 1h to 6h. The latest model system CAMSRA contains 3 trace gases: O_3, CO, and NO_2 (Wang et al. 2020b). The assimilated tropospheric column NO_2 retrievals use information from SCIAMACHY, OMI, and GOME-2. The NO_2 mixing ratio is given by the minimization of the comparison between the model's background fields and the observation values. The minimization is evaluated using National Meterological Center (NMC) method (Parrish and Derber 1992) or the forecast differences (Inness et al. 2015).

GEOS-Chem is another global 3D model for modeling tropospheric chemistry developed from assimilated meteorological data from NASA Data Assimilation Office (Bey et al. 2001). Its main idea is to simulate tropospheric O_3, NO_x, and HC by tracking 24 tracers (ibid.). GEOS-Chem also considers emissions from anthropogenic activities, biomass burning, and natural sources. It's horizontal spatial resolution is 2.5^o x 2^o in the simulation of the NO_x-O_x-HC interaction (Grajales and Baquero-Berna 2014) and it divides the vertical space from the surface to the atmospheric pressure of 0.01 hPa into 72 model layers (Global Modeling and Assimilation Office 2021).

The NO_2 surface concentrations can be inferred from tropospheric NO_2 vertical columns by Equation H.1 (Jeong and Hong 2021),

$$S_A = \frac{S_L}{C_L} * C_A \tag{H.1}$$

where S_A is the inferred NO_2 surface concentrations, S_L is the surface level NO_2 mixing ratio provided by EAC4, C_2 is the tropospheric NO_2 columns provided by EAC4, and C_A is the tropospheric NO_2 vertical columns from satellite.

Similar to EAC4, GEOS-Chem also provides values of S_L and C_L so that the NO_2 surface concentrations can be calculated from tropospheric NO_2 vertical columns in the same way (Lamsal et al. 2008).

Lamsal et al. (ibid.) refined Equation H.1 and proposed another way of inferring NO_2 surface concentrations from satellite columns (Equation H.2),

$$S_A = \frac{v * S_L}{v * C_L - (v-1) * C_L^F} * C_A \tag{H.2}$$

where v is the ratio of the local tropospheric NO_2 vertical column to the mean satellite field over a GEOS-Chem grid, and C_L^F is the simulated free tropospheric (i.e. range from 750 hPa to 250 hPa) NO_2 column over the GEOS-Chem grid.